EPRI | ELECTRIC POWER
RESEARCH INSTITUTE

Evaluation of a Spent Fuel Repository at Yucca Mountain, Nevada

2008 Progress Report

Evaluation of a Spent Fuel Repository at Yucca Mountain, Nevada

2008 Progress Report

1016631

Final Report, December 2008

EPRI Project Manager
A. Sowder

DISCLAIMER OF WARRANTIES AND LIMITATION OF LIABILITIES

THIS DOCUMENT WAS PREPARED BY THE ORGANIZATION(S) NAMED BELOW AS AN ACCOUNT OF WORK SPONSORED OR COSPONSORED BY THE ELECTRIC POWER RESEARCH INSTITUTE, INC. (EPRI). NEITHER EPRI, ANY MEMBER OF EPRI, ANY COSPONSOR, THE ORGANIZATION(S) BELOW, NOR ANY PERSON ACTING ON BEHALF OF ANY OF THEM:

(A) MAKES ANY WARRANTY OR REPRESENTATION WHATSOEVER, EXPRESS OR IMPLIED, (I) WITH RESPECT TO THE USE OF ANY INFORMATION, APPARATUS, METHOD, PROCESS, OR SIMILAR ITEM DISCLOSED IN THIS DOCUMENT, INCLUDING MERCHANTABILITY AND FITNESS FOR A PARTICULAR PURPOSE, OR (II) THAT SUCH USE DOES NOT INFRINGE ON OR INTERFERE WITH PRIVATELY OWNED RIGHTS, INCLUDING ANY PARTY'S INTELLECTUAL PROPERTY, OR (III) THAT THIS DOCUMENT IS SUITABLE TO ANY PARTICULAR USER'S CIRCUMSTANCE; OR

(B) ASSUMES RESPONSIBILITY FOR ANY DAMAGES OR OTHER LIABILITY WHATSOEVER (INCLUDING ANY CONSEQUENTIAL DAMAGES, EVEN IF EPRI OR ANY EPRI REPRESENTATIVE HAS BEEN ADVISED OF THE POSSIBILITY OF SUCH DAMAGES) RESULTING FROM YOUR SELECTION OR USE OF THIS DOCUMENT OR ANY INFORMATION, APPARATUS, METHOD, PROCESS, OR SIMILAR ITEM DISCLOSED IN THIS DOCUMENT.

ORGANIZATION(S) THAT PREPARED THIS DOCUMENT

Electric Power Research Institute (EPRI)

NOTE

For further information about EPRI, call the EPRI Customer Assistance Center at 800.313.3774 or e-mail askepri@epri.com.

Electric Power Research Institute, EPRI, and TOGETHER…SHAPING THE FUTURE OF ELECTRICITY are registered service marks of the Electric Power Research Institute, Inc.

CITATIONS

REPORT SUMMARY

In June 2008, the U.S. Department of Energy (DOE) submitted a license application to the U.S. Nuclear Regulatory Commission (NRC) for the construction of a geologic repository at Yucca Mountain, Nevada, for the disposal of spent nuclear fuel and high-level radioactive waste. The license application was accepted for formal NRC review in September 2008. Throughout the more than 20-year history of the Yucca Mountain project, EPRI has performed independent assessments of key technical and scientific issues to facilitate an understanding of overall repository performance. This report presents background on the overall project and detailed information on EPRI's Yucca Mountain-related activities during calendar year 2008.

Background

The governing U.S. Environmental Protection Agency (EPA) standards and NRC regulations are probability-based. This probabilistic nature and the long time frames of interest associated with geologic disposal led to the development of the total system performance assessment (TSPA) methodology for demonstrating repository performance and regulatory compliance. As part of the license application preparation, the DOE has developed a TSPA; the NRC, the designated regulator for this facility, has done likewise. A similar analytical tool, the Integrated Multiple Assumptions and Release Code (IMARC), has also been developed by EPRI to provide an independent probabilistic performance evaluation of the proposed Yucca Mountain repository. Throughout the year, EPRI has investigated aspects of direct interest to its members, such as the feasibility of direct disposal of dual-purpose canisters at Yucca Mountain. EPRI has also continued to review and evaluate the technical basis supporting Yucca Mountain performance assessments, including 1) the likelihood and consequences of potentially disruptive volcanic and seismic activity, 2) additional performance margin provided by internal waste package components and the fuel itself, and 3) fundamental corrosion processes such as stifling of corrosion crevices and microbiologically influenced corrosion. Such issues are considered important to the overall determination of the suitability of the Yucca Mountain site to serve as a geologic repository.

Objective

To provide an independent assessment of key technical and scientific issues associated with the proposed geologic repository at Yucca Mountain, Nevada.

Approach

EPRI has developed and maintained IMARC to provide an independent probabilistic evaluation of the radiological performance of the proposed Yucca Mountain site under various conditions. IMARC has specifically been used to calculate probability-weighted mean dose to the reasonably maximally exposed individual (RMEI) located at the compliance point on the site boundary, one of the performance criteria established in the applicable NRC regulations. To address specific

subjects in key technical and scientific areas, EPRI has assembled a team of experts versed in the respective fields. The subjects vary from year to year and often arise from issues raised by those directly involved in the Yucca Mountain project as well as external interested parties. Wherever possible and appropriate, EPRI uses cautious but realistic assumptions in the performance of its various analyses and investigations, as recommended by the National Academy of Sciences (NAS) in its *Technical Bases for Yucca Mountain Standards* (TYMS) report.

Results

EPRI's 2008 analyses continue to show that the proposed Yucca Mountain repository will result in doses to the RMEI located downstream from the proposed facility that are well within both the regulatory limits established for the pertinent post-closure 10,000-year and 1 million-year compliance periods established in 40 CFR 197. EPRI also continues to observe that the use of overly conservative assumptions and approaches in TSPA modeling by the DOE lead to overestimated RMEI doses for the various scenarios investigated. Following are several key results from 2008 EPRI work:

- Direct disposal of at least some dual-purpose canisters is feasible.

- Volcanic hazard estimates for Yucca Mountain are overly conservative. EPRI's more realistic probability estimate for igneous events intersecting the repository falls below the regulatory threshold for considering the consequences of igneous activity.

- Peak seismic ground motion estimates for Yucca Mountain are overestimated.

- Internal waste package components (inner vessel and canister) and spent fuel itself provide additional and potentially significant performance margin for the repository.

- Waste package corrosion crevices, once formed, stifle rather than continue to propagate.

EPRI Perspective

EPRI believes that the proposed repository design submitted for license review in June 2008 is capable of maintaining any resulting dose levels to the public at extremely low levels, even in the face of various postulated events of low probability. Accordingly, the repository is expected to exceed performance criteria and regulatory limits by a significant margin. EPRI finds DOE assessments of the proposed repository performance to be overly conservative. Use of more realistic scenarios and input data result in a more appropriate estimate of performance, exhibiting a significant margin of compliance with respect to established regulatory criteria.

Keywords

Yucca Mountain
High-Level Radioactive Waste
Spent Fuel Disposal
Total System Performance Assessment

EXECUTIVE SUMMARY

In June, 2008, the U.S. Department of Energy (DOE) submitted a license application (LA) to the U.S. Nuclear Regulatory Commission (NRC) to initiate construction of a geologic repository at Yucca Mountain (YM), Nevada, for the storage of spent nuclear fuel (SNF) and high-level radioactive waste (HLW). This license application was accepted for formal review in September, 2008.

Investigations to determine the suitability of a site at Yucca Mountain to serve as a geologic repository have been underway since the early 1980's. Throughout most of this period, the Electric Power Research Institute (EPRI) has been performing its own scientific and technical investigations and reviews to provide an independent, third party perspective on site suitability and project-related scientific and technical issues.

This report provides information to EPRI's members, NRC, DOE, independent technical review bodies (such as the Nuclear Waste Technical Review Board and the Advisory Committee on Nuclear Waste and Materials), and the public regarding activities performed by EPRI and its consultants during CY 2008 related to the Yucca Mountain Project (YMP). These activities reflect scientific and technical developments that have arisen during the year and progress by the Department of Energy towards finalization and submission of the LA for repository construction. During 2008, EPRI sponsored activities to address a number of key issues that have the potential to significantly impact the ability of the proposed repository to be designed, constructed and operated in a manner that is in compliance with established regulations.

During 2008, the DOE and NRC focused their activities on the continued resolution of outstanding technical/scientific issues and preparation for the submittal of the LA and the review of the tendered documents. Significant resources were expended by the YMP towards the development of a comprehensive LA that addresses all of the issues raised in the NRC's Yucca Mountain Review Plan (NUREG – 1804), the updating and finalization of the Total System Performance Analysis (TSPA) required to support the LA and the updating and finalizing of Analysis/Model Reports (AMRs) intended to document the scientific basis for the license application. The final U.S. Environmental Protection Agency (EPA) standard establishing individual public dose limits for Yucca Mountain was issued on October 15, 2008 and became effective November 14, 2008. The conforming NRC regulation had not been issued at the time this report was prepared. In 2008, DOE also continued the development of the Transportation, Aging and Disposal (TAD) canister concept.

During 2008, the EPRI-sponsored work paralleled the activities of other stakeholders. Primary among these efforts were in-depth, independent evaluations that addressed the following subjects:

- IMARC - In 2007, EPRI commissioned an independent peer review of its Yucca Mountain TSPA code, IMARC. The full International Review Team (IRT) report will be published in 2009 concurrently with a parallel report on the latest revisions to the IMARC code (IMARC 10), including EPRI's response to the results of the IRT review. An advanced copy of the executive summary from the IRT review is provided in Appendix A of this report.

- Summary of Dual Purpose Canister (DPC) Disposal Review - EPRI evaluated the feasibility of direct disposal of Dual Purpose Canisters at Yucca Mountain based on a comparison of repository post-closure performance for a representative DPC design and for the TAD. EPRI concludes that at least some fraction of DPCs would be suitable for direct disposal at Yucca Mountain.

- Summary of Probabilistic Volcanic Hazards Analysis (PVHA) – During 2008, EPRI sponsored an independent expert elicitation to assess the likelihood of a future volcanic event intersecting the proposed Yucca Mountain repository footprint. The objectives for this study were to develop a better understanding of the generation of conceptual models and expert elicitation techniques used in a PVHA, and through the process of elicitation, to develop independent insights into and probability estimates for future igneous events in the Yucca Mountain region (YMR). The results of EPRI's assessment, which considers more recent and extensive geological and structural data obtained since the publication of DOE's 1996 PVHA study, indicate that the annual probability of such an event falls below the regulatory threshold for consideration of 1×10^{-8}.

- Igneous Intrusive Impacts - The objective of this work was to address a number of assumptions that have been made regarding the performance of magma within drifts at the proposed Yucca Mountain repository during the course of an igneous intrusive event. The EPRI studies demonstrated how pulses of magma entering a drift would extend only a limited distance from the point of entry and contact only a small number of waste packages, thus significantly attenuating recent bounding estimates of the effects of igneous intrusion on peak dose rate.

- Constraints on Post-Closure Ground Motion – A preliminary version of a probabilistic seismic hazard (PSH) model for Yucca Mountain (YM) has been recently developed by EPRI. Preliminary post-closure PSH estimates show peak ground acceleration (PGA) and peak ground velocity (PGV) to be around 0.7 to 1.1 g and 80 to 100 cm/sec, respectively, for the 10^6 year return period and 95th percentile level. These values are considerably lower than the PGA and PGV derived from the original YM PSH model for an equivalent return period and percentile level.

- Corrosion Behavior of the Stainless Steel Inner Vessel and TAD Canister of a TAD-bearing Waste Package – EPRI performed an assessment of the corrosion behavior of the stainless steel inner vessel and TAD canister following failure of the outer Alloy 22 corrosion barrier. Following a review of the current specifications for the design of the TAD-bearing WP, the environmental conditions to which the inner vessel and TAD canister will be exposed following WP failure were reviewed. Various forms of corrosion of stainless steel were then considered. Based on this corrosion assessment, the

inner stainless steel components of the WP (i.e., inner vessel + TAD canister) is considered to be capable of providing a significant barrier to water ingress and radionuclide release for a substantial time period (on the order of 50,000 – 500,000 years) following the failure of the outer Alloy 22 vessel.

- Microbiologically Influenced Corrosion (MIC) may affect the long-term integrity of the Engineered Barrier System (EBS) in the Yucca Mountain Repository. As such, the potential for, and extent of, MIC was assessed and suitable models were developed for predicting the long-term behavior of the engineered barriers. It is concluded that microbial effects will not compromise the safety of the overall disposal system.

- Revised Source-Term Model for the Dissolution of Commercial Spent Nuclear Fuel - It is well known that the solubility of the UO_2 matrix of spent fuel under oxidizing conditions (as (U(VI)) is several orders of magnitude higher than that under reducing conditions (as U(IV)). Because of this fact, and because of experimental studies performed under aerobic conditions, there is a perception that commercial spent nuclear fuel (CSNF) will undergo rapid alteration upon exposure to the drift environment in the Yucca Mountain (YM) repository. However, this experimental evidence was obtained under conditions that do not represent the whole range of conditions to which the fuel will be exposed at YM. It was determined that basing estimates of UO_2 dissolution rates on more appropriate conditions will lead to lower long-term, UO_2 dissolution rates.

- Mechanistic Studies of the Crevice Corrosion of Alloy 22 in Chloride-Nitrate Solutions - Crevice corrosion of Alloy 22 is one of a number of potential corrosion processes of interest for the waste packages in the proposed Yucca Mountain repository. However, knowledge about the factors controlling the propagation of crevice corrosion is limited. Conservatively, the DOE have chosen to assume that, once initiated, crevices will continue to propagate at a constant rate. This study performed by EPRI involved preliminary electrochemical and surface analysis of the crevice corrosion of Alloy 22 in chloride solutions at a temperature of $120^{\circ}C$. The current results of these studies indicate that nitrate ions inhibit the propagation of localized attack in addition to inhibiting the initiation of crevice corrosion. This work, in conjunction with the research from DOE and CNWRA, indicates that corrosion crevices will stifle rather than continuing to propagate as assumed by DOE; the exact mechanism behind this stifling process remains undetermined.

In addition to the above topics, during 2008 EPRI also investigated the potential occupational risk consequences resulting from the construction and operation of the proposed repository, the potential for a criticality event in a DPC should these canisters be used for direct placement within the repository and activities related to the eventual transportation of spent nuclear fuel and high level waste to Yucca Mountain from sites around the country.

EPRI personnel and consultants also continued to monitor on-going YM-related regulatory discussions and activities, review YM-related documents issued by all stakeholders, and attend and make presentations at numerous technical, scientific and regulatory meetings and forums addressing YM-related subjects of interest.

EPRI analyses to-date continue to show that, for the scenarios investigated, probability-weighted mean annual doses to a Reasonably Maximally Exposed Individual (RMEI) living downstream of the proposed Yucca Mountain repository will be extremely small. The analyses indicate that the peak RMEI dose will be significantly lower than the levels specified in the recently released EPA regulations across the entire time period of interest, i.e., up to one million years following permanent closure of the repository.

ACKNOWLEDGMENTS

CONTENTS

LIST OF FIGURES

LIST OF TABLES

1
INTRODUCTION

Investigations to determine the suitability of a site at Yucca Mountain (YM), Nevada, to serve as a geologic repository for the disposal of spent nuclear fuel (SNF) and high-level radioactive wastes (HLW) have been underway since the early 1980's. Throughout most of this period, the Electric Power Research Institute (EPRI) has been performing its own independent scientific and technical investigations and reviews to provide a third party perspective on site suitability and project-related scientific and technical issues.

During 2008, the major Yucca Mountain Project-related development was the U.S. Department of Energy's (DOE) completion and submission to the U.S. Nuclear Regulatory Commission (NRC) of a license application (LA) for repository construction. That application was submitted to the NRC for docketing review on June 3, 2008 and accepted by the NRC staff for formal review on September 8, 2008. With this acceptance and initiation of the formal review activities, the Yucca Mountain Project (YMP) has entered into a new and challenging period.

This report provides information to EPRI's members, the NRC, the DOE, independent technical review bodies (e.g., the Nuclear Waste Technical Review Board (NWTRB) and the Advisory Committee on Nuclear Waste and Materials (ACNW&M)), and the public regarding Yucca Mountain related activities performed by EPRI and its consultants during CY 2008. These activities reflect issues of scientific and technical interest and/or contention that have arisen over the past 2-3 years and that EPRI believed warranted further, independent investigation. In addition, this report provides a brief summary of the background of the YMP and the unique regulatory review process that is associated therewith.

The major organizations participating in Yucca Mountain activities are the NRC and its contractor, the Center for Nuclear Waste Regulatory Analyses (CNWRA), and the YMP, which is composed of the DOE, its Management and Operating (M&O) contractor (Bechtel SAIC LLC (BSC)), the Lead Laboratory (Sandia National Laboratory), and other contributing parties including additional National Laboratories and the U.S Geological Service (USGS). During 2008, these organizations focused their activities on the continued resolution of outstanding technical/scientific issues, the preparation and submittal of the LA and its supporting documents, and the planning for and initiation of the formal review of the tendered documents. Significant resources were expended by the YMP towards the completion of the LA and the updating and finalization of Analysis/Model Reports (AMRs) and other documents intended to provide the scientific basis for the LA. These efforts entailed the completion of the preliminary project design and pre-closure risk assessment, the post-closure Total System Performance Assessment (TSPA-LA), and the further population of the Licensing Support Network (LSN), an electronic database of documents that is required by 10 CFR Part 2 and is intended to expedite the public hearing process if and when the NRC staff approves the LA. In addition, the project awaited the promulgation by the U.S. Environmental Protection Agency (EPA) of the final regulations

required to establish the criteria for the licensing of the facility following the remand of previously promulgated standards by the U.S. Court of Appeals in July, 2004 for further consideration of the time period of applicability. The EPA formally issued the applicable standard (40 CFR Part 197) on October 15, 2008, and it became effective November 14, 2008.

During 2008, the EPRI-sponsored work paralleled the activities of the other stakeholders in the effort to ensure that an independent, third party perspective on issues of scientific and technical interest were made publicly available for review by all interested parties. Primary among these efforts were in-depth, independent studies that addressed the following topics:

- During CY 2008, the EPRI team received and addressed the results of an independent assessment of its TSPA code, IMARC, which had been commissioned in 2007. The purpose of that assessment and the associated follow-on activities was to identify and resolve any potential deficiencies in the code and to ensure that it accurately reflects the on-going status of the project. (See Section 5.2)

- Summary of Dual Purpose Canisters (DPC) Review - EPRI evaluated the feasibility of direct disposal of DPCs at Yucca Mountain (See Section 5.3)

- Summary of PVHA Review – A summary of the methods used and results of an EPRI sponsored Probabilistic Volcanic Hazards Analysis (See Section 5.4)

- Igneous Intrusive Impacts– A discussion of the potential performance of magma within the Yucca Mountain repository drifts and the potential impact of the magma on the waste packages stored within the drifts. (See Section 5.5)

- Constraints on Ground Motion - A discussion of the preliminary development of a simplified and updated probabilistic seismic hazard (PSH) model for the proposed YM repository site. (See Section 5.6)

- Corrosion Behavior of the Stainless Steel Inner Vessel and TAD Canister of a TAD-bearing Waste Package – An assessment of how the stainless steel WP inner barrier and TAD canister will perform once the WP outer barrier has been breached. (See Section 5.7)

- An Assessment of the Threat from Microbiologically Influenced Corrosion to the Lifetime of the Engineered Barrier System in the Yucca Mountain Repository - A description of a decision-tree approach used to decide whether MIC is a significant threat to the integrity of the engineered barriers. (See Section 5.8)

- A Revised EPRI Source-Term Model for the Dissolution of Commercial Spent Nuclear Fuel – The development of a new model describing the manner in which Commercial Spent Nuclear Fuel (CSNF) would degrade following failure of the engineered barriers and access to the repository environment. (See Section 5.9)

- Mechanistic Studies of the Crevice Corrosion of Alloy 22 in Chloride-Nitrate Solutions – A study of the factors controlling the propagation of crevice corrosion in Alloy 22. (See Section 5.10)

- Transportation – A description of EPRI's activities during 2008 related to the transportation of CSNF to the YM repository. (See Section 5.14)

The EPRI team also investigated the potential occupational risk consequences resulting from the construction and operation of the proposed repository (See Section 5.12) and the potential for a criticality event in a DPC should these canisters be used for direct placement within the repository (See Section 5.13).

In addition, the EPRI team reviewed project-related documents, identified issues of potential interest to and contention within the technical and scientific communities, and developed numerous scientific and technical papers for presentation at HLW-related meetings and forums. (See Section 5.15)

EPRI analyses to-date continue to show that, for the scenarios investigated, probability-weighted mean annual doses to a Reasonably Maximally Exposed Individual (RMEI) living downstream of the proposed Yucca Mountain repository will be extremely small. EPRI analyses continue to demonstrate that the risks to the public associated with the transport of SNF and other radioactive material to the Yucca Mountain site will also be extremely small.

2
BACKGROUND

2.1 Summary of Legislation Leading to the Designation of Yucca Mountain

The Nuclear Waste Policy Act (NWPA) of 1982 (as amended) established the course for the siting, characterization, and licensing a deep geologic repository for permanent disposal of CSNF and HLW at Yucca Mountain, Nevada. The NWPA also established the separate roles for the EPA for environmental standard setting, and the NRC for independent review, oversight, and licensing of DOE for the construction and operation of the YM repository. NRC is also responsible for the implementation of the EPA's siting criteria and reviewing and approving any application for a repository license.

The NWPA also established a rigorous path for the regulatory review and licensing of a geologic repository site. That path includes a multiple part licensing process to assure that the repository, if determined suitable, would be constructed, operated, and permanently closed in a manner that would ensure the protection of public health and safety.

2.2 Establishment of Regulations and Requirements

As discussed above, the NWPA directed the EPA to establish the primary regulatory limits to ensure the protection of the health and safety of the public. In addition, the NRC was directed to implement those requirements and ensure that any application demonstrates compliance with the established regulatory criteria. The final EPA standard issued in October 2008, 40 CFR 197 (EPA, 2008), is based on input from the National Academy of Sciences (NAS) Technical Bases for Yucca Mountain Standards (TYMS) report and an extensive, seven year revision process following a successful court challenge to one of the provisions, (i.e., the establishment of the regulatory period of interest) in the original 2001 version of the regulation. At the time of preparation of this report, the conforming NRC regulation (10 CFR 63) implementing the EPA standard had not been issued.

Among other things, the final EPA standard:

- maintains a 15 mrem/year limit for doses that could be received by the Reasonably Maximally Exposed Individual (RMEI) during the first 10,000 years (as originally proposed in the 2001 regulation) and establishes a 100 mrem/year standard for the period from 10,000 to 1 million years;

- directs the NRC to use the arithmetic mean of the distribution of projected doses to determine compliance with both the 150 μSv/yr (15 mrem/yr) dose standard applicable

for the first 10,000 years after closure and the 1 mSv/yr (100 mrem/yr) peak dose standard applicable between 10,000 and 1 million years after closure;

- retains §197.36 as originally proposed, with two modifications. First, the probability threshold for Features, Events and Processes (FEPs) to be considered for inclusion in performance assessments conducted to show compliance with § 197.20(a)(1) is now stated as an annual probability of 1 in 100 million (1 x 10^{-8} per year). Because the same FEPs included in these performance assessments will also be included in performance assessments conducted to show compliance with § 197.20(a)(2), the same probability threshold applies in all cases;

- adds a provision to address a potential effect of seismicity on hydrology that was identified by NAS. The final rule now requires the potential effects of a rise in the ground-water table as a result of seismicity to be considered. If NRC determines such effects to be significant to the results of the performance assessment, it shall specify the extent of the rise for DOE to assess; and

- retains the previous provision related to climate change allowing NRC to characterize climate change beyond 10,000 years using constant conditions.

The final EPA standard also:

- indicates that DOE's analysis must include all potential pathways of radionuclide transport and exposure"; (63.311)

- establishes thee characteristics of the Reasonably Maximally Exposed Individual (RMEI) as a hypothetical person who is located on the site boundary and who meets certain other specified criteria; (63.312)

- establishes the permissible concentration limits for radionuclides in the groundwater exiting the site boundary;

- mandates that there shall be a multi-part regulatory period of interest for the repository extending up to one million years;

- directs that any assessment of the safety aspects of the proposed repository should be probability based; and

- establishes that the repository should include multiple natural and engineered barriers to ensure compliance with the applicable regulations.

Licensing of the geologic repository involves consideration of activities during two distinct time periods:

- The "pre-closure period," extending from the initiation of construction through the period in which the SNF and HLW is received at the Yucca Mountain site by the DOE and

eventually emplaced within the repository. The pre-closure period ends with the permanent closure of the repository; and

- The "post-closure" period following permanent closure of the repository.

As required by the regulations, risk-based performance assessments, a Pre-closure Safety Assessment (PCSA) for the pre-closure period, and a Total System Performance Assessment (TSPA) for the post-closure period, have been developed by the DOE for the activities to be conducted during both time periods. The risk estimates used in the respective assessments are based on the results of the scientific investigations conducted as part of the site characterization efforts or on demonstrated performance of equipment and/or material.

The risk-based performance assessments: (1) identify potentially relevant "features, events, and processes" (FEPs) and event sequences; (2) establish the probability of occurrence of the FEPs or events; (3) estimate the resulting consequences of the reasonably probable FEPs and events should they occur; and (4) evaluate the ability to meet established performance objectives. These requirements were established in the original version of 10 CFR Part 63 and are reiterated (with additional details) in the Yucca Mountain Review Plan (NUREG 1804), the NRC document intended to serve as a guide for the DOE in the preparation of its application and to facilitate the review by the NRC staff of any license application (LA) tendered by the DOE.

2.3   The Regulatory Review Process

The DOE's license application to construct the repository at Yucca Mountain was submitted to the USNRC on June 3, 2008 and was accepted for docketing (i.e., formal review) by the NRC staff on September 8, 2008. This acceptance initiates an extended, multi-part review period and heralds a new phase for the Yucca Mountain Project in which the progress of the project, as well as the identification and resolution of issues of technical and scientific interest, is controlled by the regulators [i.e., the NRC staff and Atomic Safety and Licensing Board (ASLB) Panels] rather than the DOE. This Licensing Phase succeeds the Site Characterization, Site Certification and Pre-Licensing phases that preceded it.

The NRC staff review of the License Application will culminate with the issuance of a Staff Safety Evaluation Report (SSER) detailing the staff's findings. If the staff recommends that the "Construction Authorization" license be granted, the Staff Safety Evaluation Report (SSER), along with the amended License Application, will then serve as the basis for the adjudicatory hearings to be held by one or more Atomic Safety and Licensing Board (ASLB) panels.[1] Parties to these proceedings will be admitted by the ASLB panel(s) based upon the potential impact of the project on their interests and well-being.

---

[1] Traditionally, a single, three person ASLB panel is assigned to each application. However, given the breadth and scope of the issues surrounding the licensing of a repository and the time limitations for licensing activities mandated by the NWPA, there are indications that more than one ASLB panel will be assigned to the Yucca Mountain docket and each panel may consist of more than three members.

2.4   The Public Hearing Process

The public hearing process is the second phase of the NRC review process of an application to build a repository at Yucca Mountain. The hearings will be held by one or more Atomic Safety and Licensing Boards appointed by the NRC. As the Nuclear Waste Policy Act of 1982 (as amended) mandated that the regulatory review of any application to build a repository must be conducted within a 36 month period (with the potential for a single 12 month extension), the model schedule contained in NRC regulations for YM licensing shows hearings extending over a period of three months with the obvious potential for extensions due to appeals and agreements among the parties and the ASLBs. All activities associated with the public hearing process will be conducted in accordance with the regulations contained in 10 CFR Part 2. Parties to the hearings will be, as a minimum, the applicant (DOE), the NRC staff, the State of Nevada, affected Native American tribes, and affected local governments. Other entities, such as the nuclear power industry, may be admitted as parties upon a showing that they have a vested interest in the activities to be conducted. Various issues (i.e., "contentions") may be raised by the various parties and, if accepted by the ASLB(s), will serve as the basis for the hearings and the participation of additional parties.

Once the actual administrative hearings are held, each admitted party to the process may put forth expert witnesses whose testimony will support their respective positions and counsel for all parties will have the right to cross-examine witnesses from the other parties. Any of the parties involved in the hearing process may choose to enter the information and conclusions contained within previously issued EPRI reports into the record to the extent that they deem appropriate.

Upon completion of the hearings, the Hearing Board(s) will render its/their decision regarding the issues that were in contention and the overall acceptability of the proposed repository. Following the decision by the ASLB, the NRC Commissioners may review and approve the ASLB's decision or set aside that decision and assume responsibility for approval or disapproval of the application.

2.5   References

EPA, 2001. 40 CFR 197. *Public Health and Environmental Protection Standards for Yucca Mountain, Nevada: Final Rule*, Volume 66, Number 114, pp 32074 – 32135, June 13, 2001.

EPA, 2005. 40 CFR 197. *Public Health and Environmental Protection Standards for Yucca Mountain, Nevada: Proposed Rule*, Volume 70 Federal Register, Number 161, pp 49104 – 49065, August 22, 2005.

EPA, 2008. 40 CFR 197. *Public Health and Environmental Protection Standards for Yucca Mountain, Nevada: Final Rule*, Volume 73 Federal Register, Number 200, pp 61256 – 61289, October 15, 2008.

EPRI, 2005. *Yucca Mountain Licensing Standard Options for Very Long Time Frames, Technical Bases for the Standard and Compliance Assessments*, Electric Power Research Institute, Palo Alto, CA: 2005. 1011754.

NAS (National Academy of Sciences), 1995. *Committee on Technical Bases for Yucca Mountain Standards, Technical Bases for Yucca Mountain Standards* (TYMS). National Research Council, National Academy Press, Washington, D.C. 1995

NRC, 2002. 10 CFR Part 63, *Disposal of High-Level Radioactive Wastes in a Geologic Repository at Yucca Mountain, Nevada*. November 2001.

NRC, 2003. *Yucca Mountain Review Plan*. Revision 2, NUREG 1804, U.S. Nuclear Regulatory Commission, Washington, D.C., July 2003.

NRC, 2005. 10 CFR Part 63. *Implementation of a Dose Standard After 10,000 Years: Proposed Rule*, SECY – 05-0144, U.S. Nuclear Regulatory Commission, Washington, D.C., August 10, 2005.

3

YUCCA MOUNTAIN PROJECT ACTIVITIES DURING 2008

To date, the Yucca Mountain Project has gone through four distinct phases. In Phase 1 (1982-1987), the DOE was investigating multiple sites within the continental US in an attempt to determine which would be the best candidate for a repository for spent nuclear fuel and high-level radioactive waste. In Phase 2 (1987-2002), DOE focused its efforts on characterization activities related to the Yucca Mountain site and region. The Site Characterization phase was completed in February, 2002 when the Secretary of Energy made a recommendation to the President that a repository could be built at Yucca Mountain. That recommendation was subsequently submitted to and approved by Congress as was required by the NWPA. In Phase 3 (2002 – 2008), the DOE completed its investigations of the Yucca Mountain site and undertook the development of a License Application to be submitted to the US NRC. Phase 3 effectively ended when the LA was submitted to the NRC for a docketing review on June 3, 2008. Phase 4 (September, 2008 to the present) will involve the regulatory review of the LA by the NRC staff and its consultants followed by public hearings to be conducted by one or more Atomic and Safety Licensing Boards (ASLBs).

The primary focus of activities conducted by the Yucca Mountain Project (YMP: DOE, its Management and Operations (M&O) contractor, BSC, and Sandia National Laboratory, the "Lead Laboratory") during 2008 was on:

- The preparation of the construction License Application and revision and updating of the supporting documents (i.e., Analysis/Model Reports) associated therewith;
- Finalizing the risk-based Preclosure Safety Analysis (PCSA) and the Total System Performance Analysis (TSPA) required to support the LA;
- Awaiting information on and determining how to respond to revised EPA and NRC regulatory standards;
- Completion of the preliminary project design intended to serve as the basis for the License Application;
- Issuance of a Final supplement to the 2002 Environmental Impact Statement (FSEIS) incorporating and addressing the latest changes in the design of the project and updating information on the transportation of SNF and HLW to the YM site;
- Issuance of a Supplemental EIS (SEIS) addressing the selection and implementation of transportation routes for movement of the radioactive material to Yucca Mountain;
- Continued implementation of and populating the Licensing Support Network (LSN); and
- Development of a conceptual design for the Transportation, Aging and Disposal (TAD) canisters to be used for the transfer of SNF from the nuclear plant sites to Yucca Mountain.

Over 120 Analysis/Model Reports (AMRs) were originally developed by DOE to document the results of the site characterization activities and other technical/scientific investigations that have been conducted through the years by the DOE on Yucca Mountain-related subjects. It is anticipated that approximately 90 of these documents will serve as the primary basis for the post-closure compliance assessment in the LA. Since their initial development, DOE has continued to update and upgrade many of these documents, especially those that have been identified as the key supporting documents to the LA. The most recent versions of these documents are posted on the LSN.

Establishing a design for the surface and subsurface facilities is a prerequisite for the submission of any License Application. The introduction in early 2006 of the Transportation, Aging and Disposal (TAD) canister concept in which the spent fuel will be loaded into specially designed canisters at the various reactor sites and then moved to Yucca Mountain where they will be loaded directly into the permanent storage waste packages affected the design and operation of the pre-closure facilities. Throughout 2008, the Project funded some of the dry cask storage and transportation cask vendors to further develop TAD designs and the operational details associated with their use. To date, only limited detailed information on this concept has been made publicly available by the DOE. The Project also completed the general design of surface facilities required for their handling at the Yucca Mountain site.

During 2008, activities related to the potential transportation of nuclear waste to Yucca Mountain from existing sites around the country continued as well. However, progress in this area was relatively limited as the transportation activities slowed consistent with a stretch out of the project schedule that now foresees the storage of the first waste in 2017 (or later if required funding is not made available). It can be expected that these activities will accelerate when the licensing activities associated with the repository proceed.

In October, 2007, the Department of Energy released for public comment and review the Draft Supplemental Environmental Impact Statement for a Geologic Repository for the Disposal of Spent Nuclear Fuel and High-Level Radioactive Waste at Yucca Mountain, Nye County, Nevada – Nevada Rail Transportation Corridor and Draft Environmental Impact Statement for a Rail Alignment for the Construction and Operation of a Railroad in Nevada to a Geologic Repository at Yucca Mountain, Nye County, Nevada (DOE/EIS-0250F-S2D and DOE/EIS-0369D) (Draft Nevada Rail Corridor SEIS and Draft Rail Alignment EIS). The FSEIS and rail corridor FEIS were submitted to the NRC along with DOE's license application for the Yucca Mountain repository in June 2008 and were docketed along with the LA in September, 2008.

4
EPRI'S ROLE IN YUCCA MOUNTAIN ISSUES

4.1 Background

Besides the obvious interest on the part of the nuclear power generation industry in the Yucca Mountain Project as a location to dispose of spent nuclear fuel, the industry also has a significant interest in the manner in which funds provided by the Nuclear Waste Fund (NWF) are being spent. The NWPA (at Section 111 (b) (4)) indicated that one of the primary purposes of the Act was:

> "to establish a Nuclear Waste Fund composed of payments made by the generators and owners of such waste and spent fuel, that will ensure that the costs of carrying out activities relating to the disposal of such waste and spent fuel will be borne by the persons responsible for generating such waste and spent fuel."

Since the late-1980's, the electric power utilities with nuclear power plants have been collecting a 1 mil/kW-hr tax on nuclear generation from their customers, the ratepayers. This tax translates into more than $700 million per year that is deposited in the NWF for activities associated with the development of the repository and associated transportation activities. To date, in excess of $19.5B has been placed in NWF. Owing to these interests, EPRI has provided an independent perspective on technical and scientific issues that could impact the progress of the project and, in turn, the expenditure of funds from the NWF.

EPRI has been performing Yucca Mountain-related tasks and monitoring the activities of the overall Yucca Mountain Project for almost 20 years. The overall goal of EPRI's Yucca Mountain Project-related activities have been to focus on (1) providing independent (i.e., from a party not prospectively involved in the eventual licensing proceedings) technical information and analyses addressing Yucca Mountain-related technical and scientific subjects of potential interest, including the technical basis for the safe transport of spent fuel to the repository; (2) establishing the technical basis for resolving generic spent fuel storage and transportation issues impacting nuclear plant operability (i.e., loss of full core discharge capabilities), license extension of independent spent fuel storage installations (i.e., dry storage beyond 20 years), and timely decommissioning; and (3) assessing the impacts of various advanced fuel cycle schemes on spent fuel and HLW management efficiency.

In keeping with those objectives, EPRI has provided:

- An independent perspective on the characteristics of the Yucca Mountain site and the surrounding region;

- Additional insights into the safety basis for the evolving design of a repository at Yucca Mountain;

- Additional insights on issues related to the transportation of SNF to Yucca Mountain; and

- Additional Yucca Mountain-related data via sponsored analyses and experiments.

Through these activities, EPRI has endeavored to ensure that adequate information developed from an independent perspective exists to support a risk-informed resolution of important Yucca Mountain Project-related technical and scientific issues.

4.2 Post-closure Analytical Philosophy

The performance of the proposed Yucca Mountain repository and the ability to comply with established regulatory criteria are dependent upon a combination of natural and engineered barriers. The Natural Barrier System consists of:

- The unsaturated zone (UZ) above the repository horizon that acts to damp pulses of rainwater entering deep into the mountain and, to a more limited extent, divert some groundwater away from the repository;

- The UZ below the repository that limits the transport of any radionuclides that may be released from the repository via slow flow pathways and sorption; and

- The saturated zone (SZ) downstream of the repository that also limits transport of radionuclides via slow flow and sorption,

The Engineered Barrier System (EBS) is comprised of:

- The waste package, which is designed to contain the radioactive waste forms for extended periods of time;

- The drip shield, which is designed to divert any moisture entering the repository away from the waste package, thereby reducing the likelihood of corrosion and extending the waste package lifetime and limiting release of radionuclides;

- The spent fuel cladding, which can significantly delay the time at which water can contact the waste form once the waste package has failed, and

- The waste form itself.

The combined performance of the natural and engineered barriers is intended to ensure compliance with the applicable regulatory limits.

The analyses performed by EPRI, including those discussed in this report, have, in great part, addressed the capability of the various natural and engineered barriers to perform their required function. Many of EPRI's analyses have resulted in conclusions that demonstrate significantly greater margins between the calculated values and the previously proposed regulatory limits than comparable analyses performed by the YMP and/or the NRC and its contractor. The basic reason for this is that the EPRI team has followed the philosophy that it is appropriate to use more realistic ("cautious but reasonable") data and assumptions rather than using extremely conservative assumptions, such as those often used by the DOE and NRC. EPRI's IMARC code is the only TSPA that has implemented this philosophy, the use and implications of which are discussed in greater detail below.

The EPA's regulation 40 CFR 197 (EPA, 2001, 2008) indicates that the standards to be applied to an application for a license to construct the repository should be based on the concept of "reasonable expectation" and that this concept is intended to be "cautiously realistic." This latter phrase is similar to the phrase "cautious but reasonable" that was used by the National Academy of Sciences (NAS) TYMS Committee (NAS, 1995) and by the International Committee on Radiation Protection (ICRP) in various reports and standards to describe the type of assumptions that should be made to support available technical information related to any assessment of the suitability of a geologic repository site. This approach is different than that followed by the DOE and NRC in that the latter organizations have often chosen to use multiple, conservative assumptions when performing their analyses.

The use of multiple conservative assumptions often leads to results that have limited physical meaning. Use of conservatisms introduces biases into the analyses that will likely cause some components of the system to appear more or less important than they would otherwise. Furthermore, use of conservative assumptions and values makes the Yucca Mountain system appear to perform worse than it would using a more "cautious but reasonable" approach. EPRI is of the opinion that the use of the "cautious but reasonable" approach is not only consistent with the philosophy supported by the TYMS committee but would also result in a more realistic portrayal of the potential performance of the repository if the methodology and philosophy were followed by all parties.

As a result, EPRI has attempted to maintain this "cautious but reasonable" approach in its independent analyses, wherever possible, specifically to provide an independent, alternative and more realistic perspective. For example, although DOE analyses indicate that the radiological dose risk to the public associated with the transport of radioactive material to Yucca Mountain is extremely small, EPRI analyses (using more "cautious but reasonable" assumptions) have indicated that the dose risk will be a fraction of that estimated by the DOE.

4.3 Summary of EPRI 2008 Yucca Mountain-Related Activities

Primary among EPRI's Yucca Mountain-related tasks through the years has been the development of the Integrated Multiple Assumptions and Release Code (IMARC) TSPA model to probabilistically evaluate the anticipated performance of the Yucca Mountain repository. As the use of TSPA is paramount in evaluating the long-term performance of the repository, the development of an independent model and code has served to provide an important alternative method for checking the assumptions used by and results associated with both the NRC's and the DOE's performance assessment efforts. The IMARC code, now in its ninth revision (and soon to be in the tenth), is intended to calculate probability-weighted mean doses to the reasonably maximally exposed individual (RMEI) in the vicinity of the Yucca Mountain site. This is the performance objective for the repository established by 10 CFR Part 63 as it was originally issued.

In 2007, EPRI commissioned an independent peer review of IMARC to obtain an unbiased perspective regarding the performance of the IMARC code. The results of that review, the full Independent Review Team (IRT) report, will be published in 2009. Based on the comments and suggestions received from the International Review Team, along with the incorporation of revised models and data provided by EPRI's IMARC team, EPRI is in the process of revising the

interim IMARC version 9 to version 10. A comprehensive report that both updates and consolidates all components of IMARC 10 will be published concurrently with the IRT report in early 2009 and will include the EPRI response to the IRT review. Status of the IMARC TSPA code, the IRT report, and related EPRI's ongoing activities is provided in Section 5.2. An advanced copy of the executive summary from the IRT review is provided in Appendix A of this report.

In addition to the IMARC-related activities, EPRI has commissioned and managed the performance of numerous scientific and technical evaluations of and investigations into issues considered to have the potential to have a significant impact on the Yucca Mountain Project. Primary EPRI projects during 2008 included:

Summary of Dual Purpose Canister Disposal Review – DOE has adopted an approach to disposal of CSNF at Yucca Mountain that calls for the repackaging of all spent nuclear fuel into standardized transportation, aging, and disposal (TAD) canisters. However, a substantial inventory of spent nuclear fuel is already safely packaged in dual-purpose canisters (DPCs) at the reactor sites. In 2008, EPRI evaluated the feasibility of direct disposal of DPCs at Yucca Mountain based on a comparison of repository post-closure performance for a representative DPC design and for the TAD and found only minor differences between the two. EPRI therefore concludes that direct disposal of DPCs is feasible on technical grounds and that at least some fraction of DPCs would be suitable for direct disposal at Yucca Mountain. A more detailed description of these activities is provided in Section 5.3.

Summary of Probabilistic Volcanic Hazards Analysis (PVHA) – During 2008, EPRI sponsored an independent expert elicitation to assess the likelihood of a future volcanic event intersecting the proposed Yucca Mountain repository footprint. The objectives for this study were to develop a better understanding of the generation of conceptual models and expert elicitation techniques used in a PVHA, and through the process of elicitation, to develop independent insights into and probability estimates for future igneous events in the Yucca Mountain region (YMR). EPRI's assessment of the likelihood of a future volcanic event intersecting the Yucca Mountain repository footprint considers more recent and extensive geological and structural data obtained since the publication of DOE's 1996 PVHA study and the knowledge gained from this analysis can be used to better understand the results from the DOE sponsored PVHA activities and to independently evaluate repository performance. The results from EPRI's independent PVHA indicate that the probability of an igneous event intersecting the repository footprint within the 1 million year compliance period is significantly below the 10^{-8} per year threshold for considering consequences of such an event in performance assessments. A more detailed description of these activities is provided in Section 5.4.

Igneous Intrusion Impacts – The objective of this work was to address a number of assumptions that have been made regarding the performance of magma within drifts at the proposed Yucca Mountain repository during the course of an igneous intrusive event. More specifically, this study addressed whether: (1) all drifts will rapidly fill with magma following an intersection of a dike with a drift; (2) all waste packages in drifts will be engulfed in magma; and (3) the waste packages contacted by magma will be damaged and fail, providing no protection for the stored spent nuclear fuel and high level radioactive waste from groundwater. The EPRI studies demonstrated how pulses of magma entering a drift would extend only a limited distance from the point of entry and contact only a small number of waste packages, thus significantly

attenuating recent bounding estimates of the effects of igneous intrusion on peak dose rate. A more detailed description of these activities is provided in Section 5.5.

Constraints on Post-closure Ground Motion – A preliminary version of a probabilistic seismic hazard (PSH) model for Yucca Mountain (YM) has recently been developed by EPRI. The model has been implemented within the publicly-available OpenSHA framework (www.opensha.org). An important feature of the new PSH model is that the source model has been greatly simplified from that of the original YM PSH model, and can therefore be readily interrogated. The source model comprises the eight most active faults in the surrounding region, and one "area source" within which uniformly-distributed background seismicity parameters are defined. A simple logic tree is constructed to quantify epistemic uncertainties in the fault parameters (seismic moment rate, maximum magnitude) and in the background seismicity parameters (a-value, b-value and cutoff maximum magnitude). Implementation of the model in OpenSHA also allows the PSH model to incorporate a range of attenuation models, in particular the Next Generation Attenuation (NGA) models. Preliminary post-closure PSH estimates show peak ground acceleration (PGA) and peak ground velocity (PGV) to be around 0.7 to 1.1 g and 80 to 100 cm/sec, respectively, for the 10^6 year return period and 95th percentile level. These values are considerably lower than the PGA and PGV derived from the original YM PSH model for an equivalent return period and percentile level. A more detailed description of these activities is provided in Section 5.6.

Corrosion Behavior of the Stainless Steel Inner Vessel and TAD Canister of a TAD-bearing Waste Package – During 2008, EPRI performed an assessment of the corrosion behavior of the stainless steel inner vessel and TAD canister following failure of the outer Alloy 22 corrosion barrier. Following a review of the current specifications for the design of the TAD-bearing WP, the environmental conditions to which the inner vessel and TAD canister will be exposed following WP failure were reviewed. Various forms of corrosion of stainless steel were then considered including: atmospheric corrosion, general corrosion (GC), localized corrosion (LC) in the form of pitting and crevice corrosion, stress corrosion cracking (SCC), and microbiologically influenced corrosion (MIC). Based on this corrosion assessment, the potential lifetime of the stainless steel components inside a TAD-bearing WP (i.e., the stainless steel WP inner cylinder and the TAD) was addressed. A more detailed description of these activities is provided in Section 5.7.

Microbiologically Influenced Corrosion (MIC) – Microbial activity is a potential threat to the long-term integrity of the Engineered Barrier System in the Yucca Mountain Repository. As such, the potential for, and extent of, MIC must be assessed and suitable models developed for predicting the long-term behavior of the engineered barriers. There are two broad approaches to assessing the threat posed by MIC; first, to determine whether the environment will support microbial activity and, if so, where and when it will occur, and second, to estimate the maximum amount of damage that could occur if microbial activity in the repository is possible.

A decision-tree approach was used by EPRI to present evidence for both of these approaches and to decide whether MIC is a significant threat to the integrity of the engineered barriers. It was concluded that microbial effects will not compromise the safety of the overall disposal system because they will not lead to either early waste package (WP) failures or to a large number of simultaneous failures, both factors that can lead to an increase in the peak dose. A more detailed description of these activities is provided in Section 5.8.

Revised Source-Term Model for the Dissolution of Commercial Spent Nuclear Fuel – It is well known that the solubility of the UO_2 matrix of spent fuel under oxidizing conditions (as (U(VI)) is several orders of magnitude higher than that under reducing conditions (as U(IV)). This fact and the results from a number of experimental studies performed under aerobic conditions has led to the perception that commercial spent nuclear fuel (CSNF) will undergo rapid alteration upon exposure to the drift environment in the Yucca Mountain (YM) repository. However, this experimental evidence was obtained under conditions that do not represent the whole range of conditions to which the fuel will be exposed at YM. For example, the drip tests performed at the Argonne National Laboratory were conducted using used fuel samples with relatively short post-irradiation decay times such that significant β and γ-radiation fields existed. Except for CSNF in any waste package (WP) that is initially defective, the β and γ fields will have decayed to negligible levels long before the WP has failed, with atmospheric O_2 and, depending upon the time of container failure, the oxidizing radiolysis products of α-radiation, as the only oxidants to support dissolution of the spent fuel. Beta and γ-radiation have a significant effect on the dissolution behavior of spent fuel due to the polarization of the electrochemical corrosion potential (ECORR). Basing estimates of UO_2 dissolution rate on data obtained under high β and γ fields will likely lead to conservatively high estimates of actual long-term, UO_2 dissolution rates. A more detailed description of these activities is provided in Section 5.9.

Mechanistic Studies of the Crevice Corrosion of Alloy 22 in Chloride-Nitrate Solutions – Crevice corrosion of Alloy 22 is one of a number of potential corrosion processes of interest for the waste packages in the proposed Yucca Mountain repository. However, knowledge about the factors controlling the propagation of crevice corrosion is limited. Conservatively, the DOE have chosen to assume that, once initiated, crevices will continue to propagate at a constant rate. A study performed by EPRI during 2008 involved preliminary electrochemical and surface analysis of the crevice corrosion of Alloy 22 in chloride solutions at a temperature of $120^{\circ}C$. A coupled electrochemical technique has been used to follow the propagation of crevice corrosion following artificial initiation achieved by applying a constant current to the creviced sample. Experiments have been conducted in $CaCl_2$-$NaNO_3$ mixtures with different total salinities and NO_3^-:Cl^- ratios and in 5 mol·dm^{-3} NaCl solution with and without the addition of $NaNO_3$. A limited amount of surface analysis has been conducted on the crevice samples following the test. The current results indicate that, as well as inhibiting the initiation of crevice corrosion, nitrate ions also inhibit the propagation of localized attack, although the mechanism by which they do so is not understood at present. A more detailed description of these activities is presented in Section 5.10.

Transportation Activities – During 2008, EPRI continued to follow activities associated with the potential transportation of spent nuclear fuel and high-level radioactive wastes from their existing locations around the country to the Yucca Mountain repository. Key activities in this area included the performance of a review of a Final Supplemental Environmental Impact Statement (FSEIS) for the Yucca Mountain repository and a companion EIS on the Nevada Rail corridor (Rail FEIS) (DOE 2008a, DOE 2008b) that was issued by the DOE in June, 2008. EPRI's review of the FEIS and Rail FEIS was intended to determine what changes, if any, were made to the incident-free and accident risk analysis associated with the transport of SNF to Yucca Mountain. It was found that the analyses that were performed were generally consistent with those contained in the draft 2007 EIS documents that had been previously reviewed. A more detailed description of these activities is provided in Section 5.14.

<u>Other Activities</u> – In addition to the above topics, during 2008 EPRI also conducted a comparison of the results of IMARC 9 with the TSPA developed by DOE as part of the License Application (TSPA-LA), and investigated the potential occupational risk consequences resulting from the construction and operation of the proposed repository, and the potential for a criticality event in a DPC should these canisters be used for direct placement within the repository. More details on these projects are provided in Sections 5.11, 5.12 and 5.13 respectively.

EPRI personnel and consultants also continued to monitor on-going YM-related regulatory discussions and activities, to review YM-related documents issued by all stakeholders and to attend and make presentations at numerous technical, scientific and regulatory meetings and forums addressing YM-related subjects of interest. A list of presentations made and technical/scientific papers submitted during 2008 by the EPRI HLW project team is provided in Section 5.15.

4.4   References

DOE, 2008a, *Final Supplemental Environmental Impact Statement for a Geologic Repository for the Disposal of Spent Nuclear Fuel and High-Level Radioactive Waste at Yucca Mountain, Nye County, Nevada* (DOE/EIS-0250F-S1), U.S. DOE, Office of Civilian Radioactive Waste Management, June 2008.

DOE, 2008b, *Final Supplemental Environmental Impact Statement for a Geologic Repository for the Disposal of Spent Nuclear Fuel and High-Level Radioactive Waste at Yucca Mountain, Nye County, Nevada – Nevada Rail Transportation Corridor and Final Environmental Impact Statement for a Rail Alignment for the Construction and Operation of a Railroad in Nevada to a Geologic Repository at Yucca Mountain, Nye County, Nevada* (DOE/EIS-0250F-S2 and DOE/EIS-0369), U.S. DOE, Office of Civilian Radioactive Waste Management, June 2008.

EPA, 2001. *40 CFR 197. Public Health and Environmental Protection Standards for Yucca Mountain, Nevada: Final Rule*, Volume 66, Number 114, pp 32074 – 32135, June 13, 2001.

EPA, 2008. *40 CFR 197. Public Health and Environmental Protection Standards for Yucca Mountain, Nevada: Final Rule*, Volume 73 Federal Register, Number 200, pp 61256 – 61289, October 15, 2008.

NAS (National Academy of Sciences), 1995. *Committee on Technical Bases for Yucca Mountain Standards, Technical Bases for Yucca Mountain Standards* (TYMS). National Research Council, National Academy Press, Washington, D.C. 1995.

5
EPRI ACTIVITIES DURING 2008

5.1   Introduction

Throughout its many years of involvement with the Yucca Mountain Project, EPRI activities have focused on the technical and scientific investigations necessary to characterize the site, provide an adequate technical basis for Yucca Mountain regulations, develop approaches to evaluating the ability of the repository system to limit release and transport of radionuclides from the repository to the biosphere, evaluate conservatisms in the YMP pre-closure safety analyses, and follow transportation-related YMP developments. In 2008, EPRI addressed a number of issues that were believed to have the potential to impact repository performance or the quantitative assessment of that performance. The areas of primary EPRI involvement during 2008 and the results of those activities are discussed in detail in the following sections.

5.2   IMARC Status Report

5.2.1 Discussion

In 2007 EPRI commissioned an independent peer review by a team of international experts of EPRI's IMARC 9 code (EPRI 2006) for total system performance assessment (TSPA). This International Review Team (IRT) conducted its review following the guidelines and protocols of the International Atomic Energy Agency's (IAEA's) Improvements on Safety Assessment Methodology (ISAM) (IAEA, 2004). This ISAM methodology was adopted as a review framework to ensure a systematic review of the IMARC 9 draft report, as well as to conform to international standards. A paper on the IRT review was presented by one of the IRT members at the 12th International High-level Radioactive Waste Management Conference, September 7-11, 2008 in Las Vegas, Nevada (Garisto, Bennett and Andersson, 2008). The conclusions of the IRT review are briefly summarized below. An advanced copy of the IRT report Executive Summary is provided in Appendix A. A separate EPRI report detailing the findings of the IRT review will be published in the first quarter of 2009.

The IRT found that the IMARC 9 code provides an integrated presentation of the total repository system and captures the main processes and their interactions for a repository located at Yucca Mountain, Nevada. The IRT concurs that IMARC 9 is "fit for purpose" in the sense that it provides a risk-based methodology for integrating information from various disciplines affecting long-term repository performance. The IRT found that the models and databases in the IMARC 9 code conformed to performance analyses that are consistent with a "reasonable expectation" approach as presented in the US EPA's then-existing 40 CFR Part 197 safety standard for a repository at Yucca Mountain (EPA, 2001). The same approach is included in the final standard

that was issued after the IRT completed its review (EPA, 2008). IMARC 9 was judged to be a well-integrated performance assessment tool, which focuses on those processes that could affect the long-term safety and regulatory compliance of a repository located at Yucca Mountain.

Several opportunities for expanding and refining the capabilities of the IMARC 9 code were also identified in the IRT review. The IRT recommended, for example, that EPRI continue to move away from remaining conservative assumptions whenever possible, towards more scientifically credible and realistic assumptions, to help identify and prioritize risk-sensitive processes. In particular, conducting additional sensitivity analyses using IMARC 9 was urged as an approach to improve confidence in the model. The IRT also strongly supported ongoing verification and code inter-comparisons to gain additional insights into the various assumptions and modeling approaches and for enhancing the scientific credibility of the model. Most of the recommendations from the IRT review related to documentation. The IRT identified a number of areas in which the documentation of the model could be improved and suggested several graphical ways to improve and clarify the capabilities of the IMARC 9 code.

EPRI is now in the process of updating the IMARC code (IMARC 10) in response to the recommendations of the IRT review, the latest progress in the Yucca Mountain program, and advances in EPRI's own independent program. As discussed elsewhere in this report, the Yucca Mountain Project submitted a license application LA to the NRC for construction of the proposed Yucca Mountain repository on June 3, 2008, which was subsequently accepted for formal review in September 2008 following a docketing review. DOE's LA includes a significant update of the supporting repository Total System Performance Assessment (TSPA)(OCRWM, 2008). The new version of IMARC will reflect the latest information and data presented in the LA, as well as information derived from independent EPRI studies.

EPRI intends to publish its revised IMARC 10 model report, along with response to the IRT review as a combined report in the first quarter of 2009. The IRT review and the IMARC 10 update (with EPRI response to IRT review) will be released concurrently as separate EPRI reports.

5.2.2 References

EPA, 2001. 40 CFR 197. *Public Health and Environmental Protection Standards for Yucca Mountain, Nevada: Final Rule*, Volume 66, Number 114, pp 32074 – 32135, June 13, 2001.

EPA, 2008. 40 CFR 197. *Public Health and Environmental Protection Standards for Yucca Mountain, Nevada: Final Rule*, Volume 73 Federal Register, Number 200, pp 61256 – 61289, October 15, 2008.

EPRI, 2006. *Evaluation of a Spent Fuel Repository at Yucca Mountain, Nevada: 2006 Progress Report*. Electric Power Research Institute, Palo Alto, CA: 2006. 1013445.

Garisto, N., D. Bennett and J. Andersson, 2008. *A Peer Review of the Yucca Mountain IMARC Total System Performance Assessment EPRI Model*, in Proceedings of the 12th International High-level Radioactive Waste Management Conference, September 7-11, 2008 in Las Vegas, Nevada, American Nuclear Society, La Grange Park, IL.

IAEA, 2004. *Improvement of Long-Term Safety Assessment Methodologies for Near-surface Disposal Facilities.* Volume II: Review and Enhancement of Safety Assessment Approaches and Tools. IAEA-ISAM, International Atomic Energy Agency, Vienna.

OCRWM, 2008. *Yucca Mountain Repository License Application*. DOE/RW-0573, Rev. 0, Office of Civilian Radioactive Waste Management, Washington DC.

5.3   Direct Disposal of Dual-purpose Canisters (DPCs)

5.3.1 Introduction

The U.S Department of Energy (DOE) has proposed standardized disposal waste packages for the Commercial Spent Nuclear Fuel (CSNF) and High Level Radioactive Waste (HLW) destined for Yucca Mountain. In recent years, a design-basis disposal canister system, with a 21 PWR or 44 BWR fuel assembly capacity, became the basis for the Department's evaluation of the long-term, post-closure performance of the repository system. In 2005, DOE announced the evolution of this design-basis into the transportation, aging, and disposal (TAD) canister design as the exclusive disposable canister for emplacement of CSNF in the Yucca Mountain repository. The DOE-proposed approach recognizes that in addition to TADs, a finite number of dual-purpose canisters (DPCs), representing 10 – 25% of CSNF disposal inventory, could be shipped to Yucca Mountain. These would eventually be opened at Yucca Mountain and the CSNF assemblies would then be transferred into TAD canisters for emplacement in the repository. The empty DPCs would be managed as low-level radioactive waste (DOE, 2008a; 2008b).

At present, a significant quantity of CSNF is already safely packaged in DPC's at the commercial reactor sites. If it could be demonstrated that there are no physical or technological constraints associated with the direct emplacement of DPC's into the repository within a suitable Alloy 22 Waste Package (WP) similar to that to be used with the TADs, an acceptable alternative solution would exist that could be considered for implementation if problems arose with DOE's preferred approach. Therefore, EPRI has evaluated the feasibility and consequences of direct DPC disposal with respect to long-term performance of the repository. The results were published in EPRI (2008a).

EPRI (2008a) found that there are no known technical barriers to direct disposal of at least some of the DPCs. Peak temperatures at the rock wall and in the rock pillars will not result in excessive rock spalling and extensive pillar dry-out. Therefore, EPRI argues that at least some of the DPCs anticipated to be in existence at the time DOE is ready to accept CSNF at Yucca Mountain *can* be disposed of directly by inserting them inside an appropriate waste package.

5.3.2 Approach

To evaluate the feasibility and consequences of direct DPC disposal, EPRI (2008a) assessed long-term performance of the repository against several criteria:

- Size – to determine if the inner DPC canister plus a modified disposal overpack (modified to fit the DPC canister, but otherwise dimensionally consistent with the proposed TAD design)

will fit inside the proposed disposal drift diameter, and still allow room for installation of the invert, pedestal, drip shield, and rock support;

- Rock wall temperature – to determine if direct disposal of DPCs will cause rock wall temperatures to exceed ~200°C. This temperature limit is a reasonable upper bound that would prevent significant rock expansion leading to potentially significant rock spallation. However, previous EPRI analyses have suggested that this temperature limit could be increased to ~225°C (EPRI, 2006a), if necessary.

- Seismicity and rockfall – to determine if there are any special issues with respect to the ability of DPCs to withstand anticipated seismic and rockfall events;

- Pillar dry-out – to determine if the water saturation in some of the rock between the disposal drifts remains above zero, thereby allowing passage of groundwater infiltrating from above the repository to below the repository. While beneficial, EPRI contends that it is not necessary to maintain water saturation in the pillar above zero at all times (EPRI, 2006a, 2007a);

- Criticality – to determine if DPCs will remain sub-critical during the post-closure period, or if critical for some scenarios, whether the canisters are likely to become prompt critical (EPRI, 2007b, 2008a, 2008b); and

- Long-term dose to the RMEI (reasonably maximally exposed individual) – to compare the peak RMEI dose in the post-closure period due to the disposal of CSNF in DPCs with that due to the disposal of TADs.

General TAD design criteria are described in the Yucca Mountain license application (DOE, 2008a, 2008b); specific design criteria for TAD construction will be established by commercial vendors based on DOE requirements as established in the TAD Performance Specification issued by DOE. The EPRI analysis described herein was intended to determine the actual number of DPC's that may exist at the time that the repository is ready to accept Spent Nuclear Fuel, the potential impacts of increased decay heat loadings, any pre- and post-closure dose implications, the number of transportation shipments that might be required and any criticality concerns that might arise as a result of the direct disposal of DPCs.

For the purposes of the EPRI analysis, a commercially available DPC was selected as the design-basis for comparison with the TAD design. The two primary criteria for the selection of a reference DPC were: (1) the pertinent design information is publicly available, and (2) the DPC represents one of the larger, higher capacity designs available in the industry to provide a conservative estimate of the effects of DPC disposal.

The DPC selected for this purpose was designed by Holtec International (Holtec, 2004, 2005a, 2005b, 2005c).[2]

The 32 PWR assembly DPC contains approximately 1.5 times the inventory of a 21 PWR TAD design; the 68 BWR assembly DPC contains approximately 1.5 times the inventory of a 44 BWR TAD. The design-basis DPC is 1.73 m in diameter not including the waste package outer and inner cylinders and closure ends (Holtec, 2005a). This diameter is comparable to the diameters of the previous Yucca Mountain 21 PWR/44 BWR disposal canisters and the Waste Package to

---

[2] The use of the Holtec design is for illustrative purposes only and does not represent an endorsement or recommendation of the product by EPRI.

be used for TAD disposal (1.69 m diameter) (DOE, 2008a; 2008b). Therefore, physical emplacement of existing DPCs within waste packages should not require any modifications to existing drift dimensions and plans for handling equipment, and drip shield design and installation for the Yucca Mountain repository. The only potentially significant difference would be the 50% higher spent fuel capacity of the DPC with associated increases in radionuclide inventory and decay heat production.

The Yucca Mountain Supplemental Environmental Impact Statement (YMSEIS) assumes that no DPCs or storage-only systems would be unloaded at reactor sites during the Proposed Action (DOE, 2008c). The YMSEIS also assumes that a total of 307 DPCs and storage-only canister-based systems would be shipped to the repository and unloaded at the repository under the 70,000 MTHM repository case and that a total of 966 DPCs would be shipped to the repository and unloaded at the repository under the Full MTHM acceptance case (DOE 2008d, Transportation File, Trans data_Summary.xls).

As of May 2008, approximately 625 DPCs had been loaded into Independent Spent Fuel Storage Installations (ISFSIs) for on-site storage at commercial nuclear power plant sites. EPRI projects that an additional 1,530 DPCs could be loaded at reactor sites between 2008 and 2020, resulting in a total of 2,155 DPCs. This projection of DPCs loaded through 2020 assumes that nuclear operating companies continue to load DPCs rather than TAD canisters for on-site storage through 2020, although it is possible that TAD loading would occur at an earlier date should they become available.

As part of its estimate, EPRI projected CSNF discharges for all currently operating nuclear power plants. Average annual spent nuclear fuel discharges were expected to be in the range of 2,100 to 2,300 MTHM per year through 2020. Using current and planned CSNF storage pool capacities and the projected CSNF discharges, EPRI estimated that approximately 1,700 MTHM of dry storage capacity would be needed annually at nuclear power plant sites through 2020. The projection of additional on-site storage assumed that all U.S. licensed nuclear power plants continue to operate through the end of their 60-year extended licenses; that lifetime capacity factors average approximately 90%; and that average discharge fuel burnups gradually increase to 58,000 MWD/MTU for PWRs and 46,400 MWD/MTU for BWRs.

In estimating the number of DPCs loaded through 2020, EPRI assumed:

- Plants with existing ISFSIs that are loading CSNF into metal dual-purpose casks would continue to do so through 2020;[3]
- Plants with existing ISFSIs would continue to load CSNF into packages with similar capacities through approximately 2013;
- Plants with new ISFSIs would load high capacity DPCs (32-PWR or 61/68 BWR); and
- From approximately 2014 forward, all CSNF would be loaded into higher capacity DPCs at existing and new ISFSIs (except at those sites currently loading CSNF into metal dual-purpose casks as noted in the first bullet, above).

---

[3] EPRI projects that as many as 135 dual-purpose metal casks could be in storage at reactor sites by 2020. In addition, approximately 101 metal dry storage casks or other storage-only systems have already been loaded for dry storage at reactor sites.

Thus, as shown in Table 5-1, EPRI estimated that utilities could load as many as 2,155 DPCs at reactor sites through 2020. Utilities have also loaded 220 canister-based storage-only dry storage systems – the YMSEIS assumes that some of these canisters would be transported to the repository for repackaging at the repository. Including these systems in the calculation led EPRI to estimate that as many as 2,375 DPCs and canister based systems could contain CSNF at commercial facilities by the year 2020.

For the purposes of assessing the feasibility of direct disposal of DPCs at Yucca Mountain, results from two calculations are presented. The first represents a bounding case in which 100% of CSNF is emplaced using DPC-based waste packages. The second represents a more realistic case in which a mixture of 2100 DPCs and 5010 TADs are emplaced.

5.3.3 Thermal Analysis

One key consideration determining the feasibility of direct DPC disposal is the impact of the decay heat load from the DPCs (as compared to the heat load from the proposed TADs) on EBS and repository performance. The inventory in the design-basis DPC is higher than the 21 PWR/44 BWR design chosen for the TAD canister. As a result, the heat generation rate from a DPC is expected to be higher than for a TAD canister. In previous high decay heat loading calculations, EPRI compared its results to a target drift rock wall temperature of <200°C and determined whether the pillar (the rock between drifts) would completely dry out, thereby precluding drainage between drifts, and, if so, for how long (EPRI, 2006a, 2007c). The same basis used for the previous evaluation was used in this study. The thermal analysis was conducted for the bounding 100% DPC case. This assumption is conservative in that it overestimates the heat loading that would be generated under a more realistic disposal scenario in which DPCs would only represent a fraction of the total CSNF disposal inventory at Yucca Mountain.

EPRI simulated coupled heat and mass transfer in the Yucca Mountain repository loaded with DPCs using a two-dimensional model implemented with the TOUGH2 numerical simulator developed by Lawrence Berkeley National Laboratory (Pruess et al., 1999). The conceptual model is shown in Figure 5-1. The vertical extent of the thermal model is 750 meters and covers 29 major geological groups and subgroups from the ground surface to the water table. The repository horizon is located in a 100-m thick Topopah Spring welded tuff unit (tsw35), approximately 300 m below the surface and 300 m above water table.

Table 5-1
Estimated dry storage systems loaded at nuclear power plant sites through 2020.

Package Type	Number of Packages Loaded
Storage-Only Canister Systems	220
Dual-Purpose Canister Systems	2,155
Dual-Purpose Metal Casks	135
Storage Only Metal Casks	101

To be consistent with the DOE proposed drift-to-drift spacing of 81 meters, the horizontal dimension of the model spans 40.5 meters, from the radial center of the emplacement drift to the middle plane between two adjacent drifts.

All the geological units are assumed to be fractured, albeit to differing extents. To model fractured flow and transport, a dual-porosity and dual-permeability approach has been used. The top and bottom boundaries are assumed to be at a constant temperature and pressure. The top boundary is also assumed to be open for gas flow upwards and downwards and for liquid flow (i.e., infiltration) only downward. The bottom boundary allows both gas and liquid flow in both upward and downward directions.

Using these boundary conditions and a set of assumed initial conditions for pressure, temperature, and saturation distributions, the model was run without heating from the waste packages until a steady state was reached. This steady state represents the condition when the liquid flux into the water table is approximately equal to the infiltration rate at the top boundary. Benchmarking of the model against DOE modeling results (BSC, 2005) indicated very good agreement (EPRI, 2006a).

Key parameters needed to populate the model are outlined below and are described in detail in EPRI (2008a):

- Geological (thickness, elevation)
- Hydrological (porosity, permeability, van Genuchten parameters)
- Thermal and physical (density, thermal conductivity, specific heat)
- Boundary conditions (pressure, temperature, infiltration rate)
- Decay heat history
- Geometry

(a) Vertical cross section.   (b) Detailed discretization on drift scale.
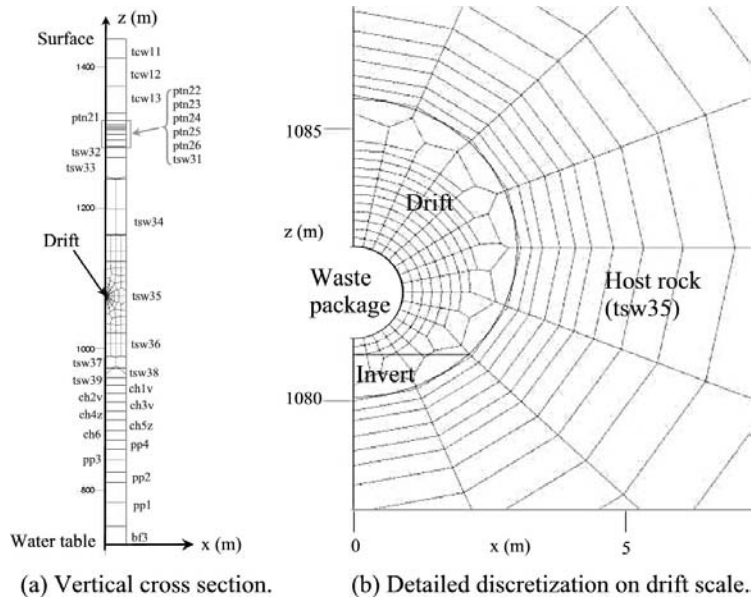
Figure 5-1
Illustration of conceptual model for simulating coupled heat transfer and flow surrounding a DPC in the Yucca Mountain repository.

Geological data were derived primarily from DOE sources (BSC 2000; 2003a; 2003b; 2004a; 2005). Numerical grids required for TOUGH2 analysis were generated using WinGridder (Pan et al. 2001) using stratigraphic data also provided in EPRI (2008a). The drift, invert, and waste package parameters were adapted from BSC (2005), as shown in Table 5-2. Linear capillary pressure and relative permeability relations were used for the drift. Linear capillary pressure and Leverett's functions for relative permeability (Pruess et al. 1999) were used for the invert. The maximum capillary pressure in the invert was assumed to be 833 Pa. The irreducible water saturation in the invert was assumed to be 0.1. The geometry of these components in the model is shown in Figure 5-2. For simplicity, the drip shield was implicitly included in the model by adjusting thermal parameters within the drift. The infiltration rate used in the analysis is shown in Table 5-3.

The design-basis DPC chosen for the EPRI analysis accommodates significantly more (~50% more) CSNF assemblies than the TAD canister design. To facilitate comparison with previous EPRI and DOE TSPA analyses, the decay heat for this larger DPC was assumed to increase proportionally with the increase in number of CSNF assemblies. The drift ventilation efficiency (86.3%) and repository ventilation period (first 50 years) were assumed to remain the same as the current repository design basis. The resulting decay heat projection is shown in Figure 5-3.
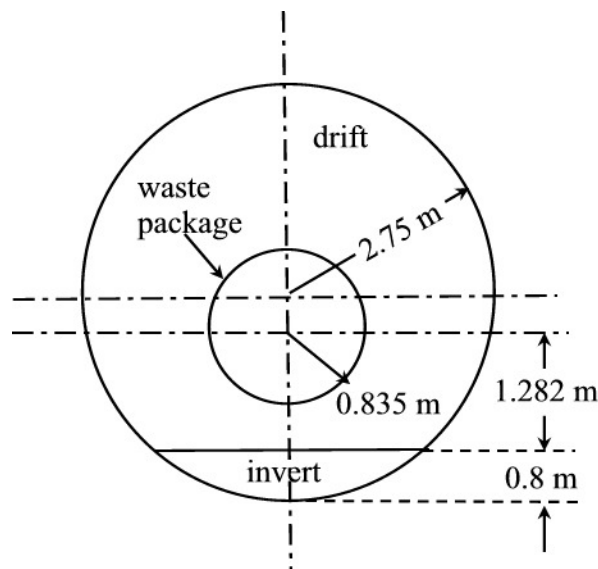
Figure 5-2
Geometry of drift, waste package, and invert in the model.

Table 5-2
Drift, invert, and waste package parameters.

Component	Permeability [m^2]	Porosity	Specific Heat [J/kg-K]	Density [kg/m^3]	Thermal conductivity [W/m-K]
Waste package	0.0	0.0	488.86	8189.0	14.42
Drift	10^{-9}	1.0	901	0.0	8.0
Invert	6.15×10^{-10}	0.545	948	2530.0	0.55

Table 5-3
Infiltration rates used for calibration and comparison (BSC 2005).

Time [yrs]	Infiltration rate [mm/yr]
0 – 600	6
600 – 2,000	16
2,000 – 100,000	25
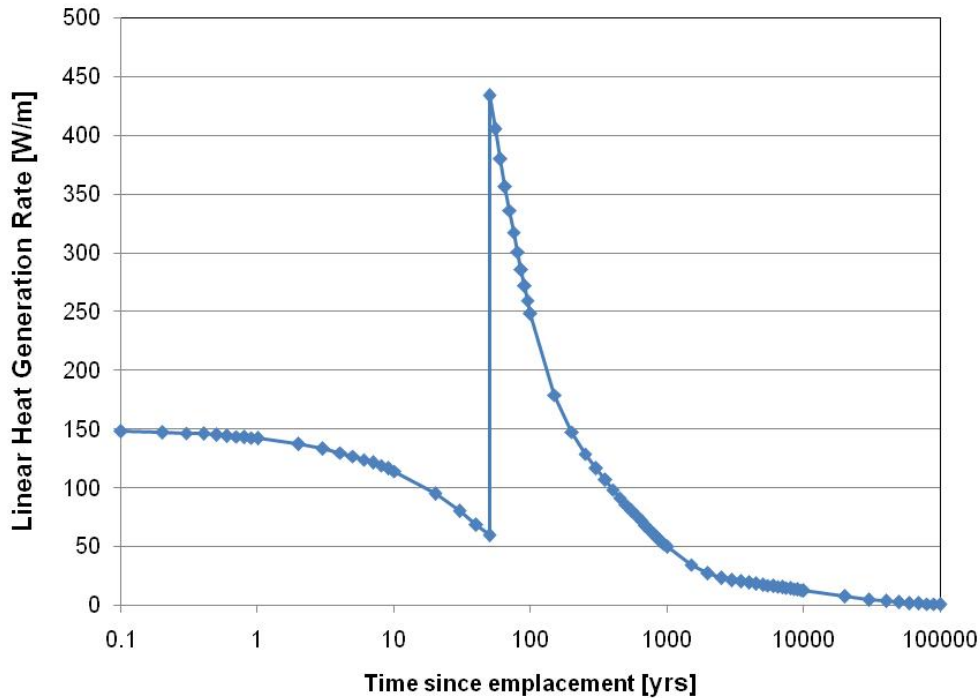
Figure 5-3
DPC heat generation rate with ventilation. The jump in the curve is associated with the time at which ventilation ceases, assumed to be at the end of a 50 year operational period for this curve.

5.3.3.1   Thermal Effects in Repository System for 100% DPC Disposal Case

In Figure 5-4A, the temperature histories are presented for the waste package, several locations of the drift wall, and in the drift pillar (the middle plane between the two drifts) for the scenario in which 100% of the TADs are replaced with DPCs. The maximum temperature calculated for the waste package was 228 °C, less than the constraint of 250 °C. The maximum drift wall temperatures calculated were 199 °C at the crown, 188 °C at the base, and 202 °C at the side.

The temperatures on the drift wall are close to DOE's 200 °C temperature constraint on rock. The minimal excess is not expected to impact the performance of the host rock. First, as shown in Figure 5-4A, the time period during which the temperature exceeds 200 °C by just 2° C is less than 10 years. Furthermore, this only happens on the side of the drift, which would be unlikely

to cause problems with the host rock surrounding the drift during the earliest timeframe, i.e., < 100 years following permanent repository closure. Secondly, this result was generated assuming a 100% DPC inventory for the repository, which, as stated above, is a bounding assumption. If direct disposal of DPCs does take place, it is likely that the emplaced CSNF waste packages would comprise a mixture of DPCs and TADs; this approach allows for a flexible thermal management strategy to reduce wall temperatures as needed.

In addition, the disposal of cooler co-disposed (i.e., containing both HLW and SNF) waste packages would provide additional margin for meeting thermal loading limits. Taking into account the inclusion of cooler non-CSNF waste packages and the likely inclusion of a substantial number of cooler TAD bearing waste packages, the argument can be made that the actual average linear heating rate will be less than that of a 100% DPC disposal inventory (and below the DOE host rock temperature constraint of 200 °C). Nevertheless, EPRI conducted a separate study of thermal effects on rock mechanics to quantitatively determine the thermal effect of exclusive DPC disposal. This thermal-mechanical analysis is presented in Section 5.3.4.

The maximum pillar temperature shown in Figure 5-4A is 87 °C, below the boiling point at the repository horizon (96°C). The resulting fracture water saturation at the drift crown and the pillar (the middle plane) is shown in Figure 5-4B. It can be seen that there is a brief period (< 300 years) of dry out at the pillar, which does not occur in the all TAD canister scenario (EPRI, 2007c). Although the pillar temperature remains below the boiling point, the fracture dries out due to an imbalance between the evaporation rate and the condensation rate arising from the higher heating associated with the DPCs.

In the previous analysis (EPRI 2007c), the relative importance of a pillar dry-out phenomenon was studied extensively. Two conclusions of that study are relevant here:

1. In cases of complete pillar dry-out, the dry-out period is much shorter than, and bracketed by, the dry-out period of the emplacement drift, effectively preventing water that may collect above the drift from dripping onto waste packages during the pillar dry-out period. Water preferably flow towards the pillar and accumulates there, and eventually drains once the dry-out period ends.

2. Three-dimensional analysis shows that under increased heating and low infiltration conditions, dry-out occurs in pillars near the drift center but not the drift edge. The axial heat and mass transfer due to the presence of cooler rock outside the repository allows water to drain towards the drift edge and downwards, as well as through cooler, open pillars near the drift edge.

5.3.3.2   Thermal Analysis for the 2100 DPC/5010 TAD Loading Case

EPRI (2008a) estimated that there could be approximately 2100 DPC waste packages by 2020; this value has been adopted here as a more reasonable design basis for the fraction of waste packages that could be received as DPCs at Yucca Mountain in a strategy mixing TADs and DPCs. Assuming the same total inventory of the repository, which is currently designed to be contained in 8160 TADs, this means that the CSNF inventory could be contained in 2100 DPCs and 5010 TADs for a total of 7110 waste packages. Assuming that the DPCs are interspersed with TADs throughout the repository, this means that the average heat loading per waste package would be 14.8 percent greater in a mixed TAD-DPC repository than in a TAD-only repository.
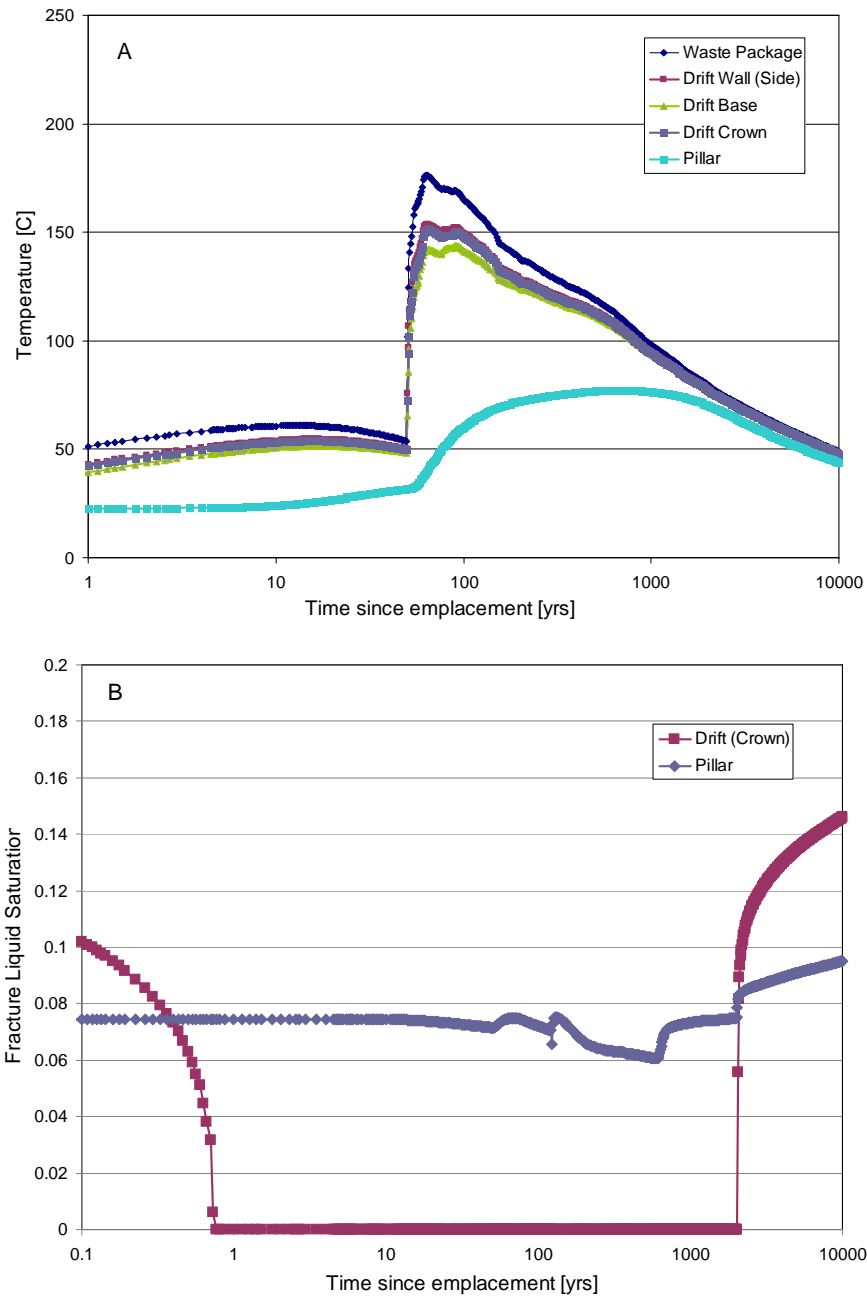
Figure 5-4
Thermal effects in repository system for 100% DPC disposal case: (A) temperature of waste package, drift wall, and drift pillar as a function of time, and (B) fracture water saturation vs. time at the drift crown and pillar centerline.

In Figure 5-5A, the temperature histories are presented for the waste package, several locations on the drift wall, and in the drift pillar (the middle plane of the two drifts). The temperature profiles are similar to the base case repository design containing only TADs. None of the thermal

limits in the current repository specifications have been exceeded. The saturation profiles in time are shown in Figure 5-5B, demonstrating that the pillar centerline does not dry out at any time.

Consequently, it is concluded that a reasonable mixture of TADs and DPCs can be disposed at Yucca Mountain without requiring modification of current design specifications or exceeding temperature limits established in the license application.

The detailed analysis undertaken by EPRI, which included a number of conservative assumptions, indicates that there is no significant thermo-hydrological impact of direct disposal of DPCs at Yucca Mountain. This finding holds even for the bounding case in which 100% of the CSFN is emplaced in DPC-bearing waste packages, which results in a 50% higher heat generation load relative to the exclusive TAD emplacement approach. The maximum waste package temperature calculated was 228 °C, which is less than the DOE thermal constraint of 250 °C. The maximum rock temperature calculated was 202 °C for a limited number of years, just marginally higher than the established DOE rock constraint of 200 °C.

This temperature exceedance could be readily addressed by interspersing a mixture of DPCs and TADs to decrease the average heat production per unit drift length. The calculations indicated that the inter-drift pillar briefly dries out, but EPRI (2007c) has shown that this type of dry-out period does not significantly impact repository performance. In addition, for the more likely case in which a mixture of DPC and TAD-bearing waste packages would be emplaced together (2100 DPCs and 5010 TADs), it is unlikely that any DOE-imposed temperature or pillar dry-out criterion would be exceeded.

5.3.4 Thermal-Mechanical Analysis

EPRI also conducted detailed thermal-mechanical analyses based on the temperature profiles determined for the 100% DPC disposal scenario for CSNF. EPRI adopted the same strategy used by DOE of dividing the lithophysal rock mass into 5 strength/moduli categories, Category 1 being the weakest and Category 5 being the strongest (EPRI, 2006b). The behavior of a drift in Category 3 (medium) lithophysal tuff subjected to drift wall temperatures up to 200°C was analyzed using the Fast Lagrangian Analysis of Continua (FLAC) numerical model (Itasca, 2008).
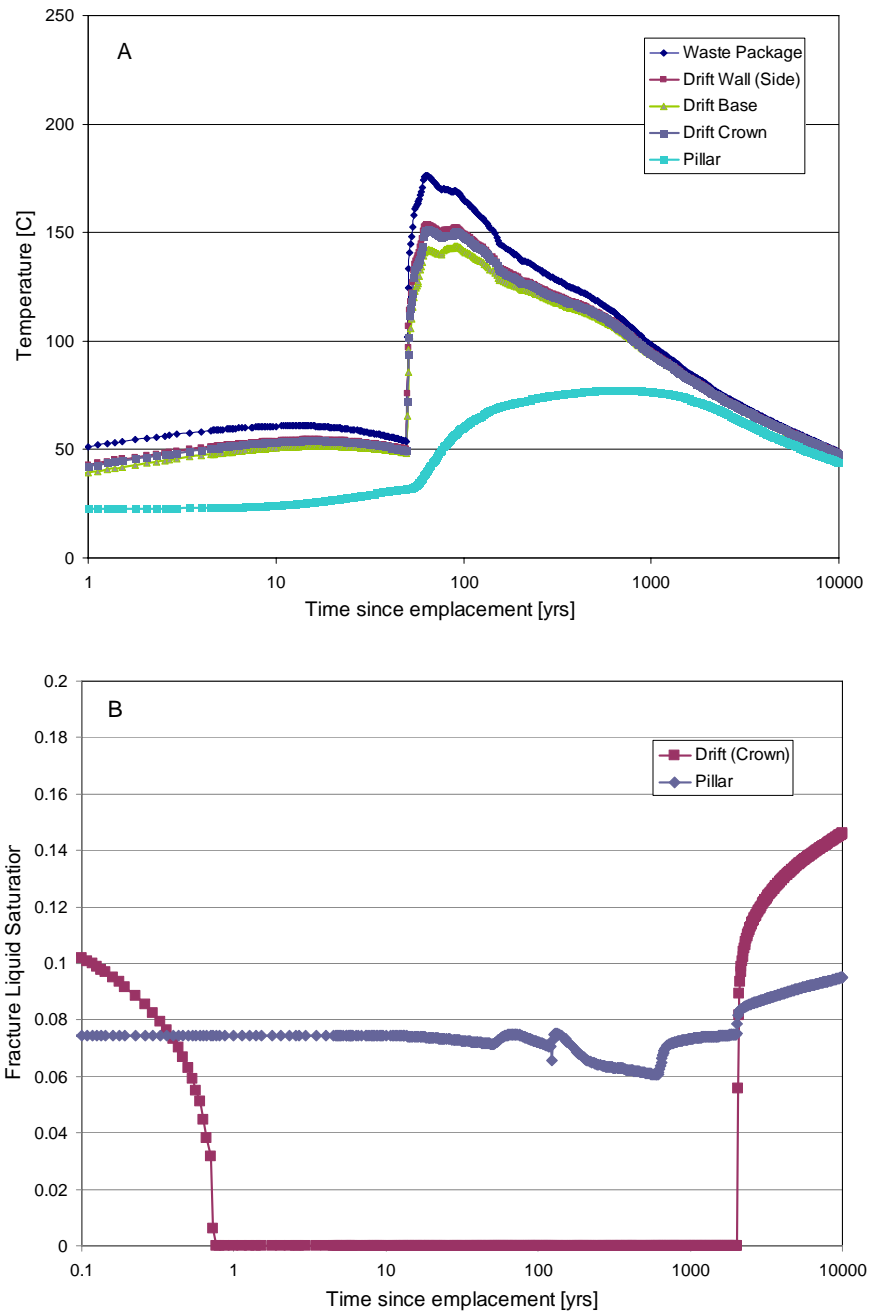
Figure 5-5
**Thermal effects in repository system for 2100 DPC/5010 TAD disposal case: (A)
Temperature of waste package, drift wall, and drift pillar as a function of time, and (B)
fracture water saturation vs. time at the drift crown and pillar.**

The analysis reported here is identical to the FLAC analyses reported in EPRI (2007a) except
that higher drift wall temperatures were considered. The drift wall temperature vs. time profile
used is shown in Figure 5-6.
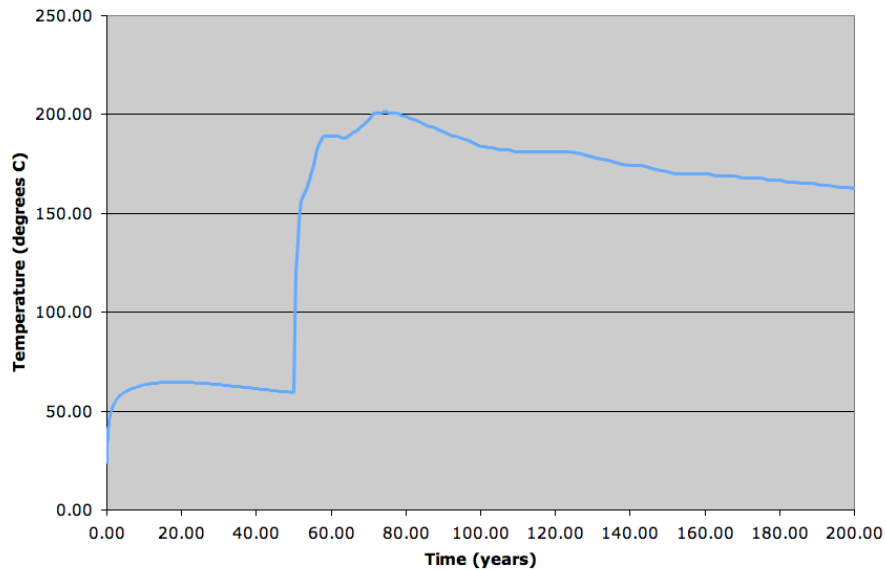
Figure 5-6
Drift wall temperature vs. time.

Simulation results at 85 years following repository closure are presented in Figure 5-7. Figure 5-7A shows predicted rock damage around the drift at 85 years (elements that have yielded), and Figure 5-7B shows the distribution of the rock mass cohesion around the drift at 85 years. Figure 5-7A indicates a zone of possible spalling with a thickness of about 0.6 meters around the drift. However, Figure 5-7B indicates that the rock mass retains most of its strength in the damage zone, and therefore extensive spalling is not predicted to occur. In particular, Figure 5-7B indicates reductions in cohesion in the damage zone of only 5 to 20%. Thus, the drift is expected to remain stable with only minor rockfall occurring from within the first 0.6 meters.

Table 5-4
Properties for Category 3 lithophysal tuff used in the FLAC simulation. G=shear modulus, K=bulk modulus, Co=cohesion, ϕ=friction angle, To=tensile strength, k=conductivity, s=specific heat, a=thermal expansion coefficient, ** α=7.46e-6 for temps < 100 °C, α=9.1e-6 for 100<temp<125, α=9.98e-6 for 125<temp<150, α=11.74e-6 for 150<temp<175, α=13.09e-6 for temp>175.

Rock Type	Elastic Properties		Rock Mass Strength Properties			Strain Softening Properties		Temperature Properties		
	G	K	Co	ϕ	To	Min values	γc	k	S	α
	GPa	GPa	MPa	deg	MPa	Co, ϕ, To		W/m°K	J/kg°K	/°C
Cat3 lith	4.51	6.01	5.1	35	1.8	1e4, 29,1e4	0.02	2.0	920	**

The results shown in Figure 5-7 were based on a γc value of 0.02. To justify this value (the importance of γc is discussed in EPRI (2007a)), a FLAC simulation of a uniaxial test was conducted with these properties and the results agree well with the results from an actual uniaxial test performed on lithophysal tuff (EPRI 2008a). As discussed in EPRI (2007a), progressive

spalling could occur around drifts for rocks that exhibit very steep strain softening slopes. However, FLAC modeling indicates that actual strain softening slopes for lithophysal tuff are very shallow, and therefore progressive spalling is not expected.

Thermal-mechanical modeling indicates that some yielding is expected to occur around the drifts under the higher drift wall temperatures. For comparison, a yield zone of about 0.6 meters thick is predicted in the Category 3 lithophysal tuff when subjected to drift wall temperatures up to 200 °C, compared with a yield zone about 0.3 meters for the current Yucca Mountain design with maximum drift wall temperatures of about 150 °C. However, the increased yielding is not expected to result in any significant rockfall, because the rock strength within the yielding zone is still 80 to 95% of its initial rock mass strength. As it is likely that any repository operations emplacing DPC-bearing waste packages would co-mingle cooler waste packages for thermal management, EPRI concludes from the bounding case examined that thermal-mechanical factors do not present significant obstacles to direct DPC disposal at Yucca Mountain.
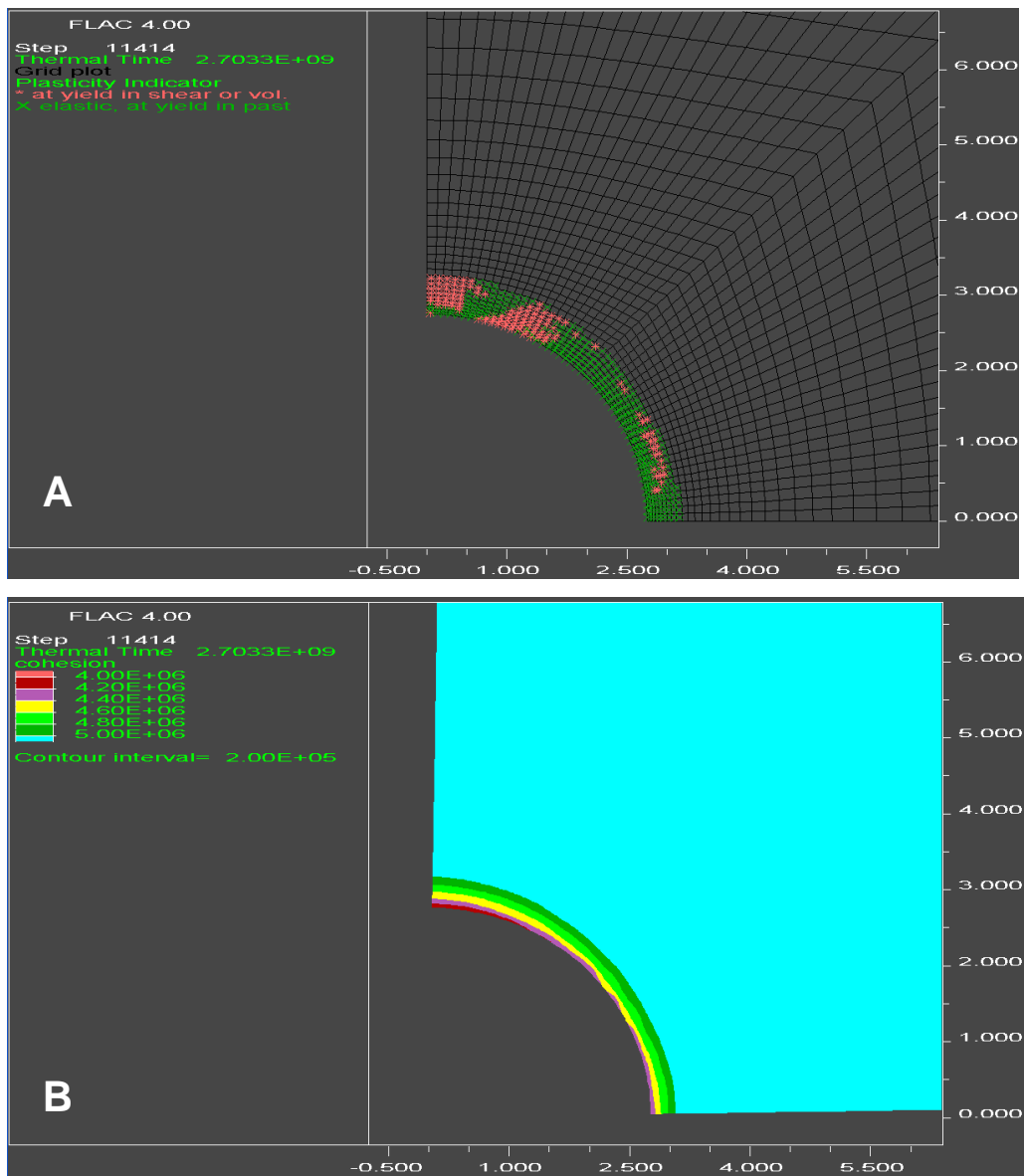
Figure 5-7
FLAC simulation results at 85 years: (A) Damage zone around the drift at 85 years as indicated by elements that have yielded, and (B) Distribution of rock mass cohesion around the drift.

5.3.5 Corrosion

A key repository performance driver is the rate of failure of the components of the engineered barrier system, in particular the titanium drip shield (DS) and Alloy 22 waste packages. Calculations of the rates of corrosion processes affecting the DS and WP for the 100% DPC/0% TAD repository case were performed by EPRI using a stand-alone model called EBSCOM.

The EBSCOM code uses Monte Carlo techniques to take into account uncertainty and variability in the prediction of DS and WP lifetimes. Uncertainty arises from the use of abstracted conceptual corrosion models, which are necessarily simplifications of the actual complex corrosion processes, and from uncertainty in the values of various input parameters. Variability results from variation in, for example, material properties, environmental conditions (both spatial and temporal variation), and the quality of the manufactured WP and DS.

A single run of the EBSCOM code typically comprises 1,000,000 individual realizations. In a given realization, an individual DS is coupled to an individual WP and the computation is performed until such time that all components of the engineered barrier system have failed.

EBSCOM is largely a thermally driven code. Thus, the temperature, and how it evolves over time, is the principal environmental parameter determining the rate of various corrosion processes. However, environmental variability is also included in the EBSCOM model, primarily based on the different seepage water "bins" defined by the DOE (BSC 2004b) and their effect on various corrosion processes – principally localized corrosion (LC) and stress corrosion cracking (SCC).

The EBSCOM code was used to evaluate the corrosion behavior for the thermal profile presented in Section 5.3.4. These temperatures are not sufficiently different from the baseline temperature curves for the 21-PWR or TAD waste packages to influence the corrosion behavior of the Alloy 22 WP (EPRI, 2006a). Consequently, EPRI concludes that the corrosion rate of Alloy 22 for DPC disposal, even for the bounding case of a repository containing 100% DPCs and no TADs, is identical to the corrosion rate of Alloy 22 for TAD disposal.

5.3.6 TSPA Analyses for Nominal and Alternative Scenarios

EPRI has conducted independent assessments of the total system performance of the candidate spent nuclear fuel (SNF) and high level radioactive waste (HLW) repository at Yucca Mountain, Nevada, since 1989. EPRI's total system performance assessment code is formally known as the Integrated Multiple Assumptions and Release Code (IMARC). The latest version, IMARC 9, is used here for the evaluation of DPC disposal. IMARC 8 is described in detail in EPRI (2005a). IMARC 9 uses the IMARC 8 model, but includes several parameters that have been updated since the publication of IMARC 8.

The use of IMARC 9 results in a number of conservatisms. The engineered barrier system in IMARC 9 reflects the DOE approach to waste package design preceding the TAD design, including the use of a thinner Alloy 22 WP outer shell than is now being contemplated. (i.e., 20 mm-thick Alloy 22 for the old design vs. 25 mm-thick Alloy 22 for the TAD design). For consistency and a common point of reference, calculations were performed using Yucca Mountain project design information and data from 2005. Consequently, inventory values and solubility, sorption, and the many other TSPA input parameters have previously documented by EPRI (2005a). IMARC is now being updated (i.e., IMARC 10) by EPRI to reflect the latest design assumptions.

The TSPA inventory basis from EPRI (2005a) has been used to estimate the inventory in a DPC waste package by increasing the per package inventory by 50 percent. To maintain the overall

inventory within the current design basis of 70,000 MTHM, the number of waste packages was reduced by 0.67 to compensate for the higher capacity of the design basis DPC.

5.3.6.1   Nominal Scenario

The overall repository performance for the 10^6 year compliance period for disposal of 100% of the larger (32-PWR) DPC versus the 21-PWR canister is presented in Figure 5-8 for EPRI's "nominal" case (i.e., the 'nominal' repository evolution scenario includes no seismic, rockfall, or igneous events) and the pre-TAD DOE waste package design The two curves are very similar. Figure 5-9 provides total dose and doses by radionuclide for the TAD-analog (21-PWR disposal canister bearing waste package, Figure 5-9A and the EPRI DPC design-basis (32-PWR) waste package, Figure 5-9B.
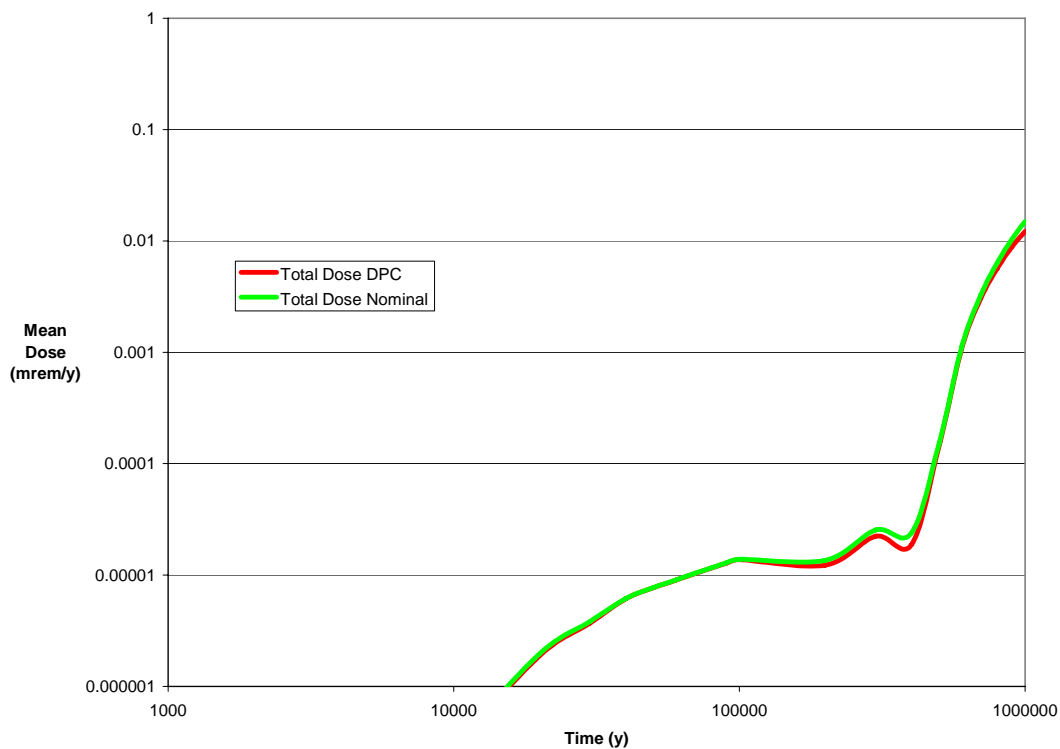
Figure 5-8
Comparison of the total mean dose rate for 100% DPC disposal and the IMARC 9 nominal repository evolution assessment.

Based on these analyses, EPRI has concluded that the TSPA results for the case of direct disposal of larger DPCs is comparable to TSPA results for the 21 PWR waste package disposal, and that either type of waste package provides adequate performance under the nominal repository disposal scenario at Yucca Mountain. Likewise, these results can be extended to a comparison of TAD disposal with disposal of DPCs, with both having a comparably thicker WP outer shell.

5.3.6.2   Alternative Scenarios

In addition to the nominal repository evolution scenario, EPRI (2004, 2005a, 2005b, 2005c, 2006b) conducted analyses related to alternative scenarios for the behavior of the repository. The EPRI analyses of these repository evolution scenarios were founded on an independent assessment of the geology, volcanic hazard, and seismology at Yucca Mountain. This independent assessment identified a number of conservatisms in the approaches used by DOE in their assessments. The assessments in this chapter are therefore based on EPRI's assessments of the alternative repository evolution scenarios.

5.3.6.2.1   Igneous

EPRI (2004, 2005a, 2005b) evaluated the potential for disruption of the repository performance in the event of an igneous event intersecting the repository. The EPRI analyses focused strongly on the performance of the waste package in either an eruptive or intrusive igneous event. The waste packages form the primary barrier to releases in the igneous scenario. The WP configuration is basically the same for either TAD or DPC disposal. Consequently, it was concluded that the consequences to the repository resulting from an igneous event would be the same for DPC disposal or for TAD disposal.

5.3.6.2.2   Seismic

EPRI (2005c, 2006b) carried out independent assessments of the consequences of seismic events at Yucca Mountain on the post-closure performance of the repository. It was noted that the prior analyses carried out by DOE contained a number of significant conservatisms, and as a result the EPRI analyses represent a more reasonable estimate of the performance of the repository from a single, large, low probability event (EPRI, 2005c), and the performance associated with multiple, smaller events (EPRI, 2006b).

EPRI (2006b) presented the results of EPRI's evaluations of the potential effects of sequences of multiple seismic events on the total system performance assessment (TSPA) of a repository at Yucca Mountain, and to implement a TSPA for a single sequence of seismic events. The TSPA was carried out for a base case analysis and two sensitivity cases, all of which represent the behavior of the repository under a series of events with a 10^5 year return interval, with a peak ground velocity of 0.75 m/s. The EPRI base case analysis is closest to a reasonable expectation analysis, though with several key conservative simplifying assumptions, whereas the sensitivity cases include additional conservative assumptions.

The conclusion of both EPRI (2005c) and EPRI (2006b) was that seismic effects increase doses at early times as a result of early waste package failures, but that the peak dose is not strongly affected by seismic activity. The results for a 21-PWR waste package were calculated as shown in Figure 5-10.

Based on the similar physical dimensions and mass of the EPRI design basis DPC and the TAD, it was concluded that EPRI's prior analyses (EPRI, 2005c, 2006b) of potential seismic damage to the TAD Alloy 22 WP can be applied to the DPC WP. Consequently, the only change to a TSPA analysis of the seismic scenario compared to an analysis of a 21 PWR waste package is (as in the nominal scenario) an increase in the inventory of an individual waste package and a decrease in the number of the total number waste packages emplaced. The behavior of the DPC was assumed to be essentially the same as that of the 21 PWR waste package during a seismic event, and the resulting TSPA analysis is indistinguishable from one performed for the 21 PWR canister (Figure 5-10).

5.3.6.2.2   Criticality

DOE (2008e) evaluated a variety of features, events, and processes (FEPs) that could have the potential for leading to conditions associated with criticality in a TAD in the first 10,000 years using an event tree approach to quantify the cumulative probability of the sequence of conditions necessary to generate criticality. For a number of these conditions, DOE (2008a) used extremely conservative assumptions, and assigned a probability of unity for some branches of the event tree clearly associated with low probability conditions.
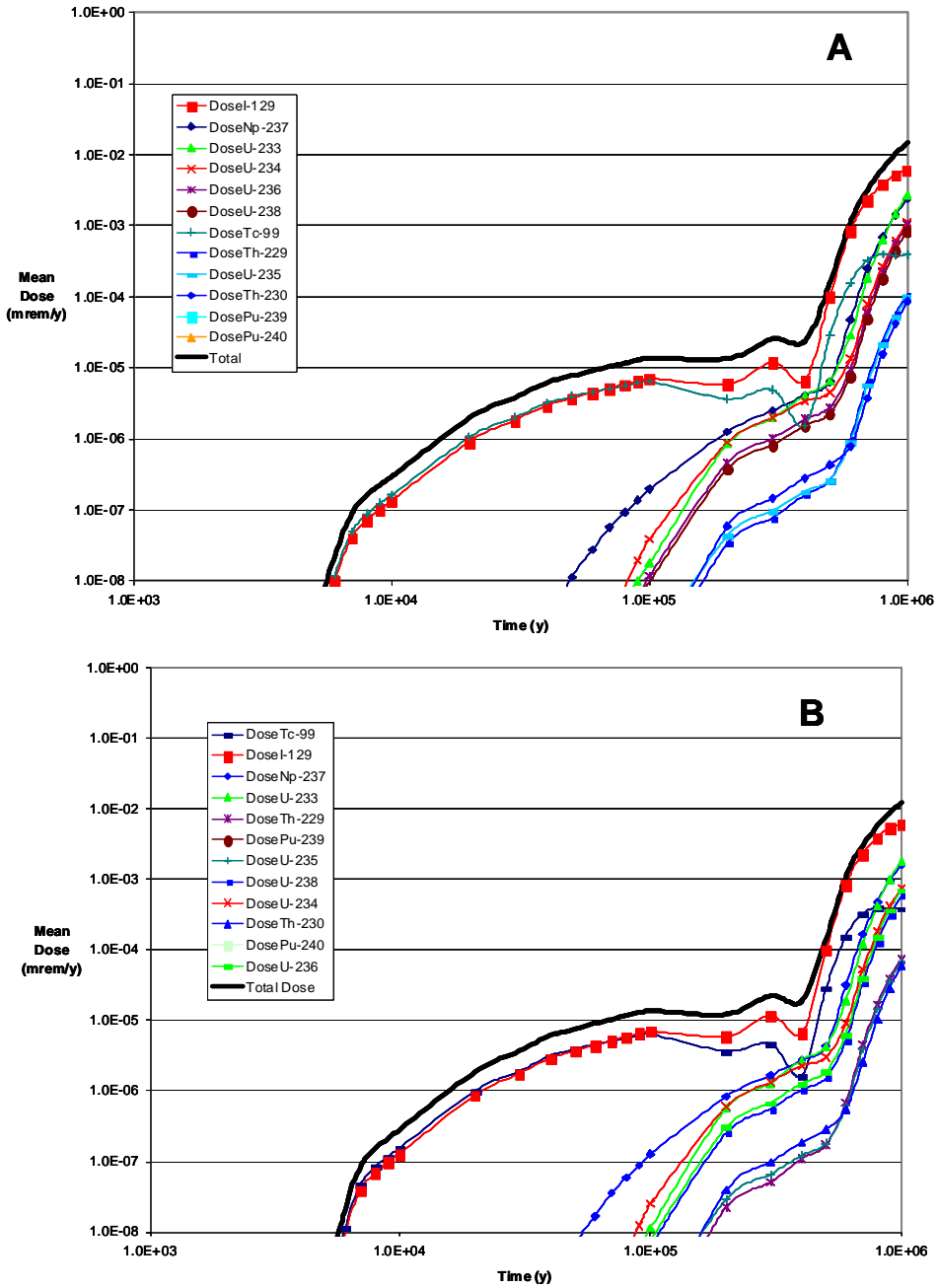
Figure 5-9
IMARC 9 results for (A) TAD analog (21 PWR waste package) and (B) the EPRI design-basis DPC (32 PWR waste package). Both simulations assume a 20 mm Alloy 22 outer waste package thickness vs. the 25 mm thickness now specified by DOE in the LA (2008).
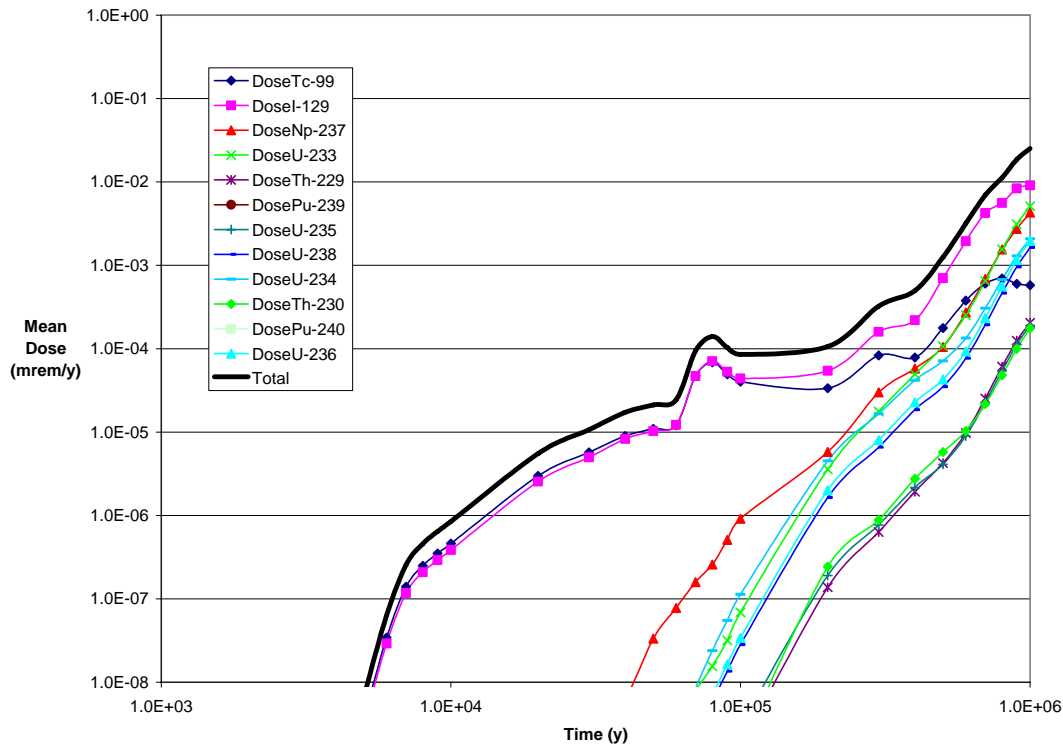
Figure 5-10
TSPA results for repeated seismic events calculated using IMARC 9, with a 21 PWR waste package (excerpted from EPRI, 2006b). Doses from a TAD-based disposal system would be less sensitive to seismic events due to the thicker disposal overpack (25 mm vs. the 20 mm used here).

Therefore, the resulting conservative DOE probability estimates for a post-closure criticality event are likely to overestimate criticality risks by several orders of magnitude. Even with DOE's extremely conservative approach, the resulting probability fell below the regulatory cutoff for screening scenarios (10^{-8} annual frequency), and post-closure criticality was screened from further consideration in the TSPA.

EPRI (2007b) provided an initial, extremely bounding evaluation of the nuclear reactivity potential of conditions associated with flooding, corrosion, and collapse of TAD canister structures in the Yucca Mountain repository. EPRI (2007b) considered the potential for transient long-term degradation processes such as corrosion to lead to changes in the configuration of fuel in the TAD, which had been speculated to have the potential for allowing criticality to occur. EPRI (2007b) concluded that these transient criticality events could only be possible based on highly conservative or non-mechanistic inputs and assumptions.

The prerequisite conditions for post-closure criticality would be the same for DPCs as for TADs. For criticality transients in TADs to occur, EPRI (2007b) concluded that the satisfaction of the requisite series of conditions would not be satisfied based on the following grounds:

- Condition 1: The waste package breach occurs in a highly selective manner, i.e., only at the top, in order to allow groundwater to completely fill the waste package. Current

understanding of corrosion of the Alloy 22 waste package outer barrier suggests that the predominant mechanism for corrosion is general corrosion, which would preclude this type of selective failure (see, e.g., EPRI, 2005d Appendix B; DOE, 2008f Section 6.3.5).

- Condition 2: The zone of failure on the top of the waste package is sufficiently large such that groundwater can enter the waste package via advection. This condition would be commonly associated with failure by general corrosion rather than localized corrosion. Therefore, the occurrence of the Condition 1 is unlikely to be associated with the second condition.

- Condition 3: Groundwater entering the breached waste package removes essentially all of the boron from the neutron poison material (e.g., borated stainless steel or aluminum). This condition requires groundwater to flow over or be present in the appropriate sections of the waste package such that boron removal occurs. In its initial bounding evaluations, EPRI (2007b) did not postulate a credible geochemical mechanism for the selective removal of boron.

- Condition 4: A sufficient amount of groundwater accumulates in the waste package such that it can fully immerse a significant portion of the waste package internals. This condition is unlikely to occur for an Alloy 22 WP that has failed by general corrosion, as general corrosion will likely lead to breaching of the bottom portions of the waste package as well as the top (see, e.g., EPRI, 2005d Appendix B; DOE, 2008f Section 6.3.5). This, in turn, would drain some fraction of the waste package before the waste package could fill to any significant extent.

- Condition 5: A very rapid collapse of the flux traps occurs. In its initial bounding evaluations, EPRI (2007b) did not postulate a mechanism by which this condition could occur. Presumably, a very rapid collapse of the flux traps might be possible during a seismic event if: the flux trap steel is degraded nearly to the point of loss of structural integrity prior to the seismic event; the seismic event is of sufficient energy to cause complete mechanical failure of the flux traps. For the newer, higher capacity DPCs, flux traps are not part of their design. Therefore, the potential for this condition would not even exist for some DPCs.

- Condition 6: A sufficient number of adjacent flux traps collapses simultaneously. In its initial bounding evaluations, EPRI (2007b) did not postulate a mechanism by which this condition could occur. As discussed in the previous bullet, this could only occur under the conditions listed above, and it would be even less likely that several of the adjacent flux traps would completely collapse during a seismic event. This condition is not applicable to the newer, higher capacity DPCs without flux traps.

The pre-requisites for transient post-closure criticality in the post-10,000 year period were therefore seen to consist of (1) conditions that are inconsistent with the expected corrosion behavior of Alloy 22, (2) conditions that require a more significant flow of groundwater than expected into the drifts at Yucca Mountain, or (3) conditions for which there is no credible physical mechanism to allow them to occur. Therefore, it was concluded that the likelihood of criticality in a DPC waste package would be comparable to that in a TAD; that is, the probability is anticipated to be below the regulatory cut-off for inclusion in TSPA as a FEP.

EPRI is in the process of updating its extremely bounding scenario results in EPRI (2007b) for the purpose of better evaluating criticality by comparing determining whether the calculated $k_{effective}$ (k-eff) in the scenarios considered is greater than 1. The results for this update (EPRI, 2008b, *in press*) are summarized in Section 5.13. For this case, k-eff was estimated for a

horizontal waste package containing a DPC canister with 32 PWR assemblies in which varying amounts of water were assumed to be present. This analysis concluded that k-eff will not approach 1 until the waste package containing the DPC is well more than half-filled with water (EPRI, 2008b, *in press*). As indicated above, it is unlikely that the waste package will fill with water to any great extent as breaching of the waste package is as likely to occur on the bottom as on the top. Also, even if a breach allows significant introduction of water inside the DPC canister, further corrosion of the waste package would also likely lead to drainage of water. Accordingly, EPRI concludes that it is extremely unlikely that a waste package containing either a TAD or a DPC canister would reach criticality.

A TSPA sensitivity analysis was conducted by EPRI to illustrate the minimal impact that an unlikely criticality event would have on repository performance based on the following assumptions:

- Despite the low probability of occurrence, a criticality event occurs. Results presented below are therefore seen to be conditional doses, which assume the event occurs.

- Given the low probability of occurrence, it was assumed that the conditions for criticality occur in only one waste package.

- The effect of the criticality event is complete loss of integrity of the WP outer and inner cylinders and the physical form of the CSNF. As a result, all of the inventory of fission products in the waste package (I-129 and Tc-99) acts as an instantaneous release fraction. Similarly, since the structural integrity of the fuel is lost, no credit is taken for alteration of the fuel, and the alteration rates are set to small values.

- The criticality event was assumed to produce 25 percent more fission products than exist in the disposed inventory for those packages experiencing a criticality (DOE, 1998).

- The criticality event was assumed to destroy the cladding, so the cladding was assumed to be completely failed at time zero.

- The event was assumed to occur in the first 1000 years following repository closure, to demonstrate the highest potential for consequences for the purpose of this sensitivity calculation. It is noteworthy, however, that the occurrence of criticality depends on significant amounts of water entering the waste package, which is not considered to be a credible scenario during the first 1000 years.

These assumptions form the basis of a sensitivity analysis, and do not represent a credible future evolution of the disposal facility. The assumptions used to implement the sensitivity analysis are described in detail in EPRI (2008b, *in press*). The only notable risk consequences are associated with the early release fraction; the criticality event does not affect the mean dose at long times after the event occurs. Results from this analysis are presented in Figure 5-11, compared to the nominal TSPA results for waste disposal in TADs. The criticality event produces an early peak from the activation products I-129 and Tc-99. The release from the criticality event is transient, and once the radionuclides from the criticality waste package have left the disposal system, the dose curve returns to the nominal behavior.
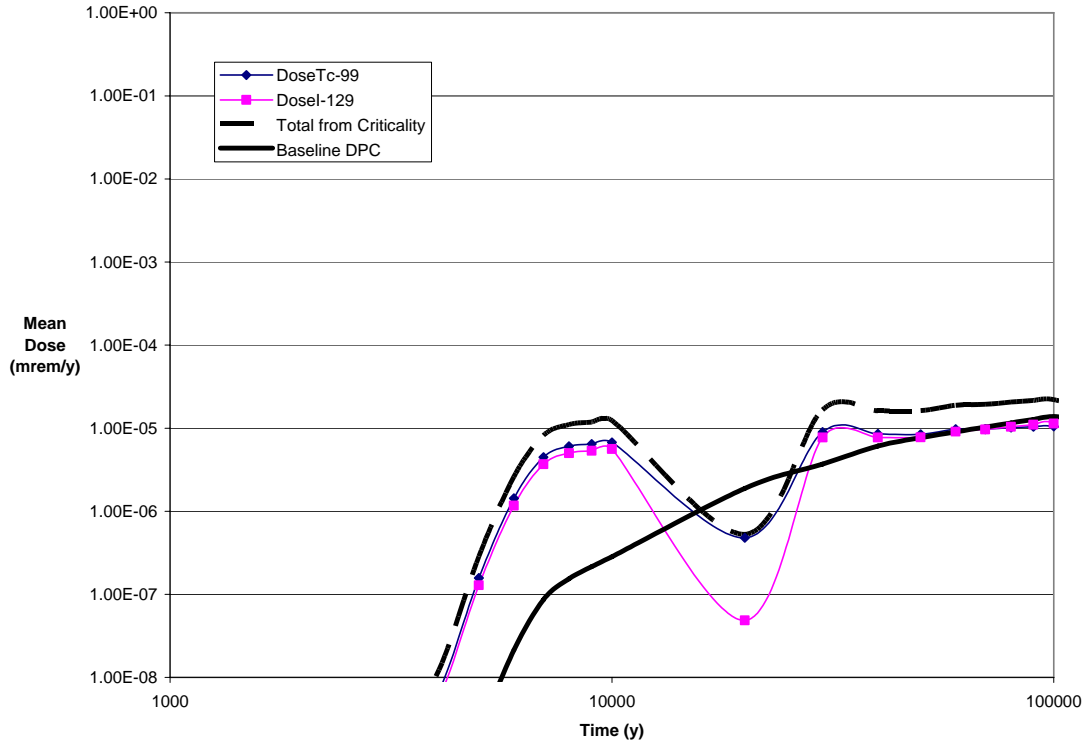
Figure 5-11
TSPA calculation for the consequences of a criticality event in the repository. These results are conditional on the event occurring, even though it is extremely low probability.

As a result of this analysis, it is concluded that criticality can be omitted from consideration in the post-closure period from the perspective of consequence, as well as from the perspective of probability. This conclusion is valid for both the scenarios involving the use of TADs and a large fraction of loaded and yet-to-be loaded DPCs.

5.3.7 Conclusions

Direct DPC disposal was examined to determine if there would be any significant issues relative to thermal effects, thermal-mechanical effects, corrosion, TSPA of the nominal repository evolution scenario and credible alternative repository evolution scenarios, as well as criticality. EPRI has concluded that there are very small differences in performance of DPCs in the post-closure period compared to performance of TADs. Criticality is also extremely unlikely for both TADs and DPCs. As such, no technical obstacles have been identified that would preclude the use of at least some fraction of DPCs for disposal of commercial spent nuclear fuel (CSNF) in a geologic repository at Yucca Mountain.

5.3.8 References

BSC, 2000. *Calibrated Properties Model*. MDL-NBS-HS-000003, REV00, Bechtel SAIC Company, Las Vegas, Nevada.

BSC, 2003a. *Drift-Scale Coupled Processes (DST and THC Seepage) Models*, MDL-NBS-HS-000001, REV02, Bechtel SAIC Company, LLC, Las Vegas, Nevada.

BSC, 2003b. *Analysis of Hydrologic Properties Data*, MDL-NBS-HS-000014 REV00, Bechtel SAIC Company, LLC, Las Vegas, Nevada.

BSC, 2004a, *Calibrated Properties Model*, MDL-NBS-HS-000003, REV02, Bechtel SAIC Company, LLC, Las Vegas, Nevada.

BSC, 2004b. *Drift Degradation Analysis*, Bechtel SAIC Company report to DOE, ANL-EBSMD-000027, REV 03, ICN 00. Bechtel SAIC Company, LLC, Las Vegas, Nevada.

BSC, 2005. *Drift-Scale THC Seepage Model*, MDL-NBS-HS-000001, REV4, Bechtel SAIC Company, LLC, Las Vegas, Nevada.

Damjanac, B. and P. Cundall. 2004. HC Itasca Technical Memorandum to Jerry King, Strain levels related to damage, estimated from laboratory results on large core samples of lithophysal tuff, reference 04-2133-6-13TM.

DOE, 1998. *Disposal Criticality Analysis Methodology Topical Report*. YMP/TR-004Q, Rev. 0. Las Vegas, Nevada.

DOE, 2003. *The Potential of Using Commercial Dual Purpose Canisters for Direct Disposal. Draft Report TDR-CRW-SE-000030 REV 00*. Office of Civilian Radioactive Waste Management, Washington DC.

DOE, 2006. Preliminary Transportation, Aging, and Disposal Canister System Performance Specification Revision A. WMO-TADCS-0000001. Office of Civilian Radioactive Waste Management.

DOE, 2007. *Total System Performance Assessment Data Input Package for Requirements Analysis for TAD Canister and Related Waste Package Overpack Physical Attributes Basis for Performance Assessment*. TDR-tDIP-ES-000006. Rev00A, March 2007.

DOE, 2008a. *Yucca Mountain Repository License Application*. U.S. Department of Energy, Office of Civilian Radioactive Waste Management, DOE/RW-0573, Rev. 0, June 2008.

DOE, 2008b. *Civilian Radioactive Waste Management System Waste Acceptance System Requirements Document,* Revision 5, ICN 01. DOE/RW -0351. U.S. Department of Energy, Office of Civilian Radioactive Waste Management.

DOE, 2008c, *Final Supplemental Environmental Impact Statement for a Geologic Repository for the Disposal of Spent Nuclear Fuel and High-Level Radioactive Waste at Yucca Mountain, Nye County, Nevada* (YMSEIS), DOE/EIS-0250F-S1.

DOE, 2008d. *YMSEIS Calculation Packages in Support of Final Supplemental Environmental Impact Statement for a Geologic Repository for the Disposal of Spent Nuclear Fuel and High-Level Radioactive Waste at Yucca Mountain, Nye County*, DOE/EIS-0250F-S1.

DOE, 2008e. *Screening Analysis of Features, Events, and Processes for License Application.* ANL-DSO-NU-000001 Rev 00, February 2008. Office of Civilian Radioactive Waste Management.

DOE, 2008f. *Total System Performance Assessment Model/Analysis for the License Application.* MDL-WIS-PA-000005 REV00, January 2008. Office of Civilian Radioactive Waste Management.

EPRI, 2004. *Potential Igneous Processes Relevant to the Yucca Mountain Repository: Extrusive-Release Scenario Analysis and Implications*, Electric Power Research Institute, Palo Alto: 2004. 1008169.

EPRI, 2005a. *EPRI Yucca Mountain Total System Performance Assessment Code (IMARC) Version 8 – Model Description*, Electric Power Research Institute, Palo Alto CA: 2005. 1011813.

EPRI, 2005b. *Program on Technology Innovation: Potential Igneous Processes Relevant to the Yucca Mountain Repository: Intrusive-Release Scenario, Analysis and Implications.* Electric Power Research Institute, Palo Alto, CA: 2005. 1011165.

EPRI, 2005c. *Program on Technology Innovation: Effects of Seismicity and Rockfall on Long-Term Performance of the Yucca Mountain Repository – 2005 Progress Report*, Electric Power Research Institute, Palo Alto, CA: 2005. 1011812.

EPRI, 2005d. *Program on Technology Innovation: Evaluation of a Spent Fuel Repository at Yucca Mountain, Nevada – 2005 Progress Report*, Electric Power Research Institute, Palo Alto, CA: 2005. 1010074.

EPRI, 2006a. *Room at the Mountain: Analysis of the Maximum Disposal Capacity for Commercial Spent Nuclear Fuel in a Yucca Mountain Repository*, Electric Power Research Institute, Palo Alto, CA: 2006. 1013523.

EPRI, 2006b. *Program on Technology Innovation: Effects of Multiple Seismic Events and Rockfall on Long-Term Performance of the Yucca Mountain Repository*, Electric Power Research Institute, Palo Alto, CA: 2006. 1013444.

EPRI, 2006c. *Program on Technology Innovation: EPRI Yucca Mountain Spent Fuel Repository Evaluation – 2006 Progress Report,* Electric Power Research Institute, Palo Alto, CA: 2006. 1013445.

EPRI, 2007a. *Program on Technology Innovation: Yucca Mountain Post-Closure Criticality – 2007 Progress Report*, Electric Power Research Institute, Palo Alto, CA: 2007. 1015128.

EPRI, 2007b. *Program on Technology Innovation: Room at the Mountain Analysis of the Maximum Disposal Capacity for Commercial Spent Nuclear Fuel in a Yucca Mountain Repository*, Electric Power Research Institute, Palo Alto, CA: 2007. 1015046.

EPRI, 2007c. *Program on Technology Innovation: Analysis of Thermal Spalling of Tuff Host Rock for the Yucca Mountain Repository*, Electric Power Research Institute, Palo Alto, CA: 2007. 1015390.

EPRI, 2008a. Feasibility of Direct Disposal of Dual-Purpose Canisters in a High-Level Waste Repository, Electric Power Research Institute, Palo Alto, CA: 2008. 1018051.

EPRI, 2008b. *Feasibility of Direct Disposal of Dual-Purpose Canisters – Options for Assuring Criticality Control,* Electric Power Research Institute, Palo Alto, CA: 2008. 1016629 (*in press*).

Holtec International, 2004. *MPC-24/24EF Fuel Basket Assembly Licensing Drawing Package*. Drawing Package ID 3925.

Holtec International, 2005a. *MPC Enclosure Vessel Licensing Drawing Package*. Drawing Package ID 3923.

Holtec International, 2005b. *MPC-32 Fuel Basket Assembly Licensing Drawing Package*. Drawing Package ID 3927.

Holtec International, 2005c. *MPC-68/68F/68FF Fuel Basket Assembly Licensing Drawing Package*. Drawing Package ID 3928.

Itasca, 2007. Itasca Consulting Group, Inc., 111 Third Avenue South, Suite 450, Minneapolis, MN 55401, http://www.itascacg.com

NWTRB, 2007. Nuclear Waste Technical Review Board, letter dated April 19, 2007.

5.4   Probabilistic Volcanic Hazard Analysis for the Yucca Mountain Region

5.4.1 Introduction

The probability of a volcanic hazard in the Yucca Mountain Region (YMR) is a critical factor in the overall assessment of a proposed geologic repository for high-level radioactive waste and spent nuclear fuel at Yucca Mountain. Before the U.S. Nuclear Regulatory Commission (NRC) grants a license to U.S. Department of Energy (DOE) for construction and operation of such a facility, DOE must demonstrate compliance with the U.S. Environmental Protection Agency (EPA) standards and conforming NRC regulations that establish, among other things, protective public dose limits over a defined timeframe. The final EPA standards for Yucca Mountain (40 CFR 197) released on October 15, 2008 call for consideration in the regulatory review process of

features, events, and processes with an annual probability of occurrence exceeding 10^{-8} per year. In Section 197.36 of this standard, EPA explicitly directs DOE to "...assess the effects of ... igneous scenarios, subject to the probability limits in paragraph (a) of this section for very unlikely features, events, and processes" that result from the igneous event intersecting the repository and damaging the waste packages such that radionuclides are released to the environment.

The probability of volcanic hazard at a specific location depends on the potential for occurrence of volcanic events in the future, and this is best evaluated based on the history of volcanic activity at that site. However, relevant past volcanic events in the YMR are rare in terms of frequency and periodicity. Infrequent basaltic volcanoes have occurred in the vicinity of the proposed Yucca Mountain repository site during the past 10 million years, as recognized in a 2007 report from the NRC's Advisory Committee on Nuclear Waste and Materials (ACNWM, 2007). The important question to be answered for repository performance assessments and, more specifically, the Yucca Mountain License Application review is, "How rare are these events?" Probabilistic volcanic hazard analyses (PVHA) provide an approach for answering this question.

DOE completed an initial PVHA study in 1996, which utilized a combination of group and individual expert elicitations to quantify the probability of volcanic disruption in the YMR. The DOE's performance assessment for the LA (OCRWM, 2008) has incorporated the mean probability value obtained in the DOE 1996 PVHA study of 1.7 x 10^{-8} per year (CRWMS M&O, 1996, pp. 4-1). As this value narrowly exceeds the regulatory threshold of 10^{-8} per year (NRC, 2005) for exclusion[4] from the YMP licensing review process, DOE is required to include the effects of igneous intrusion and eruption in its Total System Performance Assessment supporting the LA (TSPA-LA). Results from the TSPA-LA show igneous intrusion to be the dominant dose contributor to the reasonably maximally exposed individual (RMEI) at one million years.

In keeping with EPRI's focus on the most risk-important features, events, and processes that should be addressed to determine the "reasonable expectation" of repository performance (per 40 CFR 197), EPRI has sponsored its own expert elicitation based study to provide an independent analysis of the probability of volcanic hazard at Yucca Mountain. The results of this study were published in November 2008 as EPRI Report No. 1018059, "Independent Probabilistic Volcanic Hazard Analysis for the Yucca Mountain Region" (EPRI, 2008) Through this study, EPRI seeks a better understanding of volcanic hazard estimates for the YMR and the models and methodologies used to obtain such estimates. The volcanic hazard in question is the intersection of an ascending volcanic dike with the cross-sectional area (footprint) of the proposed repository at Yucca Mountain. This independent volcanic hazard analysis takes into account more recent geological and structural data published since the DOE 1996 PVHA. Although the scope of this effort was somewhat limited due to time constraints, EPRI considers the approach taken for this study and resulting probability estimates to be fit for purpose and on par with those reported for the individual Subject Matter Experts (SME) in the DOE's 1996 PHVA.

The DOE has also sponsored an update to the 1996 PVHA, the PVHA-U, which utilizes the same elicitation process used previously with a new panel of experts and incorporates relevant

---

[4] EPA's 40 CFR Part 197 standard for Yucca Mountain allows for the exclusion of extremely rare (a frequency of below 10^{-8} per year) events from performance assessment of long-term safety.

information obtained for the YMR since the 1996 study. The final PVHA-U report was not available at the time that EPRI's 2008 PVHA work was conducted.

5.4.2 Approach

The approach taken by the EPRI PVHA team to calculate the annual frequency of an igneous (volcanic) event intersecting the footprint of the proposed repository within the next 1,000,000 years follows the approach used in the DOE 1996 PVHA (CRWMS M&O, 1996)[5]. The calculation requires that an igneous event be well defined, including quantification of characteristic features and the identification of the factors governing the location and timing of a future igneous event in the YMR.

The probability calculation requires an understanding of a potential igneous event in the region of interest as well as an assessment of the spatial, temporal and geometric characteristics of the event. EPRI's independent PVHA study also considers the same new geochemical, geophysical, seismological, geodetic and age-dating data collected since DOE's initial 1996 PVHA report as has been addressed by the DOE's PVJHA-U team (*e.g.*, Brocher *et al.*, 1998; Day *et al.*, 1998; Perry *et al.*, 1998; Fridrich, 1999; Fridrich *et al.*, 1999; Potter *et al.*, 2002; 2004; Perry *et al.*, 2005; Valentine *et al.*, 2005; 2006; 2007; Parson *et al.*, 2006; Valentine and Krough, 2006; Valentine and Perry, 2006; 2007; Gaffney *et al.*, 2007; Perry, 2007; Valentine and Keating, 2007; Keating *et al.*, 2008). In particular, the EPRI calculation includes information from drilling (Perry *et al.*, 2005; Perry, 2007) and characterization, including dating, of various anomalous features identified by recent high resolution aeromagnetic surveys (O'Leary *et al.*, 2002; Perry *et al.*, 2005) buried under alluvial deposits that have been speculated to be additional volcanic centers (Perry *et al.*, 2004; Smith and Keenan, 2005).

This EPRI study also considers structural factors that demonstrably have controlled the actual eruptive location of volcanic centers that have occurred in the Yucca Mountain region in the last 12 million years (Valentine and Perry, 2006; 2007; Gaffney *et al.*, 2007; Keating *et al.*, 2008).

EPRI's Probabilistic Volcanic Hazard Assessment (PVHA) calculation is comprised of five steps:

1. Review recent data and develop EPRI's independent conceptual model for a potential igneous event in the YMR in the next 1,000,000 years.

2. Define and characterize EPRI's potential igneous event that may intersect the repository footprint.

3. Identify EPRI's region of interest and geometric characteristics of the potential igneous event.

4. Identify the time of interest and temporal pattern of events.

---

[5] The draft EPA regulations in effect in 1996 required the assessment to address the first 10,000 years following permanent repository closure, thus the DOE 1996 PVHA addressed potential volcanic events over only the next 10,000 years. The revised EPA standards recently released require the assessment of potential volcanic events to address the period extending 1,000,000 years following permanent repository closure. This is the time period addressed in the EPRI PVHA calculation.

5. Identify the factors that influence the spatial occurrence of a potential igneous event allowing for alternative spatial as well as temporal models.

Although acquisition and analysis of physical data are the primary methods of determining the probability of an igneous event intersecting the proposed repository, the complexity of the igneous process and limitations in knowledge of the process and related parameters requires the use of expert elicitation. Accordingly, each of these steps requires some degree of expert elicitation processes to obtain the information necessary to conduct a probabilistic volcanic hazard calculation for the YMR. The DOE has utilized the expert elicitation process in its volcanic hazard analyses and the NRC has formally recognized the role and value of the elicitation process in Yucca Mountain performance assessment and regulatory review (NUREG-1563, Kotra *et al*., 1996). The NRC describes expert elicitation as a process for incorporating expert judgment into defensible quantitative calculations. Recognition is given by the NRC for the potential for expert elicitation to support model building to complement and supplement other sources of scientific and technical information, such as data collection, analyses, and experimentation. In NUREG-1563, the NRC provides general guidance on when expert elicitation is appropriate, describes acceptable procedures for conducting expert elicitation in the context of the YMP and recommends its use in the Yucca Mountain high-level waste program.

EPRI has long taken an active interest in evaluating the potential for an igneous-event scenario impacting a repository at Yucca Mountain (EPRI, 1992; 1996). This project is a continuation of that interest.

5.4.3 The EPRI PVHA Expert Elicitation Process

In sponsoring its own independent PHVA study, EPRI sought to provide seeks to provide an independent, technically defensible analysis of the potential hazards to a repository at Yucca Mountain resulting from a volcanic event. The methodology employed in this PVHA study for EPRI is consistent with the systematic elicitation steps and procedures as presented in the US Nuclear Regulatory Commission's NUREG-1563 (Kotra *et al.*, 1996) and NUREG/CR-6372 (Budnitz *et al.,* 1997); the latter document was jointly sponsored by EPRI, DOE and NRC.

Elicitation sessions were performed during a period spanning from the beginning of April 2008 to the end of June 2008, allowing ample time for training and support of personnel, gathering and interpreting information, and numerous iterations of the elicitation process if needed.

5.4.4 Review of Data and Conceptual Model Development

5.4.4.1   Background Information (Step 1)

The first step in EPRI's development of an independent conceptual model includes the evaluation of trends in Yucca Mountain field data such as location of volcanoes in the YMR, geochemistry, eruption volume and lithostatic pressure as well as recent tectonic models. The recent (< 12 Ma) volcanism in the YMR, a region that extends north of the repository to the Timber Mountain caldera complex and south of the repository to Amargosa Valley (Figure 5-12), is characterized by a monogenetic eruption style (*i.e.*, single eruption at one eruptive center)

and basaltic composition of erupted material (Crowe *et al*., 1983; 1988). Polygenetic eruption (multiple eruptions over time at the same eruptive center) of more silicic material ended over 12 million years ago in southern Nevada, and are not relevant examples for future volcanism in the YMR. In the YMR, post-caldera basalt centers (< 12 Ma) are divided into four groups based on age and location (Table 5-5).

Table 5-5
Volcanic centers in the Yucca Mountain region that are considered in the development of EPRI's conceptual model of an igneous event.

Volcanic center	Estimated Age (Ma)	Volume (km³)
Group 1		
Western Crater Flat (RQ4T)	11.1	2.5
Kiwi Mesa	11	>2.5
Solitario Canyon	10.7 or 11.4	na
Dome Mountain	10.5	10.0
Skull Mountain	10.2 ±0.5	>2.5
Anomaly A	10.1	0.06
Jackass Flat	9.5	2.5
Little Skull Mountain	8.4 ±0.4	>2.5
Group 2		
Silent Canyon/Pahute Mesa	9.1 ±0.7**	>0.7**
Basalt Ridge	9.1±0.7 (2 sigma)	>0.07
East Basalt Ridge	8.8±0.1 (2 sigma)	>0.03
Scarp Canyon	8.7±0.3**	>1.0**
Frenchmen Flat	8.6	>1.0**
Paiute Ridge	8.58±0.07 (2 sigma)	>1.0**
Rocket Wash	8.0±0.2**	>1.0**
Nye Canyon (complex at least 3 events)	6.3±0.2 (youngest), 6.8 ±0.2; 7.2±0.2**	>1.0**
Group 3		
Anomaly C-D	4.8±0.005	0.190[d]
Thirsty Mesa	4.63±0.02[a]	2.28
Anomalies F-H	3.8±0.005	0.063
Anomaly B	3.8±0.005	1.227
Pliocene Crater Flat	3.71±0.02 [a]	0.56
Buckboard Mesa	2.87±0.06 [a]	0.84
Group 4		
Makani (Northern) Cone	1.076±0.026 [a]	0.005[b2]
Black Cone	0.986±0.047 [a]	0.061
Red Cone	0.977±0.027 [a]	0.055
NE Little Cone	0.78±0.045 [d]	0.014[b]
SW Little Cone	0.78±0.045 [d]	0.02[b]
Hidden Cone (SB)	0.373±0.042 [a]	0.07[c2]
Little Black Peak (SB)	0.323±0.027 [a]	0.03[c2]
Lathrop Wells	0.076 ±0.005 [a]	0.09[b]

[a] Valentine and Perry (2006) and Sawyer *et al*. (1994); [b] SNL (2007); [c] Valentine and Keating (2007); [d] PVHA-U workshop DOE; **Perry *et al*., 1998; [2] Valentine and Perry (2007).

Trace element chemistry provides a means of understanding where in the earth's mantle magma was generated and what processes were active during the generation and ascent of magma. The observed trend in trace element data (Ce to Yb isotopic ratios) in magma and eruptive volumes suggest that a future volcanic event will be at least similar to Group 4 (Farmer *et al.*, 1989; 1991; Perry *et al.*, 1998; Perry, 2007). Therefore, EPRI believes that the next igneous event, if one were to occur, would be similar in size (or smaller) and other characteristics to the Group 4 basalt centers that have previously occurred in the Yucca Mountain region.

Basaltic volcanism coincides with episodes of crustal extension in the area known as the Crater Flat domain (CFD) (Figure 5-12; Fridrich *et al.*, 1999). The CFD was one of the most active tectonic zones in the Great Basin before 11.6 Ma ago (Fridrich *et al.*, 1999). Rates of extension in the CFD since 11.6 Ma ago have followed a declining trend that continues to the present day. Volcanic centers in Groups 1-4 that are located within the CFD are all alkali basalt. The average volume of erupted material from volcanic centers within the four groups (Table 5-5) follows a declining trend that appears to correlate with the declining extension rate, indicating that CFD volcanism is waning and that the location of any future eruption would be southwest of the proposed location for the repository at Yucca Mountain. The trend in trace element geochemistry also supports the hypothesis that volcanism in the YMR is in a waning phase.

The potential location of a future igneous event is of prime interest for the probability calculation of an igneous event intersecting the proposed Yucca Mountain repository. Areas where extension has been highest in the CFD correlate strongly with the location of post-Miocene volcanism. The location of the proposed repository lies within the northeast (NE) area of the CFD that has experienced very little extension and no post-Miocene (< 10 Ma) volcanism; these observations indicate that the Yucca Mountain region is less prone to future eruptions than the southeastern (SE) portion of the CFD (see Figure 5-12).

Recent field studies sponsored by DOE (Valentine and Perry, 2006; Keating *et al.*, 2008) of basaltic centers in Group 3-4 suggest that magma from these volcanoes ascended through the near-surface crust through pre-existing faults. While magmas can ascend from the mantle via self-propagating dikes with sufficient driving pressures (Lister, 1990), recent numerical models (Gaffney *et al.*, 2007; Keating *et al.*, 2008) using pre-existing structure in the YMR have demonstrated that low-volume magmas cannot generate the pressure required to sustain a self-propagating dike approaching the surface. Therefore, low volume magmas in an extensional tectonic environment will favor a pre-existing pathway (fault) that is perpendicular (N30E) to the regional least compressive stress direction and has a dip that is 60° or greater (Gaffney *et al.*, 2007; Keating *et al.*, 2008).

Figure 5-12
The structural domains and boundaries of the Yucca Mountain region, including the Crater Flat Domain located west of the thick black line and portions of adjacent domains (taken from Fridrich (1999)).
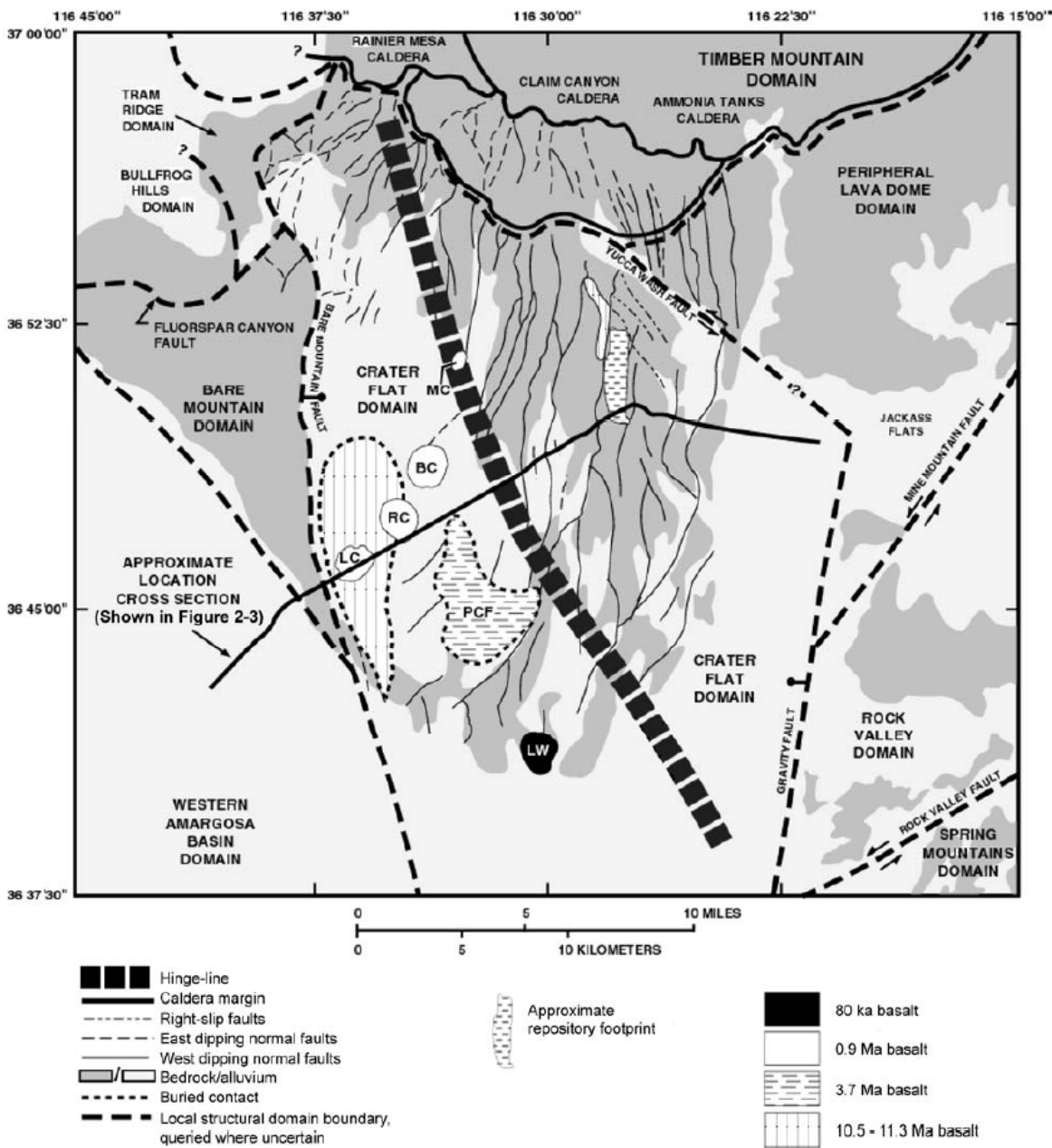
NOTE: Basalts of different ages are shown in relation to basin structure (modified from Fridrich et al. 1999, Figure 1). The 80-ka age of the Lathrop Wells volcano is from Heizler et al. (1999). MC = Makani Cone; BC = Black Cone; RC = Red Cone; LC = Little Cones; LW = Lathrop Wells volcano; PCF = Pliocene Crater Flat.

Lithostatic pressure is a governing parameter for evaluating the probability of the location of a future event. Lithostatic pressure is derived from free-air gravity data (Oliver *et al*., 1995) and provides information on topography and density of crustal materials (Turcotte and Schubert, 2002), including areas of topographic lows (basins and/or low-density material such as alluvial fill) and topographic highs (ridges or mountains) and higher density material (bedrock). Magma tends to erupt into low topographic areas and through low density material.

5.4.4.2 Conceptual Model (Step 1)

Also part of the first step in the EPRI PVHA study was the development of an independent conceptual model for volcanic activity in the YMR based on trends in field data that include geochemistry, eruptive volume, and location of Groups 1-4 volcanoes in the YMR, as well as tectonic modeling with the following features:

- Any eruption in the YMR in the next 1,000,000 years would occur within the SW region of the CFD, removed from the immediate vicinity of the proposed repository and along a pre-existing fracture oriented perpendicular (N30E) to the least compressive stress field of the region and with a dip angle near vertical. Extensional trends indicate that the NE region of the CFD that hosts the repository site is less prone to future eruptions than the SW region.

- The eruption would be alkali basalt, with eruption characteristics similar to Group 4 volcanoes located within the CFD typified by the Lathrop Wells basalt center.

- Magma would erupt at the surface first along a single fissure; subsequent activity would concentrate along a segment of the fissure initiating the development of a scoria cone and effusion of lava from its base. The source of magma would be from partial melting of the lithospheric mantle.

- The volume of magma would not be greater than the range of volumes for magmas related to the Group 4 Quaternary YMR volcanoes. The magma volume could be less than that of the Group 4 volcanoes based on the decreasing trend of eruptive volume with time.

- It is also conceivable that future partial melting of lithospheric mantle may be insufficient to produce a sufficient volume of magma that would be capable of reaching repository depth; thus one possible future scenario would include no eruptions in the YMR.

The EPRI PVHA team excluded other volcanic fields, such as the Lunar Crater and Cima volcanic fields, from its probability calculation as these do not meet the criteria for an appropriate analog as described in Appendix D of EPRI (2008). The criteria for an appropriate analog include: alkali basalt geochemistry with trace element chemistry, crystallinity, and volatile content similar to the basalts of the < 4.8 Ma YMR volcanoes; monogenetic eruption volumes less than 0.1 km^3; and an extensional tectonic setting.

5.4.4.3 Igneous Event Definition (Step 2)

For this study, the term "event definition" describes the expected characteristics of an igneous event that may intersect the repository footprint at the proposed depth of 300 m below the

surface of Yucca Mountain. The EPRI PVHA team defined its igneous event based on the type of volcanic event that may occur in the next 1 Ma. EPRI believes that the Crater Flat basalt centers younger than 1.1 Ma in age in Group 4 (Table 5-5) best represent characteristics of a possible future volcanic event in YMR (EPRI, 2004; 2005; 2007). A more detailed discussion of natural analogues and their application to PVHA is provided in Appendix D of EPRI (2008).

The EPRI PVHA team defines an igneous event in its probability calculation as a dike ascending from depths greater than 8-10 km. The characteristic features of an igneous event, including horizontal dike length and azimuth, would be similar to those from Group 4 basalt centers (those most appropriate as an analogue for a potential future igneous event) and other analog volcanoes in the area. DOE (Valentine *et al*., 2005; 2006; Keating *et al*., 2008) has conducted detailed field studies of Quaternary volcanoes in the YMR listed as Group 4 volcanoes in Table 5-5.

Table 5-6
EPRI's range of values for event parameters.

Dike length	0.6-2.4 km (1.8 km - mean)
Dike width	1-12 m (15 m maximum – swelling)
Number of dikes	1-2 (1 - mean)
Dike spacing	250-1500m
Dike orientation	Pre-existing N30E ± 15° faults

Dike length distributions and relative probabilities are determined from data collected from analog volcanoes in the YMR that include Groups 3 and 4 (Table 5-5). The expected event would most likely be a single dike with a length that ranges from 0.6 to 2.4 km (Table 5-6).

Dike widths at the repository level are expected to be less than 15 m (Table 5-6) and are considered to be negligible in the calculation relative to the model's spatial scale. In addition, refining the model's spatial scale would likely not increase the relevance of dike width significantly as dike length is many orders of magnitude greater than width.

Dike orientation is governed by the mechanics of magma transport through the lithosphere. In the YMR, evidence supports vertical dikes transporting magma to the surface for basalts that occurred since the Pliocene (Valentine and Perry, 2006; Gaffney *et al*., 2007), including that presented in Table 5-5. The DOE believes that the location of a future eruption in a waning volcanic system, such as in the Crater Flat basin, is controlled mainly by the magma source zone and structure (Valentine and Perry, 2006; Valentine and Keating, 2007). All Quaternary Crater Flat (Group 1) volcanoes have erupted on pre-existing faults. Therefore, as concluded by DOE, fault capture is an important mechanism for shallow magma ascent (Valentine and Perry, 2006).

Based on these DOE findings, the EPRI PVHA team believes that a future dike in the YMR would follow pre-existing faults oriented (N30E) perpendicular to the least compressive stress field of the region and with a dip angle near vertical. A fault map was used to generate a spatial model as a function of azimuth with areas with existing faults having higher probabilities than areas with no pre-existing faults. The EPRI approach represents an important departure from that used in the DOE 1996 PVHA. Experts involved in the 1996 PVHA considered that a dike could breach the surface anywhere in the YM region (*i.e*., all areas of the region are equally likely and pre-existing faults are not favored) and considered N30E as the most probable orientation (Table 5-6).

5.4.4.4 Region of Interest (Step 3)

Step 3 of EPRI's PVHA study involves defining the region of interest. Two areas of interest were defined by the EPRI PVHA team for its calculation, one large region and one smaller region (Figure 5-13). The larger region encompasses areas around the Yucca Mountain block in which the repository is located and includes Jackass Flat to the east, areas north such as Thirsty Mesa and Sleeping Buttes volcanoes, and areas south into the Amargosa Valley, and areas west bounded by the Bare Mountain fault (Figure 5-13, red box). The larger region is used by the EPRI PVHA team to evaluate each volcanic event in the YMR with respect to event definition and its relevant geometric characteristics for predicting a future igneous event. The smaller region considered by EPRI is essentially the Crater Flat structural domain (see Figure 5-12; Figure 5-13, yellow box) with boundaries defined by major faults: the Bare Mountain fault to the west, the Yucca Mountain fault to the north and the Gravity fault to the east as it is the area where the majority of volcanism in the YMR has occurred within the last 1 Ma. This smaller region delineates EPRI's area of interest for its temporal and spatial models.
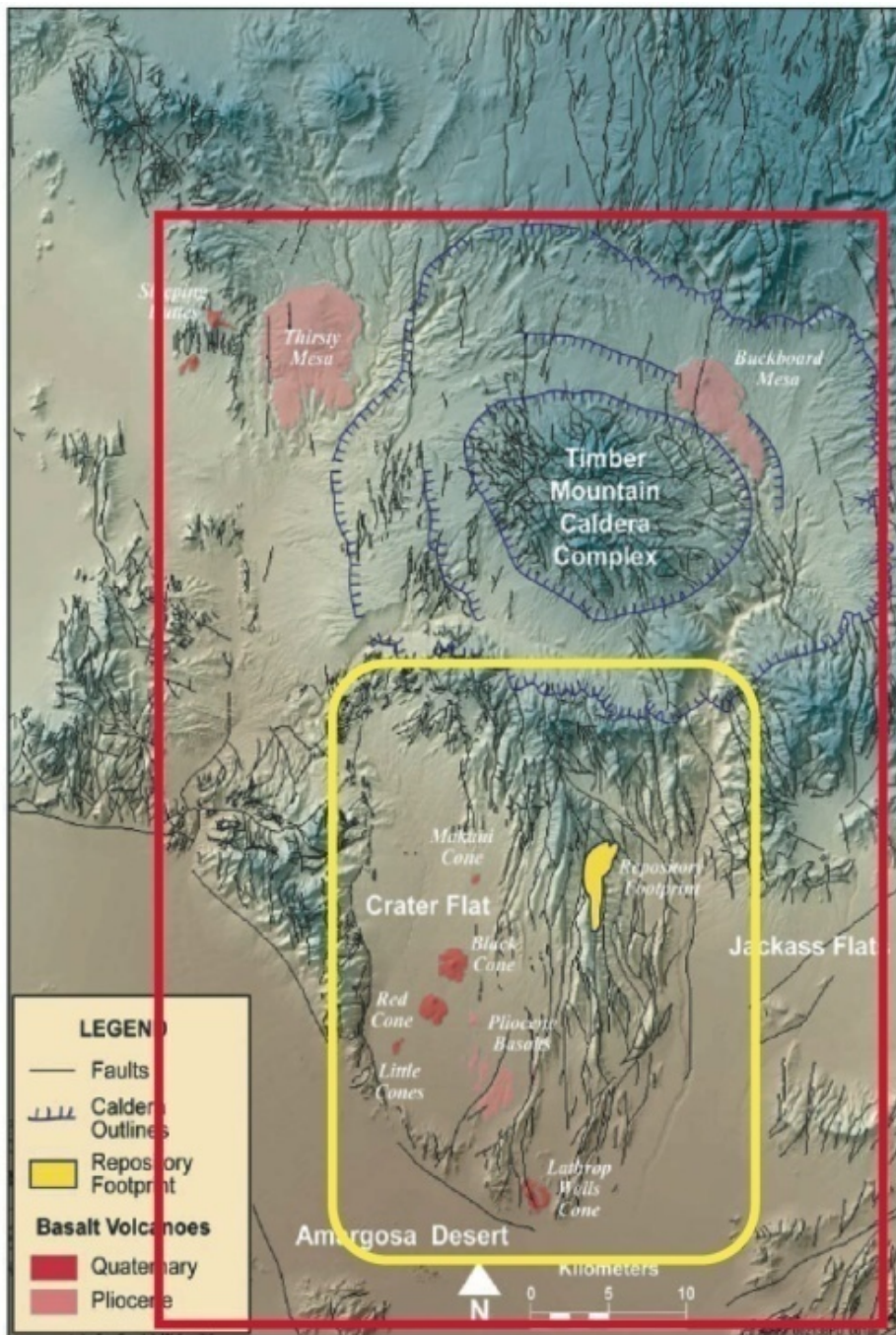
Figure 5-13
Region of interest defined by red box. The yellow box defines the area EPRI considers in its spatial models (adapted from OCRWM, 2008).

5.4.5 Model Structuring and Specification

The structuring and specification (quantifying variables and the relationships between variables) of the required temporal and spatial models derived from the EPRI conceptual require extensive expert input and iteration through the elicitation process. The EPRI elicitation process generally

employed a combination of two common approaches: (1) an assessment of a probability, or quantile, for a given value of the variable of interest (*e.g.*, asking for the probability that the next volcanic event will occur within the next million years), or (2) an assessment of a value of the variable of interest given a probability (*e.g.*, asking for the value, in years, at which there is an equal chance that a volcanic event will occur before or will occur after).

5.4.5.1   Temporal Models (Step 4)

The fourth step in the EPRI PVHA calculation involves the identification of temporal factors for igneous events. The EPRI PVHA study considers two temporal conceptual models. The Tectonic-Cluster model assumes that events are controlled by a regional tectonic event that initiates partial melting in the lithospheric mantle in one of the structural domains within the YMR that then initiates a period of igneous activity followed by a period of dormancy. The Fault-Initiated model assumes that expected events are associated with localized fault movement. The time of interest defines the rate of recurrence of an igneous event in the region of interest.

A logic tree illustrates the two temporal models considered in this study (Figure 5-14). Each node represents an aspect of the model. A single line between two nodes indicates that the right node is used without uncertainty, while a branching line indicates alternative models when the lines go to separate nodes or simply uncertainty in the parameters of the model when the branches go to the same node.
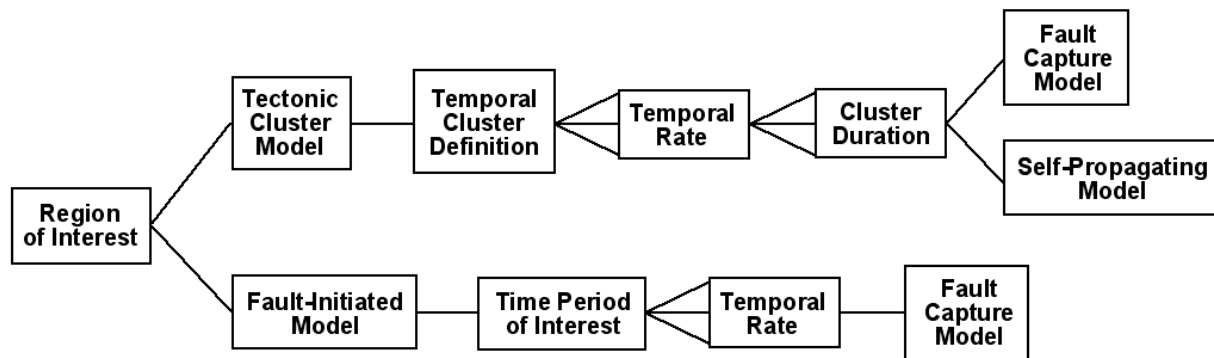
Figure 5-14
Logic tree for EPRI's temporal model for estimating the probability of an igneous event intersecting the proposed repository.

5.4.5.1.1   *The Tectonic-Cluster Temporal Model*

This model assumes that an igneous event is triggered by a regional tectonic event that initiates partial melting in the lithospheric mantle in one of the structural domains in the YMR. Cluster rate and duration are determined from the four clusters. The historical timeframe of interest extends back 1.1 Ma from the present. The two domains that seem to be most sensitive or active are the CFD and the domain that includes Group 2 basalt centers such as Pauite Ridge and Basalt Ridge.

Volcanic centers that are excluded from the clusters are: Rocket Wash, Buckboard Mesa and Thirsty Mesa as they are situated on a caldera ring fracture; Kiwi Mesa, Skull Mountain, and

Little Skull Mountain because they are located in a different structural domain (Rock Valley Domain, Figure 5-12) and have compositions that are more intermediate (andesitic) in character; Dome Mountain because it is an andesitic basalt and is located on a caldera ring fracture; and Nye Canyon basalts because they are primitive (more mafic) basalts and occur as a complex.

Table 5-7
Clusters recognized for the Tectonic-Cluster Temporal Model. Values in parentheses ( ) denote duration of volcanic cluster activity for Cluster 1 and Cluster 2 if Jackass Flat is considered in Cluster 2. Durations are used to assign relative probabilities to cluster duration. Sources of data are the same as those for Table 5-5.

Volcanic center	Estimated Age (Ma)	Duration (Ma)
Cluster 1		1.6 (1.0)
Western Crater Flat (RQ4T)	11.1	
Solitario Canyon	10.7 or 11.4	
Anomaly A	10.1	
Jackass Flat	9.5	
Cluster 2		0.5 (0.9)
Silent Canyon/Pahute Mesa	9.1 $\pm$0.7**	
Basalt Ridge	9.1$\pm$0.7 (2 sigma)	
East Basalt Ridge	8.8$\pm$0.1 (2 sigma)	
Scarp Canyon	8.7$\pm$0.3**	
Frenchmen Flat	8.6	
Paiute Ridge	8.58$\pm$0.07 (2 sigma)	
Cluster 3		1.1
Anomaly C-D	4.8$\pm$0.005	
Anomalies F-H	3.8$\pm$0.005	
Anomaly B	3.8$\pm$0.005	
Pliocene Crater Flat	3.71$\pm$0.02 [a]	
Cluster 4		1.0
Makani (Northern) Cone	1.076$\pm$0.026 [a]	
Black Cone	0.986$\pm$0.047 [a]	
Red Cone	0.977$\pm$0.027 [a]	
NE Little Cone	0.78$\pm$0.045 [d]	
SW Little Cone	0.78$\pm$0.045 [d]	
Lathrop Wells	0.076 $\pm$0.005 [a]	

The Tectonic-Cluster model is characterized by periods of roughly constant volcanic activity followed by periods of dormancy. The event times during the period of roughly constant activity are assumed to follow a homogeneous Poisson process, with the duration of the active period modeled separately. The EPRI model considers the age of volcanic events to estimate the timing of the next volcanic event. Four distinct episodes of volcanic activity are recognized and are referred to as clusters. These clusters are defined in Table 5-7 as Clusters 1-4. Cluster 4 is the one that is most relevant to future event in the YMR. The duration of the Cluster 4 volcanic activity is defined by two cluster situations: either the cluster is still active or it has recently gone dormant. If active, then the periodicity of volcanic activity within the cluster (Cluster 4) is used to predict future events. If dormant, then the periodicity between each of Clusters 1-4 is considered sufficiently long that a new cluster is unlikely to be initiated within the next 1 Ma. The current tectonic cluster is considered to initiate with the Makani cone event. Thus, 6 events are considered representative of the current tectonic cluster: Makani Cone; Black Cone; Red

Cone; Southwest Little Cone; Northeast Little Cone; and Lathrop Wells. The oldest of these is Makani Cone, dated at 1.076 Ma. More detail on the Tectonic-Cluster model is provided in EPRI (2008).

5.4.5.1.2   Fault-Initiated Temporal Model

This model assumes that each event is triggered or associated with fault motion as postulated for the eruptive event at Lathrop Wells (Parson *et al*., 2006). Although the rate of extension in CFD has been constant and fairly low relative to the past 10 Ma, field measurements have indicated that fault movement in CFD has been episodic over the past 0.5 Ma. Volcanoes in Groups 3 and 4 located in CFD are considered in this model. The historical time frame of interest spans a 1 Ma period beginning 4.8 Ma before the present. The recurrence rate is determined from the data shown in Table 5-7.

The Fault-Initiated model assumes a relatively constant rate of fault motion over the last 4.8 Ma, and thus event times are modeled as a homogeneous Poisson process over this period of time. Eleven events were considered representative within the region of interest: Anomaly C; Anomaly D; Southeast Crater Flat; Anomaly B; Anomalies F, G, and H (considered one event), Black Cone, Red Cone, Makani Cone, Southwest Little Cone, Northeast Little Cone, and Lathrop Wells. The oldest of these is Anomaly C, dated at 4.8 Ma (Table 5-7). EPRI (2008) provides a detailed discussion of the Fault-Initiated model and its application.

5.4.5.1.3   Elicited Temporal Rate Information

To complete the temporal model, a characterization of the possible dormant state is needed to capture the possibilities that: (1) the CFD may have gone dormant with the Lathrop Wells event; (2) the CFD may have gone dormant following that volcanic event; or (3) it may become dormant within the next 1 Ma. The elicited normal model implies that the probability that the volcanic system had already gone dormant is about 0.54, which supports the directly elicited value of 0.55 given above. Use of a value from the distribution other than 0.55 has no effect on the overall probability of volcanic hazard at 1 Ma because the system is dormant by that time.

A key parameter for elicitation is the relative likelihood of the two models; that is, how much better is one model believed to represent the CFD volcanic regime than the other. This value was elicited as a 3:1 ratio in favor of the Fault-Initiated model over the Tectonic-Cluster model, which corresponds to a 0.75 probability that the Fault-Initiated model better explains the volcanic activity. The value of 0.75 was used as a median value for the branch probability. The Tectonic-Cluster model branch was assigned a corresponding probability of 0.25. More detail on the elicitation of temporal rate information is provided in EPRI (2008).

5.4.5.2   Spatial Model (Step 5)

The fifth step in the EPRI PVHA calculation process involves the identification of the factors that influence the *spatial occurrence* of a potential igneous event allowing for alternative spatial, as well as temporal, models. Two spatial models are considered for the EPRI analysis: a Fault Capture model, and a Self-Propagating Dike model. A logic tree illustrates the two spatial

models considered in this study (Figure 5-15). This figure extends from the temporal model presented in Figure 5-14. A single line between two nodes indicates that the right node is used without uncertainty. A branching line between two nodes indicates that the right node is used with uncertainty.
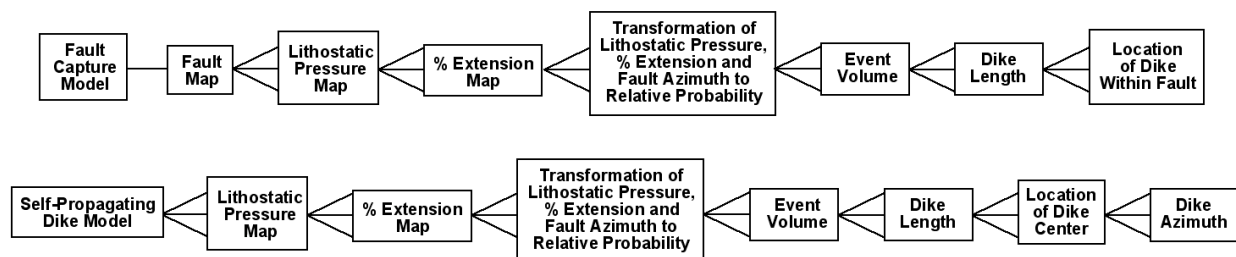
Figure 5-15
Logic tree for EPRI's spatial model for estimating the probability of an igneous event intersecting the proposed repository.

5.4.5.2.1   Fault Capture Model

The Fault Capture Model is based on recent DOE studies that demonstrate low volume (< 1.0 km^3) magmas tend to ascend through the crust along the path of least resistance (Parson *et al.*, 2006; Valentine and Perry, 2006; 2007; Gaffney *et al.*, 2007; Keating *et al.*, 2008). Initially, magma will migrate through the lithosphere as a self-propagating dike following a direction, N30E in the YMR, perpendicular to the regional least compressive stress direction. As the dike approaches the surface, it will intersect and follow a fracture with a similar orientation (N30E) and a steep dip angle (> 60°). In the Fault Capture Model, only pre-existing faults are considered as possible locations for dikes. Relative probabilities are assigned to faults that have been mapped in the Yucca Mountain region (Potter *et al.*, 2002; Day *et al.*, 1996) with the consideration of fault orientation relative to the regional stress field (Stock *et al.*, 1985).

The EPRI expert team considers lithostatic pressure to be a governing parameter for evaluating the probability of the location of a future event. EPRI's conceptual Fault Capture model assumes that the lowest range of lithostatic pressure corresponds to areas with the highest likelihood for an event to occur, whereas the highest positive values (mountains and ridges) denote areas with the least likelihood for an event to occur. Intermediate lithostatic pressure values are assigned intermediate relative probabilities via elicitation.

Extension rate is a third governing parameter that the EPRI expert team uses to evaluate the probability of the location of a future event in its Fault Capture model. EPRI uses the total cumulative extension measured through the CFD. Areas with the highest relative probability values are those where extension has been highest over the last 10 Ma, which corresponds to the western region of Crater Flat basin. Areas with the lowest relative probability values correspond to areas that have experienced the lowest percentage of extension over the last 10 Ma.

5.4.5.2.2   Self-Propagating Dike Model

The Self-Propagating Dike model assumes magma will ascend in a self-propagating dike that will reach the surface with little influence from the pre-existing structure or topography. The

dike will follow a path that is perpendicular to the least compressive stress direction. The probability distribution for event azimuth is assigned with respect to the regional stress field. This alternative model accounts for the uncertainty of an event that may not follow the Fault Capture model. A similar approach was used by the DOE's experts in the elicitation process in the 1996 PVHA where a probability distribution for event orientation is assigned with respect to the regional stress field. This model also considers lithostatic pressure and cumulative extension data in its evaluation of the location of a potential future event. The same relative probability models used for lithostatic pressure and extension in the Fault Capture model are applied to the Self-Propagating Dike model.

For the Self-Propagating Dike model, extension and lithostatic pressure are the only factors that determine the location of a dike. Each grid cell in the map within the region of interest is assigned a probability based on normalizing the relative probabilities that are generated in the previous step. This probability map is used directly to evaluate the probability that a dike intersects the repository.

5.4.5.3   Elicitation of Extension and Lithostatic Pressure Maps

The elicited extension and lithostatic pressure maps formed the basis of the spatial modeling component of the model. In the simulations, values of extension and lithostatic pressure were obtained for each 1 km by 1 km grid cell. These values were used to predict the probability of a dike in the cell based on the relationships described in EPRI (2008; Section 4.3) that relate extension and pressure to probability of formation of a dike.

5.4.5.4   Elicitation of the Non-Common Variables for Spatial Models

The Fault-Initiated temporal model is consistent only with the Fault Capture spatial model. For the Tectonic-Cluster temporal model, the Self-Propagating Dike model is also considered plausible. The Self-Propagating Dike model assumes that sufficient pressure is built up such that magma will ascend in a self-propagating dike that is not affected by pre-existing structure or topography. The dike in this model will follow a path that is perpendicular to the least compressive stress direction. The Fault-Initiated model, instead, forms dikes that follow the path of least resistance associated with faults in the existing fault structure.

The spatial models were evaluated for relative likelihood in the same way that the temporal branches were evaluated. The relative likelihood of the Fault Capture model was elicited to be 50 times greater than that of the Self-Propagating Dike model. Consequently, the conditional probability of the Fault Capture model was set at 0.9804. The conditional probability of the Self-Propagating Dike model was set at a corresponding probability of 0.0196.[6]

---

[6] This section presents certain intermediate probability values using up to four significant figures in order to accurately reflect the ratios through which these values were elicited. Such precision should not be interpreted as a reflection of the true precision of the values or confidence in those values. Final probabilities are presented using two significant figures.

5.4.6 Results from Combined Simulations

The results from combined simulations accounting for the probabilities assigned to the three possible branches (summarized in Table 5-8), are described here. EPRI (2008) provides an in depth discussion of individual elements and simulation results. The Fault-Initiated temporal model with Fault Capture is the largest contributor with a probability of 0.75. The Tectonic-Cluster temporal model with Fault Capture is the next largest contributor with a probability of 0.2451. Third in prominence is the Tectonic-Cluster temporal model with Self-Propagating Dikes with a probability of 0.0049. The net effect of the model branches and the current tectonic cluster being complete gives a probability of 0.1375 that the rate is zero at the 10 ka time period and a probability of 0.25 that the rate is zero at the 1 Ma time period. Summary statistics for the model outputs are given in Table 5-9. The results are provided for 10 ka and 1 Ma, since those are the primary timeframes of interest for performance assessments and regulatory compliance. However, the time dependency of the Tectonic-Cluster model generates results that can vary with time (Figure 5-16).

Table 5-8
Probabilities assigned to the three temporal-spatial branches considered in EPRI model.

Temporal Model and Probability	Spatial Model and Probability	Probability for Combined Temporal and Spatial Model Branch
Fault-Initiated 0.75[a]	Fault Capture 1.0000	0.75
Tectonic-Cluster 0.25	Fault Capture 0.9804[b]	0.2451
	Self-Propagating Dike 0.0196	0.0049

[a]Probability derived from elicitation of a 3:1 preference for the Fault-Initiated temporal model.
[b]Probability derived from elicitation of a 50:1 preference for the Fault Capture spatial model.

Table 5-9
Summary statistics for annual frequency of intersection.

	5th Percentile	First Quartile	Median	Mean	Third Quartile	95th Percentile	99th Percentile
Fault-Initiated							
10 ka or 1 Ma	1.97E-09	2.88E-09	3.68E-09	3.85E-09	4.63E-09	6.30E-09	7.71E-09
Tectonic-Cluster, Fault Capture							
10 ka (unconditional)	0	0	0	3.87E-09	7.33E-09	1.38E-08	1.91E-08
10 ka (conditional on >0)	2.99E-09	5.46E-09	7.77E-09	8.49E-09	1.07E-08	1.64E-08	2.16E-08
Tectonic-Cluster, Self-Propagating Dike							
10 ka (unconditional)	0	0	0	5.68E-09	1.08E-08	2.02E-08	2.81E-08
10 ka (conditional on >0)	4.40E-09	8.01E-09	1.14E-08	1.24E-08	1.57E-08	2.41E-08	3.15E-08
Combined Simulation							
10 ka	0	2.52E-09	3.60E-09	3.88E-09	4.86E-09	8.72E-09	1.48E-08
1 Ma	0	1.18E-09	3.16E-09	2.90E-09	4.27E-09	6.04E-09	7.51E-09

6.2.1 Comparison with the Regulatory Threshold

EPRI's PVHA calculation yields an annual frequency of intersection that is significantly lower than the established regulatory threshold of 1×10^{-8}. As can be seen from Figure 5-16 and Table 5-9, for a time 10,000 years after repository closure, EPRI's estimate for igneous-event probability ranges from a 5th percentile of 0.0 to a 95th percentile of 8.72×10^{-9} per year, with a mean value of 3.88×10^{-9} per year. The probability decreases over time, and at 1,000,000 years after repository closure, the estimate for igneous-event probability ranges from a 5th percentile of 0.0 to a 95th percentile of 6.04×10^{-9} per year, with a mean value of 2.90×10^{-9} per year. The decrease in probability values between 10,000 and 1,000,000 years (Figure 5-16) is attributable to the time-dependent influence of EPRI's Tectonic-Cluster Temporal model (*i.e.*, events triggered by regional tectonic episode) imposed on the baseline of the Fault-Induced Temporal model.
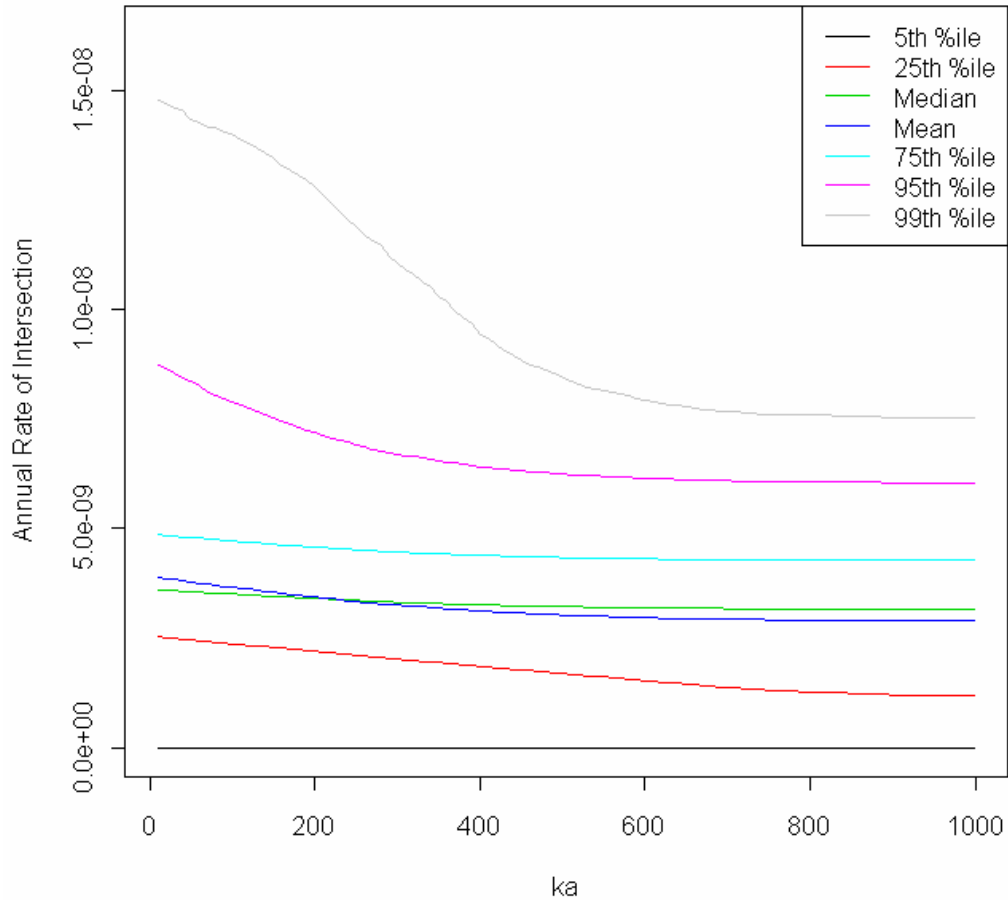
Figure 5-16
Summary statistics (composite annual frequency of intersection) of the full combined simulation results, as a function of time.

5.4.7 Comparison with the DOE 1996 PHVA

As illustrated in Figure 5-17, EPRI's calculated annual frequency of intersection is an order of magnitude lower than the aggregated mean value of the probability of intersection reported in DOE's 1996 PVHA. The results from the 1996 PVHA are presented in an aggregate probability distribution that defines the annual frequency of intersection of an igneous event through the footprint of the repository as a mean value of 1.5×10^{-8} (5.4×10^{-10} and 4.9×10^{-8} at the 5th and 95th percentiles, respectively).
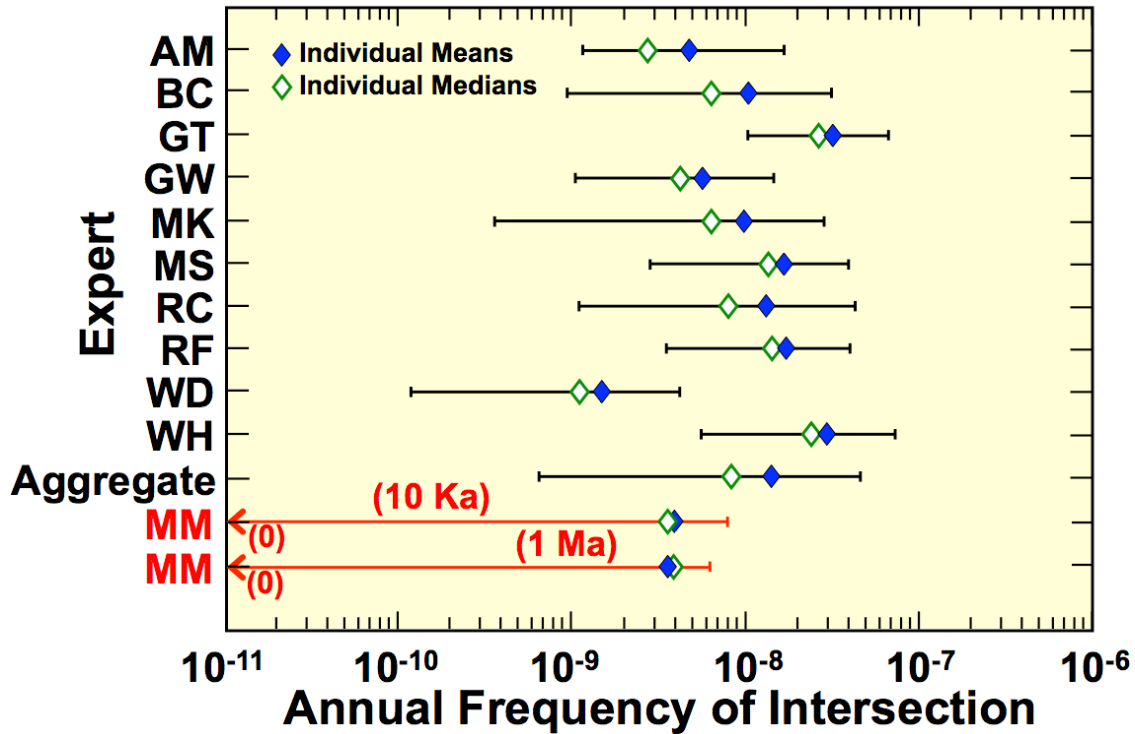
Figure 5-17
Comparison of EPRI's PVHA Calculation with the DOE's 1996 PVHA Results (Modified from CRWMS M&O, 1996). [AM=Dr. Alexander McBirney, U. Oregon; BC=Dr. Bruce Crowe, LANL; GT=Dr. George Thompson, Stanford U.; GW=Dr. George Walker, U. Hawaii; MK=Dr. Mel Kuntz, USGS; MS=Dr. Michael Sheridan, State U of NY; RC=Dr. Richard Carlson, Carnegie Institute of Washington; RF= Dr. Richard Fisher, U. California, Santa Barbara; WD=Dr. Wendell Duffield, USGS; WH= Dr. William Hackett, WRH Associates; Aggregate=Combination of all DOE 1996 PHVA experts results; MM=Dr. Meghan Morrissey, Colorado School of Mines; EPRI PVHA expert.] Note: DOE 1996 PVHA results are for the first 10,000 years of post-closure period only.

While the EPRI calculation follows the 1996 PVHA framework (CRWMS M&O, 1996), it is fundamentally different in several important aspects:

- The calculation is based on the more recent geological and structural data obtained by the DOE.

- EPRI's temporal model allows for time-dependence rather than treating the 1,000,000 years as static.

- EPRI's spatial models do not rely explicitly on the locations of existing igneous events but rather on the geologic characteristics of the region that indicate propensity for future igneous activity.

- The Fault Capture spatial model is simulated explicitly using fault maps rather than approximated by probability distributions for dike azimuth across the region.

- The Fault Capture spatial model is considered a more realistic description of igneous activity relative to the Self-Propagating Dike model and, therefore, receives greater weighting.

Without studying each model from the DOE 1996 PVHA in detail (*i.e.,* running the actual model and performing sensitivity analyses, which are outside the scope of this study), it is not possible to positively identify and rank the underlying factors contributing to the differences between PVHA models and results. Except for the final probability estimates, the results are generally not directly comparable. For example, where a larger region of interest is used, it is likely that the temporal rate of events is higher while the spatial rate is lower. However, some substantive differences can be identified, particularly with regard to new data and the use of structural information.

5.4.7.1   New Data

A considerable amount of new data has become available since the DOE 1996 PVHA. Figure 5-17 shows a summary of the DOE 1996 PVHA experts' selections of values or functions used in their PVHA calculations. Many of these values might be improved and uncertainty reduced (likely, but not necessarily) by incorporating the new data. However, new data can also lead to revision of the models used in the PVHA. Model revision based on new information can also lead to increases or decreases in uncertainty.

The definition of an event can be updated based on recent data. For the DOE 1996 PVHA calculations, a volcanic event is defined as a spatially and temporally distinct batch of magma ascending from the mantle as a dike or a dike system plus the eruptive products. Spatially, it is the midpoint of the dike system line element (length, azimuth and location). An event length is defined as the total length of a dike system or the total distance of aligned vents observed at the surface. Recent DOE field studies of dike-conduit relationship (Valentine and Perry, 2006) at basaltic volcanoes < 4.8 million years old in the Yucca Mountain region demonstrate that each basaltic cone represents a single eruption characterized by a single dike, scoria cone and lava flow field.

In most models (including all of the 1996 PHVA models and EPRI's present model), a longer event length or dike system length has a higher probability of intersecting the repository than shorter event lengths. Some DOE 1996 PVHA experts assumed Crater Flat Quaternary vents represent one event. The width and number of dikes defining the system do not contribute to the DOE 1996 PVHA. The DOE 1996 PHVA experts agreed that the orientation of dikes is N30E with a length distribution having 0.6 km as the 5th%, 10.1 km as the 95th%, a maximum of 17-50 km and 4.0 km as the mean (CRWMS M&O, 1996). Some DOE experts considered a bimodal probability distribution to reflect the influence of the local stress field and vent alignment. Many DOE experts assumed that many of the cones in the region align and, therefore, form a buried fissure from which the experts constrain the event length. Based on the more recent DOE field studies, event lengths so defined are now recognized to be artificial; therefore the DOE 1996 PVHA results appear to overestimate the probability of an igneous event intersecting the repository.

At the time of the DOE 1996 PVHA study, there were several buried aeromagnetic anomalies identified and not yet studied in sufficient detail to determine whether or not they were volcanic events. As such, the experts in the DOE 1996 PVHA used a hidden event factor to probabilistically adjust the number of volcanic events in the region for use in establishing the temporal rate. Most of the major anomalies were subsequently investigated to provide a better

basis for establishing an historical event count for the region. Keeping other factors constant, the uncertainty in the temporal rate has decreased for data-driven models, such as EPRI's.

For the DOE 1996 PVHA, event counts have a high degree of uncertainty for each volcanic event used by the different experts because of the limited available field data related to eruptive history of each volcanic center in the YMR. For example, basalt centers in the northern Crater Flat area (referred to in the DOE 1996 PVHA as 1.0 Ma Crater Flats), which include Makani Cone, Black Cone, Red Cone, SW and NE Little Cones), are considered by DOE's experts as an event represented by a weighted probability as one to seven event counts, with the majority of experts considering it to represent a single event (Tables 3-1:3-11 in CRWMS M&O, 1996). The uncertainties related to poorly constrained data increase the annual frequency of intersection (CRWMS M&O, 1996). Event counts factor into the recurrence rate of an event, which is an extremely sensitive parameter in the DOE 1996 PVHA calculation (CRWMS M&O, 1996). Detailed field studies performed by DOE since the DOE 1996 PVHA (Valentine *et al.*, 2006) now indicate igneous events < 4.8 million years old should be counted as single events with a much lower degree of uncertainty. Similar studies at other basaltic volcanoes in the Yucca Mountain region (summarized in SNL, 2007) have improved the understanding of volcanism in the area and have improved confidence in hazard models. Based on the recent DOE field studies, event counts in the DOE 1996 PVHA incorporate uncertainty that can be significantly reduced in DOE's presently on-going PVHA calculation, PVHA-U. EPRI considers all the new data and interpretations of the volcanic history in the YMR over the past 5 Ma in its PVHA calculation as illustrated by the incorporation of data in development of the EPRI conceptual model (EPRI, 2008, Section 3, Tables 3-1 and 3-2).

5.4.7.2   Structural Information

The biggest fundamental difference between EPRI's model and the DOE 1996 PVHA models lies in the use of structural information. Some experts in the DOE 1996 PVHA use structural information (*e.g.,* in construction of zonation models), but the structural information is not utilized throughout their analyses. EPRI's model restricts attention to a structurally bounded region (Bare Mountain Fault, Yucca Mountain Fault, and Gravity Fault), while some DOE 1996 PVHA experts incorporate a much broader region that includes the other structural domains adjacent to the CFD. For the spatial models, many of the DOE 1996 PVHA experts use some type of proximity models. That is, the spatial probabilities are driven (at least in part) by the location of previous volcanic events via a spatial smoothing model. The spatial smoothing can assign high probability to a location near a previous volcano regardless of the underlying structure of that location. EPRI's spatial model does not use a proximity model, but rather utilizes data that reflect relevant conditions at a given location. Finally, EPRI's model utilizes the structural aspect of existing faults for dike propagation, while all of the DOE 1996 PVHA models utilize self-propagating dikes for placing an event.

The Fault Capture model is the most distinguishing feature of the EPRI PVHA model. While the model does allow for some unrestricted dike locations via the Self-Propagating Dike model, the structural constraints of the Fault Capture model are a feature not captured by the DOE 1996 PVHA models. The proposed site of the Yucca Mountain repository was originally chosen in part due to the lack of faults that intersect the Yucca Mountain block (Brocher *et al.*, 1998). For low-volume events that are likely to utilize pre-existing faults, the choice of this low-fault location should indeed induce lower risk from volcanic intrusion. Results presented in Table 5-9

show a marked difference in the annual rate of intersection for the structurally unrestricted Self-Propagating Dike model and the structurally constrained Fault Capture model. The rate is lower when the structural constraints are imposed.

Full-scale sensitivity analyses of the EPRI model were beyond the scope of this study and were not performed. However, some preliminary analyses were performed with respect to the fault map, which was implemented without uncertainty. Uncertainty was not incorporated primarily because no good mechanism is available for simulating new fault maps adhering to existing structural constraints. In addition, it is deemed conservative (*i.e.*, leading to a higher probability of intersection) to utilize the map as given due to the potential biases in data collection. The geology of the Yucca Mountain block has been studied extensively. The Crater Flat region has been studied to a lesser extent due, in part, to the extensive surficial alluvial deposits that make fault mapping more difficult. EPRI's PVHA subject-matter expert considered it likely that the fault map under-represents the number of faults in the western, southern, and eastern portions of the map. Adding a new fault to the map that does not intersect the repository leads to a lower overall rate of intersection, while adding a fault that *does* intersect would increase the overall rate. EPRI's SME considers that, due to the extensive characterization of the Yucca Mountain block, the probability of an omitted fault within the repository boundary is small, whereas there are likely a large number of omitted faults that lie outside of the repository boundary. In light of this, the estimate of the probability of intersection developed by the EPRI PVHA team is considered to be conservative.

5.4.8 Conclusions

The independent analysis performed by a team commissioned by EPRI has generated some new insights into the PVHA for Yucca Mountain. The EPRI PVHA study supports the view that reasonable and appropriate PVHA estimates for a Yucca Mountain repository should be based on use of appropriate volcanic analogues and geological information from the YMR. Probability estimates influenced by analogue information from outside areas are of debatable relevance to the specific tectonic-volcanic setting of the YMR. The analysis of recent geologic data indicates that smaller, structurally constrained volcanic events are the most appropriate analogues for the YMR PVHA. Incorporation of this recent information leads to an estimate of the probability of intersection of an igneous event with the repository footprint (for similar temporal rates) that is significantly below the regulatory threshold of 10^{-8} per year established in 40 CFR 197. The EPRI model provides estimates that are similar to the estimates of many of the individual experts participating in DOE's 1996 PVHA but the model also suggests that the DOE estimate of the overall volcanic hazard to the proposed repository may be overstated.

5.4.10 References

ACNWM (Advisory Committee on Nuclear Waste and Materials), 2007. *Igneous Activity at Yucca Mountain: Technical Basis for Decision Making*. Presentation to the US NRC, Washington, DC. pp. 241.

Brocher T., Hunter W., Langenheim, V., 1998, Implications of seismic reflection and potential field geophysical data on the structural framework of the Yucca Mountain–Crater Flat region, Nevada, Geological Society of America Bulletin, v. 110; no. 8; p. 947–971.

Budnitz, R. J., G. Apostolakis, D. M. Boore, L. S. Cluff, K. J. Coppersmith, C. A. Cornell, and P. A. Morris, 1997. *NUREG/CR-6372, Recommendations for Probabilistic Seismic Hazard Analysis: Guidance on the Use of Experts*; US NRC and Lawrence Livermore National Laboratory, Washington, D. C. and Livermore, CA.

Crowe, B., S. Self, D. Vaniman, R. Amos, and F. Perry, 1983. "Aspects of potential magmatic disruption of a high level radioactive waste repository in southern Nevada," *Journal of Geology*, 91, 259.

Crowe, B., C. Harrington, L. McFadden, F. Perry, S. Wells, B. Turrin and D. Champion, 1988. *Preliminary Geological Map of the Lathrop Wells Volcanic Center*, LA-UR-88-4155.

CRWMS M&O (Civilian Radioactive Waste Management System Management and Operating Contractor), 1996. *Probabilistic Volcanic Hazard Analysis for Yucca Mountain, Nevada*. BA0000000-01717-2200-00082 REV 0. Las Vegas, Nevada: CRWMS M&O. ACC: MOL.19971201.0221.

Day, W.C., C.J. Potter, D.S. Sweetkind and W.R. Keefer, 1996. "Structural Geology of the Central Block of Yucca Mountain," Chapter 2-I of *Seismotectonic Framework and Characterization of Faulting at Yucca Mountain, Nevada*. Whitney, J.W., ed. Milestone 3GSH100M. Denver, Colorado. U.S. Geological Survey. TIC: 237980. ACC: MOL.19970129.0041.

Day, W.C., R.P. Dickerson, C.J. Potter, D.S. Sweetkind, C.A. San Juan, R.M. Drake II, and C.J. Fridrich, 1998. "Bedrock Geologic Map of the Yucca Mountain Area, Nye County, Nevada." *Geologic Investigations Series* I-2627. Denver, Colorado: U.S. Geological Survey. ACC: MOL.19981014.0301.

EPRI, 1992. "Volcanic Occurrences" in *Demonstration of a Risk Based Approach to High Level Waste Repository Evaluation: Phase 2*, Electric Power Research Institute, Palo Alto, CA: 1992. TR-100384.

EPRI 1996. "Probabilistic Volcanic Hazard Assessment at Yucca Mountain," in *Yucca Mountain Total System Performance Assessment, Phase 3*, Electric Power Research Institute, Palo Alto, CA: 1996. TR-107191.

EPRI, 2004. *Potential Igneous Processes Relevant to the Yucca Mountain Repository: Extrusive -Release Scenario, Analysis and Implication*, Electric Power Research Institute, Palo Alto, CA: 2004. 1008169.

EPRI, 2005. *Potential Igneous Processes Relevant to the Yucca Mountain Repository: Intrusive-Release Scenario*, EPRI Report 1011165, Electric Power Research Institute, Palo Alto, CA.

EPRI, 2007. *Yucca Mountain Spent Fuel Repository Evaluation, 2007 Progress Report*, Electric Power Research Institute, Palo Alto, CA: 2007. 1015045.

EPRI, 2008. *Independent Probabilistic Volcanic Hazard Analysis for the Yucca Mountain Region*, Electric Power Research Institute, Palo Alto, CA: 2008. 1018059.

Farmer, G. L., F. V. Perry, S. Semkin, B. Crowe, D. Curtis and D. J. DePaolo, 1989. "Isotopic evidence on the structure and origin of subcontinental lithospheric mantle in southern Nevada," *J. Geophysical Research*, V. 94, p 7885-7898.

Farmer, G. L., D. Broxton, R. Warren and W. Pickthorn, 1991. "Nd, Sr and O isotopic variations in metaluminous ash-flow tuffs and related volcanic rocks at the Timber Mountain/Oasis Valley caldera complex, SW Nevada – Implications for the origin and evolution of large-volume silicic magma bodies," *Contributions to Minerology and Petrology*, V: 109, 53-68.

Fridrich, C.J., 1999. "Tectonic Evolution of the Crater Flat Basin, Yucca Mountain Region, Nevada." Chapter 7 of *Cenozoic Basins of the Death Valley Region*. Wright, L.A. and Troxel, B.W., eds. Special Paper 333. Boulder, Colorado: Geological Society of America. TIC: 248054.

Fridrich, C.J., J.S. Whitney, M.R. Hudson and B.M. Crowe, 1999. "Space-Time Patterns of Late Cenozoic Extension, Vertical Axis Rotation, and Volcanism in the Crater Flat Basin, Southwest Nevada." Chapter 8 of *Cenozoic Basins of the Death Valley Region*. Wright, L.A. and Troxel, B.W., eds. Special Paper 333. Boulder, Colorado: Geological Society of America.

Gaffney, E.S., B. Damjanac and G. Valentine, 2007. "Localization of volcanic activity: 2. Effects of pre-existing structure," *Earth and Planetary Science Letters*, 263, no.3-4 p. 323-338.

Keating, G.N., G.A.Valentine, D. Krier, F.V. Perry, 2008. "Shallow plumbing systems for small volume basaltic volcanoes," *Bull. of Volcanology*, vol. 70: 563-582.

Kotra, J.P., M.P. Lee, N.A. Eisenberg, and A.R. DeWispelare, 1996. *Branch Technical Position on the Use of Expert Elicitation in the High-Level Radioactive Waste Program*, NUREG-1563, U.S. Nuclear Regulatory Commission, Washington, D.C..

Lister, J.R., 1990. "Buoyancy driven fluid fracture: the effects of material toughness and of low-viscosity precursors," *Journal of Fluid Mechanics*, 210, 263-280.

Liu, J. S., 2001. *Monte Carlo Strategies in Scientific Computing*, Springer-Verlag, New York, New York.

NRC, 2005. Rule Making Issue SECY 05-0144, Proposed Rule: 10 CFR 63, Implementation of a Dose Standard after 10,000 Years, NRC, Washington, D.C.

O'Leary, D.W., E.A. Mankinen, R.J. Blakely,V.E. Langenheim, and D.A. Ponce, 2002. *Aeromagnetic expressions of buried volcanoes near Yucca Mountain, Nevada*, U.S. Geol. Surv. Open File Report, 02-020.

OCRWM (Office of Civilian Radioactive Waste Management), 2008. *Total system performance assessment model/analysis for the license application Vol. 1*. MDL-WIS-PA-000005 REV00. Las Vegas, NV.

Oliver, H.W., Ponce, D.A., and Hunter, W.C., eds., 1995, *Major results of geophysical investigations at Yucca Mountain and vicinity, southern Nevada*, U.S. Geological Survey Open-File Report 95-74, 184 p.

Parson, T., G.A. Thompson and A.H. Cogbill, 2006. "Earthquake and volcano clustering via stress transfer at Yucca Mountain, Nevada," *Geology*, 34: 785-788.

Perry, F.V., A.H. Cogbill and R.D. Oliver, 2004. "Reducing uncertainty in the hazard of volcanic disruption of the proposed Yucca Mountain radioactive waste repository using a high-resolution aeromagnetic survey to detect buried basaltic volcanoes in alluvial-filled basins," *Geol. Soc.Am.* Abstr. Programs, 36(5), 33.

Perry, F.V., 2007. "Response to Expert Data Requests and Examples of Geologic Data incorporated into Hazard Models," presentation at Probabilistic Volcanic Hazard Analysis Update Workshop 4, May 2007.

Perry, F.V., A.H. Cogbill and R.E. Kelley, 2005. "Uncovering buried volcanoes at Yucca Mountain: new data for volcanic hazard assessment," *Eos*, Trans. Am. Geophys. Union 86: 485-488.

Perry, F.V., B.M. Crowe, G.A. Valentine, and L.M. Bowker, 1998. *Volcanism Studies: Final Report for Yucca Mountain Project*, Los Alamos National Laboratories, LA-13478, Tables 1.2, 2.A and 2.B.

Potter C.W., D. Day, D.S. Sweetkind and R.P. Dickerson, 2004. "Structural geology of the proposed site area for a high-level radioactive waste repository, Yucca Mountain, Nevada," *Geological Society of America Bulletin*, v. 116; no. 7/8; p. 858–879.

Potter C.W., R.P. Dickerson, D.S. Sweetkind, R.M. Drake, E.M. Taylor, C.J. Fridrich, C.A. San Juan and D. Day, 2002. "Geologic map of the Yucca Mountain region, Nye County, Nevada," U.S. Geological Survey Geologic Investigations Series Map I-2755, scale 1:50,000, p. 37.

Sawyer, D., R. Fleck, M. Lanphere, R. Warren, D. Broxton and M. Hudson, 1994. "Episodic caldera volcanism in the Miocene southwestern Nevada volcanic field: Revised stratigraphic framework, 40Ar/39Ar geochronology and implication for magmatism and extension," *Geological Society of America Bulletin*, V. 106: 1304-1318

SNL (Sandia National Laboratory), 2007. *Characterize eruptive process at Yucca Mountain, Nevada*, ANL-MGR-GS-000002 REV03. Las Vegas, NV. pp. 6.3-23

Stock, J.M., J.H. Healy, S.H. Hickman, and M.D. Zoback, 1985. "Hydraulic fracturing stress measurements at Yucca Mountain, Nevada, and relationship to the regional stress field," *Journal of Geophysical Research.*, *90*(B10), 8691-8706.

Turcotte, D.L. and G. Schubert, 2002. *Geodynamics 2nd Edition*. Cambridge University Press, 456 pp.

Valentine, G., F. Perry, D. Krier, G. Keating, R. Kelley, and A. Coghill, 2006. "Small volume basaltic volcanoes, eruptive products and processes, and post eruptive geomorphic evolution in Crater Flat (Pleistocene) southern Nevada," *GSA Bulletin* 118:1313-1330.

Valentine, G.A, D.J. Krier, F.V. Perry and G. Heiken, 2005. "Scoria cone construction mechanisms, Lathrop Wells volcano, southern Nevada," *Geology* 33:629-632.

Valentine G.A, D.J. Krier, F.V. Perry, and G. Heiken, 2007. "Eruptive and geomorphic processes at the Lathrop Wells scoria cone volcano," *Jour. Volcanology and Geothermal Res*, 161:57-80.

Valentine, G.A. and F. Perry, 2006. "Decreasing magmatic footprints of individual volcanoes in waning basaltic field," *Geophys. Research Letters*, 33:L14305.

Valentine, G.A. and F. Perry, 2007. "Tectonically controlled, time-predictable basaltic volcanism from a lithospheric mantle source (central Basin and Range Province, USA)," *Earth and Planetary Science Letters* 261, 201–216

Valentine, G.A. and G. Keating, 2007. "Eruptive styles and inferences about plumbing systems at Hidden Cone and Little Black Peak scoria cone volcanoes (Nevada, USA)," *Bull. of Volcanology* DOI10.1007

Valentine, G.A. and K.E. Krough, 2006. "Emplacement of shallow dikes and sills beneath a small basaltic volcanic centers – The role of pre-existing structure (Pauite Ridge, southern Nevada, USA)," *Earth and Planetary Science*, 246: 217-230.

Valentine, G.A., 2006, "Igneous scenarios," Presented at DOE/NRC Technical Exchange on Total System Performance Assessment (TSPA) for Yucca Mountain, Las Vegas, NV.

5.5   Processes Limiting Igneous Intrusive Impacts

5.5.1 Introduction

This section presents a quantitative assessment of the expected behavior of lava inside an emplacement drift at the proposed repository at Yucca Mountain. The objective of this work is to address a number of assumptions that have been made regarding the performance of magma within drifts at the proposed Yucca Mountain repository during the course of an igneous intrusive event. More specifically, this section discusses whether: (1) all drifts are rapidly filled with magma following an intersection of a dike with a drift; (2) all waste packages in drifts are engulfed in magma; and (3) the waste packages contacted by magma are damaged and fail, providing no protection for the waste from groundwater (SNL, 2007, Section 5.1). DOE chooses to use the term magma in reference to the behavior of gas depleted magma that at the surface would be referred to as lava. EPRI uses the term lava to refer to gas depleted (< 1 wt% H_2O) magma instead of referring to it as magma. In this section, the two terms are used interchangeably.

Results from EPRI's analysis demonstrate how pulses of lava entering a drift would extend only a limited distance from the point of entry and contact only a small number of waste packages,

thus significantly attenuating recent bounding estimates of the effects of igneous intrusion on peak dose rate.

In the unlikely event that an igneous dike intersected the proposed repository, EPRI has analyzed the expected behavior of lava inside emplacement drifts filled with nuclear waste packages based on characteristic features of lava flows observed at Quaternary Crater Flat (QCF) volcanoes and theoretical lava cooling models. EPRI described the geologic setting and physical volcanology of many of the volcanic centers in the Crater Flat Volcanic Zone (CFVZ) in its 2004 and 2007 technical reports (EPRI, 2004; 2007) based on recent field studies conducted by DOE, (Valentine *et al.*, 2005; 2006; 2007; Valentine and Perry, 2006). The DOE studies focused on five Quaternary Crater Flat volcanoes (Red Cone, Black Cone, Little Cones and Makani Cone) that provided detailed descriptions of the eruptive deposits, eruption processes and emplacement mechanisms.

There are several major features that all five Quaternary basalt centers share, including a scoria cone, one to two lava fields, lava flows containing rafted sections of the scoria cone, and pyroclastic deposits (Table 1 in Valentine *et al.*, 2006). The eruptive products (lava and pyroclastics) are interpreted to have erupted from a single source area near the base of the cone and not from multiple distributed vents (Valentine *et al.*, 2006). Quaternary volcanoes in CFVZ (Table 5.7-1) are comprised of a single pyroclastic cone (scoria cone) with one or two lava flows extending from the base. The lava flow fields associated with Quaternary scoria cones in CFVZ all appear to extend from the base on a scoria cone and to be composed of lava terraces (Valentine *et al.*, 2006). The implication of lava extending from the base on the scoria cone is that venting of volcanic material is concentrated along a single segment of a fissure and not multiple vents and fissure segments (Valentine and Perry, 2006). EPRI uses these data to construct a conceptual model for its analysis of lava entering a drift. The analysis by EPRI follows a similar approach used to evaluate the cooling history of lava flowing inside a lava tube. EPRI believes that the lava tube system is an appropriate analog for evaluating the lava-drift system as long as the depth of the repository is considered in the assessment.

5.5.2 Conceptual Model

EPRI's conceptual model is based on the eruptive history at Lathrop Wells and other QCF volcanoes. As illustrated in Figure 5-18, a single dike is expected to reach the surface producing a fissure eruption that quickly transitions to a cone building and conduit developing Strombolian event and contemporaneous effusion of lava. For modeling purposes, a drift is inserted at the repository depth allowing EPRI to analyze the conditions of lava entering the drift environment.
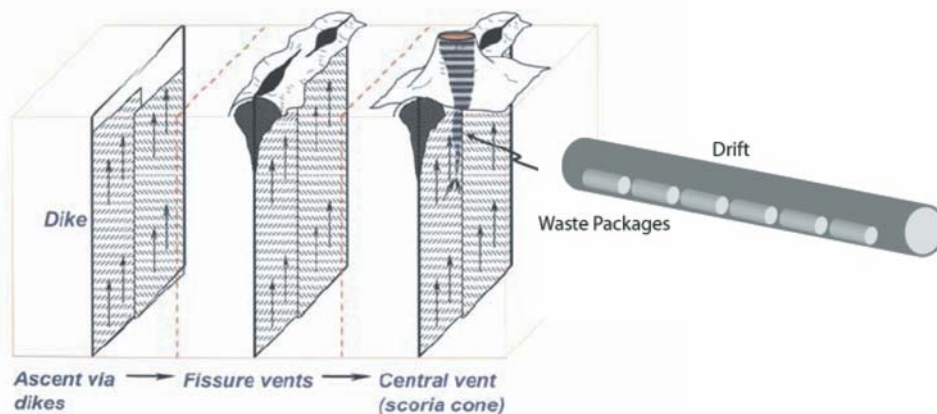
Figure 5-18
Conceptual model of an expected dike propagating to the surface and intersecting a drift (adapted from Valentine, 2006).

Field observations of Quaternary lava flow fields provide constraints on flow conditions from the fissure/dike. Lava terraces and lava ridges are two features common to all Quaternary lava fields associated in the Yucca Mountain area (Valentine *et al.*, 2006). Lava terraces are step-like features in the Quaternary lava flows that form by multiple pulses of lava from the same source (Valentine *et al.*, 2006). The periodicity of lava pulses is sufficiently long to allow the previous lava flow to cool and form multiple benches or terraces (Valentine *et al.*, 2006, p. 1321). These features suggest that lava effusion is not a continuous process but an intermittent process characterized by pulses of lava.

5.5.3 Numerical Method

EPRI quantitative analysis for evaluating the expected flow behavior of lava inside a drift follows the approach developed for evaluating the cooling history inside a lava tube (Keszthelyi, 1995). The lava tube system is an appropriate analog for the lava-drift system as long as conditions at repository depth are considered.

The lava tube approach (Keszthelyi, 1995) evaluates and quantifies various modes of heat transfer that may act on a lava flow inside a lava tube (Figure 5-19). In Figure 5-19, the main heat loss mechanisms inside a lava tube include boiling of rainwater, thermal erosion of the walls and floor, atmospheric convection in the porous wall rock, radiation from an opening to the surface (skylight), degassing, and conduction. The main heat input mechanisms are latent heat from crystallization and viscous dissipation.
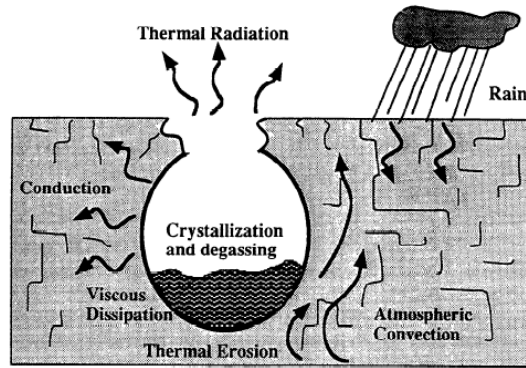
Figure 5-19
Sketch of different heat transfer mechanisms that work on lava inside a lava tube (from Figure 1 in Keszthelyi, 1995).

In the case of lava entering a repository drift, only four of the heat mechanisms are applicable, degassing, conduction, viscous dissipation and latent heat. Rain is not expected to reach the drift and, therefore, is neglected in the calculation. Thermal erosion (extracting the latent heat of fusion) is also neglected following the arguments made by (Keszthelyi, 1995) that "for any reasonable erosion rate ($\partial h / \partial t \ll 1 m / day$), the direct heat loss through thermal erosion is completely trivial." Air convection through the wall rock is neglected given the low permeability expected for the drift walls ($< 10^{-11}$ m^2, (Detournay et al., 2003)), yielding a low Rayleigh number (< 10) and negligible convection (Keszthelyi, 1995). Thermal radiation is also neglected because the calculations assume the diameter of the lava flow is equal to the diameter of the drift.

Degassing is neglected in the lava tube model calculation because lavas are essentially depleted in volatiles as they ascend to and erupt at the surface. In the case of lava inside a drift, once the lava has decompressed from conditions of the dike (~10 MPa) to conditions inside the drift (0.1 MPa), lava will be essentially degassed.

In the lava-drift system, three heat transfer mechanisms act on the lava as it flows down the drift: conduction, viscous dissipation and crystallization. Each of these terms is defined in the thermal budget (Equation 5-1). The thermal budget model for the lava-drift system assumes that the area lava moves into is circular and that lava enters the drift under steady state flow conditions. These assumptions yield the following thermal budget equation (Keszthelyi, 1995):

$$Q_{cond} = Q_{visc} + Q_{xstal}.$$ **eq. 5-1**

Where, Q_{cond} is the conduction term and is calculated assuming a buried hot pipe in an infinite half space expressed by (Keszthelyi, 1995):

$$Qcond = 2\pi \Delta T\, k / \cosh^{-1}(2ho/D + 1)$$ **eq. 5-2**

Where ΔT is the temperature differential between lava and wall rock, k is thermal conductivity of the wall rock, h_o is the depth of buried pipe (drift), D is pipe (drift) diameter (Keszthelyi, 1995). Q_{visc} is the viscous dissipation term and is defined as:

$$Q_{visc} = \rho_l \, g \, \psi \, \frac{\partial z}{\partial x} \qquad \text{eq. 5-3}$$

Where ρ_l is the density of lava, g is gravity, ψ is the volumetric flow rate, and $\delta z/\delta x$ is pipe (drift) slope (Keszthelyi, 1995). Q_{xstal} is the crystallization term that accounts for latent heat from cooling and crystallization defined by:

$$Q_{xstal} = \frac{\delta T}{\delta x} \, \psi \rho_l \left(C_p + L \frac{\delta X_c}{\delta T} \right) \qquad \text{eq. 5-4}$$

Where, $\delta T/\delta x$ is the cooling rate with distance inside the pipe (drift), C_p is heat capacity of lava, L is latent heat of crystallization of lava, and $\delta X/\delta T$ is the increase in volume fraction of crystals per degree of cooling (Keszthelyi, 1995). The three modes of heat transfer are assumed to be constant with respect to time. This assumption is conservative and will contribute to underestimating the cooling rate of lava inside a drift.

For the purpose of evaluating the flow behavior of lava inside a drift, Equation 5-1 is solved for the cooling rate with the distance ($\delta T/\delta x$) in Equation 5-5 with direct substitution of Equations 5-2 and 5-3 for Q_{cond} and Q_{visc}, respectively:

$$\frac{\delta T}{\delta x} = (Q_{cond} - Q_{visc}) / \psi \rho_l \left(C_p + L \frac{\delta X_c}{\delta T} \right) \qquad \text{eq. 5-5}$$
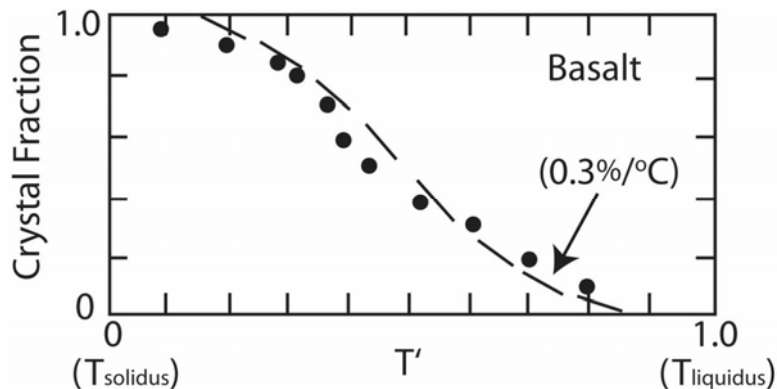
Figure 5-20
Crystal volume fraction (*X*) as a function of temperature *T' (= T-T$_s$/T$_l$-T$_s$)* adapted from Figure 5b in (Marsh, 1981). Arrow denotes line segment for d*X/dT* selected for the calculation. The dashed line is the analytical function fitted to experimental data (Marsh, 1981).

Table 5-10 lists the values that are used in the cooling with distance calculation (Equation 5-5). The temperature difference is obtained from the eruption temperature (975-1,010°C for QCF basalts (Nicholis and Rutherford, 2004)), and the bulk temperature of the wall rock (25-100°C, (EPRI, 2004)). Values for thermal properties for the magma or lava for alkali basalts in Yucca Mountain are from Table 1-2 in Detournay et al. (2003). The effective diameter of the drift is assumed to be 3.2 m to account for the presence of waste packages. Neglecting the presence of the waste packages would result in an underestimation of the magma temperature loss down the length of a drift as the relatively cold waste packages (as compared to the temperature of the

magma) will absorb a significant amount of heat from the lava. The drift is assumed to be essentially flat and a slope of 0.1% is assumed. One of the parameters that the calculation is quite sensitive to is the fraction of crystallization per degree of cooling ($\delta X/\delta T$). The value for $\delta X/\delta T$ is strongly dependent on temperature (Figure 5-20) ranging up to ~0.70%/°C at temperatures midway between the solidus and liquidus, and ~0.30%/°C at temperatures approaching the solidus and liquidus (Marsh, 1981; Wright and Okamura, 1977). A value of 0.3%/°C is used because the temperature of lava will decrease by 20°C as it decompresses upon entering a drift.

5.5.4 Results

Results from Equation 5-5 are plotted (Figure 5-21) in terms of cooling with distance as a function of volumetric flow rate using values listed in Table 5-10. The solid line (Figure 5-21) shows the cooling trend for lava as it flows down the length of the drift in the absence of waste packages (solid line). The trend of the line indicates that high flow rates allow lava flows to lose less heat with distance due to latent heat being the dominant mode of the three heat transfer mechanisms in the model. In contrast, Figure 5-21 suggests that slow moving lava flows tends to cool faster along shorter distances due to the higher heat loss into the surrounding wall rock than the gain from latent heat of crystallization. The dashed lines in Figure 5-21 show the effect of the presence of waste packages inside a drift. The waste packages have a thermal conductivity that is one order of magnitude greater than wall rock (Table 5-10) allowing more heat (an order of magnitude more) to be removed from the lava flow than by the wall rock over the same distance. Because lava will be in contact with waste packages as it flows in a drift, the interpretation of lava flow behavior is based on the cooling rate distances associated with waste packages (dashed line Figure 5-21).

Table 5-10
Values for parameters applied to thermal budget calculation for magma (lava) entering a drift including references for the source of value.

Parameter	Unit	Value	Source
Temperature contrast, DT	°C	975	(EPRI, 2004)
Thermal conductivity of (dry) wall rock, k	W/m K	1.2	(Detournay et al., 2003)
Thermal conductivity of waste package	W/m K	14.42	(BSC, 2005)
Depth of drift, h_o	M	300	(EPRI, 2004)
Diameter of drift with packages, D	M	3.2	(EPRI, 2004)
Lava density, r_l	kg/m^3	2200	(Detournay et al., 2003)
Gravity, g	m/s^2	9.81	
Drift slope, dz/dx	%	0.1	(Keszthelyi, 1995)
Heat capacity of lava, C_p	J/kg K	1100	(Detournay et al., 2003)
Latent heat of lava, L	kJ/kg	350	(Harris and Rowland, 2001)
Crystal fraction with cooling, dX/dT	%/°C	0.30	(Marsh, 1981; Wright and Okamura, 1977)
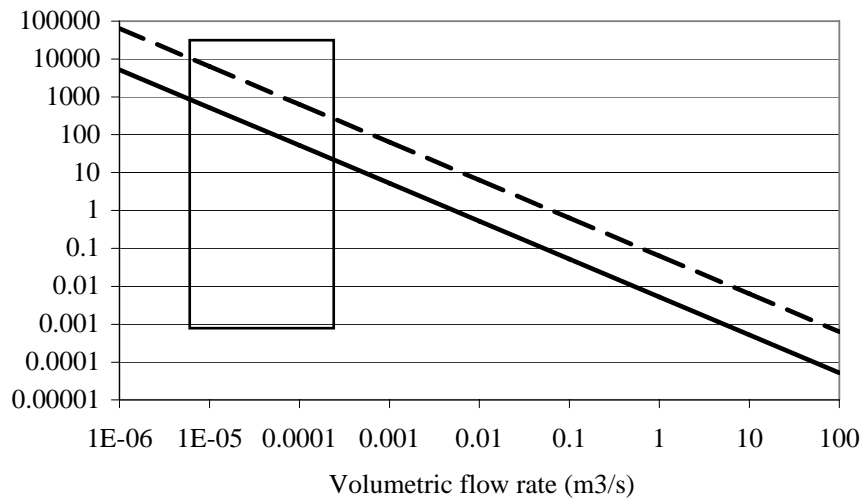
Figure 5-21
Cooling distance of lava inside a drift as a function of volumetric flow rate and *dX/dT* calculated from Equation 5-5 (log-log scale). The solid line is for lava in contact with wall rock (1.2 W/m-K); the dashed line is for lava in contact with waste packages (14.42 W/m-K). As the lava cools and continues to crystallize, the volumetric flow rate will decrease limiting the flow length of the lava. The box defines the anticipated conditions inside a drift at YM.

5.5.5 Discussion

The lava cooling distance values expected inside a repository drift are inferred from Figure 5-21 from the volumetric flow rate. The volumetric flow rate of lava entering a drift is estimated by considering the analytical relationship between eruption rates and flow lengths as shown in Figure 5-22 (Kilburn, 2000). Expected eruption rates (volumetric flow rates) for future basaltic lavas at the surface in the Yucca Mountain region are obtained from lava flow lengths observed in Lathrop Wells and other Quaternary lavas in the Crater Flat region (Table 1 in Valentine and Perry, 2006). Observed lava flow lengths in Quaternary Crater Flat basalt flow fields range between 0.4 and 1.8 km that according to Figure 5-22, correspond to volumetric flow rates on the scale of 0.001-0.1 m^3/s.

Lower volumetric flow rates are expected at repository depth than at the surface when decompression effects are considered. In general, magma decompresses inside a dike as it approaches the surface and releases volatiles once it erupts onto the surface. Lathrop Wells and Quaternary Crater Flat basaltic lava flows are assumed to have erupted onto the earth's surface with minimum decompression. Lava (referring to magma containing < 1 wt. % H_2O) that enters a drift would decompress from 7-10 MPa (lithostatic pressure) as it enters a drift. Rapid decompression of lava from 7-10 MPa with a volatile content of < 1 wt.% would result in undercooling ($20°C$), which in turn would result in decompression degassing and crystallization (Sparks and Pinkerton, 1978) at the point of entry into the drift. According to Figure 5-23 (note arrows), degassing and crystallization would increase the viscosity of lava entering the drift and decrease the volumetric flow rate inside the drift. For instance, alkali basalt typical of an expected eruption in Yucca Mountain would contain approximately3-5% phenocrysts prior to entering the drift and would have a viscosity on the order of10^2 Pa-s. Magma undergoing decompression from 7-10 MPa to 0.1 MPa upon entering a drift would experience cooling of approximately$20°C$ and would lose on the order of 1 wt.% H_2O via degassing (Sparks and Pinkerton, 1978).
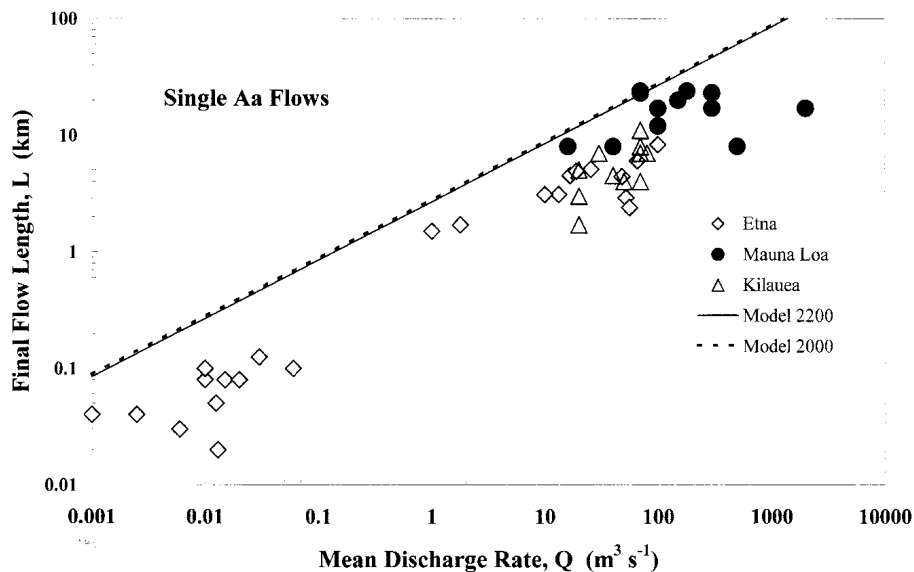
Figure 5-22
Final lava flow length as a function of discharge or effusion rate measured at Etna and Hawaiian volcanoes (Figure 8b in (Kilburn, 2000). Lava flow lengths observed at Quaternary volcanoes in Crater Flat are < 0.4-1.8 km (Valentine and Perry, 2006) that yield eruption rates of 0.001-0.1 m^3/s.

Undercooling basalt 20°C would increase the crystallinity to 10-20% (Figure 5-20) and would increase the viscosity 1-2 orders of magnitude (10^3-10^4 Pa-s). Increased viscosity would decrease the flow velocity of lava in the drift in the vicinity of the point of entry as described by the expression for the maximum flow velocity (*u*) in a pipe (Equation 6-34 in Cas & Wright, 1987):

$$u_{max} = \frac{R^2 dp}{4\mu\, dx},$$ **eq. 5-6**

where R is pipe radius, dp/dx pressure gradient and μ is viscosity. The decrease in flow velocity will decrease the volumetric flow rate by a similar magnitude in the drift. Under such conditions, volumetric flow rates of 0.001-0.00001 m^3/s are expected inside a drift with corresponding cooling with distance values of 100-1000°C/km (Figure 5-23). Eruption temperatures can be expected to drop 20°C upon entering a drift due to decompression degassing., Consequently, this cooling plus the cooling with distance rates described above indicate that lava experiencing decompression and degassing will approach its solidus temperature (950°C) within 5-150 m if the dependency of viscosity on temperature and crystallization are not considered. Incorporating the temperature and crystallinity dependences of viscosity results in accelerated cooling distance, resulting in a trend of decreasing volumetric flow rate (Figure 5-23). Together, these arguments suggest in-drift lava flow lengths on the order of 10 m.

In line with EPRI's views, the Advisory Committee on Nuclear Waste and Materials (ACNWM, 2007) stated in their final report on "Igneous Activity at Yucca Mountain: Technical Basis for Decision Making," that "the major factors in determining risk from the intrusive scenario, in addition to the probability of the event, are the number of waste packages affected by the intruding molten rock (magma) (determined by the viscosity of the magma …" (p. xi). The ACNWM believes that the flow rate of magma inside a drift "strongly depends on the magma viscosity and the rate of solidification as it contacts the relatively cold drip shield, waste packages and drift walls" (ACNWM, 2007). Recent work by Marsh and Coleman (2006) demonstrates that magma viscosities expected for a future igneous event at Yucca Mountain would be several orders of magnitude greater than previously assumed by DOE and that would reduce the rate of magma entry into drifts. The ACNWM also states that "the potential critical effects of quenching and solidification on waste packages and drift walls have not fully been evaluated by DOE or NRC" (ACNWM, 2007; p.31). The ACNWM provides a detailed discussion on their viscosity analysis in Section 6.2.1.2 in their report and concludes that magma (lava) at YM region will be wet, relatively immobile basalts (ACNWM, 2007).
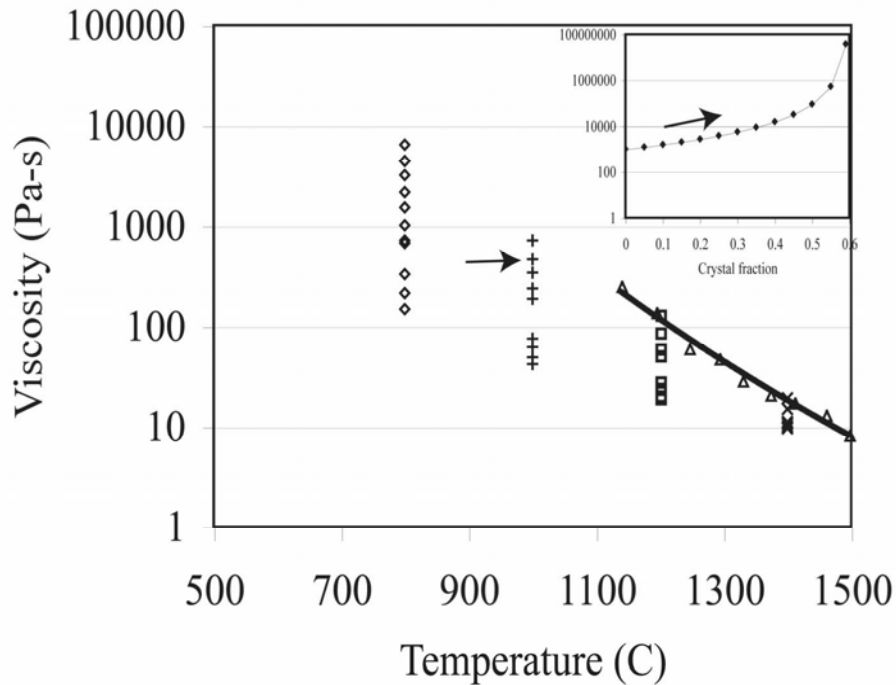
Figure 5-23
Viscosity as a function of temperature and H$_2$O content for crystal -free basaltic magma (Griffiths, 2000). Inset is viscosity as a function of crystal content at 1,000°C calculated using Einstein-Roscoe equation with a crystal free starting viscosity denoted by the arrow (EPRI, 2005). Y-axis log scale.

5.5.7 Conclusions

The expected behavior of in-drift lava at Yucca Mountain has been evaluated by EPRI using the approach of (Keszthelyi, 1995) for assessing the thermal budget inside a lava tube. This approach evaluates and quantifies various modes of heat transfer that may act on a lava flow inside a lava tube. The main heat loss mechanisms inside a lava tube include atmospheric convection in the porous wall rock, radiation, thermal erosion, boiling of water, degassing, and conduction. The main heat input mechanisms are latent heat from crystallization and viscous dissipation. For lava entering an emplacement drift, each mechanism from the model is evaluated to determine its applicability to the drift.

Three modes of heat transfer are assumed to occur inside the drift: conduction, viscous dissipation and latent heat crystallization yielding a thermal budget (Keszthelyi, 1995). For the purpose of evaluating the flow behavior of lava inside a drift, the thermal budget has been solved for the cooling with the distance from the lava entry point . Low volumetric flow rates are expected inside a drift because as lava enters a drift it will decompress from 7-10 MPa to 0.1 MPa. Rapid decompression of magma with < 1 wt.% H$_2$O results in 20°C undercooling (Sparks and Pinkerton, 1978) and 10-20% crystallization. This raises the viscosity 1-2 orders of magnitude and decreases the flow velocity in the drift at the point of entry. Under these conditions, in-drift volumetric flow rates of 0.001-0.00001 m^3/s are expected, which correspond

to cooling with distance rates in the range of 100-1000°C/km. These cooling rates indicate that, upon entering a repository drift, lava will approach its solidus temperature (950°C) after an in-drift travel distance on the order of 10 meters. EPRI's analysis demonstrates that lava will enter only a fraction of the drifts and that only a small number of waste packages will be entombed by lava. Moreover, the rapid cooling of lava upon contact with a waste package results in the formation of a protective barrier on the waste package. EPRI therefore concludes that realistic assessment of igneous consequences at Yucca Mountain should consider the dramatic effects of viscosity and cooling on lava flow behavior within emplacement drifts. Neglecting such important effects will lead to overly conservative estimates of the consequences of igneous intrusion for repository performance.

EPRI's analysis of expected lava cooling behavior inside the drift environment demonstrates the important differences in cooling and crystallization mechanisms experienced by lava erupting onto the earth's surface versus lava entering a drift located 300 m below the surface. These results support previous EPRI hypotheses (EPRI, 2004; 2007) that lava inside a drift will not: a) fill all repository drifts at Yucca Mountain following an igneous intrusion event, and b) erupt onto the surface via a secondary dike i.e., the dog-leg scenario proposed by Woods et al. (2002). Results from this lava cooling analysis supports EPRI's view (EPRI, 2004; 2007) that lava entering an emplacement drift would result in only partially filling of the drift and would form a protective barrier, entombing the waste packages with which that it comes into contact.

5.5.8 References

ACNWM (Advisory Committee on Nuclear Waste and Materials), 2007. *Igneous Activity at Yucca Mountain: Technical Basis for Decision Making*, pp. 241.

BSC, 2005. *Drift-Scale THC Seepage Model*, MDL-NBS-HS-000001 REV4, Bechtel SAIC Company, LLC, Las Vegas, Nevada, USA, 2005.

Cas, R.A.F. and J.V. Wright, 1987. *Volcanic Successions, Modern and Ancient*. Allen and Unwin Ltd., UK. p.528

Detournay, E., L. Mastin, A. Pearson, A. Rubin and F. Spera, 2003. *Final Report of the Igneous Consequences Peer Review Panel*, Bechtel SAIC Company LLC, Las Vegas. NV. pp. 86.

EPRI, 2004. *Potential Igneous Processes Relevant to the Yucca Mountain Repository: Extrusive-Release Scenario, Analysis and Implication*, Electric Power Research Institute, Palo Alto, CA: 2004. 1008169.

EPRI, 2005. *Potential Igneous Processes Relevant to the Yucca Mountain Repository: Intrusive-Release Scenario*, Electric Power Research Institute, Palo Alto, CA: 2005. 1011165.

EPRI, 2007, *EPRI Yucca Mountain Spent Fuel Repository Evaluation – 2007 Progress Report*, Electric Power Research Institute, Palo Alto, CA: 2007. 1015045.

Griffiths, R.W., 2000. "The Dynamics of Lava Flows," *Annual Reviews of Fluid Mechanics*, 32: 477-518.

Harris A.J. and S.K. Rowland, 2001. *FLOWGO: a kinematic thermo-rheological model for lava flowing in a channel*, *Bull. Volcanol*. 63:20-44.

Keszthelyi, L., 1995. "A preliminary thermal budget for lava tubes on the Earth and planets," *J. of Geophysical Research* 100:20,411-20,420.

Kilburn, C.R.J., 2000. "Lava flows and flow fields," in *Encyclopedia of Volcanoes*, H. Sigurdsson (ed.), Academic Press.

Marsh, B., 1981. "On the crystallinity, probability of occurrence and rheology of lava and magma," *Contrib. Mineral Petrol.* 78:85-98.

Nicholis, M. and M. Rutherford, 2004. "Experimental constraints on magma ascent rate for the Crater Flat volcanic zone hawaiite," *Geology*, 32, 489.

SNL (Sandia National Laboratory), 2007. *Characterize eruptive process at Yucca Mountain, Nevada,* ANL-MGR-GS-000002 REV03, Las Vegas, NV, pp. 6.3-23.

Sparks R.S.J. and H. Pinkerton, 1978. "Effect of degassing on rheology of basaltic lava," *Nature* 276: 385-386.

Valentine, G.A. and F. Perry, 2006. "Decreasing magmatic footprints of individual volcanoes in waning basaltic field," *GRL* 33:L14305

Valentine, G. A., 2006, "Igneous scenarios," Presented at DOE/NRC Technical Exchange on Total System Performance Assessment (TSPA) for Yucca Mountain, Las Vegas, NV.

Valentine G., F. Perry, D. Krier, G. Keating, R. Kelley, A. Coghill, 2006. "Small volume basaltic volcanoes, eruptive products and processes, and post eruptive geomorphic evolution in Crater Flat (Pleistocene) southern Nevada," *GSA Bulletin* 118:1313-1330.

Woods, A.W, S. Sparks, O. Bokhove, A. LeJeune, C. Connor, and B. Hill, 2002. "Modeling magma-drift interaction at the proposed high-level radioactive waste repository at Yucca Mountain, Nevada, USA," *Geophysical Research Letters,* 13.

Wright, T.L. and R.T. Okamura, 1977. *Cooling and Crystallization of Tholeiitic Basalt, 1965 Makaopuhi lava lake, Hawaii*, U.S. Geol. Surv. Prop. Paper 1004, 59 pp.

5.6 Simplified Post-closure Probabilistic Seismic Hazard Model for Yucca Mountain

5.6.1 Introduction

As part of a program to provide independent review of scientific research on, and technical assessments of, the performance of a proposed geologic repository at Yucca Mountain (YM), the Electric Power Research Institute (EPRI) is conducting its own probabilistic seismic hazard (PSH) modeling for the proposed YM repository site. The EPRI PSH model is implemented within the Java-based OpenSHA framework (www.OpenSHA.org), with an emphasis on simplicity and transparency to allow for greater understanding of key elements, such as seismic source model and treatment of uncertainty. The simplicity of EPRI's PSH model also facilitates sensitivity analyses of hazard estimates with respect to various parameters. Independent sensitivity analyses were not possible for DOE's original YM PSH model (Stepp et al., 2001), due to the great complexity of the model. The original Department of Energy (DOE) YM PSH model predicts 95th percentile peak ground accelerations (PGAs) and peak ground velocities (PGVs) of over 4g and 400 cm/sec, respectively, for return periods of 10^6 years and longer. These values represent extreme ground motions in that these levels have never been measured in the history of worldwide strong motion accelerograph recording, and are thought to be physically unrealizable (Bommer et al., 2004; Hanks, et al., 2004). Considerable effort is being directed at validation of PSH models for YM and other locations where long-term seismic hazards are of concern.

5.6.1.1 Earthquake Source Model

The earthquake sources developed for the YM model are based on the publicly available YM seismic source model developed by John Anderson at the Nevada Seismological Laboratory (personal communication, 2007), and are shown in Figure 5-24. The model comprises seven fault sources and one area source. The fault sources assume a characteristic earthquake model (Schwartz and Coppersmith, 1984), in which the magnitude is based on the length of the fault, using well-known regressions (Wells and Coppersmith, 1994). A normal distribution of uncertainty in earthquake magnitudes is assumed for the fault length-based magnitude. Recurrence intervals for the fault sources are then defined by dividing the seismic moment of the Moment magnitude (Mw) by the seismic moment rate for the fault (derived from fault slip rate estimates). For the area source, the seismicity recorded inside the box shown in Figure 5-24 is used to define parameters of the Gutenberg-Richter relationship:

$$logN/yr = a - bM \qquad \text{eq. 5-7}$$

in which N/yr is the cumulative annual number of events greater than or equal to magnitude M, and a and b are empirical parameters (Gutenberg and Richter, 1944).

Treatment of parameter uncertainty in the source model is achieved by construction of simple logic trees. An example of a fault source logic tree, along with the background seismicity logic tree, is shown in Figure 5-25.
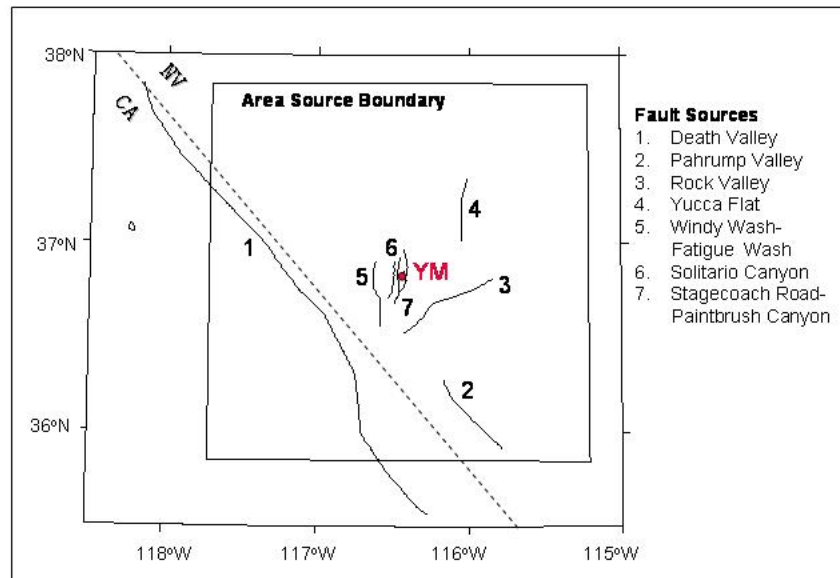
Figure 5-24
Fault sources and large background seismicity (area) source used in EPRI's Yucca Mountain (YM) PSH model.
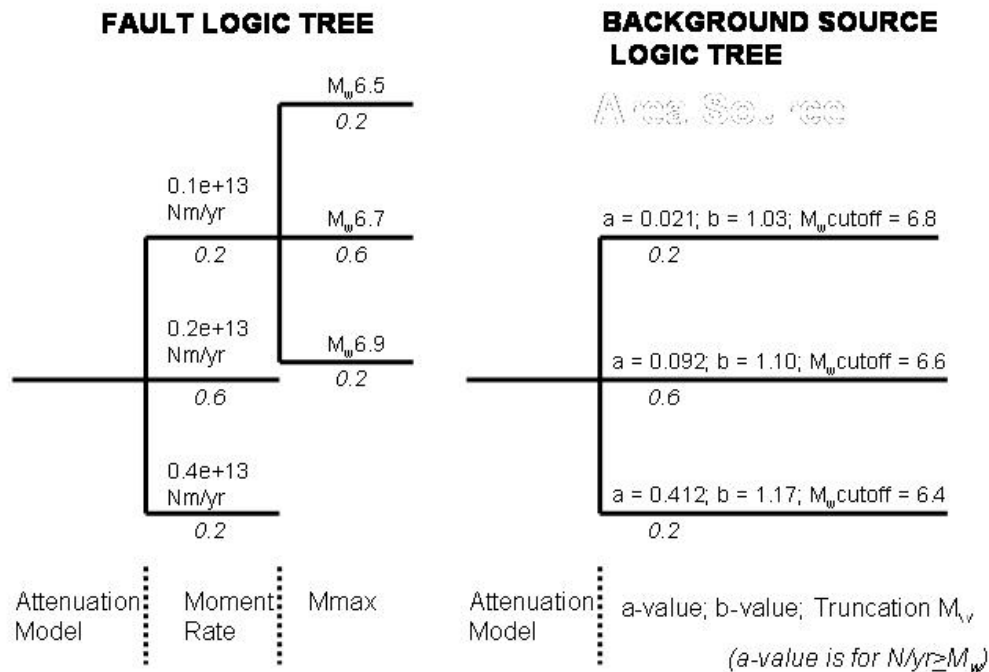
Figure 5-25
Logic tree structures developed for the treatment of epistemic uncertainty in the source model (fault source example is the Solitario Canyon Fault).

5.6.1.2   Attenuation Models

Implementation of the EPRI's PSH model in OpenSHA allows for the consideration of a range of attenuation models, in particular the Next Generation Attenuation (NGA) models. The NGA of Boore and Atkinson (2007) and Campbell and Bozorgnia (2007) have been used to date in EPRI's PSH model These NGA models incorporate the wealth of strong motion data obtained from recent large worldwide earthquakes, and therefore supersede the extensively-used attenuation models of the mid-to-late 1990s. Other NGA models are currently available but these are not used in the EPRI PSH model (Figs. 5-26 and 5-27) as EPRI's intent is to simply use a random subset of the models for its analysis.

5.6.1.3   Hazard Estimates

Hazard curves derived from the EPRI PSH model are shown in Figures 5-26 and 5-27. The two sets of hazard curves show the 5th, 15th, 50th, 84th and 95th percentiles of PGA and PGV, for the Boore and Atkinson (Figure 5-26) and Campbell and Bozorgnia (Figure 5-27) NGA models (Boore and Atkinson, 2007; Campbell & Bozorgnia, 2007). The percentiles are calculated based on 1000 Monte Carlo-based samples of the logic trees (Figure 5-25). The EPRI PSH model yields 95th percentile PGAs and PGVs of 0.7 to 1.1 g and 80 to 100 cm/sec, respectively, for the 10^6 year return time. These estimates are considerably lower than the equivalent estimates for DOE's original YM model (see Section 5.6.1), and are well within the range of strong motions recorded worldwide. Use of a greatly simplified earthquake source model, combined with the influence of the NGA models are likely to be the main factors leading to the reduced estimates of hazard in EPRI's PSH model. Deaggregation analyses show that the closest fault and background sources dominate the PGA hazard at the 10^6 year return period, but that the more distant Death Valley-Furnace Creek Fault (DVFCF) contributes 40% to the PGV hazard at the same return period. The large earthquake magnitudes and short recurrence intervals estimated for the DVFCF make this source an important contributor to the hazard at YM, despite being tens of km distant from YM.
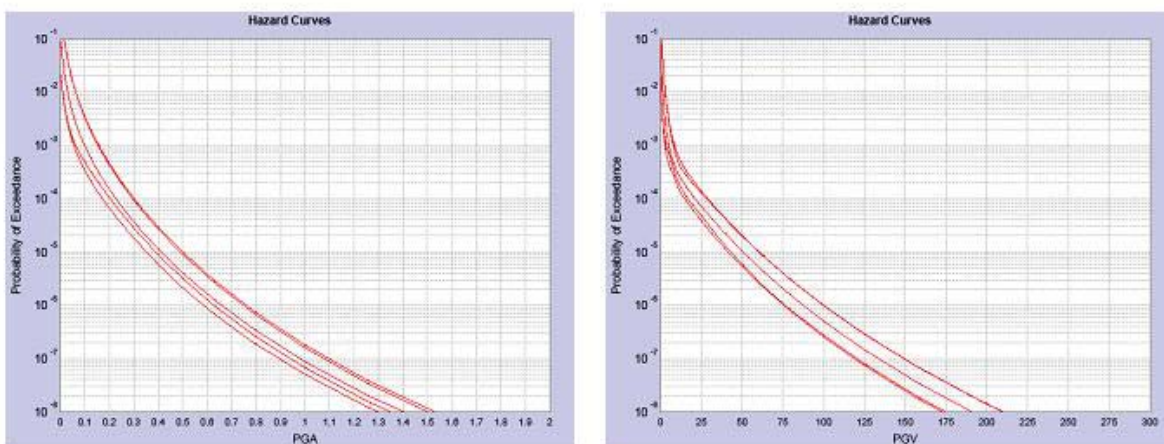
Figure 5-26
Hazard curves for PGA (left) and PGV (right), using the Boore & Atkinson NGA model.
Probability of exceedance (y-axis) range is 10^{-1} to 10^{-8}/year, and ground motion (x-axis)
range is 0 to 3 g for PGA, and 0 to 300 cm/sec for PGV.
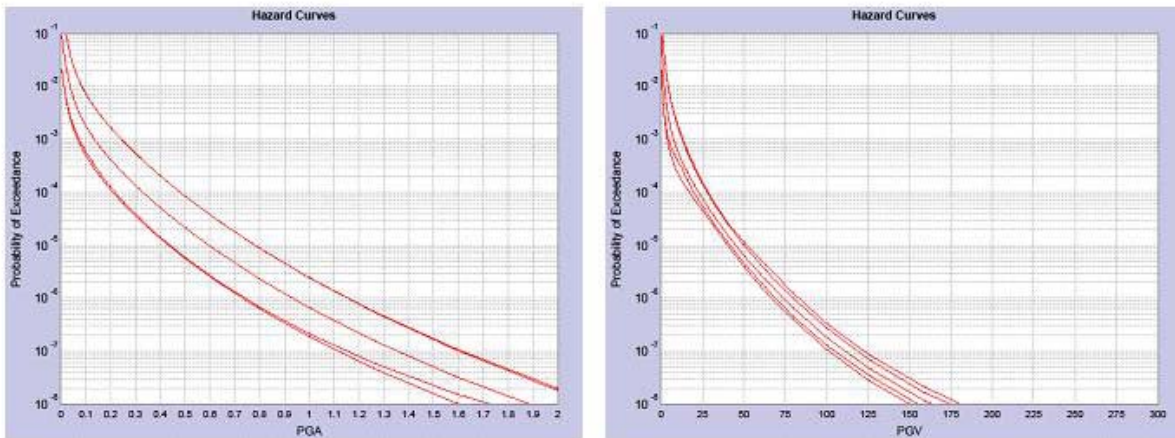
Figure 5-27
Hazard curves for PGA (left) and PGV (right), using the Campbell & Bozorgnia NGA model.
Ranges shown on y and x axes are the same as for Figure 5-26.

5.6.2 Conclusions

EPRI's simplified PSH model for YM produces ground motion estimates that fall within a range observed to date in worldwide strong motion recording, as opposed to the "extreme" ground motions produced by DOE's original YM PSH model. EPRI's PSH model is preliminary and the potential exists for further improvements, including validation against analogue criteria (such as unstable ancient geomorphic features that would be destroyed during strong motion events) in the vicinity of YM. Possible future investigations may provide a greater understanding of the strong influence of the DVFCF on the PGV hazard.

5.6.3 References

Bommer, J.J.; N.A. Abrahamson, F.O. Strasser, A. Pecker, P.Y. Bard, H. Bungum, F. Cotton, D. Fah, F. Sabetta, F. Sherbaum, and J. Studer, 2004. "The challenge of defining upper bounds on earthquake ground motions." *Seismological Research Letters*, 75, 82-95.

Boore, D.M., and G.M. Atkinson, 2007. "Boore-Atkinson NGA ground motion relations for the geometric mean horizontal component of peak and spectral ground motion parameters." *Pacific Earthquake Engineering Research Center (PEER) report* 2007/01.

Campbell, K.W and Y. Bozorgnia, 2007. "Campbell-Bozorgnia NGA ground motion relations for the geometric mean horizontal component of peak and spectral ground motion parameters." *Pacific Earthquake Engineering Research Center (PEER) report 2007/02.*

Gutenberg, B. and C.F. Richter, 1944. "Frequency of Earthquakes in California." *Bulletin of the Seismological Society of America* 34, 185-188.

Hanks, T.C. and 5 others, 2004. "Observed ground motions, extreme ground motions, and physical limits to ground motions." *International Workshop on Future Directions in Instrumentation for Strong Motions and Engineering Seismology Proceedings. May 17-21.*

Schwartz, D.P and K.J. Coppersmith, 1984. "Fault behaviour and characteristic earthquakes: examples from the Wasatch and San Andreas fault zones." *Journal of Geophysical Research* 89, 5681-5698.

Stepp, J.C.; I. Wong, J. Whitney, R. Quittmeyer, N. Abrahamson, G. Toro, R. Youngs, K. Coppersmith, J. Savy, T. Sullivan, and Yucca Mountain PSHA project members, 2001. "Probabilistic seismic hazard analyses for ground motions and fault displacement at Yucca Mountain, Nevada." *Earthquake Spectra* 17, 113-151.

Wells, D.L. and K.J. Coppersmith, 1994. "New empirical relationships among magnitude, rupture length, rupture width, rupture area, and surface displacement." *Bulletin of the Seismological Society of America* 84, 974-1002.

5.7 Corrosion Behavior of the Stainless Steel Inner Vessel and TAD Canister of a TAD-bearing Waste Package

5.7.1 Introduction

The proposed Yucca Mountain (YM) repository for the disposal of spent nuclear fuel (SNF) and high-level waste (HLW) features a multi-barrier system to limit release of radionuclides to the environment (DOE, 2008). Natural barriers, such as the unsaturated and saturated zones above and below the proposed repository elevation, are supplemented by the engineered barriers, including the waste form itself and a corrosion-resistant waste package (WP). The WP comprises an Alloy 22 outer corrosion barrier and an inner vessel constructed of stainless steel. The WP is further protected by a titanium Grade-7 drip shield designed to prevent seepage drips and rocks from contacting the WP during the thermal pulse and beyond. Together, the waste form, the WP, the drip shields, and other engineered repository design elements compose the engineered barrier system (EBS).

The function of the stainless steel inner vessel is to provide structural strength for the relatively thin Alloy 22 outer corrosion barrier. Recently, the US Department of Energy (DOE, 2006) has proposed the use of a transportation, aging, and disposal (TAD) canister for the handling and disposal of commercial spent nuclear fuel (CSNF) (DOE, 2006). The TAD canister would be used to transport the CSNF to the YM repository site (in a suitable transportation cask), to age the fuel in a suitable aging overpack (if necessary), and finally to dispose of the fuel by directly inserting the TAD canister into the waste package.

The WP is one of the primary engineered barriers in the multi-barrier system. Accordingly, understanding the long-term behavior of the WP is critical for evaluating the long-term performance of the repository system (DOE, 2008; EPRI, 2005a). For the nominal scenario, corrosion is considered to be the major threat to the integrity of the WP (DOE, 2008; King et al.,

2008), with additional failure mechanisms possible for the low-probability seismic (EPRI, 2006; James et al., 2006; SNL, 2007a) and igneous (EPRI, 2004; 2005b; King et al., 2006) disruptive event scenarios. Although credit is taken in performance assessment calculations for the Alloy 22 outer corrosion barrier, which is expected to survive intact for considerable periods of time (DOE, 2008, King et al., 2008), no credit is taken for the potential containment function of the stainless steel inner vessel or TAD canister despite the fact that they will both be sealed by welding.

This lack of credit for the containment function of the inner vessel and TAD canister results from the perception that stainless steel corrosion will be rapid relative to the degradation of the corrosion resistant Alloy 22 outer barrier. While this argument may be true during the early thermal pulse, it is not necessarily the case for the ambient environmental conditions that will prevail after several hundred thousand years, the time at which the waste packages are anticipated to fail. There could be a considerable delay between the failure of the outer Alloy 22 corrosion barrier and of the inner stainless steel vessel and TAD canister, further delaying contact of the CSNF by water and the release of radionuclides.

This section provides an assessment of the corrosion behavior of the stainless steel inner vessel and TAD canister assuming failure of the outer Alloy 22 corrosion barrier. Following a review of the current specifications for the design of the TAD-bearing WP, the environmental conditions to which the inner vessel and TAD canister will be exposed following WP failure are reviewed. Various stainless steel corrosion mechanisms are considered including: atmospheric corrosion, general corrosion (GC), localized corrosion (LC) in the form of pitting and crevice corrosion, stress corrosion cracking (SCC), and microbiologically influenced corrosion (MIC). Based on this corrosion assessment, the potential lifetimes of the non-Alloy 22 WP components, including the stainless steel inner vessel and TAD canister itself, are discussed.

5.7.2 Design and Environmental Considerations

5.7.2.1   Design of Stainless Steel Inner Vessel

5.7.2.1.1   Design of TAD-bearing Waste Package for CSNF

Preliminary performance specifications for the TAD canister have been defined (DOE 2006); however final design specifications await further development by commercial vendors. The following discussion, therefore, is based on the general requirements for the TAD canister and the TAD-bearing WP.

The TAD canister is designed to address spent nuclear fuel containment needs during dry storage at reactor sites, during transport, and aging (if needed) and direct disposal at Yucca Mountain. Prior to emplacement in the repository, the TAD canister will be loaded into an overpack composed of a 1-inch (25.4-mm)-thick Alloy 22 outer corrosion barrier with a 2-inch (50.8-mm)-thick stainless steel inner vessel (Figures 5-28 and 5-29).

LOWER SLEEVE

UPPER SLEEVE

PURGE PORT CAP

OUTER CORROSION BARRIER

INNER VESSEL

INNER LID

OUTER LID

SPREAD RING

NOTES:

1. ALL DIMENSIONS ARE REFERENCE ONLY.

COMPONENT NAME	MATERIAL	QTY REQ
OUTER LID	SB-575 (UNS N06022)	1
SPREAD RING	SA-240 (UNS S31600)	1
PURGE PORT CAP	SA-240 (UNS S31600)	1
INNER LID	SA-240 (UNS S31600)	1
INNER VESSEL	SA-240 (UNS S31600)	1
INTERFACE RING	SA-240 (UNS S31600)	1
OUTER CORROSION BARRIER	SB-575 (UNS N06022)	1
UPPER SLEEVE	SB-575 (UNS N06022)	1
LOWER SLEEVE	SB-575 (UNS N06022)	1
SUPPORT RING	SB-575 (UNS N06022)	1

NOMINAL LENGTH	NOMINAL DIAMETER	WASTE PACKAGE ASSY	LOADED MASS
230.32 IN	77.28 IN	53.500 LBM	162.000 LBM
5850.1 MM	1962.9 MM	24.300 KG	73.500 KG

00249DC_LA_1031f.ai

Figure 5-28
Exploded view of TAD-bearing waste package (after Figure 1.5.2-3, DOE 2008).
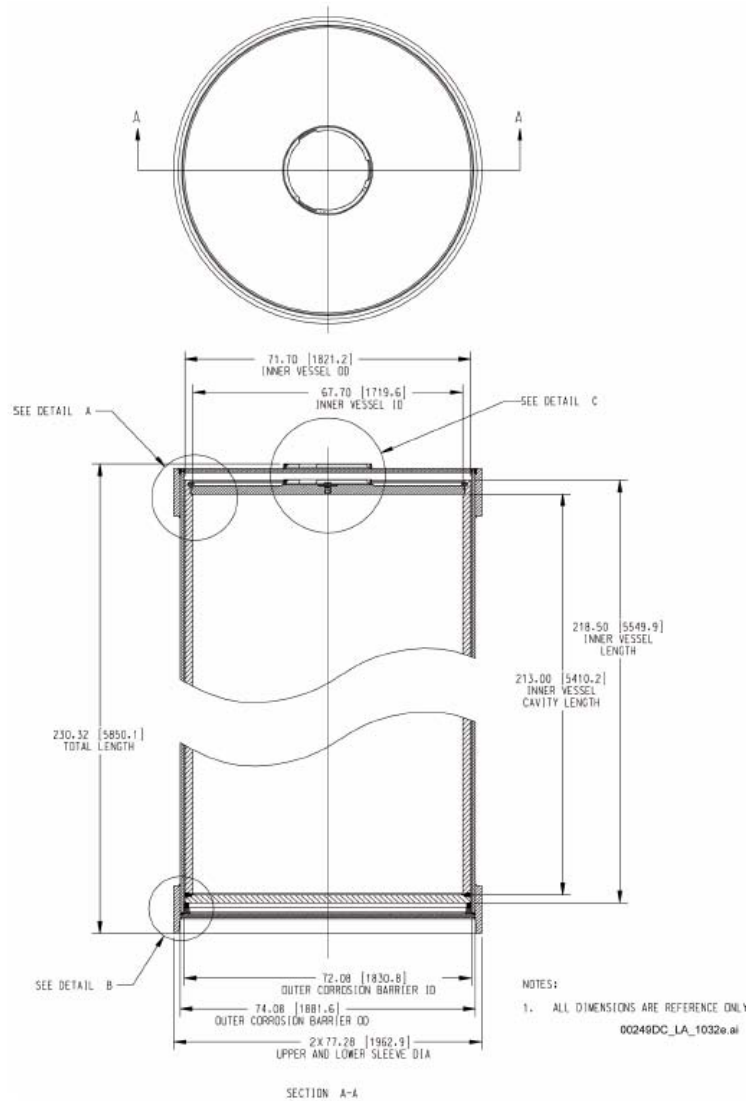
Figure 5-29
Cross section and plan view of TAD-bearing waste package (after Figure 1.5.2-3, DOE. 2008).

The overall dimensions of the TAD canister are 212 in. (5385 mm) in length by 66.5 in. (1689 mm) outside diameter. Whilst the wall thickness is not specifically defined in the preliminary performance specifications (DOE, 2006), a minimum wall thickness of 1.0 in. (25.4 mm) is specified for the License Application (LA) (DOE, 2008; SNL, 2007b).

The combined wall thickness, therefore, of the WP corrosion barrier and of the stainless steel inner vessel and TAD canister will be of the order of 4 inches, of which 3 inches will be stainless steel.

5.7.2.1.2   Material of Construction

The WP inner vessel is fabricated from Type 316 stainless steel (UNS S31600), with additional chemical content restrictions for carbon (maximum 0.020 wt.%) and nitrogen (maximum 0.10 wt.%, minimum 0.060 wt.%). These additional elemental limitations are more restrictive than the equivalent limits for Type 316L (max. 0.03 wt.% C, max. 0.10 wt.% N).

The preliminary TAD performance specifications (DOE 2006) call for the use of an American Iron and Steel Institute (AISI) 300-series stainless steel, "such as UNS S31603, which may also be designated as Type 316L." Designs for the TAD canister that would meet the performance requirements defined by DOE (SNL, 2007b) are currently being developed by commercial vendors under a DOE-led effort. In lieu of a specific design, this analysis assumes that the TAD canister is fabricated from the same grade of stainless steel as the inner vessel or a similar grade, such as Type 316L.

5.7.2.1.3   Sealing and Stress Mitigation

Prior to transportation from the reactor site, the loaded TAD canister is closed by welding of the closure lids using gas tungsten arc welding (DOE, 2008). The details of the closure welds for the stainless steel inner vessel of the TAD-bearing WP and of the Alloy 22 outer corrosion barrier are shown in Figure 5-30. Following closure, the TAD-bearing WP is pressure tested to 1.1-1.25 design pressure, followed by He leak testing. The inner vessel closure weld will not be stress relieved after welding (SNL, 2007c).
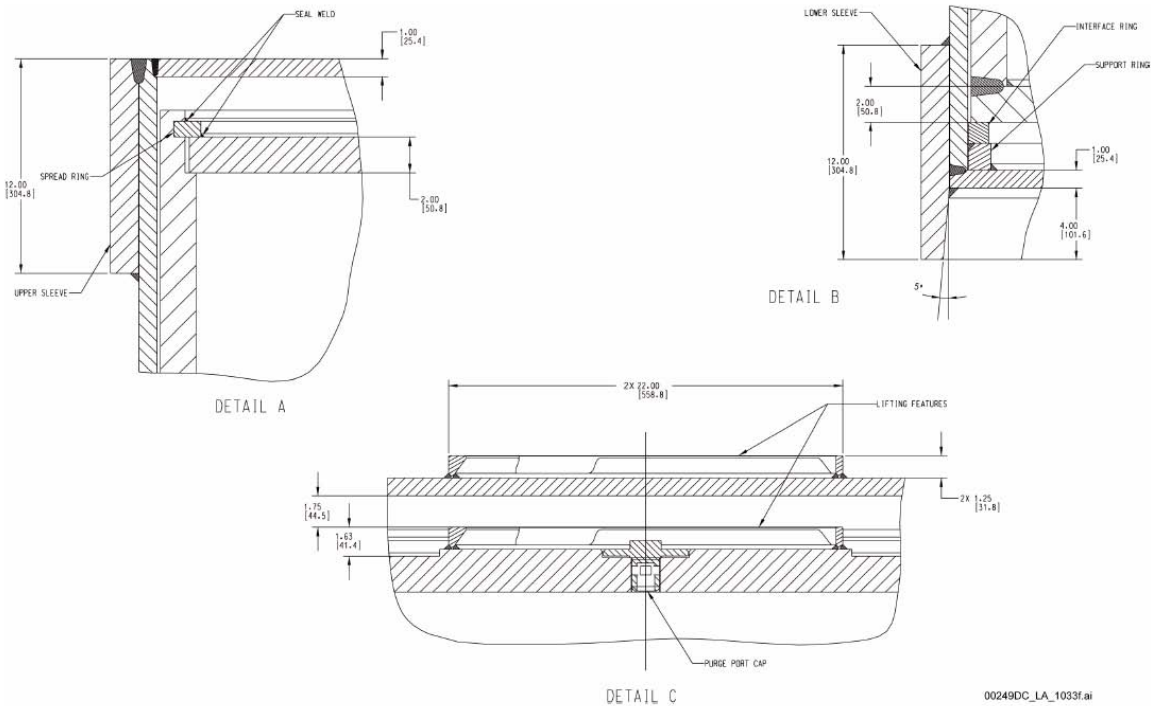
Figure 5-30
Details of closure welds for TAD-bearing waste package (after Figure 1.5.2-3, DOE 2008).

5.7.2.2 Environmental Considerations

5.7.2.2.1 Environment Prior to Disposal

The TAD canister may be exposed to various aqueous environments and thermal conditions during loading, storage at the reactor site, transportation to YM, and possible aging prior to disposal. TAD canisters will be loaded in pools at the reactor site in which the conductivity and Cl$^-$ content is maintained at low levels. Following the loading and sealing, the inside of the TAD will be drained, dried and eventually filled with (helium) inert gas. The TAD-canister atmosphere should contain a maximum of 0.2 vol.% "oxidizing" gas (i.e., O_2) (DOE, 2008).

Although attempts will be made to protect the TAD canister surface from exposure to precipitation, it is possible that the canister could be exposed to precipitation from rain or snow for brief periods of time during some stage of reactor site storage, transportation, and/or aging at the repository.

The thermal history of the TAD canister prior to disposal will depend on the fuel characteristics and on conditions under which the canister is stored, transported, and (possibly) aged. These conditions will vary on a case-by-case basis, but a design requirement is that the internal temperature shall not exceed a value of 350°C in the repository in order to maintain the CSNF cladding integrity (DOE, 2006, 2008).

Although not expected to result in more than superficial corrosion of the TAD canister prior to disposal, the surface of the canister could nevertheless be contaminated by mineral deposits that could affect the corrosion behavior following failure of the outer corrosion barrier many hundreds of thousands of years into the future.

5.7.2.2.2 Environment Following Waste Package Outer Barrier (WPOB) Failure

The environment to which the stainless steel inner vessel and TAD canister will be exposed is strongly dependent on the time of failure of the Alloy 22 outer corrosion barrier.

A maximum of one WP is expected to contain an undetected manufacturing defect severe enough to result in a through-wall penetration soon after emplacement in the repository. Depending upon the nature of the through-wall penetration, the inner vessel in this single WP could be exposed to concentrated aqueous solutions produced by the evaporation of seepage waters. However, for this to occur, the WP must not only be located in a region of the repository where seepage is possible (<1%, EPRI, 2008) but the defect must be large enough for the mass transport of water. The probability of an undetected manufacturing flaw will be small (<10^{-4}) and the probability that water will seep inside the outer corrosion barrier is even smaller (<10^{-6}). Because of the low probability of such an event, this condition is not considered further here.

For all but the maximum of one initially defected WP, the inner vessel will not be exposed to an aqueous environment until the Alloy 22 outer barrier fails by corrosion. For the current reference 25-mm-thick Alloy 22 outer layer, less than 7% of the WPs are predicted to have failed at 10^6 years, with the first corrosion failure occurring after ~400,000 years.

5.7.2.2.2.1   *Temperature*

At the time of the first expected WP corrosion failure, the temperature within the drifts will have decreased to the ambient repository temperature of 17-25°C (DOE, 2008).

5.7.2.2.2.2   *Amount and Composition of Aqueous Phase*

Because of its location in the unsaturated zone above the water table, the amount of water available in the YM repository to initiate corrosion is limited. Following the thermal transient and the return of the drift wall temperature to below the local boiling point (96°C), dripping of water from the roof of the drift is possible. If both the Ti-7 drip shield and Alloy 22 WP have failed, this water could contact the stainless steel inner vessel. In the absence of dripping, the surface of the inner vessel will be covered by a thin film of moisture provided the relative humidity (RH) exceeds approximately 60-70%, the typical critical RH for the onset of atmospheric corrosion (Shreir et al., 1993).

Tables 5-11 and 5-12 summarize the composition of representative porewaters from various lithostratigraphic units at YM. The waters are generally fresh, with total dissolved solids in the range of 300-900 mg/L and are near-neutral to slightly alkaline with a pH of 7-8. The predominant anion is HCO_3^- (130-515 mg/L), with smaller amounts of NO_3^- (3-60 mg/L), SO_4^{2-} (10-130 mg/L), F^- (1-6 mg/L), and Cl^- (20-150 mg/L).

5.7.2.2.2.3   *Oxidants*

The repository horizon is located in the unsaturated zone under Yucca Mountain at an elevation approximately 300 m above the water table. Accordingly, the drifts can be considered to be fully aerated. Predominant oxidants present in the emplacement drifts at the time of WP failure (i.e., beyond 400,000 years) are atmospheric O_2 and H_2O from condensation and infiltration.   By this time, radioactive decay will have reduced the gamma radiation field at the surface of the inner vessel and TAD canister to an insignificant level; therefore corrosion supported by the reduction of oxidizing radiolysis products, such as H_2O_2 or OH radicals, will not be important

5.7.2.2.2.4   *Microbial Environment*

Microbial activity in the drift is considered to be possible once the RH exceeds a threshold value of 96% (King, 2008). Figure 5-31 shows the predicted time to reach an RH of 95% at the surface of various WP configurations located at different locations within the repository (DOE 2008). By the time of WP failure by corrosion, all packages will be exposed to moisture conditions that will support microbial activity. Consequently, since the possibility of inoculation of the packages by airborne microbes or by microbes in seepage drifts cannot be excluded, microbial activity on the stainless steel inner vessel and TAD canister surface is possible.

Table 5-11
Representative Yucca Mountain pore-water compositions (SNL 2007d).

Sample ID		SD-9/1184.7-1184.8/UC	ESF-THERMALK-017/26.5-26.9/UC	ESF-HD-PERM-3/34.8-35.1/Alcove 5	HD-PERM-3/56.7-57.1/UC
Lithostratigraphic Unit		Tptpll	Tptpul	Tptpmn	Tptpmn
Water designation		Gp1	Gp2	Gp3	Gp4
Members in Group		21	7	3	3
Parameter	Units	Values			
pH (meas.)	pH	8.2	7.7	8.31	-
Na^+	mg/L	59	45	62	123
K^+	mg/L	4.8	14.4	9	13.8
Mg^{2+}	mg/L	0.7	7.9	17.4	16.7
Ca^{2+}	mg/L	19	62	97	59.9
Cl^-	mg/L	23	67	123	146
SO_4^{2-}	mg/L	16	82	120	126
HCO_3^-	mg/L	142	126	-	149
NO_3^-	mg/L	16	44	10	57.4
F^-	mg/L	2.2	1.4	0.76	1.3
$SiO_2(aq)$	mg/L	42	52	75	-

Table 5-12
Compositions of representative Yucca Mountain porewaters (BSC, 2003).

Porewater ID	W0	W5	W4	W6	W7
Lithostratigraphic Unit	Tptpmn	Tptpul (base)	Tptpll	Tptpll	Tptpul
Temperature (°C)	25	25	25	25	25
pH	8.3	7.6	7.4	7.9	8.0
Na^+ (mg/l)	61.5	39.0	130.0	84.0	57.0
K^+ (mg/l)	8.0	7.6	10.6	7.9	10.3
Ca^{2+} (mg/l)	101.0	94.0	82.0	56.0	120.0
Mg^{2+} (mg/l)	17.0	18.1	5.3	0.9	19.3
SiO_2(aq) (mg/l)	70.5	42.0	48.0	50.0	49.0
Cl^- (mg/l)	117.0	21.0	26.0	23.0	54.0
SO_4^{2-} (mg/l)	116.0	36.0	39.0	10.0	78.0
HCO_3^- (calc)[1]	200.0	395.0	515.0	335.0	412.0
HCO_3^- (mM)	3.3	6.5	8.4	5.5	6.8
CO_3^{2-} (mM)[2]	0.03	0.012	0.0096	0.02	0.031
NO_3^- (mg/l)	6.5	2.6	4.2	17.0	6.1
F^- (mg/l)	0.9	3.4	6.0	2.5	4.8

[1] Total aqueous carbonate as HCO_3^- (mg/l), calculated from charge balance.
[2] Based on $pK_2 = 10.34$ (Pourbaix, 1974)
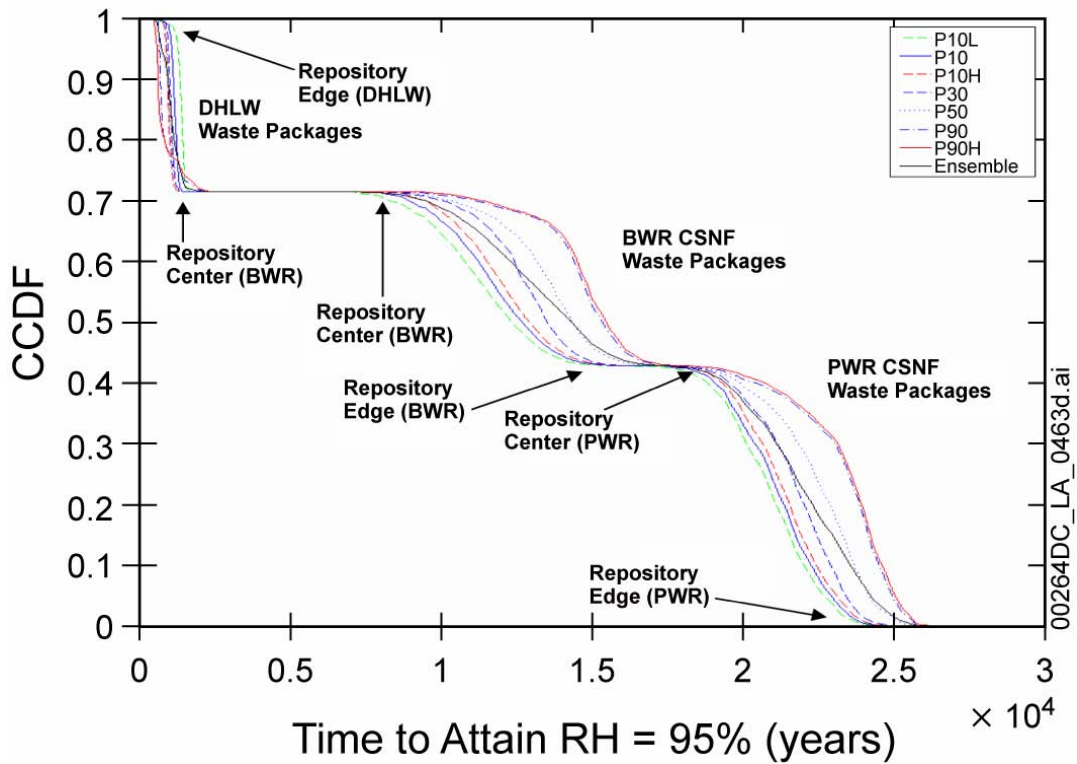
Figure 5-31
Time for waste package surface to attain a relative humidity of 95% (after Figure 2.3.5-34, DOE, 2008).

5.7.2.2.2.5   *Residual and Applied Stress*

The inner vessel will contain residual stresses of an unknown magnitude because of the lack of post-weld stress relief of the closure weld (SNL, 2007c). Applied loads on the inner vessel and TAD canister will result from the accumulation of rock on the surface of the WP. The height of the rock pile will depend on a number of factors, including: whether the drift is located in the lithophysal or non-lithophysal areas of the repository and the number and severity of seismic events (SNL, 2007a; EPRI, 2006). In lieu of more specific information, EPRI assumes that the level of residual and applied stress is greater than the threshold stress for the initiation of stress corrosion cracking of the stainless steel inner vessel and TAD canister.

5.7.2.2.2.6   *Impact of Alloy 22 Outer Barrier*

The stainless steel inner vessel will be exposed to the environment only after the Alloy 22 outer corrosion barrier has failed. Based on predictions using the EPRI EBSCOM model, the primary failure mechanism for the Alloy 22 is microbiologically-enhanced general corrosion. Theoretically, therefore, the outer corrosion barrier will have totally corroded to oxide before the stainless steel inner vessel is exposed to the environment. However, if the outer barrier is not in close contact with the inner vessel, local rupture of the outer corrosion barrier due to mechanical overload by an accumulated rock pile could occur before complete consumption of the Alloy 22. Therefore, the effects of both corrosion products and of un-corroded Alloy 22 on the subsequent corrosion of the stainless steel inner vessel are assessed.

Contact between un-corroded Alloy 22 and the Type 316L stainless steel could result in galvanic corrosion. However, the difference in electrochemical potential between the two alloys is small and no galvanic coupling is expected (ASM, 1987). He et al. (2007) found no effect on the crevice re-passivation potential for Type 316L stainless steel of coupling to Alloy 22 in 4 mol·dm^{-3} NaCl solution at a temperature of 95°C. Therefore, galvanic effects between Alloy 22 and Type 316L stainless steel will not affect the corrosion behavior of the stainless steel inner vessel.

Alloy 22 corrosion products may be present on the surface of the inner vessel (and, following failure of the inner vessel, on the TAD canister surface) in either solid or dissolved form. It could be argued that a layer of porous oxide could act as a crevice former on the stainless steel surface, but Apted et al. (2005) have shown that porous layers cannot support the requisite conditions (i.e., a differential oxygen concentration cell for passive materials) for the initiation of localized corrosion.

Therefore, the only likely effect of the Alloy 22 outer barrier on the corrosion behavior of the stainless steel inner vessel and TAD canister is the possible impact of dissolved corrosion products. The solubility of dissolved Ni, Cr, Mo, W, and Fe (the major elemental constituents of Alloy 22) will be limited because of the neutral to slightly alkaline pH expected in the repository. The other important consideration is the oxidation state of the dissolved metal ions. The higher the oxidation state, the more oxidizing the dissolved species and the more positive the potential of the stainless steel will be due to reduction of the metal ion. Based on thermodynamic data (Pourbaix, 1974), the species most likely to be present in oxidized form are Mo (as molybdate MoO_4^{2-}), W (as tungstate WO_4^{2-}), and Fe (as ferric Fe^{3+}). Even in aerated systems, it is unlikely

that Cr(VI) will be stable. Divalent nickel (Ni^{2+}) is relatively stable under relevant repository conditions. The combination of low solubility and the relatively low percentage composition of Mo, W, and Fe in the alloy suggest that any effect of dissolved Alloy 22 corrosion products on the corrosion behavior of the stainless steel TAD canister components will be minimal.

5.7.3. *Corrosion Behavior of the Stainless Steel Inner Vessel and TAD Canister*

5.7.3.1   Atmospheric Corrosion

Atmospheric corrosion could take the form of general corrosion, LC, and/or SCC, and is distinguished from other aqueous corrosion mechanisms only because these processes occur in a thin moisture film rather than in bulk solution. Thin moisture films form by condensation of water vapor from the atmosphere when the vapor pressure of water exceeds the saturated vapor pressure. The saturated vapor pressure is lower in the presence of salt contaminants, due to a process referred to as deliquescence. Much is known about the deliquescence behavior of different salts, and the critical temperature and %RH at which these salt contaminants absorb moisture from the atmosphere are also known (BSC, 2004a; Rard et al., 2005).

The most likely forms of atmospheric corrosion will be general corrosion and LC, the latter in the form of pitting or, possibly, crevice attack if any occluded regions are present. Table 5-13 summarizes observed atmospheric corrosion rates for Types 304 and 316, as well as for an unspecified grade of stainless steel. All rates are of the order of 0.01-0.05 $\mu m \cdot yr^{-1}$, with little variation between different types of atmosphere. The possibility of LC is discussed in more detail below.

Table 5-13
General corrosion rates for stainless steel under atmosphere conditions from the literature.

Grade	Temperature (°C)	Redox Conditions	Other	Rate ($\mu m \cdot yr^{-1}$)	Reference
304	Ambient	Aerated	Urban, 5-15 yrs	<0.03	Johnson and Pavlik, 1982
			Urban, 5-15 yrs	0.022	
			Marine, 5-15 yrs	0.05-2	
			Industrial/urban, 5-15 yrs	0.01	
	Ambient		Industrial/urban	0.03-3	Kearns et al., 1984
316	Ambient	Aerated	Urban, 5-15 yrs	<0.03	Johnson and Pavlik, 1982
Stainless steel	Ambient	Aerated	Various atmospheres	0.05	Dechema, 1990

5.7.3.2   General Corrosion

For those WPs subject to dripping conditions in the repository, general corrosion of the stainless steel inner vessel and TAD canister could occur in a bulk aqueous environment. A wide range of passive corrosion rates for stainless steel have been reported (Table 5-14), with higher rates reported for saline solutions. For the fresh waters expected in the case of seepage following the thermal pulse, a conservative range of general corrosion rates is 0.1-1 $\mu m \cdot yr^{-1}$.

Table 5-14
General corrosion rates for stainless steel in neutral to slightly alkaline solution from the literature.

Grade	pH	Temperature (°C)	[Cl] ($\mu g \cdot g^{-1}$)	Redox conditions	Other	Rate ($\mu m \cdot yr^{-1}$)	Reference
304	Ambient	90	7,000-43,000	Aerated	10 hrs	10-130	Morsy et al., 1979
304L	Ambient	25-100	"Freshwater"	Aerated		0.21	BSC, 2004b
304L	Ambient	27 90	"Saltwater"	Aerated		11.4 5.82	BSC, 2004b
304	Ambient	25 50 75	Interstitial clay water	Aerated		0.2-0.96 0.22-0.23 0.3-0.35	Casteels et al., 1986
316	Ambient	Ambient	19,000	Aerated	8 yrs, Pacific Ocean seawater	4	Alexander et al., 1961
316L	Ambient	30 50-100	"Freshwater"	Aerated		0.01 0.25	BSC, 2004b
316L	Ambient	27	"Saltwater"	Aerated		1.94	BSC, 2004b
316	Ambient	25 50 75	Interstitial clay water	Aerated		0.1-0.24 0.1-0.34 0.1-0.17	Casteels et al. 1986
Stainless steel	Ambient	25-40	Seawater 19,000	Deaerated	120 days	0.8	White et al., 1966
Stainless steel	Ambient	25-40		7.7 $\mu g \cdot g^{-1}$ O_2 2.17 $\mu g \cdot g^{-1}$ O_2		0.55 4.8	White et al.,1966
Stainless steel	9.8 9.4	25 80	2,000	Deaerated		0.025-0.23 0.01-0.034	Hoch et al., 1992

5.7.3.3   Localized Corrosion

Localized corrosion of stainless steel may take the form of pitting of exposed surfaces and/or of crevice corrosion of occluded areas. The assessment and prediction of LC is usually divided into initiation and propagation stages.

Initiation of localized corrosion can be assessed by comparing the corrosion potential (E_{CORR}) to the critical potential for LC. Two characteristic potentials can be used to determine the critical potential for LC, the breakdown potential (E_P and E_{CREV} for pitting and crevice corrosion, respectively) or the re-passivation potential (E_{RP} and E_{RCREV} for pitting and crevice corrosion, respectively). The re-passivation potential is the potential at which a propagating LC site will stop growing. Values for E_P/E_{CREV} and E_{RP}/E_{RCREV} can be determined for the pitting of bold surfaces or the crevice corrosion of occluded areas.

The criterion for localized corrosion can be written as:

$$E_{CORR} > E_P, E_{CREV} \qquad \text{eq. 5-8}$$

based on a film breakdown criterion, or

$$E_{CORR} > E_{RP}, E_{RCREV} \qquad \text{eq. 5-9}$$

based on re-passivation. Figure 5-32 illustrates the concept for the pitting of 316L stainless steel in Cl^- solutions at 95°C (Dunn et al., 1996). Based on the comparison of E_{CORR} and E_{RP}, pitting is possible only in aerated solution.
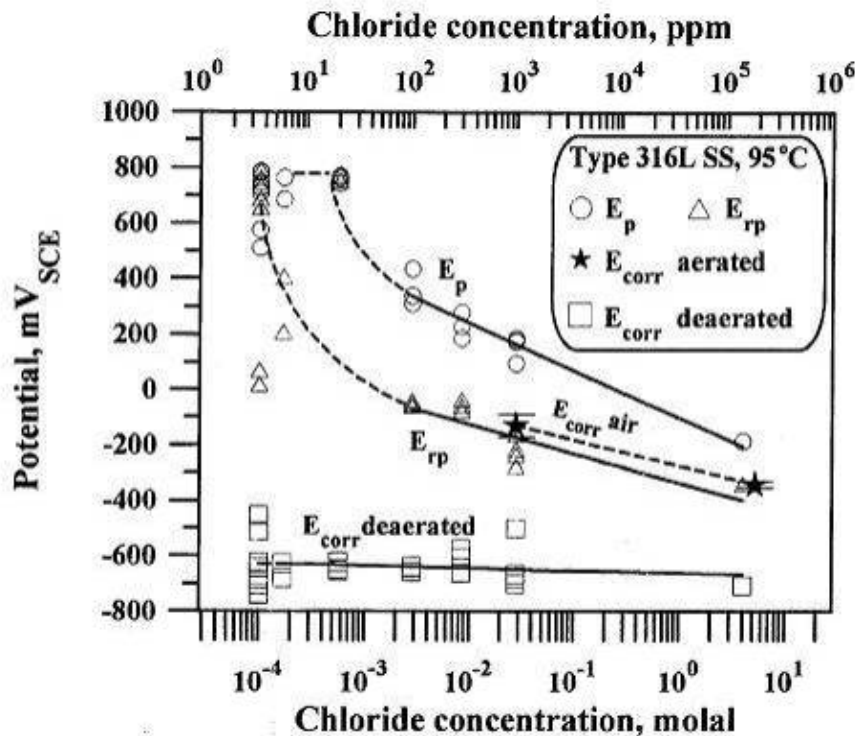
Figure 5-32
Comparison of the pitting and pit repassivation potentials for type 316L stainless steel to the corrosion potential E_{CORR} in aerated and deaerated chloride solutions at 95°C (Dunn et al., 1996).

The tendency of a stainless steel alloy to pit can be characterized by the pitting resistance equivalent number or PREN, which relates the pitting propensity to the alloy composition, particularly the Cr, Mo, and N contents (Sedriks, 1996). Nitrogen improves the pitting resistance

of stainless steels but increases the susceptibility to SCC, so the restriction of the N content for the grade of stainless steel to be used for the inner vessel is a compromise between cracking susceptibility and LC. The general form of the PREN expression is

$$PREN = \%Cr + a \cdot \%Mo + b \cdot \%N \qquad \textbf{eq. 5-10}$$

The values of a and, in particular, b tend to vary depending on whether corrosion takes the form of pitting or crevice corrosion, on the nature of the environment, and to some degree on the alloy family (Pettersson and Flyg, 2004). Figure 5-33 shows the dependence of the propensity for pitting on the PREN for various austenitic, duplex, and super-austenitic alloys.
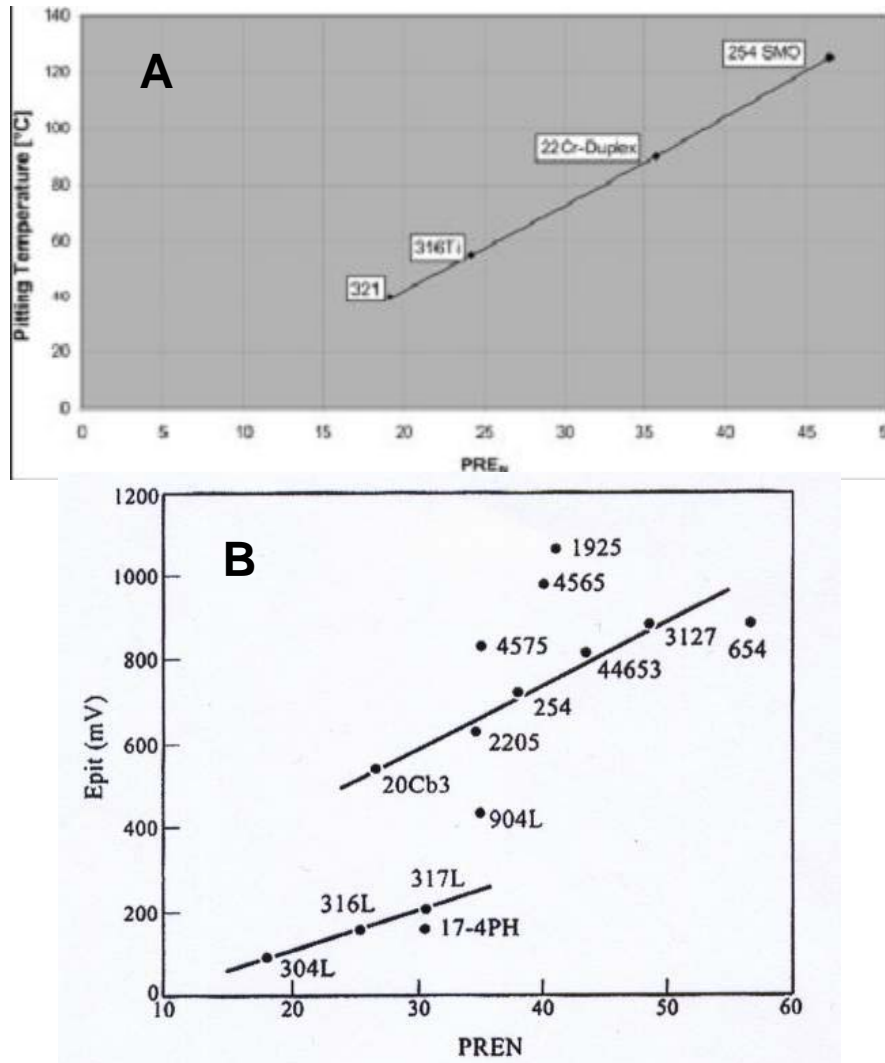
Figure 5-33
Correlation between the pitting resistance equivalent number (PREN) and pitting resistance for various austenitic, duplex, and super-austenitic stainless steels. (A) Dependence of the critical pitting temperature on PREN (Oberndorfer et al., 2004). (B) Correlation between the PREN and pitting potential (Malik et al., 1996).

The general susceptibility of a stainless alloy to LC is often presented in the form of "corrosion maps" (Figures 5-34, 5-35 and 5-36). Figure 5-34 shows the susceptibility of Type 316L (and of

a number of other stainless steels) to pitting and crevice corrosion in terms of a threshold temperature and chloride ion concentration. (In this case, "susceptibility" refers to a combination of both initiation and propagation). The threshold temperature for localized attack increases with decreasing Cl⁻ concentration, with a critical crevice temperature in fresh waters (defined here as ≤100 µg·g⁻¹ Cl⁻) of 65-70°C. Pitting occurs under more severe conditions, with a critical pitting temperature for Type 316L in fresh water of above 100°C, according to Figure 5-34. Sulfate ions inhibit the LC of austenitic stainless steels, as illustrated in Figure 5-35. The pH of the environment also affects the propensity to LC, with increasing susceptibility with decreasing pH (Figure 5-36).
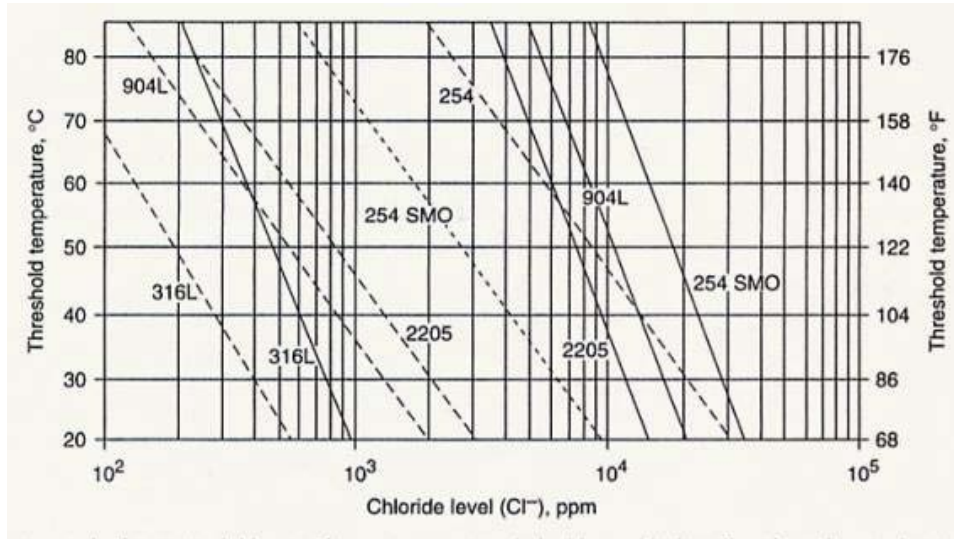
Figure 5-34
Corrosion map illustrating critical pitting and crevice corrosion temperatures as a function of chloride concentration for various stainless steels (ASM, 2005). The threshold conditions for pitting and crevice corrosion for each alloy are indicated by the solid and broken lines, respectively.
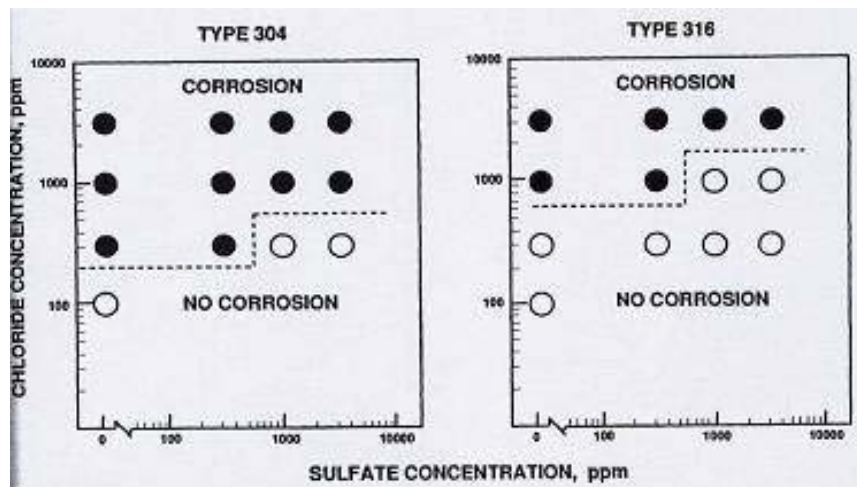
Figure 5-35
Inhibitive effect of sulfate on the crevice corrosion of types 304 and 316 stainless steel in chloride solutions (from Sedriks, 1996).
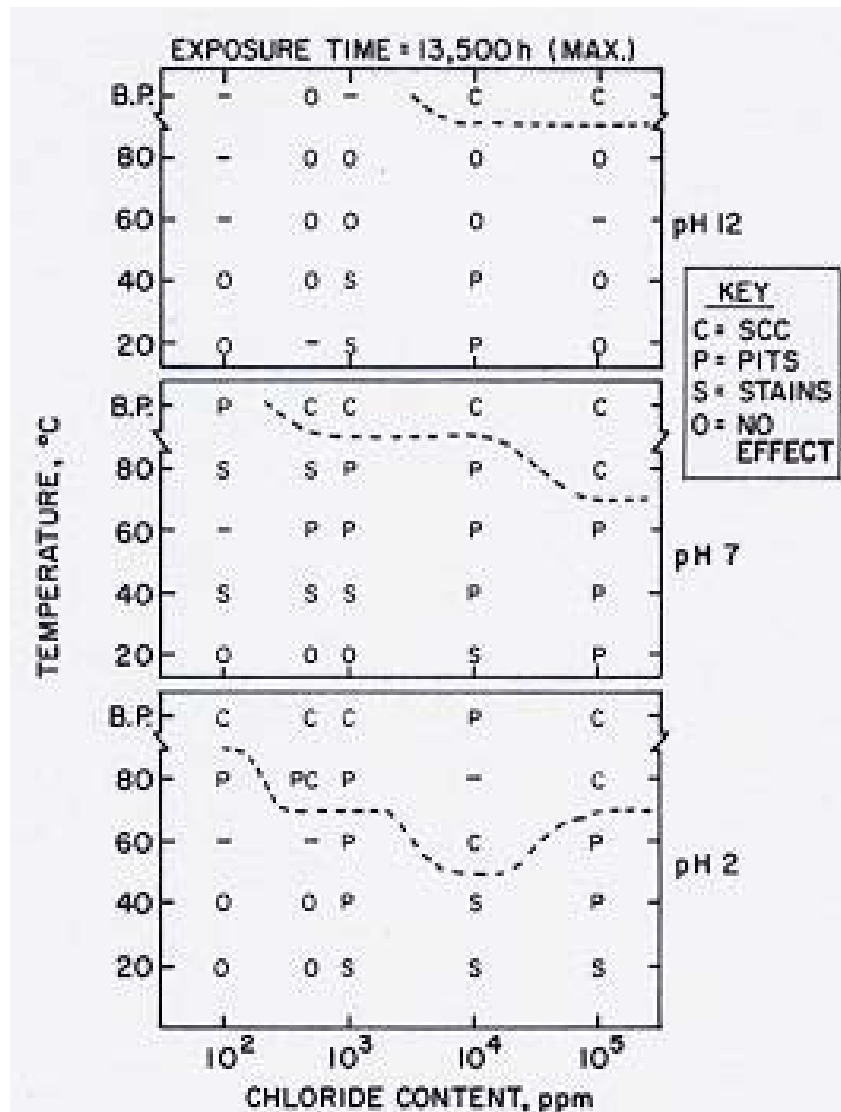
Figure 5-36
Ranges of pH, chloride concentration and temperature for the pitting and stress corrosion cracking of 304 stainless steel (Jones, 1992). The dashed curves in each figure define the transition from pitting attack (P) to SCC (C).

If LC does initiate, there is evidence that propagation is limited by stifling of the pit or crevice. Figure 5-37 shows the time dependence of the crevice corrosion rate, clearly indicating a strong tendency for the crevice to slow down with time (or "stifle"). Various factors may account for the observation of stifling, including:

1. The ohmic drop in deep pits that shifts the potential at the bottom of the pit or crevice below the repassivation potential;

2. Decreasing cathode:anode surface area ratio;

3. Mass-transport limitation of aggressive species to the bottom of actively growing pits and crevices;

4. Loss of critical pit or crevice chemistry;

5. Preferential migration of inhibitive anions into the pit or crevice; or

6. Passivation of actively growing pits or crevices due to enrichment of the alloying elements that are stable at low pH.

As only a small fraction of the failed WP will be subject to dripping, the majority of the internal stainless steel components will only be exposed to atmospheric conditions. In unsaturated systems, the extent of crevice or pit propagation can become cathodically limited as the aerial extent of the cathode is limited by the availability of water. Factors such as the high resistivity of thin liquid layers and suppression of the rate of O_2 reduction due to the increase in pH in the cathodic electrolyte can serve to inhibit localized corrosion under atmospheric conditions (Cui et al., 2005; Kelly et al., 2006).
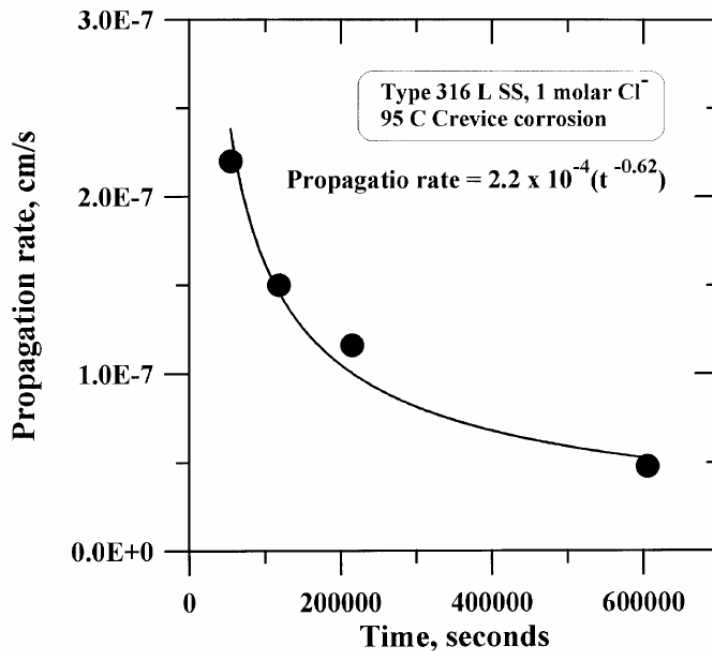
Figure 5-37
Evidence for the stifling of the crevice corrosion propagation of type 316L stainless steel
(Dunn et al., 1996).

5.7.3.4   Stress Corrosion Cracking

The anticipated procedure for WP closure does not call for stress relief of the inner vessel closure weld (SNL, 2007c). It is assumed, therefore, that significant residual tensile stress, amounting to several tens of percent of the yield stress, will render the inner vessel susceptible to SCC under appropriate conditions.

The available evidence, however, suggests that the probability of SCC of the stainless steel components in a failed WP is low because of the nature of the environment. Figure 5-38 shows the combination of temperature and Cl$^-$ concentration for the susceptibility of various stainless steels to SCC. Although the austenitic alloys tend to be more susceptible than other alloys, there is a threshold temperature of 50-60°C below which Types 304 and 316 and their low-carbon variants are immune to cracking, regardless of the Cl$^-$ concentration. This threshold temperature is supported by practical experience (McIntyre, 1987). It seems unlikely, therefore, that the stainless steel inner vessel or TAD canister will be susceptible to SCC, especially since a low-carbon content has been specified that will prevent sensitization of the weld region. However, it is difficult to completely exclude the possibility of cracking as localized environments and conditions that support cracking, such as microbial reduction of sulfate to thiosulphate, could form and because of the potential for high tensile stresses due to the lack of post-weld stress relief and because of external loading from an accumulated rock pile.

5.7.3.5   Microbiologically Influenced Corrosion

Austenitic stainless steels are susceptible to MIC (Little et al., 1991). Attack is often focused at weld regions, in which distinctively shaped pits are often observed. Ennoblement of E$_{CORR}$ has also been observed, possibly rendering the material more susceptible to localized corrosion. If locally acidic conditions form under biofilms due to acid-producing bacteria, de-passivation could occur at sufficiently low pH. Although the drift environment will be aerobic, local anaerobic regions could form under biofilms, raising the possibility of anaerobic microbial activity as well. It is not possible, therefore, to exclude the possibility of MIC of the stainless steel inner vessel and TAD canister.
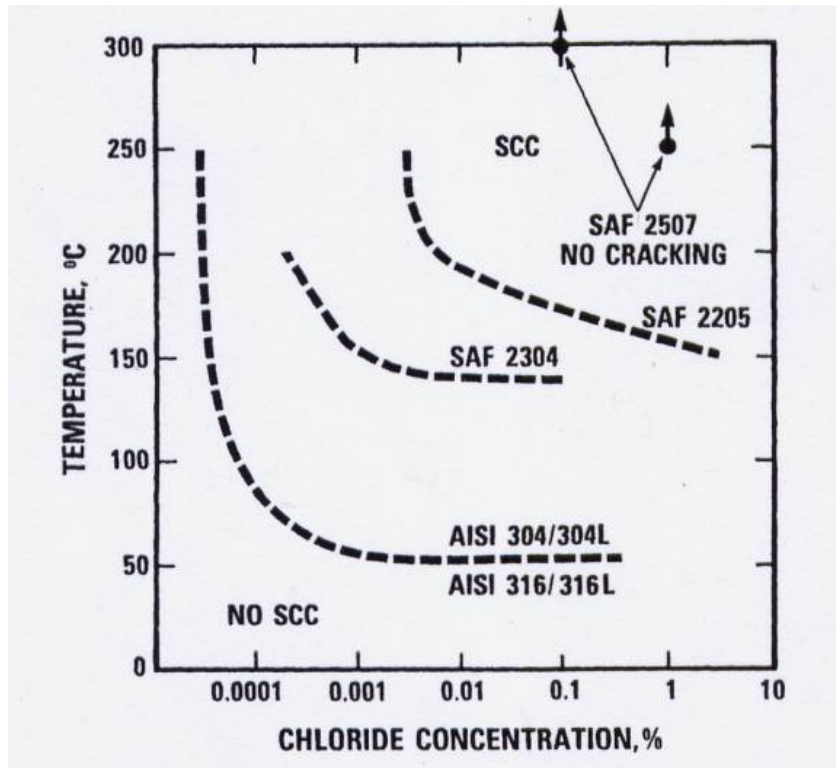
Figure 5-38
Corrosion map for the susceptibility of various austenitic and other stainless steels to stress corrosion cracking in aerated chloride environments as a function of temperature (Sedriks, 1996).

5.7.4. Lifetime Assessment

5.7.4.1   Definition of Failure

The stainless steel inner vessel and, depending upon the final design, the TAD canister, are designed to be sealed to provide containment of the CSNF. For the current assessment, initial failure of the stainless steel inner vessel is assumed to occur locally and produce a relatively small through-wall penetration, preferentially at the closure weld. A small through-wall defect, however, still provides significant mass-transfer resistance to the release of radionuclides. Therefore, final failure of the inner vessel is defined here as the complete loss of barrier function of the vessel, corresponding to significant general corrosion of the wall.

No additional credit is taken for the performance of the TAD canister as a barrier to radionuclide release. Although a small aperture in the closure weld of the inner vessel is likely to prevent significant water ingress, it would be theoretically possible for the TAD canister to start to corrode upon the initial failure of the inner vessel weld. Therefore, because the TAD canister is assumed to be thinner than the inner vessel, the TAD canister could corrode before the inner vessel has completely corroded,   thus offering little, if any, additional barrier function.

5.7.4.2   Assessment of Corrosion Processes

Because of the variability in the nature of the environment to which the stainless steel inner vessel and TAD canister will be exposed, a detailed calculation of the expected lifetime of the stainless steel components inside the WP is beyond the scope of the current report. Instead, a range of possible lifetimes is given to illustrate the potentially significant delay in the release of radionuclides as a result of the corrosion resistance of the internal components of the WP.

Based on the discussions above, the most likely degradation mechanism for the inner vessel is general corrosion. For a general corrosion rate in the range of 0.1-1 $\mu m \cdot yr^{-1}$, the estimated lifetime for the 50.8-mm-thick inner vessel is 50,000-500,000 years. However, because it is not possible to exclude the possibility of MIC, SCC, and (possibly) LC, earlier, local penetration of the inner vessel is considered possible, especially of the closure weld. No attempt is made here to model the kinetics of microbial attack or of crack growth. Instead, a penetration time of 100 years is estimated based on expert judgment.

Figure 5-39 shows the predicted fractional failed surface area of the inner vessel as a function of time following the first penetration of the Alloy 22 outer corrosion barrier. It is assumed here that the area of the weld region that fails after the estimated 100 years is equivalent to 5% of the surface area of the vessel. Following this early penetration, the remainder of the inner vessel continues to provide a significant mass-transport barrier to the ingress of water and the release of radionuclides until the body of the vessel corrodes after an estimated period of 50,000-500,000 years following initial failure of the outer Alloy 22 corrosion barrier.
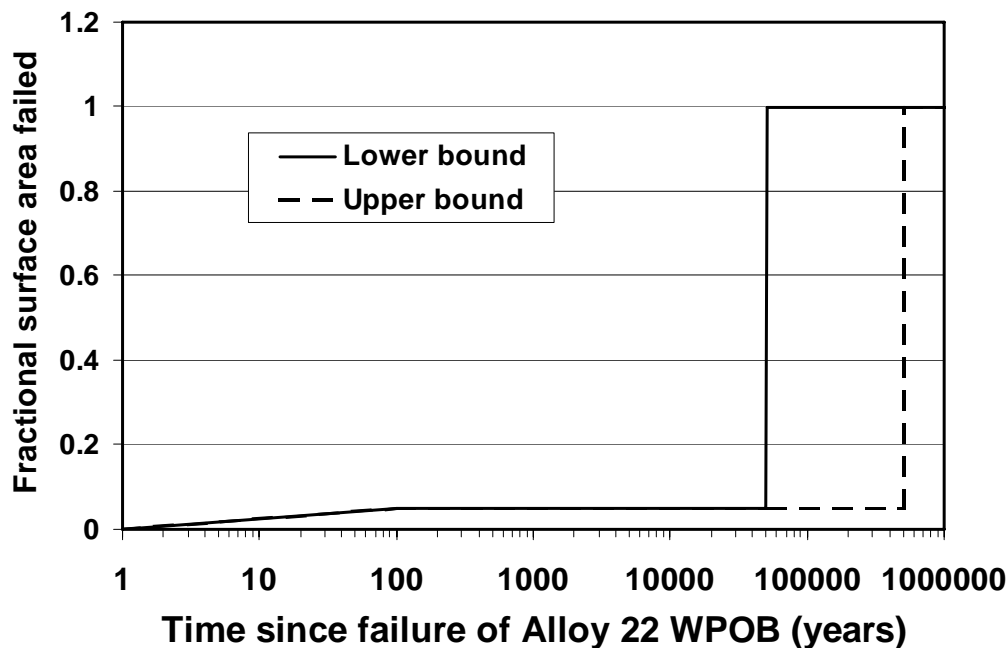
Figure 5-39
Estimated Time Dependence of the Fractional Failed Surface Area for the Stainless Steel Inner Vessel Following Failure of the Alloy 22 Outer Corrosion Barrier.

5.7.5 Conclusions

In its TSPA modeling, EPRI recognizes no performance credit for the stainless steel internal components of the waste package, which include the stainless steel inner vessel and the TAD canister. This represents a conservative approach as both containers will be sealed (welded) and will have a combined wall thickness of the order of 3 in (75 mm). Furthermore, both the inner vessel and TAD canister will be constructed from corrosion-resistant austenitic stainless steel, similar in composition to AISI Type 316L, and the repository environment will be relatively benign by the time of anticipated initial waste package failure, approximately 400,000 years or more after emplacement.

The most likely form of corrosion of the stainless steel inner vessel and TAD canister is general corrosion in humid air and, for the small number of packages exposed to dripping, in aqueous solution. Microbial activity is possible in the drift environment and may enhance the rate of general corrosion and/or promote localized attack at the welds. Localized corrosion in the form of pitting or crevice corrosion is unlikely as the temperature and chloride content of the seepage water are considered to be too low to initiate localized attack. Stress corrosion cracking is also thought to be unlikely, based more on the benign nature of the environment than on the absence of sufficient tensile stress (e.g., the closure welds will not be stress relieved).

EPRI has conducted a conservative assessment of the additional barrier credit provided by the stainless steel internal components. Despite the expected low probability of localized corrosion or stress corrosion cracking, early but localized failure of a small fraction of the inner vessel surface is assumed. Based on expert judgment, through-wall penetration of the closure weld (accounting for an estimated 5% of the entire surface area) is assumed to occur 100 years after through-wall penetration of the Alloy 22 waste package outer barrier. The inner vessel continues to provide significant mass-transfer resistance to the release of radionuclides until such time that the body of the vessel fails by general corrosion, a period estimated to be between 50,000 and 500,000 years following initial failure of the Alloy 22 waste package outer barrier. No additional credit is taken for the lifetime of the TAD canister, as it could potentially start to corrode as soon as water vapor enters the annular gap between the TAD canister and inner vessel at the time of initial penetration of the latter.

5.7.6 References

Alexander, A.L., C.R. Southwell, and B.W. Forgeson, 1961. Corrosion of metals in tropical environments, part 5 – stainless steel. *Corrosion* 17, 345.

Apted, M., F. King, D. Langmuir, R. Arthur, and J. Kessler, 2005. The unlikelihood of localized corrosion of nuclear waste packages arising from deliquescent brine formation. *Journal of Materials* 57, 2005, 43-48.

ASM (America Society for Metals), 1987. *Metals Handbook*, *9th edition, Volume 13, Corrosion*. American Society for Metals International, Metals Park, OH, 610-640.

ASM, 2005. *ASM Handbook, Volume 13B, Corrosion: Materials*. American Society for Metals International, Metals Park, OH.

BSC (Bechtel SAIC Company), 2003. *Drift Scale Coupled Processes (DST and THC) Models*, Report to DOE, MDL-NBS-HS-000001 Rev 02, Bechtel SAIC Company, Las Vegas, NV.

BSC, 2004a. *In-drift precipitates/salts model*. Report prepared for the U.S. DOE by Bechtel SAIC Company, ANL-EBS-MD-000045 Rev 02, Bechtel SAIC Company, Las Vegas, NV.

BSC, 2004b. *Aqueous corrosion rates for waste package materials*. Prepared for US DOE, ANL-DSD-MD-000001, Bechtel SAIC Company, Las Vegas, NV.

Casteels, F., G. Dresselaars, and H. Tas, 1986. *Corrosion behaviour of container materials for geological disposal of high level waste*. Commission of the European Communities Report, EUR 10398 EN, p. 3-40.

Cui, F., F.J. Presuel-Moreno, and R.G. Kelly, 2005. Computational modeling of cathodic limitations on localized corrosion of wetted SS 316L at room temperature. *Corrosion Sci*. <u>47</u>, 2987-3005.

Dechema, 1990. *Corrosion Handbook: Corrosive Agents and their Interaction with Materials, Volume 7 Atmosphere*.

DOE, 2006. *Preliminary transportation, aging and disposal canister system performance specification*, WMO-TADCS-0000001 Rev. A.

DOE, 2008. *Yucca Mountain Repository License Application*, DOE/RW-0573, Rev. 0.

Dunn, D.S., G.A. Cragnolino, and N. Sridhar, 1996. "Localized corrosion initiation, propagation, and repassivation of corrosion resistant high-level nuclear waste container materials." <u>In</u> *Proc. CORROSION/96*, NACE International (Houston, TX), paper no. 97.

EPRI, 2004. *Potential Igneous Processes Relevant to the Yucca Mountain Repository: Extrusive-Release Scenario Analysis and Implications*, Electric Power Research Institute, Palo Alto: 2004. 1008169.

EPRI, 2005a. *EPRI Yucca Mountain Total System Performance Assessment Code (IMARC) Version 8 – Model Description*. Electric Power Research Institute, Palo Alto, CA: 2005. 1011813.

EPRI, 2005b. *Potential Igneous Processes Relevant to the Yucca Mountain Repository: Intrusive-Release Scenario*, Electric Power Research Institute, Palo Alto, CA: 2005. 1011165.

EPRI, 2006. *Effects of Multiple Seismic Events and Rockfall on Long-Term Performance of the Yucca Mountain Repository*, Electric Power Research Institute, Palo Alto, CA: 2006. 1013444.

EPRI, 2008. *Occupational Risk Consequences of the Department of Energy's Approach to Repository Design, Performance Assessment and Operation in the Yucca Mountain License Application*, Electric Power Research Institute, Palo Alto, CA: 2008. 1018058

He, X., D.S. Dunn, and A. Csontos, 2007. Corrosion of similar and dissimilar metal crevices in the engineered barrier system of a potential nuclear waste repository. *Electrochimica Acta* 52, 7556-7569.

Hoch, A.R., C.C.Naish, S.M. Sharland, A.C. Smith, and K.J. Taylor, 1992. Experiments and Modeling Studies Concerning Localised Corrosion Of Carbon Steel And Stainless Steel Containers For Intermediate And Low Level Radioactive Waste, *Materials Research Society Symposia Proceedings*, Nov 30, 1992.

James, R., F. King, and J. Kessler, 2006. The Consequence of Seismic Activity on Waste Package Structural Integrity. In *Proc. 11th International High-level Radioactive Waste Management Conference*, American Nuclear Society (La Grange Park, IL), pps. 913-920.

Johnson, M.J. and P.J. Pavlik, 1982. Atmospheric corrosion of stainless steels. In *Atmosphere Corrosion*, W.H. Ailor (Ed.), p. 461.

Jones. R.H. (ed.), 1992. *Stress-Corrosion Cracking*. ASM International, Materials Park, OH.

Kearns, J.R., M.J. Johnson, and I.A. Franson, 1984. The corrosion of stainless steels and nickel alloys in caustic solutions. In *Proc. CORROSION/84*, NACE International (Houston, TX), paper no. 146.

Kelly, R.G., A. Agarwal, F. Cui, Xi Shan, U. Landau, and J. H. Payer, 2006. Considerations of the role of the cathodic region in localized corrosion. In *Proc. 11th International High-level Radioactive Waste Management Conference*, American Nuclear Society (La Grange Park, IL).

King, F., 2008. The impact of microbiologically influenced corrosion on the lifetimes of the Yucca Mountain engineered barrier system. In *Proc. 12th International High-level Radioactive Waste Management Conference*, American Nuclear Society (La Grange Park, IL), pps. 229-240.

King, F., M. Kolar, J.H. Kessler, and M. Apted, 2008. Yucca Mountain engineered barrier system corrosion model (EBSCOM)." *J. Nucl. Mater.* 379, 59-67.

King, F., R. James, S. Findlan, M. Apted, and J. Kessler, 2006. Performance of the Waste Package During an Igneous Disruptive Event. In *Proc. 11th International High-level Radioactive Waste Management Conference*, American Nuclear Society (La Grange Park, IL), pps. 835-842.

Little, B., P. Wagner, and F. Mansfeld, 1991. Microbiologically influenced corrosion of metals and alloys. *Int. Mater. Rev.* 36, 253-272.

Malik, A. U., N. A. Siddiqi, S. Ahmad, and I. N. Andijani, 1996. The effect of dominant alloy additions on the corrosion behavior of some conventional and high alloy stainless steels in seawater. *Corrosion Sci.* 37, 1521-1535.

McIntyre, D.R., 1987. *Experience survey stress corrosion cracking of austenitic stainless steel in water.* Materials Technology Institute, St, Louis, MO. MTI Publication No. 27.

Morsy, S.M., S.M. El-Raghy, A.A. Elsaed, and A.E. El-Mehairy, 1979. *Effect of cations on the corrosion of stainless alloys in saline water at elevated temperatures.* Arab Republic of Egypt Atomic Energy Establishment Report 232.

Oberndorfer, M., K. Thayer, and M. Kästenbauer, 2004. Application limits of stainless steels in the petroleum industry. Materials and Corrosion 55, 174-180.

Pettersson, R.F.A. and J. Flyg, 2004. *Electrochemical evaluation of pitting and crevice corrosion resistance of stainless steels in NaCl and NaBr.* Outokumpu report, ACOM 3-2004.

Pourbaix, M., 1974. *Atlas of Electrochemical Equilibria in Aqueous Solutions, 2nd edition.* NACE International, Houston, TX.

Rard, J.A., K.J. Staggs, S.D. Day, and S.A. Carroll, 2005. *Boiling temperature and reversed deliquescence relative humidity measurements for mineral assemblages in the $NaCl + NaNO_3 + KNO_3 + Ca(NO_3)_2 + H_2O$ system.* Lawrence Livermore National Laboratory Report, UCRL-JRNL-217704.

Sedriks, A.J., 1996. *Corrosion of Stainless Steels, 2nd edition.* John Wiley, New York, NY.

Shreir, L.L., R.A. Jarman, and G.T. Burstein, 1993. *Corrosion.* 3rd edition, Butterworth-Heinemann, Oxford.

SNL (Sandia National Laboratory), 2007d. *Engineered Barrier System: Physical and Chemical Environment.* ANL-EBS-MD-000033 REV 06. Las Vegas, Nevada: Sandia National Laboratories. ACC: DOC.20070907.0003.

SNL, 2007a. *Seismic consequence abstraction.* Report prepared for US DOE by Sandia National Laboratories, MDL-WIS-PA-000003 REV 03.

SNL, 2007b. *Total System Performance Assessment (TSPA) data input package for requirements analysis for TAD canister and related waste package overpack physical attributes basis for performance assessment.* Report prepared for US DOE by Sandia National Laboratories, TDR-tDIP-ES-000006 Rev 00A.

SNL, 2007c. *Analysis of mechanisms for early waste package/drip shield failure*, Report prepared for US DOE by Sandia National Laboratories, ANL-EBS-MD-000076 Rev 00.

White, J.H., A.E. Yanic, and H. Schick, 1966. The corrosion of metals in the water of the Dead Sea. *Corros. Sci.* 6, 447.

5.8   An Assessment of the Threat from Microbiologically Influenced Corrosion to the Lifetime of the Engineered Barrier System in the Yucca Mountain Repository

5.8.1 Introduction

Microbiologically influenced corrosion (MIC) is a potential threat to the long-term integrity of the engineered barrier system (EBS) in the Yucca Mountain Repository. Consequently, repository performance assessments need to address the potential for, and extent of, MIC with respect to the long-term behavior of repository engineered barriers, including key components such as the Alloy 22 waste package (WP) and Titanium-7 drip shield (DS). Assessment of MIC can take the form of a detailed mathematical model to quantitatively describe the rates of various processes, or expert judgments based on a scientific body of evidence that is used to exclude MIC from consideration due to unfavorable conditions for the particular materials of concern and the repository environment.

Microbes (bacterial, yeasts, fungi) could impact the corrosion behavior of the EBS in a number of ways. MIC is most often observed as corrosion underneath a biofilm which, among other features, acts to occlude the surface and promote the development of local environments than can depart dramatically from bulk conditions. Biofilms are spatially heterogeneous (Little and Wagner, 1996) and, therefore, localized corrosion can result from the separation of anodic and cathodic processes. For engineering structures, virtually all forms of MIC reported in the literature are associated with corrosion underneath a biofilm. Microbial activity can produce additional oxidants, which promote corrosion (King, 1996). This particular consequence of microbial activity is of concern for repository designs in which the amount of oxidant is limited, but is less significant for the permanently aerobic Yucca Mountain (YM) environment. More generally, H^+ produced by acid-producing bacteria could also result in additional corrosion if these acidic products contact the WP or DS surface and are not neutralized by some form of pH-buffering agent present in the system (Little and Wagner, 1996). The action of microbes can also promote forms of corrosion that otherwise would not be of concern. For example, reduced sulfur species have been shown to cause the loss of passivation of Ni-based alloys (Marcus, 1995).

Evaluating the long-term effects of MIC on the lifetime of the EBS can be approached from two general directions. The first approach involves determining the effect of the repository environment on microbial activity and predicting where and when microbes might be active (BSC, 2004a). Microbial activity, not the mere presence of microbes, is the key to understanding MIC effects. The second approach involves estimating how much damage could result assuming microbial activity exists in the repository. Such an estimate can be based on microbial kinetics or on the availability of nutrients necessary for supporting microbial activity. The two approaches are complementary, and both can be used in parallel to determine whether microbes and microbial activity pose a credible threat to EBS integrity.

A decision-tree approach is used here to determine whether MIC represents a threat to the integrity of the EBS and to the safety of the disposal system. Specifically, the following questions are addressed:

- Will microbes be present in the YM repository?

- If present, will microbes be active?

- If active, will corrosion occur?

- If corrosion occurs, will failure of the WP or DS result?

- If failure of the EBS occurs, will the performance of the disposal system be compromised?

The YM repository design incorporates a number of engineered and natural barriers that collectively form a multiple-barrier system. In a multiple-barrier system, the question is not so much whether MIC (and other corrosion processes) limits the lifetime of the EBS, but rather whether such processes impact the performance of *the entire system*. For the YM repository the performance of the system is defined in terms of the dose limit to the Reasonably Maximally Exposed Individual (RMEI). Therefore, the threat posed by MIC is only significant if it leads to either accelerated or simultaneous EBS failures and an increase in the dose to the RMEI over the assessment period. In order to evaluate the impact of MIC on repository performance, a sufficiently quantitative treatment of MIC is needed.

The YM repository provides a relatively inhospitable environment for microbial activity (BSC, 2004a). Microbial stressors in the repository include: elevated temperature, absence or lack of free water, absence or lack of nutrients and/or terminal electron acceptors, saline pore waters and evaporates, redox conditions, and radiation fields. While specific microbes can be identified that are tolerant to each of these stressors on an individual basis, combinations of multiple stressors can be expected to effectively limit microbial diversity. This diversity is critical for promoting and sustaining growth and activity, and therefore the likelihood of MIC.

An important consideration, one that will be emphasized throughout the following discussion, is the location of microbial activity relative to the WP. Clearly, microbes <u>on</u> the WP or DS surface will experience a substantially different environment and could have much greater impacts on EBS performance than microbes at some location removed from the EBS. Environmental conditions at the WP surface are generally more severe than those further away, making microbial activity on the container less likely (King, 1996; King and Stroes-Gascoyne, 1997; Meike and Stroes-Gascoyne, 2000; Stroes-Gascoyne and King, 2002). For example, the temperature and radiation field are highest at the WP surface, as is the degree of desiccation. Conversely, microbial activity is more likely in the more-hospitable environments further from the WP. Corrosion will only occur as a result of this remote activity if aggressive metabolic by-products reach the WP surface under the protective DS.

As for any corrosion process, the environmental conditions play an important role in determining whether microbes are active and whether MIC of the EBS will occur. Environmental conditions within the proposed YM repository will evolve with time (BSC, 2004b, c; Gordon, 2002). The maximum design WP surface temperature (T) is in the range 150-200°C. During this elevated temperature period water is driven away from the WP and aqueous corrosion does not occur until the container cools and the relative humidity (RH) in the drifts increases. At some point, the temperature is sufficiently low and the RH sufficiently high that surface contaminants on the WP deliquesce resulting in surface wetting and the initiation of aqueous corrosion. Once the temperature of the drift wall drops below the local boiling point (96°C), water may drip from the walls onto the WP, or more likely onto the surface of the Ti-7 drip shields emplaced over the

waste packages to protect them from dripping. The initial water contacting the WP or DS surface will be concentrated, either because it forms a thin deliquesced liquid film or because of the evaporative concentration of seepage drips. As the temperature cools and the RH increases, the concentration of the surface aqueous phase will decrease. External γ-radiation fields are likely to be <1 Gy/hr, especially since the WP is currently being designed to accept an inner Transportation, Aging and Disposal (TAD) canister, resulting in a combined wall thickness of 10-20 cm. Because there is no backfill in the proposed repository, gaseous species can diffuse freely in the drifts (or be transported by advection during the initial 50-year ventilation period). However, there is no continuous aqueous phase through which dissolved species can diffuse, so for these species transport to the WP can only occur from the roof of the drifts in the seepage drips, assuming that the drip shield is no longer intact or along the surface of the packages in continuous surface liquid films, should they be present. The repository will be permanently aerated because of the location of the repository horizon in the unsaturated zone, approximately 300 m above the current water table.

5.8.2 Decision Tree Approach to MIC of the EBS

A number of pre-requisite conditions are necessary for MIC to occur. In deciding whether MIC is a concern for the overall performance of the disposal system, it is helpful to define these pre-requisites in the form of a decision tree. In this context, a decision tree provides a simple pictorial representation of the sequence of events or processes that need to occur for MIC to lead to impact repository performance to an unacceptable degree. The decision tree is structured as a series of questions laid out in a logical sequence, each of which must be answered in the affirmative to both proceed to the next decision and for MIC to be considered as a significant process for repository performance. A general decision tree for the MIC of the EBS is shown in Figure 5-40 with the individual "decisions" discussed in detail below. The decisions lead all the way from the question of whether microbes are present through to the consequences of MIC for the performance of the repository system. The main body of the tree comprises two parallel paths, one accounting for microbial activity and MIC at the surface of the WP and DS and the other describing the possibility and consequences of microbial activity at some other location in the repository.
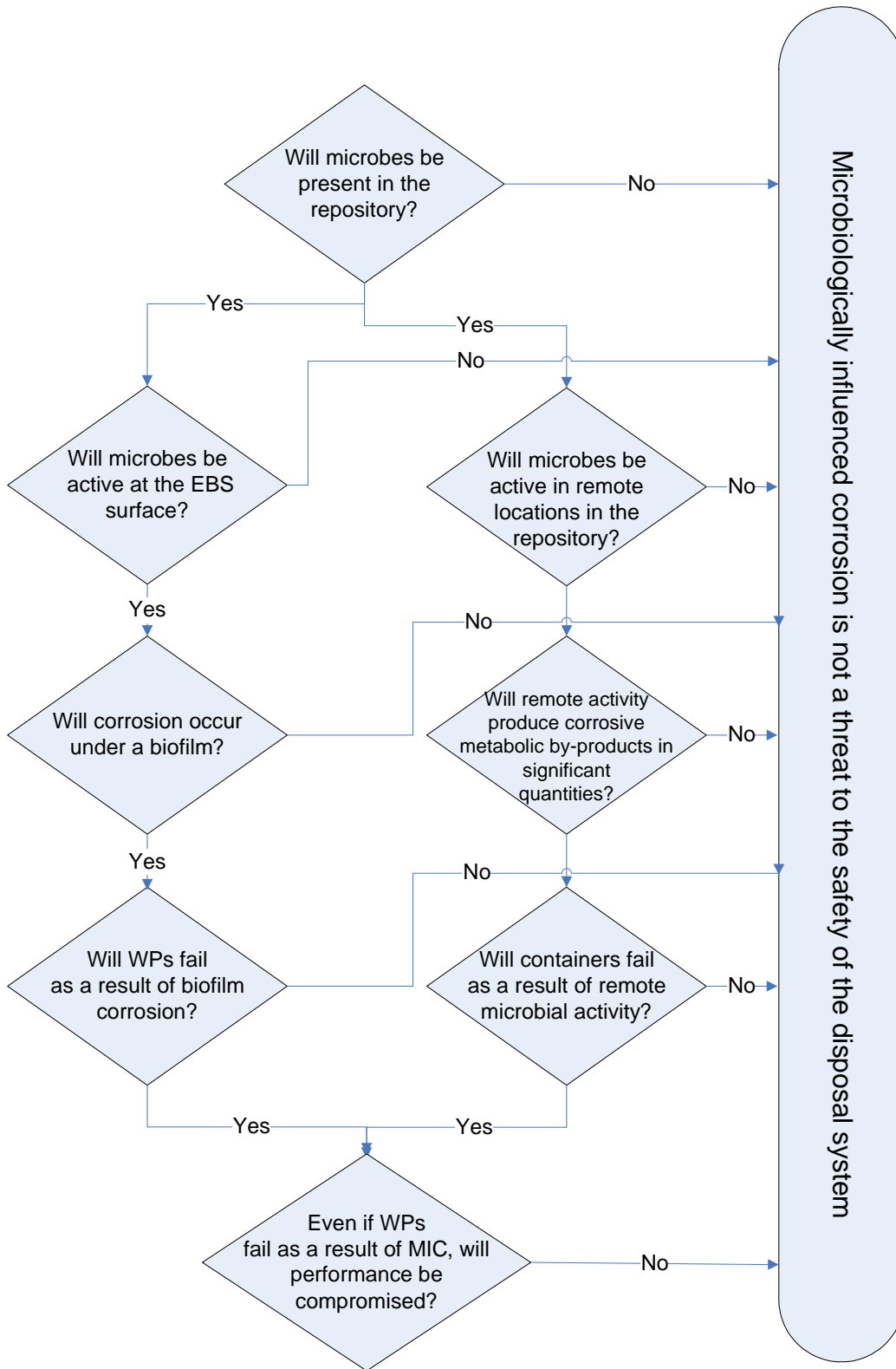
Figure 5-40
Decision Tree for Determining the Possibility and Consequences of Microbiologically Influenced Corrosion of the Engineered Barrier System.

5.8.2.1   Will Microbes Be Present in the Repository?

The first pre-requisite for MIC is the presence of microorganisms in the repository. (The term repository is used here to refer to the near-field engineered barriers and to the near-field region of the geosphere in which the presence of microbes could influence corrosion of the EBS.) Horn *et al.* (1998, 2003) and BSC (2004a) describe the results of microbial sampling at the YM site and the implications for MIC. A wide range of microbes were identified, including species tolerant of desiccation (e.g., *Bacillus*, *Clostridium*, *Arthrobacter*) and nutrient-poor conditions (e.g., *Caulobacterr*). Microbes may also be introduced during construction activities. Therefore, it appears certain that microbes will be present both in the host geological formation and in the drifts at the time of repository closure.

5.8.2.2   If Present, Will Microbes Be Active?

As noted above, it is not the presence of microbes that is of concern, but their activity. In general, the repository presents an inhospitable environment for microbes and microbial activity (BSC, 2004a). While it is always possible to identify specialized microbes that have adapted to survive in various extreme environments, the vast majority of microbes are inactive outside a relatively narrow range of optimal conditions. The combined effects of a number of sub-optimal environmental factors can severely restrict the number and diversity of active microbes in the repository and their ability to adapt to adverse conditions.

The key environmental factors that will limit microbial activity are:

Temperature

Elevated temperatures typically suppress the activity of microbes; the optimum temperature for many microorganisms falls within the 35-40°C range. Temperatures greater than 100°C are commonly used to sterilize surfaces; accordingly, WP and DS will only see significant microbial activity once the temperature has decreased to tolerable levels to allow for inoculation of the EBS surfaces. This is an important observation, since inoculation of the surface during handling and emplacement of the WP or during the ventilation period prior to the installation of the DS becomes unimportant. The thermal period following repository closure will essentially sterilize the WP surface and other EBS components.

Else *et al.* (2003) determined the limiting conditions of temperature and relative humidity for the formation of biofilms on the surfaces of metal coupons embedded in crushed YM tuff. Coupons of 316N stainless steel, Alloy 22, and an unspecified grade of Ti (but likely Ti Grade 2) were exposed to crushed tuff at temperatures of 30, 60, and 70°C at relative humidities of 100, 84, 70.5, and 32% RH, for periods of 0-18 months. No additional microbes, nutrients, or media were added. Any biofilm on the surface of the coupons was then sampled and the microbial population enumerated using standard methods.
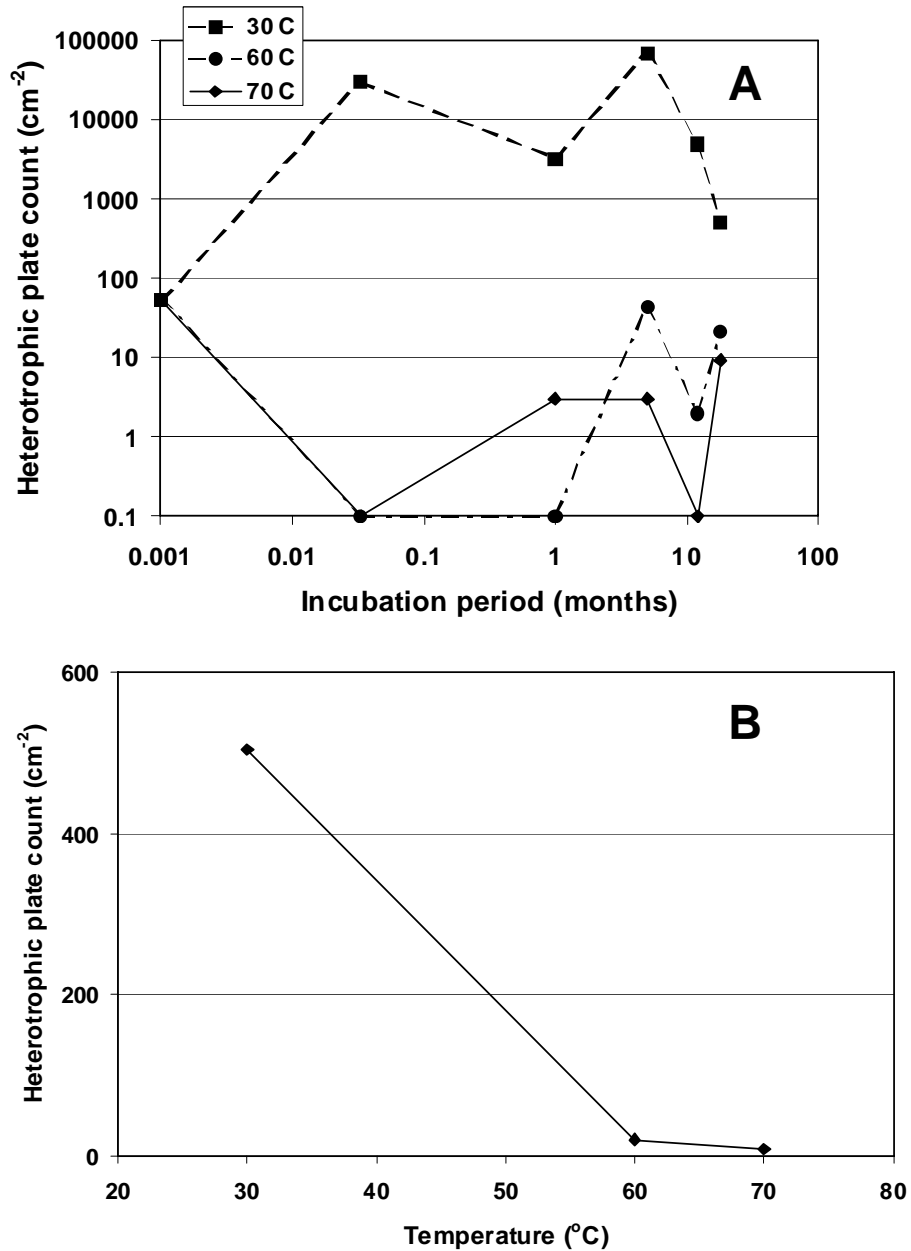
Figure 5-41
Time dependence of the surface microbial population on Alloy 22 coupons embedded in crushed YM Tuff at 100% RH, (A) as a function of incubation time at three temperatures [with zero population represented by a log scale plate count of <0.1 cm^{-2}] and (B) as a function of temperature after 18 months incubation (after Else *et al.*, 2003).

Figure 5-41 shows the time dependence of the number of culturable microbes on the surface of Alloy 22 coupons as a function temperature (Else *et al.*, 2003). These tests were conducted at 100%RH, so that the availability of water was not limiting. While microbes were observed at a temperature of 30°C, much smaller populations were observed at 60°C and 70°C, with populations of zero microbes reported in some cases (plotted as a plate count of 0.1 cm^{-2} in Figure 5-41(a)). The trend with temperature is more apparent from the data after 18 months

(Figure 5-41 (b)), for which the decline in microbial numbers with increasing temperature is clearly apparent. The trends for the 316N stainless steel and Ti coupons were similar (not shown). The trends exhibited by the microbial population were supported by evidence from SEM analyses of the surface. High microbial populations were associated with features indicative of surface colonization, whereas coupons with low microbial numbers showed no evidence for attached microbes. No evidence for corrosion was observed by Scanning Electron Microscopy (SEM) over the 18-month exposure for any of the materials studied (Else *et al.,* 2003).

Water activity and relative humidity

It is well understood that microbes require water to be active (Brown, 1990; Meike and Stroes-Gascoyne, 2000). In compacted soils and aqueous systems it is appropriate to speak in terms of water activity (a_w). In unsaturated atmospheres, the more common parameter is the relative humidity (RH), which is related to a_w by:

$$a_w = P/P_0 = RH \qquad \textbf{eq. 5-11}$$

where P and P_0 are the vapor pressure of the solution and of the pure solvent (water), respectively (Brown, 1990; Meike and Stroes-Gascoyne, 2000).

Most bacteria are inactive below a water activity of 0.96, equivalent to a relative humidity of 96%, with some specialized strains (e.g., halophiles) tolerant down to $a_w = 0.75$ (Brown, 1990). Yeasts and fungi tend to be more tolerant of low water activity than bacteria, but all microbial activity ceases below an a_w of ~0.6 (60% RH). As with other external environmental stressors, although microbes can be identified that can tolerate or adapt to tolerate low %RH, these microbes survive and/or maintain some low level of activity but do not flourish in these sub-optimal conditions.

Figure 5-42 shows the effect of %RH on the culturable microbial population on Alloy 22 specimens after exposure to crushed tuff for various periods of time (Else *et al.*, 2003). Minimal growth of microbes was observed at all RH, but especially at humidities <100% where the numbers of microbes were typically no greater than the initial population of 50-100 cm^{-2}.

Although the studies of Else *et al.* (2003) were performed using metal coupons, the results should be equally applicable to any surface, since the nature of the surface does not seem to have any impact on the extent of attachment. Thus, biofilms are also not expected to occur on rock surfaces exposed to these same limiting conditions of low humidity and high temperature. This is important as the creation of anaerobic microenvironments to support processes such as sulphate reduction requires biofilm formation.

There is some question as to the appropriate threshold %RH for the cessation of microbial activity. To maintain conservatism, DOE assumes a threshold of 75-90% RH for estimating the period during which MIC might be possible at the WP surface (BSC, 2004a). However, there is strong evidence that a more appropriate threshold is 96 %RH (or $a_w = 0.96$), as suggested by the data summarized by Brown (1990). Figure 5-43 shows the effect of the water activity on the natural microbial population in 95% saturated bentonite, adjusted by compacting the clay to different densities and/or through the addition of saline pore solution. Reductions in the number of culturable microbes for water activities <0.96 appears to occur, regardless of whether that activity is achieved through adjusting the clay density or the salinity of the pore water.

Culturability is measured in this case by taking a sample of the compacted bentonite, dispersing it in a nutrient-rich growth medium, and then counting the number of colonies formed when plated. Thus, these numbers overestimate the *in situ* microbial activity during the exposure, as other factors such as lack of water or nutrients or lack of space will limit activity within the pores of the bentonite. Instead, these results reflect the extent to which naturally occurring culturable microbes become "deactivated" by exposure to, in this case, low a_w.
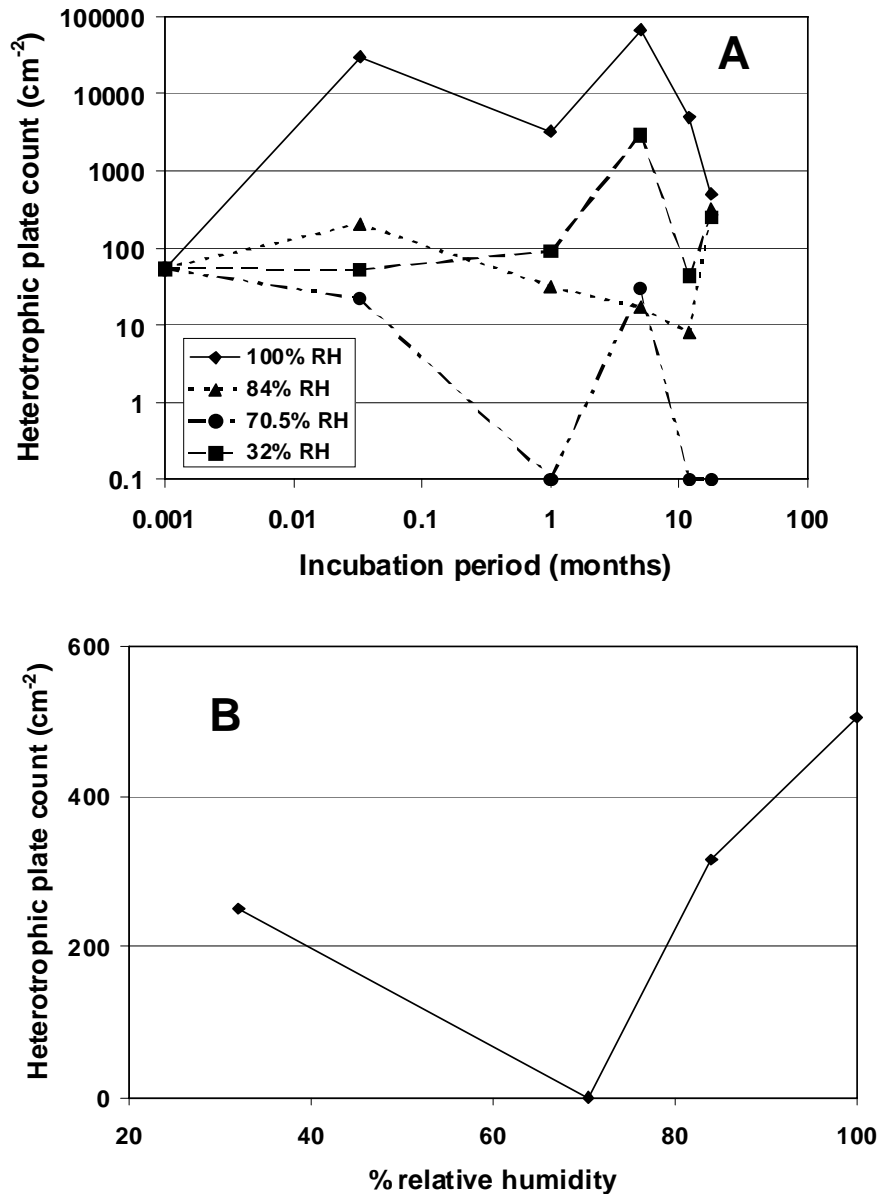
Figure 5-42
Effect of relative humidity on the microbial population on Alloy 22 coupons embedded in crushed Yucca Mountain tuff. (A) Time dependence of surface population for four relative humidity levels, and (B) Surface population dependence on relative humidity after 18 months incubation (after Else *et al.*, 2003).
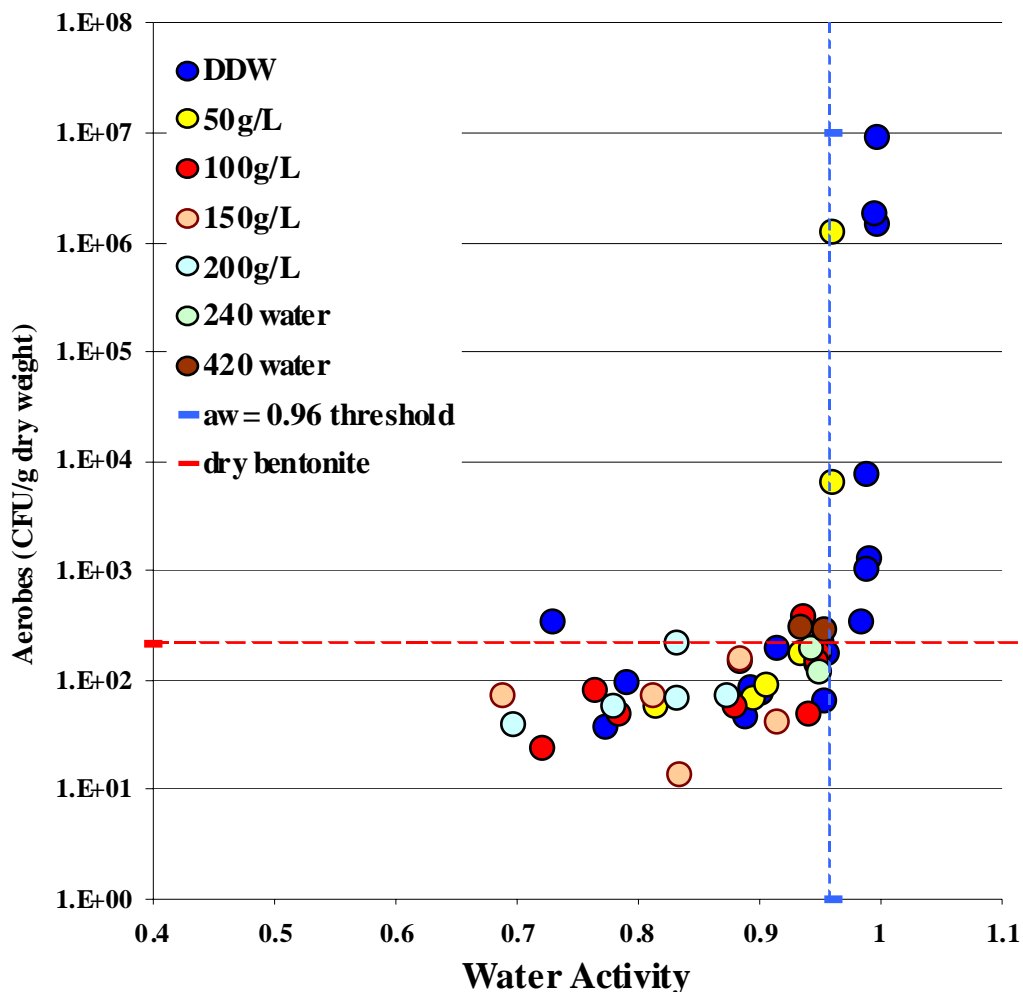
Figure 5-43
Number of culturable heterotrophic aerobes as a function of measured water activity following exposure to compacted bentonite for 40-90 days (Stroes-Gascoyne *et al.*, 2006, 2007).

The other feature of interest from Figure 5-43 is the rapid rise in post-test activity at $a_w > 0.96$. At these high water activities, which are achieved in this case by loosely compacting the bentonite with double-distilled water or a relatively low salinity simulated groundwater solution, the initial microbial population is not "deactivated" as at lower a_w, but rather it increases during the course of the exposure. This growth leads to a sharp increase in the culturable population by over four orders of magnitude over a narrow range of a_w. The water activity of 0.96, therefore, represents a threshold below which the population of culturable microbes is reduced. Whether these microbes are killed or simply rendered dormant by the low a_w is not currently known, but the important fact is that exposure to low a_w renders them inactive and unable to grow through normal metabolic activity.

The fact that the data in Figure 5-43 were obtained in a compacted bentonite system rather than in a humidity-controlled atmosphere is irrelevant to the current argument, since it is the availability of water that is the operative factor, not how that water activity or RH is achieved.

Salinity

Concentrated solutions are expected in the YM repository during the initial thermal pulse (BSC, 2004b; Gordon, 2002). The deliquescence of surface deposits or the evaporation of seepage drips will create highly concentrated aqueous solutions. If the solution is in equilibrium with the atmosphere in the drift, then the water activity in the aqueous phase will be equal to the relative humidity in the drift (BSC, 2004c). Until such time that the RH approaches 96% (based on the evidence in Figure 5-43), therefore, microbial activity will not occur.

Redox conditions

To be active, microbes require sources of nutrients and energy to support metabolic processes (Madigan *et al.,* 2000). Energy is provided by redox reactions involving the oxidation of organic matter, H_2, or other reduced species and the reduction of terminal electron acceptors (TEAs), such as O_2, NO_3^-, Fe(III), SO_4^{2-}, and CO_2. The TEAs are reduced in a well-defined sequence depending upon the amount of energy released or in electrochemical terms from the most-positive redox potential to the most negative, starting with the reduction of O_2 and progressing through the reduction of Mn(IV), NO_3^-, Fe(III), SO_4^{2-}, and CO_2. Figure 5-44 shows the redox potential ranges for various reduction and oxidation processes (Madigan *et al.,* 2000).
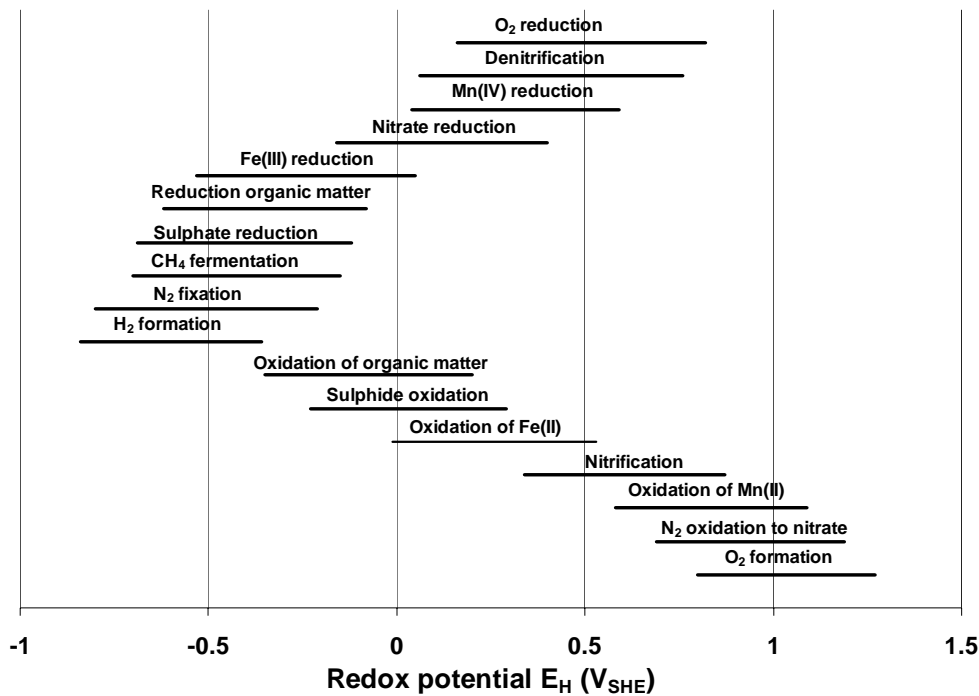
Figure 5-44
Observed ranges of redox potential for microbially mediated reduction and oxidation processes (Madigan et al., 2000).

While all of these redox reactions are possible in the YM repository, there are certain restrictions on where and when different reactions may occur. Aerobic processes will be favored throughout the repository environment, whereas anaerobic reactions will only occur in anoxic microenvironments, assuming other permissive environmental factors exist.

Little (2003) has suggested that denitrification (the use of NO_3^- as a TEA by denitrifiers) will result in an increase in the $Cl^-:NO_3^-$ ratio in the drift and, hence, the possibility of localized corrosion of the WP (BSC, 2004d). However, denitrifiers use NO_3^- as a TEA in the absence of O_2 but, since the repository will be permanently aerobic, they will preferentially consume O_2 as it results in a larger energy release. Furthermore, the emplacement of heat-generating waste in the repository will make the environment less conducive to microbial activity. Since there is currently NO_3^- present at drift level in YM, it is not apparent how the construction and operation will result in higher $Cl^-:NO_3^-$ ratios than currently exist and on which localized corrosion assessments have been based (BSC, 2004d).

Nutrients

Nutrients are required to maintain microbial activity and to support the growth of new cells. Apart from carbon and H_2O, cells also require smaller amounts of N, P and S and trace amounts of other elements (Stroes-Gascoyne, 1989). Organic carbon concentrations in YM groundwaters are low (BSC, 2004a). The range of dissolved organic carbon (DOC) contents in unpolluted groundwaters is reported to be 0-2 mg/L. Although some organic C will be introduced during construction (in the form of spilled lubricants and vehicle exhausts), institutional controls can be put in place to minimize the amount of carbon introduced into the repository. Of the various nutrients required by microbes (C, N, P, S), organic carbon is considered to be a key limiting factor (BSC, 2004a).

Radiation

Many microbes are known to be sensitive to ionizing radiation, although radiation-tolerant microorganisms have also been identified (Meike and Stroes-Gascoyne, 2000). Pitonzo *et al.* (1999a,b) studied the radiation sensitivity of indigenous microbes on YM rock samples, and reported that a dose of 2.3 kGy was sufficient to suppress microbial activity.

Although radiation can sterilize surfaces, attenuation of the radiation field by the WP wall will result in incomplete sterilization (by radiation) of the WP surface in the repository. For example, for an absorbed gamma dose rate of 0.01 Gy/hr on the surface of a TAD (DOE 2006), the estimated accumulated dose at the surface of the WP is ~190 Gy after 300 years, far less than that required to sterilize the surface based on the data of Pitonzo *et al.* (1999a, b). This radiation dose rate was calculated assuming a half-layer thickness of 1.7 cm for Cs-137 gamma radiation for the WP stainless steel inner barrier and Alloy 22 outer barrier with thicknesses of 5.1 cm (2") and 2.54 cm (1"), respectively, and an effective half-life of 30 years for the spent fuel.

Although complete WP surface sterilization may not occur, the presence of radiation in combination with other stressors will reduce the number and diversity of the microbial population.

Mass transport

Transport of species to and from the WP surface will be limited in the YM repository. In open (*i.e.*, un-backfilled) drifts located in the unsaturated zone, transport of gaseous species including water vapor will occur readily, especially during the initial ventilation period. However, the transport of dissolved species will be more limited. The only transport mechanism for dissolved nutrients and/or microbes will be via seepage drips and the subsequent transport that may occur once the drips contact the surface of the drip shield, waste package, or rock wall. Mass transport laterally in the thin adsorbed moisture films expected to form on surfaces in humid atmospheres is not a significant contributor to transport due to the small diffusive cross-sectional area.

Transport processes could play a significant role in the MIC of the EBS. It is likely that the combination of the various stressors of elevated temperature, low water activity, and limited nutrients will deplete the microbial population close to the WP surface. If this occurs, then microbial activity near the WP is only possible if this zone can be re-populated. Repopulation of the WP surface will not occur until the temperature has dropped sufficiently to allow seepage from the drift walls and then only if the drip shield has failed, a period that is estimated to range from ~30,000 yrs to >10^6 a (King and Kolar, 2006).

From the discussion above, it is apparent that there are a number of factors that will prevent microbial activity in different parts of the repository. Some of these factors, such as low water activity or RH and elevated temperatures (>100°C), are sufficient on their own to prevent microbial activity and, therefore, MIC. Others, such as radiation effects, the evolution of redox conditions, restrictive mass transport, and the limited supply of nutrients, may not be sufficient on their own to completely suppress microbial activity, but taken together with other stressors and environmental conditions will create adverse conditions for microbial activity. The existence of multiple environmental stressors provides a defense in depth against microbial growth and other metabolic activity.

To illustrate the above argument in more detail, consider the factors that will limit microbial activity both *at* the EBS surface and *away* from the engineered barriers in more-hospitable regions of the repository. Because of the initial thermal transient and its effect on the in-drift humidity and the surface temperature of the EBS, microbial activity at the EBS surface can be ruled out for a significant period of time. The factors that will limit microbial activity at the surface of the waste package are:

1. The elevated waste package surface temperature during the thermal pulse (Else *et al.,* 2003),

2. The low %RH at the surface of the waste package (Else *et al.,* 2003, Kieft *et al.,* 1997, Meike and Stroes-Gascoyne, 2000),

3. The presence of saline (low a_w) aqueous phases resulting from deliquescence of surface salt impurities and evaporation of seepage drips (if any) (Stroes-Gascoyne *et al.,* 2006, 2007),

4. The presence of a gamma radiation field (Pitonzo *et al.,* 1999a, b),

5. Limited inoculation of the waste package surface by microbes in seepage drips while the drip shields are intact and in place, and

6. Limited availability and supply of nutrients in seepage drips while drip shields are intact and in place.

These factors result in an initial abiotic phase during which biofilm formation on the waste package surface will not occur. Figure 5-45 shows approximate times for each of these factors, from which it is apparent that biofilm formation will not occur before 10,000 yrs and likely much longer. In the long-term, the possibility of MIC of the waste package is determined in part by the lifetime of the drip shield.
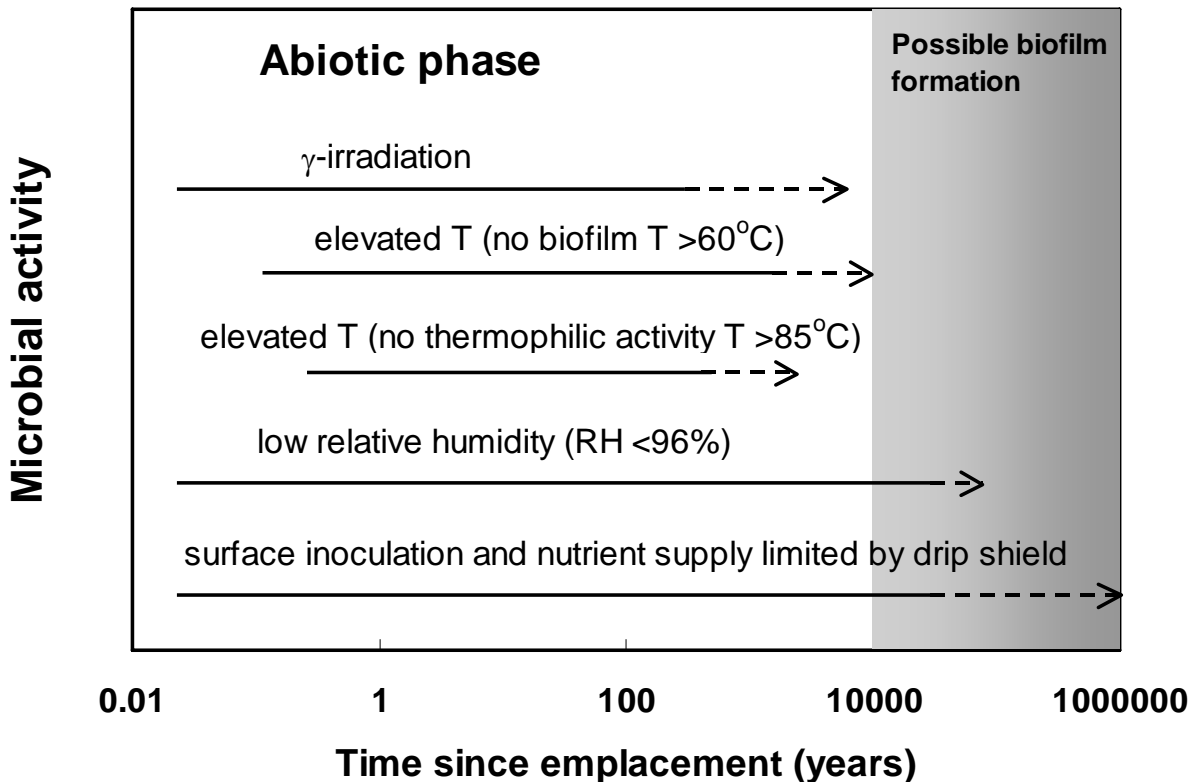
Figure 5-45
Factors that prevent or limit microbial activity at the surface of waste packages in the Yucca Mountain repository environment.

Further away from the EBS, environmental conditions are generally more favorable for microbial activity. The tuff in the drift walls will experience partial desiccation for some distance during the thermal pulse until the temperatures decreases and water moves back towards the drift wall (BSC, 2004b, c). Figure 5-46 shows schematically how the abiotic zone will initially extend further from the waste package as the temperature in the drifts and surrounding rock increases and the RH decreases. Based on tuff saturation predictions from thermohydrologic modeling (BSC, 2004c), the abiotic zone could extend up to several meters into the rock surrounding the drifts.

In answer to the question "If present, will microbes be active in the repository?" (Figure 5-40), the evidence indicates that:

*   microbes will not be active on the surface of the waste package for a minimum of 10,000 yrs and, possibly, as long as $>10^6$ yrs, but

*   microbial activity is possible further away from the WP surface once the initial thermal pulse and desiccation of the environment have diminished.

However, even in locations where microbial activity is possible, the extent and nature of that activity will still continue to be limited by factors such as the nutrient-poor environment, the redox conditions, the presence of saline pore fluids, and the restrictive mass-transport conditions.
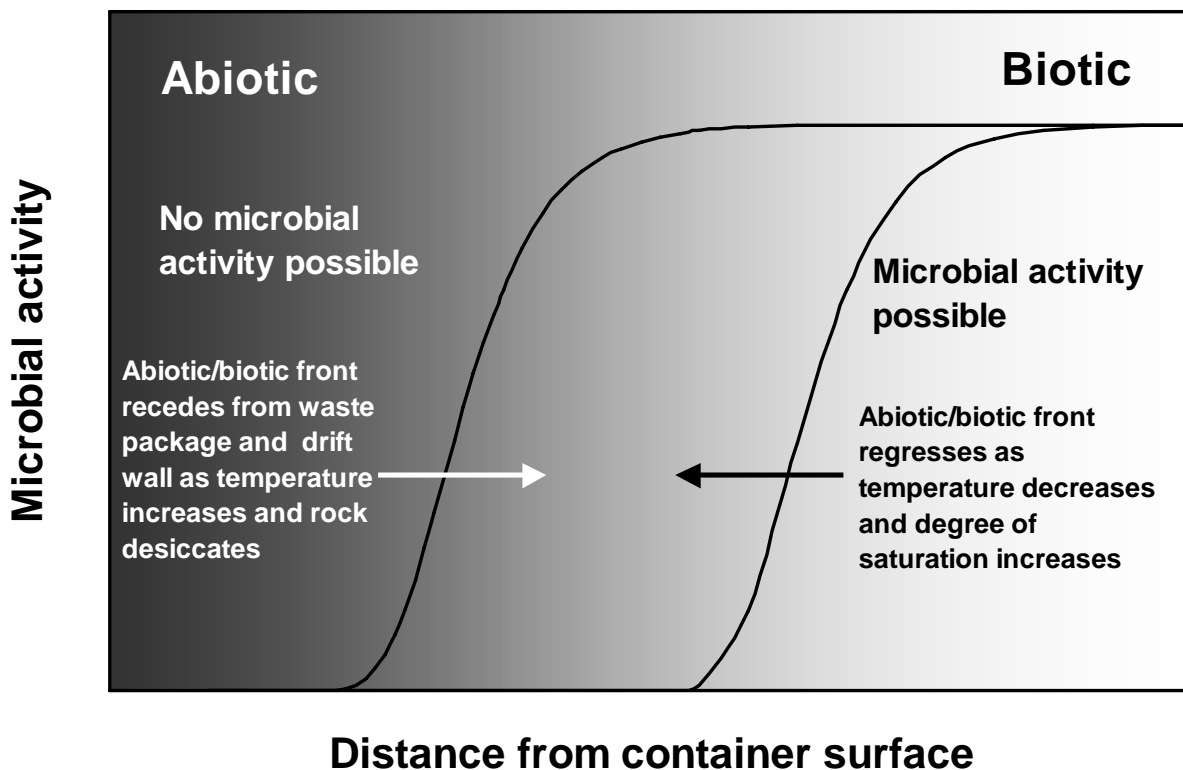
Figure 5-46
Schematic illustration of the initial recession of the abiotic zone during the thermal pulse in the Yucca Mountain repository and the subsequent regression as the temperature decreases and the relative humidity increases in the drift and rock wall.

5.8.2.3   If Active, Will Corrosion Occur?

Notwithstanding the evidence presented above that microbial activity will be limited within the repository, let us consider whether corrosion will occur if microbes are indeed active.

If the surface of the WP is colonized by active microbes, biofilm formation is a reasonable assumption. Biofilms represent a heterogeneously distributed population of different types of microbe, nutrients, and extracellular polymeric material that can create locally occluded regions and microenvironments that can host conditions that depart dramatically from those in the bulk environment (Little and Wagner, 1996; Little *et al.,* 1991). Currently, there is no reliable method to predict conditions under biofilms, so reliance must be placed on practical experience and laboratory experimental simulations of the corrosion that might occur.

The alloys proposed for use for the EBS in the YM repository are among the most-corrosion resistant alloys and are among the few materials that may be immune to MIC. Little and co-workers (Little and Wagner, 1996; Little *et al.,* 1991) have reviewed the MIC behavior of a range of candidate repository materials and concluded that Ti alloys may be the only material resistant to microbes. This resistance may result from the absence of multiple oxidation states for Ti in the corroded form, which is believed to be a pre-requisite for participation in microbially mediated corrosion processes (Lloyd *et al.,* 2004).

The MIC resistance of Alloy 22 and Ti alloys has been examined under a range of conditions. Else *et al.* (2003) exposed metal samples to simulated YM repository conditions over a range of temperatures (30-70°C) and RH (32-100%) and then characterized the surface colonization and extent of surface damage. Not only was there no evidence for surface microbial activity except at the lowest temperature and highest %RH studied, but there was also no indication of surface damage (based on SEM examination) of either material exposed for periods of up to 18 months. Lloyd *et al.* (2004) have suggested that the inherent stability of the Cr-rich oxide film on the waste package surface should render it immune to MIC. This conclusion is supported by the "accelerated" MIC tests of Horn and co-workers (Horn *et al.* 1999, 2000, 2001, 2002; Lian *et al.,* 1999; Martin *et al.,* 2004). In these experiments, Alloy 22 and Ti-7 samples were exposed to an inoculated environment containing a thiosulphate culture medium. No corrosion of the Alloy 22 samples was observed after 7 months exposure but, based on Atomic Force Microscopy measurements, some surface roughening of the Ti-7 amounting to ±1-2 μm was reported. In other experiments, minimal micro-pitting and surface roughening of Alloy 22 was observed, again after prolonged exposure to an aqueous environment enriched through the addition of glucose. It is unclear, however, how these experimental conditions relate to environments that might form on the surface of the waste package or drip shield in the YM repository.

A more likely scenario is that microbial activity will be confined to regions removed from the waste package. Under these circumstances, corrosion of the WP is only possible if aggressive metabolic by-products formed by the microbes reach the WP surface. Microbial activity could eventually occur on the walls of the drifts once the temperature has diminished and the relative humidity increased. It is conceivable that biofilms could spall and fall onto the drip shields and, if the conditions used by Horn *et al.* (2001) are relevant, cause some surface roughening of the Ti-7 drip shields. However, the drip shields will continue to protect the waste package from direct contact with biofilm material falling from the roof of the drifts while they are intact and in place, in exactly the same way that they protect the waste package from seepage drips.

In summary, assuming that microbial activity in the repository is possible:

- Alloy 22 and Ti-7 appear to offer resistance to MIC, even under "accelerated" conditions in which the material is exposed to inoculated nutrient-rich environments (Else *et al.,* 2003; Horn *et al.,* 1999, 2001; Lloyd *et al.,* 2004), and

- Waste packages in the YM repository will be protected by drip shields from direct contact with biofilms and corrosive metabolic by-products formed on the drift roof and walls as long as this barrier is in place and intact.

5.8.2.4   If Corrosion Occurs, Will Waste Packages Fail?

Assuming that MIC of the WP does occur, will corrosion be extensive enough to cause WP failure? In the absence of a biofilm on the WP surface, corrosion appears to be unlikely to cause WP failure because the extent of microbial activity in regions remote from the packages is limited. Biofilm formation is possible in the YM repository environment, but only after a considerable period of time. However, the materials may be sufficiently corrosion resistant that WP failure does not occur.

To date, extensive corrosion of Alloy 22 or Ti-7 has not been observed even under "accelerated" conditions involving the deliberate inoculation of the test environment and the addition of unlimited nutrients. Corrosion effects have been limited to surface roughening of the order of a few μm for Ti-7 (Horn *et al.,* 2001) and a reported doubling of the corrosion rate of Alloy 22 based on short-term electrochemical polarization experiments (Farmer *et al.* 2000). In contrast, there is extensive evidence for the intrinsic stability of the passive films on both materials and their resistance to localized and general corrosion (BSC, 2003, 2004d; Lloyd *et al.,* 2004). It is unlikely that microbes could produce sufficiently acidic conditions to cause dissolution of TiO_2 (pH < 1) (Pourbaix, 1974) and there is recent evidence for the repassivation of the passive film on Alloy 22 during crevice corrosion (Pan *et al.,* 2006), which further bolsters the case for the inherent corrosion resistance of Alloy 22 under acidic conditions.

In conclusion, both Alloy 22 and Ti-7 appear to possess inherently stable passive films that provide excellent corrosion resistance to both biotic and abiotic corrosion mechanisms.

5.8.2.5   If Waste Packages Fail, Will Compliance with Regulatory Dose Limits Be Compromised?

The last question on the decision tree is whether, in the unlikely event that MIC leads to WP failures, the performance of the repository will be compromised such that regulatory dose limits are exceeded. (Figure 5-40). The regulatory dose limits established for YM are based on the dose to an affected individual or receptor at a prescribed distance (18 km) downgradient from the site and is largely determined by the binding, sequestration, or retardation of radionuclides by the multiple components of the engineered and natural barriers.

The two WP failure characteristics that can lead to high doses are early failures and a narrow distribution of failure times. Early failures can lead to high doses because the waste form toxicity is at its highest and little radioactive decay has occurred within the WP before release to reduce the radioactive inventory. Simultaneous or closely timed failures lead to a higher peak dose

because failures, and the resulting radioactive releases and exposures, are not distributed over a long period of time.

Even if MIC leads to WP failures, these failures will neither occur early nor over a narrow range of time. Microbial activity is least likely to occur early in the evolution of the repository environment as it is during this period that conditions are the most inhospitable for microbial activity. It is only after the thermal transient and the relative humidity has subsequently increased that microbes will be active. Furthermore, any eventual WP failures will be distributed over long timeframes. In the YM repository, MIC of the WP is only likely after the drip shields have failed and nutrients and sufficient water can reach the waste package surface via seepage. The expected failure times of the drip shields are distributed between ~30,000 yrs and $>10^6$ years (King and Kolar, 2006); accordingly any MIC-induced waste package failures will also be distributed over a long period of time.

In conclusion, even if MIC WP failures were to occur, the repository performance and regulatory dose limits are unlikely to be compromised because such failures are expected to occur far into the future and to be distributed over a long timeframe.

5.8.3 Discussion

Figure 5-47 shows the MIC decision tree for the Yucca Mountain repository. MIC of the WPs does not compromise the overall performance and regulatory compliance of the proposed Yucca Mountain repository system.

The waste packages are protected from MIC for a long period of time, first by adverse environmental conditions during the thermal pulse and, later, by the drip shields. The combined effects of the elevated temperature and low relative humidity will prevent microbial activity at the EBS surface for a period in excess of 10^4 years. Once environmental conditions have become more favorable for microbial activity, the most likely route for the inoculation of, and the supply of nutrients to the surface of the WP is via seepage drips from the roof of the repository drifts. However, the drip shields are expected to continue to protect the waste packages from drips for periods of up to 10^6 years and beyond, thereby delaying the onset of MIC for a large portion of the 10^6 regulatory compliance period. Furthermore, the materials selected for the WP and DS (the Cr-Ni-Mo-W Alloy 22 and the Pd-containing Ti-7) are among the most corrosion resistant materials known with respect to abiotic corrosion and MIC processes.

A substantial performance margin is provided by a series of engineered and natural barriers, of which the WP and DS represent just two components. Moreover, repository performance is not reliant on any single barrier, although some barriers do provide a greater degree of containment or retardation than others. Microbial effects are not expected to compromise the repository performance or regulatory compliance because they neither lead to early nor to simultaneous WP failures, which could otherwise lead to increases in the peak dose.

Microbiologically influenced corrosion is one of a number of corrosion threats to the EBS and should be treated in the same manner as these other processes. The threat to repository performance posed by other corrosion processes is assessed by considering the most likely sequence of events that lead to WP or DS failure. Rarely is it the case that we have a complete

mechanistic understanding of a given process, and where there is uncertainty we either use expert judgment to determine the most likely behaviour or use conservatisms when assessing the impact on lifetimes.

There has been a tendency within the nuclear waste management community to assess the threat from MIC differently. This, in part, is in response to the argument from some quarters that specific strains can always be found that exist in a wide range of aggressive environments and that uncertainty with respect to long-term microbial influences requires special or unique consideration. But these arguments are not valid based on the results of microbial studies performed under *relevant* environmental conditions, including those described above. A large body of evidence indicates that multiple factors inherent to a deep geological repository like that of Yucca Mountain present a hostile environment for microbial growth. In this work, the manner in which these environmental conditions affect microbial activity has been determined and quantitative methods for making predictions about microbial activity have been developed. These methods allow the prediction, with "reasonable assurance" (NRC, 1995) that the performance and regulatory compliance of the proposed Yucca Mountain repository will not be compromised by microbially-induced corrosion of key engineered barrier system components.
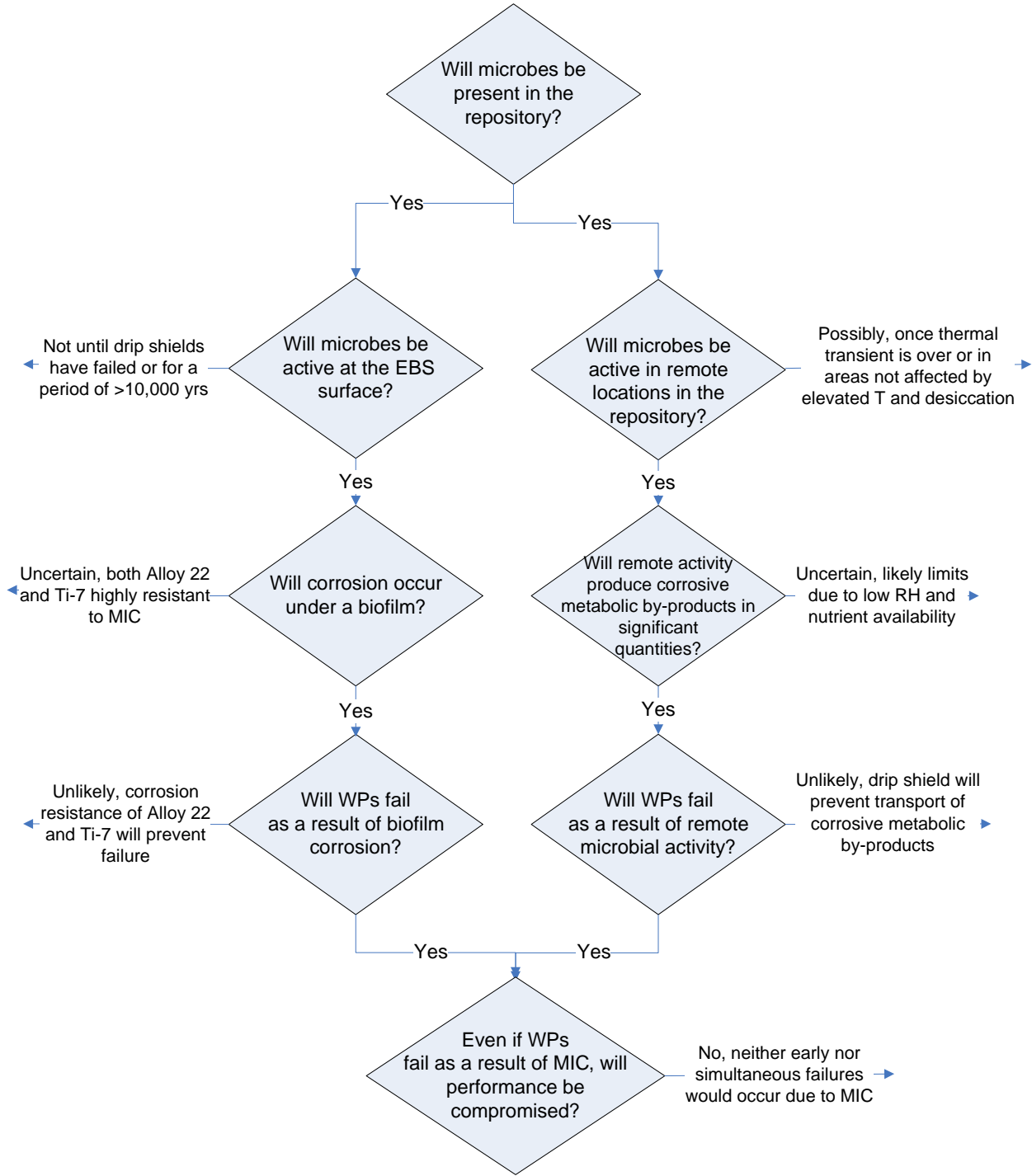
Figure 5-47
Decision tree for the MIC of waste packages in the Yucca Mountain repository.

5.8.4 References

Brown, D.A., 1990. *Microbial Water Stress Physiology*. John Wiley, Chichester.

BSC, 2003. *Technical basis document no. 6: waste package and drip shield corrosion*. Bechtel SAIC Company report to DOE, Revision 1, December 2003.

BSC, 2004a. *Evaluation of potential impacts of microbial activity on drift chemistry*. Bechtel SAIC Company report for U.S. Department of Energy, ANL-EBS-MD-000038 REV 01.

BSC, 2004b. *Engineered barriers system: physical and chemical environment model*. Bechtel SAIC Company report to DOE, ANL-EBS-MD-000033 Rev 02, February 2004.

BSC, 2004c. *Multiscale thermohydrologic model*. Bechtel SAIC Company report to DOE, ANL-EBS-MD-000049 Rev 02, October, 2004.

BSC, 2004d. *General corrosion and localized corrosion of waste package outer barrier*. Bechtel SAIC Company report to DOE, ANL-EBS-MD-000003 Rev 02, October 2004.

DOE, 2006. *Preliminary transportation, aging and disposal canister system performance specification. Revision A*. Office of Civilian Radioactive Waste Management Report, WMO-TADCS-000001.

Else, T.A., C.R. Pantle, and P.S. Amy, 2003. Boundaries for biofilm formation: humidity and temperature. *Appl. Environ. Microbiol.* 69, 5006-5010.

Farmer, J., D. McCright, G. Gdowski, F. Wang, T. Summers, P. Bedrossian, J. Horn, T. Lian, J. Estill, A. Lingenfelter, and W. Halsey, 2000. General and localized corrosion of outer barrier of high-level waste container in Yucca Mountain. *Proc. Transportation, Storage, and Disposal of Radioactive Materials* – 2000, PVP-Vol. 408 (American Society of Mechanical Engineers, New York, NY), pp. 53-69.

Gordon, G.M, 2002. Considerations related to permanent disposal of high-level radioactive waste. *Corrosion* 58, 811-825.

Horn, J., C. Carrillo, and V. Dias, 2003. Comparison of the microbial community composition at Yucca Mountain and laboratory test nuclear repository environments. *Corrosion*, 2003 (NACE International, Houston, TX), paper no. 03556.

Horn, J., S. Martin, A. Rivera, P. Bedrossian, and T. Lian, 2000. Potential biogenic corrosion of Alloy 22, a candidate nuclear waste packaging material, under simulated repository conditions. *Corrosion* 2000, NACE International, Houston, TX, paper 00387.

Horn, J., S. Martin, and B. Masterson, 2001. Evidence of biogenic corrosion of titanium after exposure to a continuous culture of *Thiobacillus ferrooxidans* grown in thiosulphate medium. *Proc. Corrosion* 2001, NACE International, Houston, TX, paper 01259.

Horn, J., S. Martin, B. Masterson, and T. Lian, 1999. Biochemical contributions to corrosion of carbon steel and Alloy 22 in a continual flow system. *Corrosion* 1999, NACE International, Houston, TX, paper 162.

Horn, J., T. Lian, and S. Martin, 2002. Microbiologically-facilitated effects on the surface compositions of Alloy 22, a candidate nuclear waste packaging material. *Corrosion* 2002, NACE International, Houston, TX, paper 02448.

Horn, J.A., A. Rivera, T. Lian, and D.A. Jones, 1998. MIC evaluation and testing for the Yucca Mountain repository. *Corrosion* 1998 (NACE International, Houston, TX), paper no. 98152.

Kieft, T.L., W.P. Kovacik, D.B. Ringelberg, D.C. White, D.L. Haldeman, P.S. Amy, L.E. Hersman, 1997. Factors limiting microbial growth and activity at a proposed high-level nuclear repository, Yucca Mountain, Nevada. *Appl. Environ. Microbiol*. 63, 3128-3133.

King, F., 1996. Microbially influenced corrosion of copper nuclear fuel waste containers in a Canadian disposal vault. *Atomic Energy of Canada Limited Report*, AECL-11471, COG-94-519.

King, F. and M. Kolar, 2006. EPRI's Engineered Barrier System Corrosion Model (EBSCOM). *Proc. 11th International High-level Radioactive Waste Management Conference*, American Nuclear Society (La Grange Park, IL), pps. 478-485.

King, F. and S. Stroes-Gascoyne, 1997. Predicting the effects of microbial activity on the corrosion of copper nuclear waste disposal containers. *Microbial Degradation Processes in Radioactive Waste Repository and in Nuclear Fuel Storage Area*s, J.H. Wolfram (ed.), Kluwer Press, Dordrecht, p. 149-162.

Lian, T., S. Martin, D. Jones, A. Rivera, and J. Horn, 1999. Corrosion of candidate container materials by Yucca Mountain bacteria. *Corrosion* 1999, NACE International, Houston, TX, paper 476.

Little, B. and P. Wagner, 1996. An overview of microbiologically influenced corrosion of metals and alloys used in the storage of nuclear wastes. *Can. J. Microbiol*. 42, 367-374.

Little, B., P. Wagner and F. Mansfeld, 1991. Microbiologically influenced corrosion of metals and alloys. *Int. Mater. Rev*. 36, 253-272.

Little, B.J., 2003. A perspective on the use of anion ratios to predict corrosion in Yucca Mountain. Corrosion 59, 701-704.

Lloyd, A.C., R.J. Schuler, J.J. Nöel, D.W. Shoesmith, and F. King, 2004. The influence of environmental conditions and passive film properties on the MIC of engineered barriers in the Yucca Mountain Repository. *Scientific Basis for Nuclear Waste Management* XXVIII, J.M. Hanchar, S. Stroes-Gascoyne, and L. Browning (eds.), *Mat. Res. Soc. Symp. Proc*. 824 (Materials Research Society, Warrendale, PA, 2004), pps. 3-9.

Madigan, M.T., J.M. Martinko and J. Parker, 2000. *Brock Microbiology of Microorganisms*. Ninth Edition. Prentice Hall, Upper Asaddle River, NJ.

Marcus, P., 1995. Sulfur-Assisted Corrosion Mechanisms and the Role of Alloyed Elements, Chapter 8, pp. 239-263, *Corrosion Mechanisms in Theory and Practice*, P. Marcus and J. Oudar (eds.), Marcel Dekker, Inc.

Martin, S., J. Horn, and C. Carrillo, 2004. Micron-scale MIC of Alloy 22 after long term incubation in saturated nuclear waste repository microcosms. *Corrosion* 2004, NACE International, Houston, TX, paper 04596.

Meike, A. and S. Stroes-Gascoyne, 2000. *Review of microbial responses to abiotic environmental factors in the context of the proposed Yucca Mountain repository*. Atomic Energy of Canada Limited Report, AECL-12101.

NRC (National Research Council), 1995. *Technical Bases for Yucca Mountain Standards*. National Academy Press, Washington, D.C.

Pan, Y.-M., K.T. Chiang, D.S. Dunn, X. He, O. Pensado, P. Shukla, and L. Yang, 2006. Independent evaluation of waste package corrosion performance under potential repository conditions. *Proc. 11th International High-level Radioactive Waste Management Conference*, American Nuclear Society (La Grange Park, IL), pps. 843-849.

Pitonzo, B., M. Rudin, and P.S. Amy, 1999a. Effect of gamma radiation on native endolithic microbes. *Radiat. Res*. 152, 71-75.

Pitonzo, B., M. Rudin, and P.S. Amy, 1999b. Resuscitation of microbes after gamma radiation. *Radiat. Res*. 152, 64-70.

Pourbaix, M. 1974. *Atlas of Electrochemical Equilibria in Aqueous Solutions*, 2nd. edition. NACE International, Houston, TX.

Stroes-Gascoyne, S., 1989. *The potential for microbial life in a Canadian high-level nuclear fuel waste disposal vault: a nutrient and energy source analysis*. Atomic Energy of Canada Limited Report, AECL-9574.

Stroes-Gascoyne, S. and F. King, 2002. Microbially influenced corrosion issues in high-level nuclear waste repositories. *Proc. Corrosion 2002 Research Topical Symposium*, NACE International (Houston, TX).

Stroes-Gascoyne, S., C.J. Hamon, C. Kohle, and D.A. Dixon, 2006. *The effects of dry density and porewater salinity on the physical and microbiological characteristics of highly compacted bentonite.* Ontario Power Generation, Nuclear Waste Management Division Report 06819-REP-01200-10016.

Stroes-Gascoyne, S., C.J. Hamon, D.A. Dixon, C. Kohle, and P. Maak, 2007. The effects of dry density and porewater salinity on the physical and microbiological characteristics of highly compacted bentonite. *Scientific Basis for Nuclear Waste Management XXX*, edited by Darrell Dunn, Christophe Poinssot, Bruce Begg (Mater. Res. Soc. Symp. Proc. 985, Warrendale, PA, 2007), paper 0985-NN13-02.

5.9 A Revised EPRI Source-Term Model for the Dissolution of Commercial Spent Nuclear Fuel

5.9.1 Introduction and Background

Oxidation of the UO_2 matrix of spent nuclear fuel results in the formation of U(VI) corrosion products, in which uranium is predominately found as the uranyl dioxocation, UO_2^{2+}. The solubility of these corrosion products under oxidizing conditions are several orders of magnitude higher than the UO_2 matrix under reducing conditions (Grenthe et al., 1992). This fact and the results of a number of experimental studies performed under oxidizing conditions (BSC, 2004, Finch et al., 1999; Finn et al., 1995; Stout and Leider, 1998) have led to the perception that commercial spent nuclear fuel (CSNF) will undergo rapid alteration upon exposure to the drift environment in the Yucca Mountain (YM) repository.

However, the experimental evidence supporting rapid CSNF alteration was obtained under conditions that are not necessarily representative of the YM environment. Drip tests performed at the Argonne National Laboratory were conducted using relatively fresh (i.e., un-aged) spent fuel samples with significant β and γ-radiation fields (Finch et al, 1999; Finn et al., 1995). Except for the case of anomalous early failures, presumably due to defective waste packages (WPs), CSNF β and γ fields will decay to negligible levels long before WP failure occurs. In the long-term, atmospheric O_2 and, depending upon the time of WP failure, oxidizing radiolysis products of α-radiation represent the only oxidants capable of supporting spent fuel corrosion. As shown below, β and γ-radiation have a significant effect on the dissolution behavior of spent fuel due to the polarization of the electrochemical corrosion potential (E_{CORR}). UO_2 dissolution rates based on data obtained under high β and γ fields will overestimate the long-term alteration and dissolution of UO_2 in the Yucca Mountain system.

Another potential source of conservatism in the DOE CSNF matrix alteration model results from the numerical fitting of experimental data obtained from flow-through dissolution tests on spent fuel and UO_2, for which unrealistically high solution volume to surface area (V:SA) ratios were used (BSC, 2004; Stout and Leider, 1998). Such conditions limit the precipitation of alteration products, which is a significant feature in the natural alteration of uraninite, i.e., naturally occurring UO_2 (Murphy and Pearcy, 1992), and is also expected to be important for alteration of CSNF under in-drift conditions at Yucca Mountain.

The environmental conditions to which the CSNF is exposed following WP failure play a significant role in determining fuel dissolution behavior. Because the proposed repository horizon is located in the unsaturated zone, the amount of water available to support fuel dissolution is limited. Although dripping is expected in some of the drifts once the temperature in the repository has fallen below the local boiling point, the vast majority of fuel will be exposed to humid air, rather than direct impact by drips. Thus, the surface of the fuel will be covered by a thin moisture film (assuming the relative humidity (RH) in the failed WP exceeds the threshold RH for condensation of water on porous surfaces of 60-70%), with a correspondingly low V:SA ratio. In the case of a failed WP situated in a drift experiencing infiltration of seepage water, the WP spent fuel inventory will be protected from direct contact with advective flow by an assortment of WP internal components, including the stainless steel inner cylinder, stainless steel TAD canister and internals, and the fuel cladding itself.

In addition to limited amounts of water and low rates of mass transport, UO_2 dissolution is also affected by the composition of the seepage water. YM seepage waters have high Si contents derived from the tuff host rock (BSC, 2003). Furthermore, the principal cation in many of these waters is Ca^{2+} (BSC, 2003). These species, in particular, have been shown to suppress the dissolution rate of spent fuel and UO_2 by up to two orders of magnitude (Santos et al., 2006a, 2006b; Shoesmith, 2000; Tait and Luht, 1997; Wilson and Gray, 1990). Recent data suggest that Ca^{2+} inhibits dissolution of UO_2 by participating in the anodic dissolution process, either inhibiting the formation of the adsorbed precursor of UO_2^{2+} or by blocking the insertion of O^{2-} species (Santos et al., 2006a). Dissolved silica promotes the precipitation of insoluble uranyl minerals, such as soddyite (($UO_2)_2SiO_4 \cdot 2H_2O$), β-uranophane ($Ca(UO_2)_2(SiO_3OH)_2 \cdot 5H_2O$), and Na-boltwoodite (($Na,K)(UO_2)(SiO_3OH) \cdot H_2O$) (Shoesmith, 2000). Both Ca and Si may also affect the creation of local acidity in nascent porous deposits on the fuel surface (Santos et al., 2006a, 2006b).

A fundamental feature of the UO_2 alteration expected for CSNF in the YM repository is the formation of a protective layer of precipitated corrosion products. In addition to the information from tests with Ca^{2+} and Si summarized above, there is other compelling evidence that a surface film will develop under the oxidizing conditions expected at YM.

Figure 5-48 shows the effect of electrochemical potential on the dissolution rate of UO_2 (Shoesmith, 2000). Under all but the most reducing conditions, the dissolution of UO_2 or spent fuel can be considered to be an electrochemical corrosion process in which the anodic dissolution of UO_2 to U(VI) is coupled to the cathodic reduction of one or more oxidants, such as O_2, H_2O_2, or various oxidizing radical species. As such, the dissolution behavior can be studied as a function of potential, in exactly the same fashion as any other corrosion process.

The dissolution rate (current) increases with increasing potential, equivalent to more oxidizing conditions. Above a potential of +0.3 V_{SCE} (denoted as Region B in Figure 5-48), the dissolution rate increases logarithmically with potential, as would be expected of an electrochemically driven process under film-free conditions. At more-negative potentials (Region A), however, the dissolution current is relatively independent of potential. Indeed, at a given potential, the current decreases with time, as indicated by the vertical lines of symbols at potentials of 0.1, 0.2, and 0.3 V_{SCE} which represent sequential measurements in single experiments. The independence of the dissolution rate with respect to potential and the decrease in current with time are both indicative of the formation of a protective film on the UO_2 surface. At potentials more-positive than +0.3 V_{SCE} the surface film is no longer protective because of acidity produced in the pores of the surface film by the hydrolysis of dissolved U(VI), which maintains an open pore structure and a non-protective surface film. The potential of +0.3 V_{SCE} represents the potential at which the rate of H^+ generation by the hydrolysis of U(VI) exceeds the rate at which the H^+ leaves the surface. Also shown in Figure 5.9.1 are the achievable ranges of E_{CORR} in the presence of various oxidants.
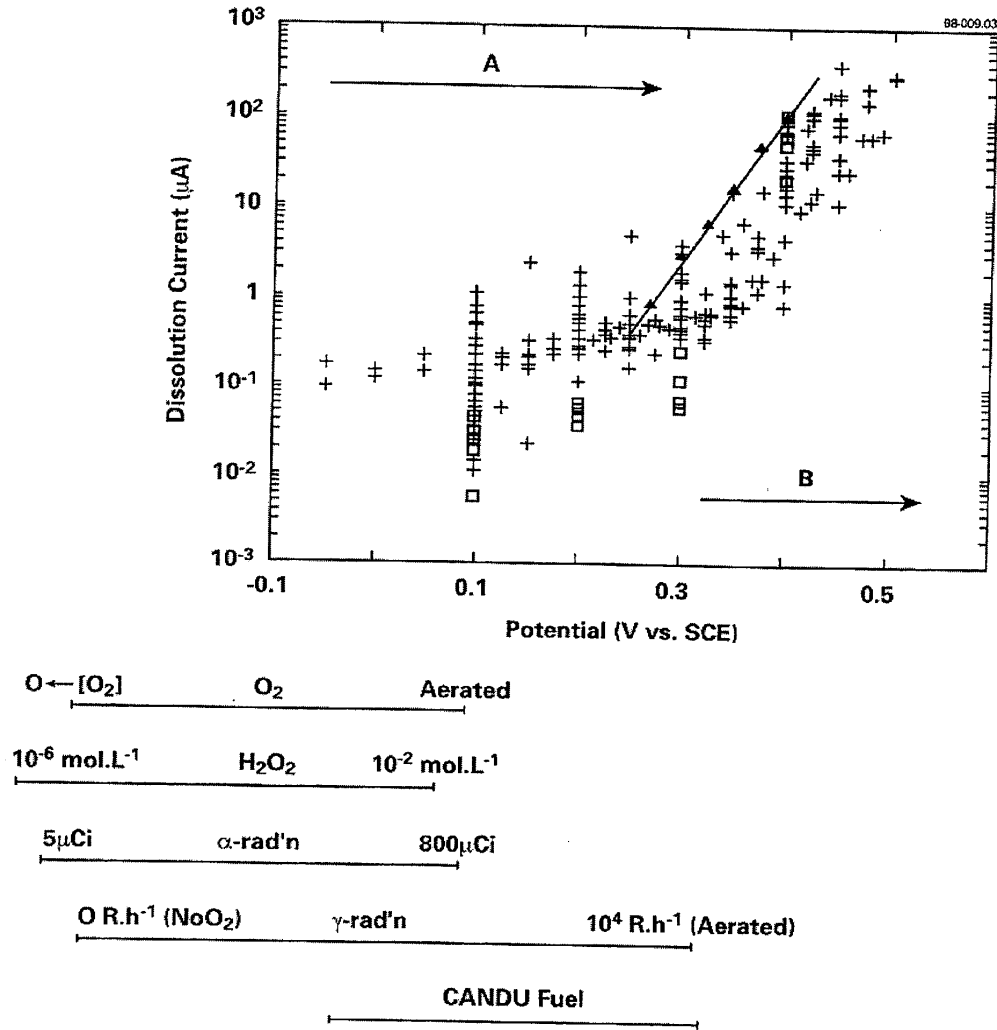
Figure 5-48
Effect of potential on the dissolution rate of UO$_2$ (Shoesmith, 2000).

Evaluation of the effect of surface film formation on the dissolution of CSNF in YM requires an understanding of whether the E_{CORR} of the fuel is in Region A (protective surface film) or Region B (non-protective surface film) indicated in Figure 5-48. Even in fully aerated environments, the potential does not exceed a value of approximately +0.1 V_{SCE}, i.e., the potential is well within the range for Region A and the formation of a protective surface film is expected. Even introduction of H$_2$O$_2$ or α-radiolysis would not result in surface oxidation sufficient to drive the potential into Region B. However, high γ-radiation fields, especially in the presence of air, are sufficient to drive the potential into Region B. For this reason, the Argonne drip tests on fresh fuel represent a conservative assessment of the dissolution behavior of CSNF under YM conditions.

Natural analogs also provide supporting evidence for the formation of protective surface films on UO$_2$ under oxidizing conditions (BSC, 2004). The most well-known such analog is that from Peña Blanca in Mexico (Murphy and Pearcy, 1992). Figure 5-49 illustrates the general paragenetic sequence of alteration phases typically observed on uranium ore deposits (BSC,

2004; Shoesmith, 2000). While not direct evidence for the formation of protective surface layers, the existence of such deposits indicate the stability of precipitated uranium phases under oxidizing conditions over geologic timeframes.
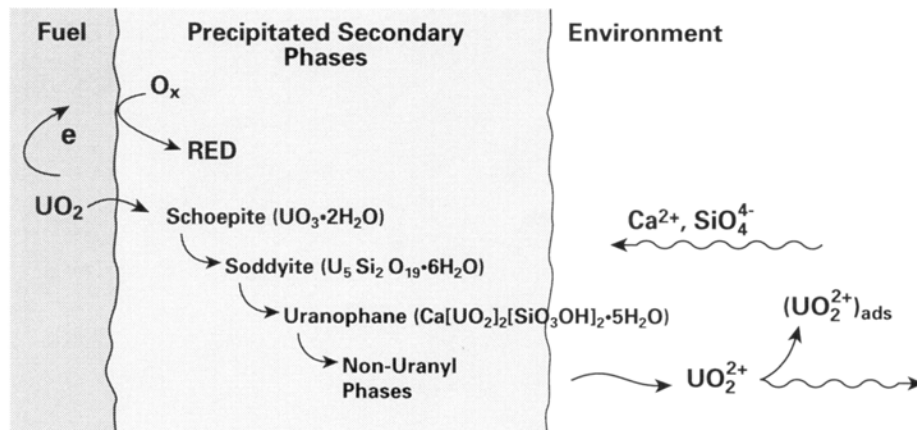
Figure 5-49
Sequence of uranium(VI) alteration products observed from natural analogs for used fuel dissolution and in laboratory studies (Shoesmith, 2000).

5.9.2 Conceptual Model

A number of features are included in the EPRI CSNF alteration model. The conceptual model described in this section forms the basis of the mathematical model described in Section 5.9.3 below.

5.9.2.1 Reaction Scheme

The EPRI conceptual model is based on the reaction scheme shown in Figure 5-50. The anodic dissolution of UO_2 as either UO_2^{2+} (interfacial rate constant k_A) or $UO_2(CO_3)_2^{2-}$ (k_B) is electrochemically coupled to the cathodic reduction of radiolytically-produced H_2O_2 (k_D) or atmospheric O_2 (k_E). Oxygen can also be produced by the interfacial decomposition of H_2O_2, which involves the coupling of the reduction reaction to the oxidation of H_2O_2 (k_C) (Shoesmith et al., 2003). It is implicitly assumed that no other oxidants are present in the system, specifically radical species formed by the β and γ-radiolysis of water.

In addition to the interfacial electrochemical reactions, a number of homogeneous reactions are included in the conceptual model. If the concentrations of dissolved UO_2^{2+} or $UO_2(CO_3)_2^{2-}$ exceed their respective solubilities, then a precipitated U(VI) solid can form (with rate constants k_1 and k_2, respectively). If there is Fe(II) present, from the corrosion of internal WP components for example, O_2, H_2O_2, and U(VI) may be consumed by the homogeneous oxidation of Fe(II) to Fe(III) (with rate constants k_3, k_4, and k_5/k_6, respectively).
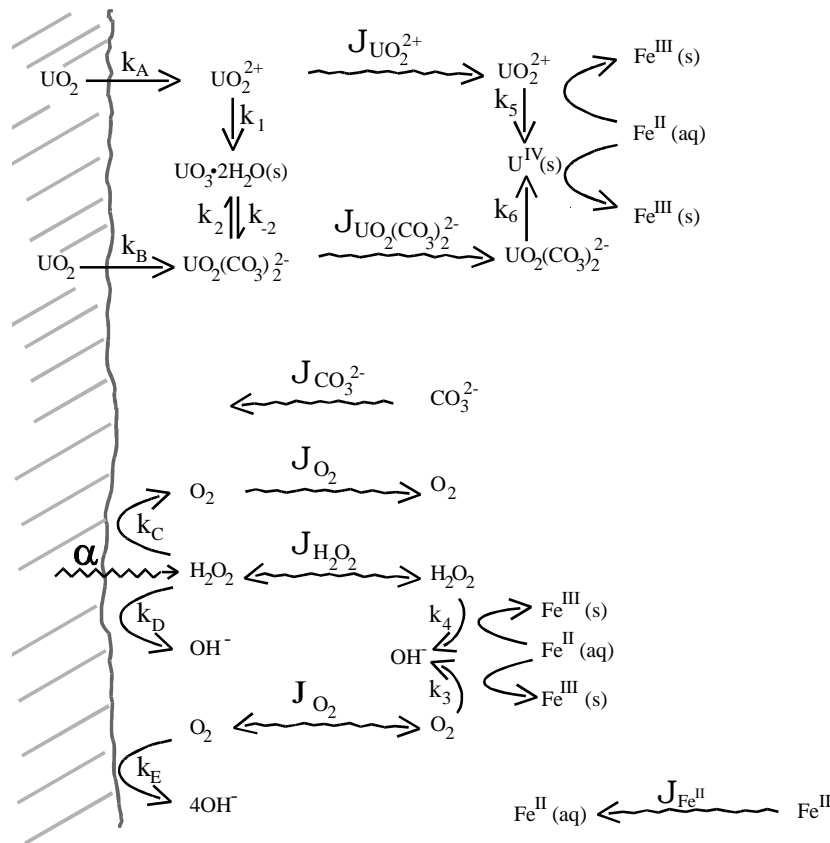
Figure 5-50
Reaction scheme for the revised EPRI CSNF alteration model. Although schoepite,
$UO_3 \cdot 2H_2O$, is shown as the stable U(VI) phase, the actual precipitated solid modeled
depends on the composition of the seepage water.

5.9.2.1   Precipitation of Surface Film

A principal feature of the EPRI conceptual model is the precipitation of surface films. Precipitation of a surface layer is assumed to occur if the concentration of dissolved U(VI) exceeds the solubility of a given solid, with the specific stable solid phase determined by the groundwater chemistry (see below).

The precipitated layer is considered to have a number of effects on CSNF dissolution behavior (Figure 5-51):

- Due to its porous nature, the film restricts the mass transport of species to and from the dissolving CSNF surface. This will restrict the supply of atmospheric O_2 to the surface, as well as the transport of dissolved U(VI) and of radiolytically-produced H_2O_2 away from the surface. (A spatially dependent generation rate is used to account for the radiolytic formation of H_2O_2 in a water layer approximately 40-μm-thick adjacent to the fuel surface).

- The precipitate modifies the yield of α-radiolysis products not only by absorbing a fraction of the incident energy, but also by effectively increasing the volume of irradiated solution if α-emitters are co-precipitated in the growing film.

- Co-precipitation retards the migration of radionuclides released by dissolution of the matrix.

- Precipitation physically blocks the surface and reduces the rates of the interfacial electrochemical process. For a porous structure of randomly sized and randomly orientated pores, it can be shown that the fraction of the surface exposed to the solution at the base of the pores is equal to the bulk porosity of the solid ε (King and Kolar, 2001).
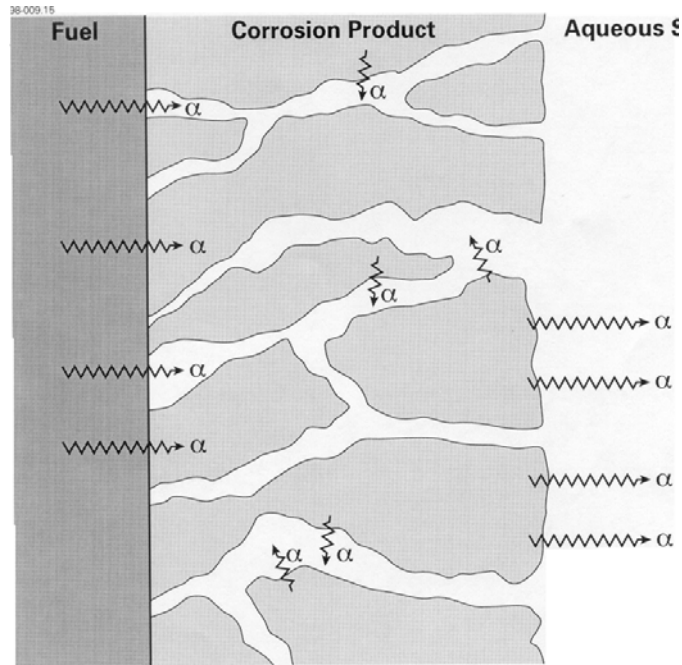
Figure 5-51
Conceptual model of a protective precipitated layer on the fuel surface.

5.9.2.3   Mass Transport Conditions

Given the location of the proposed YM repository horizon in the unsaturated zone, the availability of water and the transport of species away from the dissolving fuel surface will be limited.

Conceptually, three mass-transport scenarios are considered in the EPRI model:

1. The fuel surface is covered by a thin condensed water layer. Two variants of this scenario are considered, one in which the thickness of the water layer remains constant as the porous deposit (if any) thickens (equivalent to an increase in water volume, as the pores of the precipitated layer are also assumed to be filled with water) and another in which the volume of the water layer remains constant.

2. A dripping scenario in which the amount of water on the fuel surface increases with time. This scenario simulates the case in which there is a single defect in the top of the WP, which slowly fills with water in a "bathtub"-type effect.

3. A second dripping scenario in which dissolved U(VI) is assumed to be removed from the surface by advection. This scenario simulates either the complete disappearance of the WP outer barrier or the case in which there are defects in the top and bottom of the package which both allows seepage water to enter and dissolved U(VI) to leave the WP.

5.9.2.4 Effect of Groundwater Chemistry

The groundwater (or seepage) chemistry affects the rates of the interfacial dissolution reactions and the composition and solubility of the precipitated U(VI) phase. In seepage or ground waters rich in CO_3^{2-}, aqueous uranium speciation is dominated by uranyl carbonate complexes, e.g,, $UO_2(CO_3)_2^{2-}$, whereas the uranyl dioxo-cation (UO_2^{2+}) will predominate in carbonate-poor waters. As discussed in more detail below, the chemistry of the aqueous phase also determines the nature of the most-stable U(VI) solid phase. With time, changes in aqueous chemistry, temperature, and other environmental conditions, the uranyl alteration products can evolve as illustrated in Figure 5-49. Although the current implementation of the EPRI model does not include paragenesis of the precipitated U(VI) phase, the inclusion of the effect of a precipitated uranyl phase is considered to be a significant advancement in sophistication over existing CSNF alteration models. The exact nature of the precipitated U(VI) phase will have a smaller effect on the alteration rate than the fact that a precipitated phase is present on the surface blocking dissolution of the underlying spent fuel.

5.9.2.5 Instant Release Fraction

A fraction of the radionuclides in the fuel are located either in the fuel-cladding gap or at grain boundaries in the fuel matrix. This so-called instant release fraction (IRF) is assumed to be instantly released upon failure of the WP, which is the common approach for modeling the rapidly released fraction of the radionuclide inventory in CSNF.

5.9.2.6 Effect of Canister Internals and Cladding

No chemical or mass-transport credit is taken for any component of the WP. The CSNF is assumed to be contacted by water, either as a condensed H_2O layer or as seepage drips, immediately upon failure of the WP. Although the stainless steel inner vessel, the stainless steel transportation, aging, and disposal (TAD) canister, the fuel cladding, and any remaining part of the Alloy 22 WP outer cylinder may offer significant resistance to the transport and release of radionuclides from the failed WP, no credit is taken for these processes in the current model.

5.9.3 Mathematical Model

The conceptual EPRI model described above is formalized in a mathematical model referred to as the <u>EPRI</u> <u>C</u>SNF Alteration <u>M</u>odel (ECM) Version 1.0.

A 1-D reaction-transport equation is written for each of the species illustrated in Figure 5-50 of the general form (King and Kolar, 2001; Shoesmith et al., 2003)

$$\varepsilon_a \frac{\partial c}{\partial t} = \frac{\partial}{\partial x}\left(\varepsilon_e \tau D \frac{\partial c}{\partial x}\right) + \varepsilon_a R \qquad \qquad \textbf{eq. 5-12}$$

where c and D are the concentration and diffusion coefficient, ε_a, ε_e, and τ are the apparent and effective porosities for mass transport and the tortuosity factor of the porous medium, respectively; x and t are the spatial and temporal variables; and R is the sum of the gain and loss terms for the particular species for all reactions in which it participates. One such equation is assigned for each of the ten key species in the model listed in Table 5-15. Mass transport is treated as occurring by diffusion only, with the advective transport inherent in the "flow-through" dripping scenario simulated through appropriate choice of boundary conditions (see below). For the version of the model described here, no effect of Fe(II) formed by corrosion of the internal stainless steel components was considered. The exclusion of the effects of Fe(II) is reasonable for the current WP design, since the corrosion of the stainless steel internals is unlikely to significantly reduce the flux of atmospheric O_2 to the CSNF.

Table 5-15
Chemical species included in EPRI CSNF alteration model.

UO_2^{2+}	CO_3^{2-}
$UO_2(CO_3)_2^{2-}$	O_2
$(UO_2^{2+})_{ADS}$ [a]	H_2O_2
U(IV) (s)[b]	Fe^{2+}
U(VI) (s)[b]	Fe(III) (s)[b]

[a] Adsorbed uranyl species not shown in Figure 5-50.
[b] Precipitated phases.

These equations are solved using finite-difference methods subject to various initial and boundary conditions. The most important boundary conditions (BCs) are electrochemical expressions for each species that participates in the interfacial dissolution reactions. Together, these BCs form a mixed-potential model from which the corrosion potential of the surface and the rate of dissolution are determined (King and Kolar, 2001; Shoesmith et al., 2003). Other important BCs are those for various species at the right-hand boundary, which serve to define the three mass-transport scenarios discussed above. For example, the condensed water layer is simulated using zero-flux BCs for H_2O_2 and the dissolved U(VI) species, which cannot diffuse away, and constant concentration BCs for O_2 and CO_3^{2-}. Similar BCs are used for the dripping scenario in which water accumulates inside the failed WP. However, zero-concentration BCs are used for H_2O_2 and dissolved U(VI) for the dripping scenario in which water flows through the failed WP, in order to simulate the advective flux.

The nature of the stable U(VI) film that forms is determined through equilibrium thermodynamic modeling of various possible seepage water compositions (Table 5-16). Thermodynamic analyses are performed using EQ3NR and the YM Project's thermodynamic database data0.ymp.R2 to calculate saturation indexes for the U minerals represented in this database. The saturation index, SI, is given by

$$\text{SI} = \log (Q/K) \qquad \qquad \textbf{eq. 5-13}$$

where Q is the ion-activity product, and K represents the corresponding equilibrium constant. A negative SI for a given U mineral indicates that the seepage water is under-saturated with respect to that mineral. Positive values indicate that the water is oversaturated, and a value of 0 indicates that the water is equilibrated with the mineral of interest. For a given seepage water, the U mineral having the highest (i.e., least negative) SI value are the first to equilibrate with the seepage water if the dissolved U concentration increases as a result of spent fuel-water interactions.

Table 5-17 shows the results of the thermodynamic analyses for the various seepage waters. For all waters, the least soluble U(VI) solid is predicted to be Na-boltwoodite, with either schoepite or uranophane representing the next least-soluble corrosion product.

An important property of the precipitated layer is its porosity. Unfortunately, there are few porosity measurements available in the literature. Consequently, a value of 0.1 is used for the calculations presented here based on the total estimated porosity of a hydrated U(VI) film (King and Betteridge, 1998) and an assessment of the fraction of that porosity contributing to mass-mass transport.

Table 5-16
Compositions of representative Yucca Mountain seepage waters (BSC, 2003).

Seepage water ID	W0	W5	W4	W6	W7
Lithostratigraphic Unit	Tptpmn	Tptpul (base)	Tptpll	Tptpll	Tptpul
Temperature (°C)	25	25	25	25	25
pH	8.3	7.6	7.4	7.9	8.0
Na^+ (mg/l)	61.5	39.0	130.0	84.0	57.0
K^+ (mg/l)	8.0	7.6	10.6	7.9	10.3
Ca^{2+} (mg/l)	101.0	94.0	82.0	56.0	120.0
Mg^{2+} (mg/l)	17.0	18.1	5.3	0.9	19.3
SiO_2(aq) (mg/l)	70.5	42.0	48.0	50.0	49.0
Cl^- (mg/l)	117.0	21.0	26.0	23.0	54.0
SO_4^{2-} (mg/l)	116.0	36.0	39.0	10.0	78.0
HCO_3^- (calc)[1]	200.0	395.0	515.0	335.0	412.0
NO_3^- (mg/l)	6.5	2.6	4.2	17.0	6.1
F^- (mg/l)	0.9	3.4	6.0	2.5	4.8

[1]Total aqueous carbonate as HCO_3^- (mg/l), calculated from charge balance.

Table 5-17
Calculated saturation indexes for U minerals at 25°C for the Yucca Mountain seepage waters in Table 5 - 16.

Mineral	Pore water				
	W0	W5	W4	W6	W7
Na-boltwoodite	-3.30	-4.66	-4.46	-3.93	-4.45
Rutherfordine	-6.80	-6.04	-5.92	-6.38	-6.83
Schoepite	-4.90	-5.15	-5.33	-5.14	-5.56
UO2(OH)2(beta)	-5.02	-5.27	-5.45	-5.25	-5.67
UO3:0.9H2O	-5.09	-5.34	-5.52	-5.32	-5.75
Uranophane	-3.95	-6.28	-6.99	-5.72	-6.11

5.9.4 Results of Preliminary Analyses

Preliminary simulations were performed for one of the seepage waters in Table 5-16 (water W0) for the condensed water scenario for the case of a constant water-layer thickness. Figure 5-52 shows the predicted time dependence of E_{CORR} and of the rates of each of the individual interfacial electrochemical reactions. The value of E_{CORR} is within Region A in Figure 5-48 indicating that the surface, while oxidized, is within the potential region where a protective U(VI) film is expected. After an initial period of 30-50 years, during which H_2O_2 is a significant oxidant, dissolution is supported primarily by the cathodic reduction of atmospheric O_2.[7] For this particular seepage water composition, approximately 80% of the total dissolution occurs as UO_2^{2+}, with the remaining 20% occurring as $UO_2(CO_3)_2^{2-}$.

---

[7] For these simulations, an α-dose rate equivalent to freshly discharged spent fuel was used
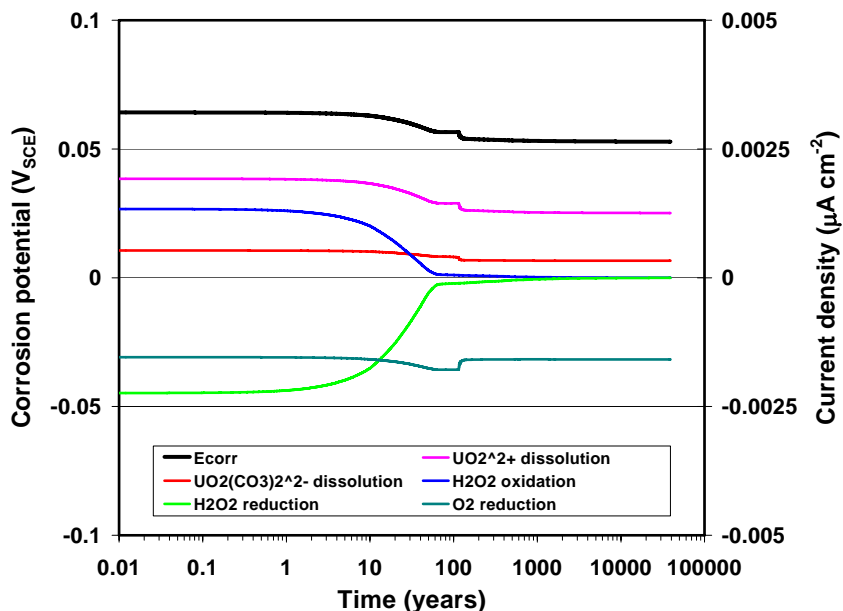
Figure 5-52
Predicted time dependence of the corrosion potential and individual anodic dissolution and cathodic reduction current densities for CSNF covered by a condensed water film.

Figure 5-53 shows the time dependence of the thickness of the Na-boltwoodite layer, the stable U(VI) solid for this seepage water. Precipitation is predicted to occur within minutes, as the initial 100-µm-thick water layer quickly becomes saturated with dissolved U(VI). The layer is predicted to increase in thickness before reaching a constant thickness of ~170 µm after approximately 1000 years. The reason for the attainment of a constant film thickness is not currently understood, since there is no mechanism by which dissolved U(VI) is removed from the surface. For the scenario modeled, one might have expected the layer to continue to thicken until all the fuel had dissolved.

The amount of altered CSNF can be determined by integrating the sum of the dissolution currents for UO_2^{2+} and $UO_2(CO_3)_2^{2-}$ (Figure 5-54). The figure shows a relatively constant dissolution rate and an overall alteration time of 30,000 years. This alteration time is ten times longer than the alteration rate in the absence of a film, as calculated from the film-free electrochemical kinetic expressions in the model. Since the assumed porosity of the film for this run was 0.1, the ten-fold reduction in rate suggests that the principal effect of the precipitated film is to physically block the dissolving surface, reducing the overall dissolution rate by the fractional surface coverage by the solid phase.[8] This conclusion is supported by the apparent constant dissolution rate, since mass-transport limitation due to diffusion of reactants to, or of products away from, the corroding surface would have resulted in a $t^{1/2}$-dependent alteration rate.

---

[8] As noted above, the fraction of the CSNF surface area exposed to the aqueous environment at the base of pores in the precipitated film is numerically equal to the bulk porosity of the film.
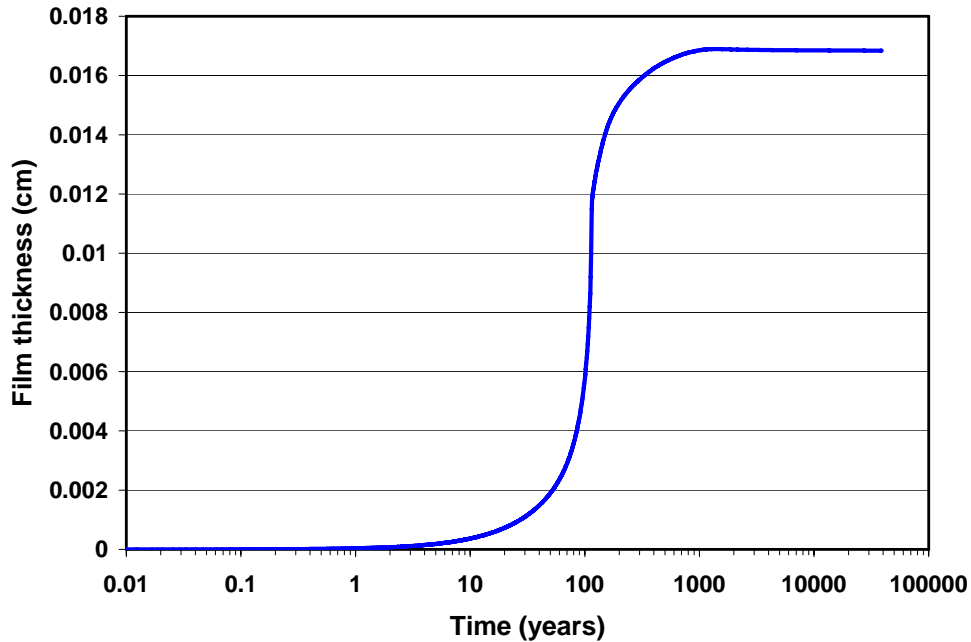
Figure 5-53
Predicted time dependence of the thickness of the precipitated Na-boltwoodite film formed on CSNF covered by a condensed water film.
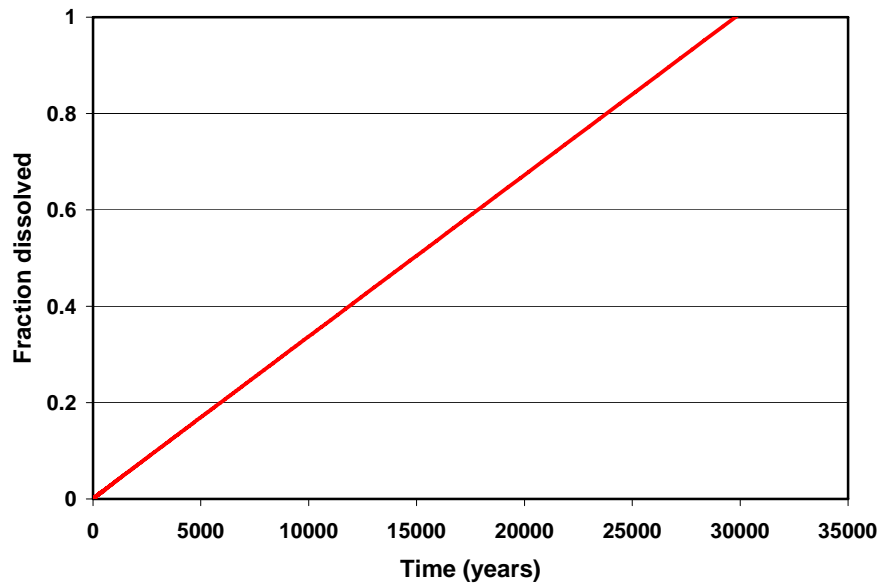
Figure 5-54
Predicted time dependence of the fraction of fuel dissolved for CSNF covered by a condensed water film.

Regardless of the nature of the rate-determining process, it is apparent that an understanding of the porosity of the precipitated U(VI) film is essential in predicting the long-term alteration behavior of CSNF.

5.9.5 Conclusions

EPRI has developed a mechanistically based model for the dissolution rate of the UO_2 matrix of commercial spent nuclear fuel in the proposed Yucca Mountain repository. The conceptual and mathematical models account for important processes affecting fuel dissolution under the expected environmental conditions, most notably the limited availability of water, the generally limited rates of mass transport, and the formation of protective U(VI) surface films. Because of these factors, complete alteration of the fuel is predicted to take 10,000's to 100,000's of years, rather than the 1000's of years predicted using conservative models based on experimental flow-through measurements (BSC, 2004).

Preliminary simulations have shown that the minimum fuel alteration time in the presence of a condensed water film is of the order of 30,000 years, approximately ten times longer than under film-free conditions. The major effect of the precipitated film appears to be to reduce the effective fuel surface area, thereby increasing the matrix alteration time.

5.9.6 References

BSC, 2003. *Drift Scale Coupled Processes (DST and THC) Models*, Report to DOE, MDL-NBS-HS-000001 Rev 02, Bechtel SAIC Company, Las Vegas, NV.

BSC, 2004. *In-Package Environment and Waste Form Degradation and Solubility*. Technical Basis Document No. 7. Revision 1, Report prepared for DOE, July 2004, Bechtel SAIC Company, Las Vegas, NV.

Finch, R.J., E.C. Buck, P.A. Finn, and J.K. Bates, 1999. Oxidative corrosion of spent UO_2 fuel in vapour and dripping groundwater at $90^{\circ}C$, *Mater. Res. Soc. Symp. Proc.*, 556, 431-438.

Finn, P.A., E.C. Buck, J.C. Hoh, and J.K. Bates, 1995. Spent fuel's behavior under dynamic drip tests, in *Proc. Global '95*, Versailles, September 11-14, 1995, 241-248, American Nuclear Society, La Grange Park, IL.

Grenthe I., J. Fuger, R.J.M. Konings, R.J. Lemire, A.B. Muller, C. Nguyen-Trung, and H. Wanner, 1992. *Chemical Thermodynamics of Uranium*, North Holland, Amsterdam.

King, F. and J.S. Betteridge. 1998. Ex situ measurements of the porosity of precipitated corrosion products on oxidized UO_2, Ontario Hydro Report No. 06819-REP-01200-0059 R00.

King, F. and M. Kolar, 2001. *Mixed-Potential Model Simulations of the Effects of Porous Film Formation on the Dissolution of Used Fuel (MPM Version 1.3),* Report No: 06819-REP-01300-10019, Ontario Power Generation, Toronto, Ontario.

Murphy, W.M. and F. and E..C. Pearcy, 1992. Source-term constraints for the proposed repository at Yucca Mountain, Nevada, derived from the natural analog at Peña Blanca, Mexico, Mat. Res. Soc. Sympos. Vol. 257, Material Research Society Pittsburgh, PA 521-527.

Santos, B.G., J.J. Noël, and D.W. Shoesmith, 2006a. The influence of silicate on the development of acidity in corrosion product deposits on SIMFUEL (UO₂), *Corros. Sci*. 48, 3852-3868.

Santos, B.G., J.J. Noël, and D.W. Shoesmith, 2006b. The influence of calcium ions on the development of acidity in corrosion product deposits on SIMFUEL UO₂, *J. Nucl. Mater*. 350, 320-331.

Shoesmith, D.W., 2000. Fuel corrosion processes under waste disposal conditions, *J. Nucl. Mater*. 282, 1-31.

Shoesmith, D.W., M. Kolar, and F. King, 2003. A mixed-potential model to predict fuel (uranium dioxide) corrosion within a failed nuclear waste container. *Corrosion* 59, 802-816.

Stout, R.B. and H.R. Leider, 1998. *Waste Form Characteristics Report*, Revision 1, Report, UCRL-ID-108314, Version 1.3, Lawrence Livermore Laboratory, Livermore, CA.

Tait, J.C. and J.M. Luht, 1997. *Dissolution Rates of Uranium from Unirradiated UO2 and Uranium and Radionuclides from Used CANDU Fuel Using the Single-Pass Flow-Through Apparatus*, Report Np. 06819-REP-01200-0006 R00, Ontario Hydro, Toronto, Ontario.

Wilson, C.N. and W.J. Gray, 1990. Measurement of Soluble Nuclide Dissolution Rates from Spent Fuel, *Mater. Res. Soc. Symp. Proc*., 176, 489.

5.10   Mechanistic Studies of the Crevice Corrosion of Alloy 22 in Chloride-Nitrate Solutions

5.10.1.   Introduction

Crevice corrosion of Alloy 22 is one of a number of potential corrosion processes of interest for the waste packages in the proposed Yucca Mountain repository (DOE, 2008; Sandia, 2007; King et al., 2008; Rebak et al., 2007; Cragnolino et al., 2004; He and Dun, 2007). Localized corrosion is only possible during the intermediate stages of the thermal pulse, and then only if the drip shields have failed and seepage water can contact the waste package surface. Under such conditions, concentration of the seepage water by evaporation on the hot WP surface could lead to aggressive concentrated brines. An alternative scenario in which localized corrosion initiates following the deliquescence of salt assemblages derived from surficial dust deposits has been shown to be highly unlikely based on multiple lines of argument (DOE, 2008; Apted et al., 2005).

The crevice corrosion of Alloy 22 has been studied in some detail, with particular attention paid to conditions leading to the initiation of localized attack (Sandia, 2007; Rebak et al., 2007; Cragnolino et al., 2004; He and Dunn, 2007). Susceptibility of a whole range of passive alloys, including Alloy 22, to localized corrosion can be evaluated by comparing the corrosion potential

E_{CORR} to a known threshold potential for initiation of localized attack. For this purpose, the DOE has selected a threshold criterion based on the re-passivation potential ($E_{R,CREV}$) measured on creviced samples (DOE, 2008; Sandia 2007), even though this potential corresponds to that at which a propagating pit ceases to grow. Predictions of crevice initiation based on this criterion are clearly, therefore, conservative. The effects of temperature, pH, Cl⁻ concentration, nitrate:chloride ratio, metallurgical condition, etc. on the values of E_{CORR} and $E_{R,CREV}$ have all been previously determined (DOE, 2008; Sandia, 2007; Rebak et al., 2007; Cragnolino et al., 2004; He and Dunn, 2007).

Factors controlling the propagation of crevice corrosion are less well understood. Consequently, DOE conservatively assumes in its WP performance assessments that, once initiated, crevices propagate at a constant rate (DOE, 2008; Sandia, 2007). In the absence of measured crevice propagation rates, a distribution of rates was defined based on the rate of general corrosion of Alloy 22 in acidic concentrated chloride solutions containing Fe(III) and other aggressive cations. DOE also considers an alternative crevice propagation model, in which the rate of crevice penetration decreases with time in a process known as stifling.

Stifling of crevice corrosion has been included in the EPRI localized corrosion model for some time (King et al., 2008; EPRI, 2000; EPRI, 2002; EPRI, 2005; King and Kolar, 2006; Shoesmith and Kolar, 1998; Shoesmith and Massari, 2001). The inclusion of stifling is based on an analogy with many other localized corrosion systems for a range of passive and non-passive materials. The EPRI corrosion model represents stifling effects via the mathematical expression:

$$D = kt^n \qquad \qquad \textbf{eq. 5-14}$$

where D is the depth of corrosion as a function of time t, n is the time exponent and k is a temperature-dependent growth constant the value of which also depends on the nature of the environment. By comparison with other systems, the time exponent is typically of the order of 0.1 to 0.5 (EPRI, 2000).

Recently, both the DOE (BSC, 2005) and CNWRA (He and Dunn, 2006, 2007) have shown that the crevice corrosion of Alloy 22 obeys a similar dependence. The DOE expression takes the form:

$$D = A + kt^n \qquad \qquad \textbf{eq. 5-15}$$

where the exponent n has been found to vary between 0.09 and 0.69, with an average value of 0.44 (BSC, 2005). The DOE sponsored experiments were performed in a range of solutions with different $[NO_3^-]:[Cl^-]$ ratios and at temperatures up to 140°C. Localized corrosion was initiated by applying an externally controlled potential and the current decay monitored as a function of time to determine values of A, k, and n.

He and Dunn (2006, 2007) measured penetration depths as a function of time for a naturally corroding crevice sample of Alloy 22 immersed in 5 mol·dm⁻³ NaCl solution at 95°C. Cupric ions (in the form of 2×10^{-4} mol·dm⁻³ $CuCl_2$) were added to the solution in order to create sufficiently oxidizing conditions to initiate localized corrosion. The average value of n reported was 0.23.

Consensus within the corrosion science community has not been reached regarding the mechanism of stifling. The principle candidates include:

1. potential (iR) drop down the crevice

2. mass-transport effects

3. loss of critical crevice chemistry by catalysis of H^+ reduction

4. loss of critical crevice chemistry by the reduction of NO_3^- (in NO_3^-:Cl^- mixtures)

5. negative shift in E_{CORR} upon the initiation of localized corrosion

This section presents the results of EPRI-sponsored preliminary electrochemical and surface analytical studies of the crevice corrosion of Alloy 22 in chloride solutions at 120°C. A coupled electrochemical technique has been used to follow the propagation of crevice corrosion following artificial initiation achieved by applying a constant current to the creviced sample. Experiments have been conducted in $CaCl_2$-$NaNO_3$ mixtures with different total salinities and NO_3^-:Cl^- ratios and in 5 mol·dm^{-3} NaCl solution with and without the addition of $NaNO_3$. Results from surface analyses conducted on a limited number of post-test crevice samples are also discussed.

5.10.2 Experimental

Crevice specimens were made from 3/16"-thick Alloy 22 plate material (Allegheny Ludlum Corp.). The Alloy 22 chemical composition is listed in Table 5-18.

Table 5-18
Elemental composition of the Alloy 22 plate.

Element	Ni	Cr	Mo	W	Fe	Co	V	Mn	Cu	Si	P	C	S
Weight %	56.53	21.23	13.43	2.64	4.51	0.904	0.170	0.154	0.065	0.072	0.015	0.0073	0.0002
Atomic %	58.99	25.01	8.57	0.88	4.95	0.940	0.204	0.172	0.063	0.160	0.030	0.037	0.0004

The Alloy 22 plate was cut into strips and bent into a "U" shape using a pair of dies. Figure 5-55(a) shows a schematic of the specimen configuration. This design avoids potential localized attack at the crevices formed by specimen contact with the washers by keeping these locations out of the solution. The surface of the specimens was polished using wet (180, 320, and 600 grit) SiC papers and rinsed in distilled water. A small wafer of PTFE (teflon) (2.2 cm x 3.0 cm x 0.2 cm) was sandwiched between the specimen and a bottom polysulfone plate to make the 2.2 cm x 1.7 cm (or 3.8 cm^2) creviced region. The crevice assembly was held together with the addition of a top polysulfone plate, and two Alloy 22 threaded bolts with four matching Alloy 22 nuts. The bolts and nuts were made from the same Alloy 22 material. A tapered crevice gap was formed by placing a 0.22 mm diameter PTFE fiber at one edge of the creviced region during assembly, which provided a 0 – 0.2 mm crevice gap once the assembly nuts were tightened. In later experiments (those in NaCl solution), a separate Alloy 22 specimen (2.2 cm × 1.7 cm × 0.5 cm), sized to fit in the Auger spectrometer chamber for post-experiment surface analysis, was inserted between the U-shaped sample and the PTFE crevice former (Figure 5-55(b)). The addition of this Alloy 22 block provided both a metal-metal and a metal-PTFE crevice in the same experiment.

(a) U sample

(b) U-shape sample and Alloy 22 block arrangement
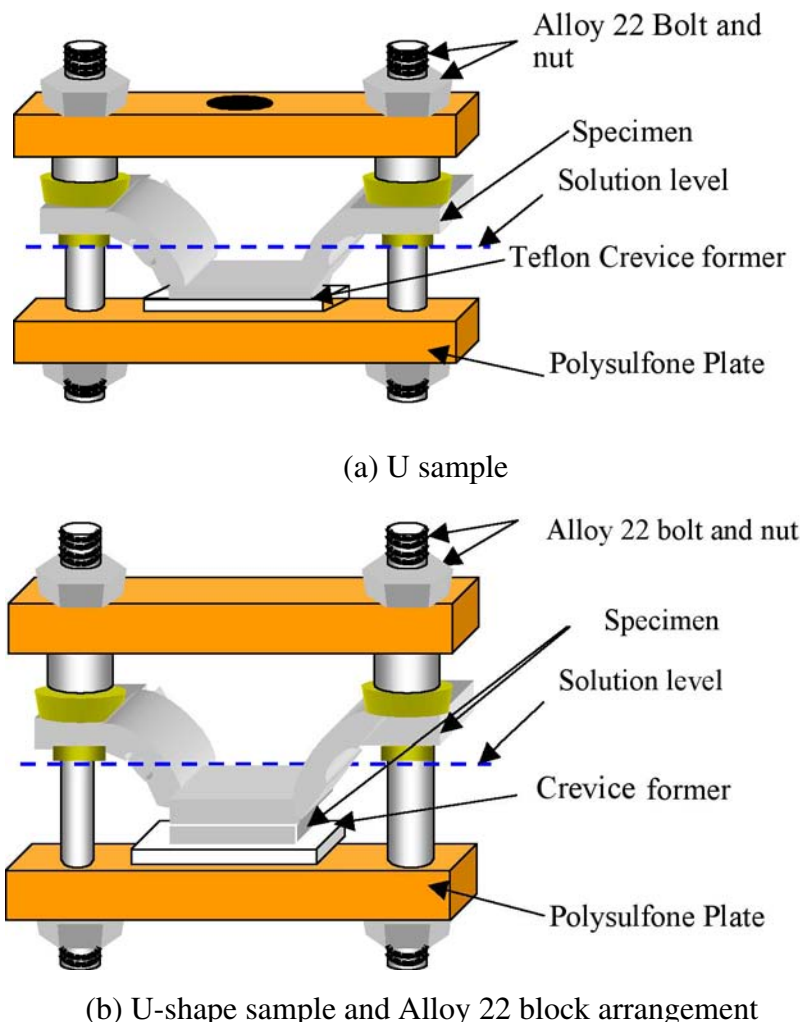
Figure 5-55
Schematic illustration of creviced electrode geometries.

Figure 5-56 shows the electrochemical test cell used to study the crevice corrosion of Alloy 22 at a temperature of 120°C. The counter electrode (CE), with a total surface area of 390 cm^2 of which 130 cm^2 was immersed in solution, was machined from the same Alloy 22 plate used for the test specimens and was formed into an annulus to surround the creviced assembly, which serves as the working electrode (WE). The creviced working electrode (Figure 5-55) was galvanically coupled to the counter electrode through a zero resistance ammeter (ZRA, model #399, AMC Instruments). A custom internal Ag/AgCl/KCl reference electrode was used to monitor the potential of the crevice couple. For tests in high Cl$^-$ concentration solutions (5 mol·dm^{-3} CaCl$_2$ and 5 mol·dm^{-3} NaCl), a saturated KCl solution was used in the reference compartment. For tests in the dilute solutions, the concentration of the Cl$^-$ in the reference compartment was the same as the test solution. All potentials have been converted to SHE (standard hydrogen electrode) unless otherwise specified. The potentials of the various Ag/AgCl/KCl reference electrodes at 120°C were estimated to be 0.110 V$_{SHE}$, 0.216 V$_{SHE}$, and 0.138 V$_{SHE}$ for the saturated KCl, 0.1 mol·dm^{-3} KCl, and 1 mol·dm^{-3} KCl solutions, respectively (King et al., 1989). A planar Alloy 22 electrode was included in the cell, in the form of a bar having the same composition as the working electrode. Finally, a glass liner was inserted

between the electrochemical cell and the autoclave wall to isolate the solution from the pressure vessel.
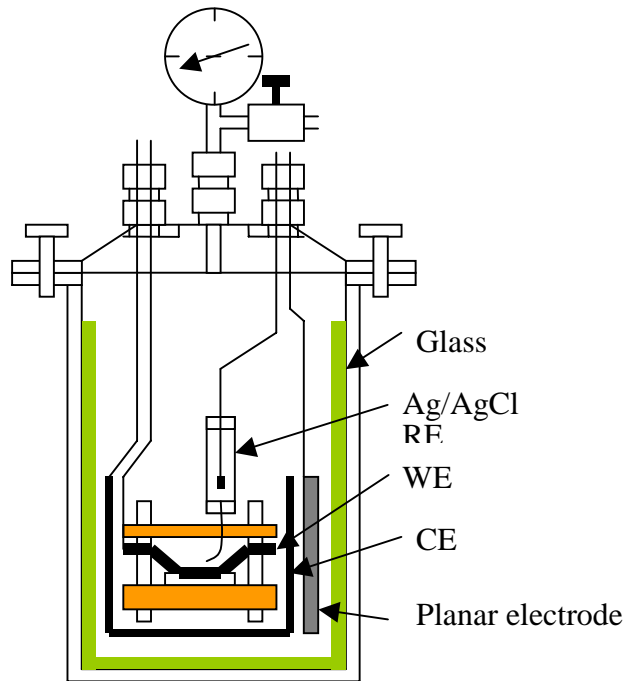
Figure 5-56
Schematic of glass-lined autoclave and the experimental arrangement. RE, WE, and CE stand for reference electrode, working electrode, and counter electrode, respectively.

Two sets of solutions were used in this study. A number of tests were performed in $CaNO_3$ + $NaNO_3$ mixtures with varying chloride concentration and $[NO_3^-]$:$[Cl^-]$ ratio. The most saline solutions comprised 5 mol·dm^{-3} $CaCl_2$ with either 1 mol·dm^{-3} or 0.5 mol·dm^{-3} $NaNO_3$ (solutions A and B, respectively, Table 5-19), with $[NO_3^-]$:$[Cl^-]$ ratios of 0.1 and 0.05. Two other, more dilute $CaNO_3$ + $NaNO_3$ solutions, each with a $[NO_3^-]$:$[Cl^-]$ of 0.05, were also used (solutions C and D, respectively, Table 5-19). The main purpose for using these more-dilute solutions was to determine whether there was any change in the $[NO_3^-]$:$[Cl^-]$ ratio in the bulk solution, and by inference also in the crevice solution, at the end of the test. A second set of tests was performed in 5 mol·dm^{-3} NaCl solution, with additions of 0, 0.1 mol·dm^{-3}, or 0.5 mol·dm^{-3} $NaNO_3$ (solutions E, F, and G, Table 5-19), providing $[NO_3^-]$:$[Cl^-]$ ratios of 0, 0.02 and 0.1, respectively.

Table 5-19
Composition of the test solutions.

Solution	[NO_3^-]:[Cl^-] ratio	Composition (mol·dm^{-3})		
		CaCl$_2$	NaCl	NaNO$_3$
Solution A	0.1	5.0	--	1.0
Solution B	0.05	5.0	--	0.5
Solution C	0.05	0.05	--	0.005
Solution D	0.05	0.5	--	0.05
Solution E	0	--	5.0	0
Solution F	0.02	--	5.0	0.1
Solution G	0.1	--	5.0	0.5

Before each test, the solution (300 cm^3) was aerated by bubbling with air for 4-12 hours. To prevent boiling of the solution upon heating, the pressure vessel was over-pressurized with 100 psi of high-purity Argon gas. All tests were performed at a temperature of 120°C in order to promote crevice initiation. The current between the working and the counter electrodes and the potential of the creviced sample versus the reference electrode were recorded using the ZRA. The potential between the planar electrode and the reference electrode was monitored using a Gamry Corrosion Measurement System (Gamry Instruments, Warminster, PA). Table 5-20 lists the experimental conditions for each of the tests performed.

Table 5-20
Description of test conditions.

Specimen Number	Sample type[a]	Test solution	Initiation condition[b]	Coupling time (days)
3	U type	Solution B	10 μ A/cm^2 for 6 hrs	11
4	U type	Solution A	10 μA/cm^2 for 6 hrs 10 μA/cm^2 for 6 hrs	20
5	U type	Solution C	10 μA/cm^2 for 6 hrs	20
6	U type	Solution C	20 μA/cm^2, 2 hrs +10 μA/cm^2, 2 hrs	20
7	U type	Solution D	10 μA/cm^2 for 6 hrs	8
15	U type + flat	Solution E	10 μA/cm^2 for 11 hrs	11
11	U type + flat	Solution F	10 μA/cm^2 for 11 hrs	10
12	U type + flat	Solution F	10 μA/cm^2 for 11 hrs	3
10	U type + flat	Solution G	10 μA/cm^2, 11 hrs 26 μA/cm^2, 24 hrs	1

[a]The "U type" crevice specimen and the "U type + flat" crevice specimen are shown in Figs.1 (a) and (b), respectively.
[b]10 μA/cm^2 corresponds to a total current of 38.8 μA.
[c]The coupling time is the duration of the test following the initiation period.

An initial test (not listed in Table 5-20) was performed without applying a potential or current to the creviced working electrode. After 24 hrs at 120°C, the coupled current was less than 0.5 μA, suggesting a failure to initiate localized corrosion. In all subsequent tests, localized corrosion was initiated artificially by applying a constant current to the working electrode (Table 5-20).

After each experiment, the creviced specimen was carefully rinsed with distilled water and photographed using an optical microscope (DM ILM, Leica Microsystems), and the corrosion products were ground away sequentially until the measured thickness was within ± 10 μm of the original thickness. The corroded surface was photographed following each round of polishing.

The ratio of NO_3^- to Cl^- on the creviced surface was measured using X-ray photoelectron spectroscopy (XPS), using a Kratos Ultra XPS spectrometer with a focused monochromatic Al Kα X-ray (1486.7 eV, source operating at 14 keV and 15 mA). To confirm the results of the XPS, Auger electron spectroscopy (AES) was also used in this work to determine the elemental composition of the creviced surface for certain samples.

5.10.3 Results and Discussion

5.10.3.1   Concentrated CaCl$_2$ + NaNO$_3$ Solution

Figures 5-57 and 5-58 show the crevice potential (E$_c$), planar electrode potential (E$_p$), and crevice current (coupled current, I$_c$) as a function of time in Solutions A and B, respectively. The crevice was initiated by applying a constant current density of 10 μA/cm^2 between the working electrode and the counter electrode. When the initiation current was stopped, the crevice electrode and the counter electrode were coupled together.

Initiating crevice corrosion for a [NO$_3^-$]:[Cl$^-$] ratio of 0.1 (Solution A, Figure 5-57) was difficult. Following the initial galvanostatic polarization, the coupled current was of the order of 0.6 μA for the first three days of the test, suggesting minimal initiation had occurred. Therefore, a second initiation step was applied, after which the coupled potential dropped by a few tens of mV and the coupled current increased marginally (to ~0.8 μA). However, the magnitude and frequency of the current noise fluctuations increased, suggesting a certain amount of activity within the crevice, presumably associated with film breakdown and repair events. Following the test, the creviced sample exhibited only three visible areas of attack in the region of the tightest crevice gap. Sequential polishing indicated that the maximum depth of corrosion was 117 μm after 20 days exposure (average penetration rate of 5.9 μm/day), with attack focused at grain boundaries.
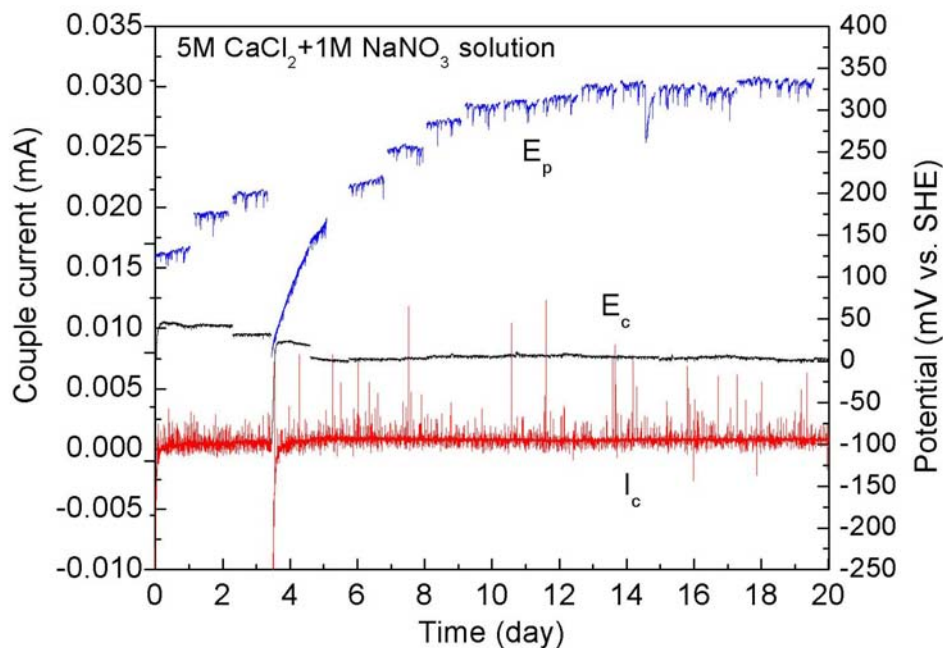
Figure 5-57
Time dependence of the coupled current (I$_c$) and potential (E$_c$) and the potential of the planar electrode (E$_p$) in solution A (5 mol·dm^{-3} CaCl$_2$ + 1 mol·dm^{-3} NaNO$_3$) following initiation at a current density of 10 μA·cm^{-2} initially and again after three days.
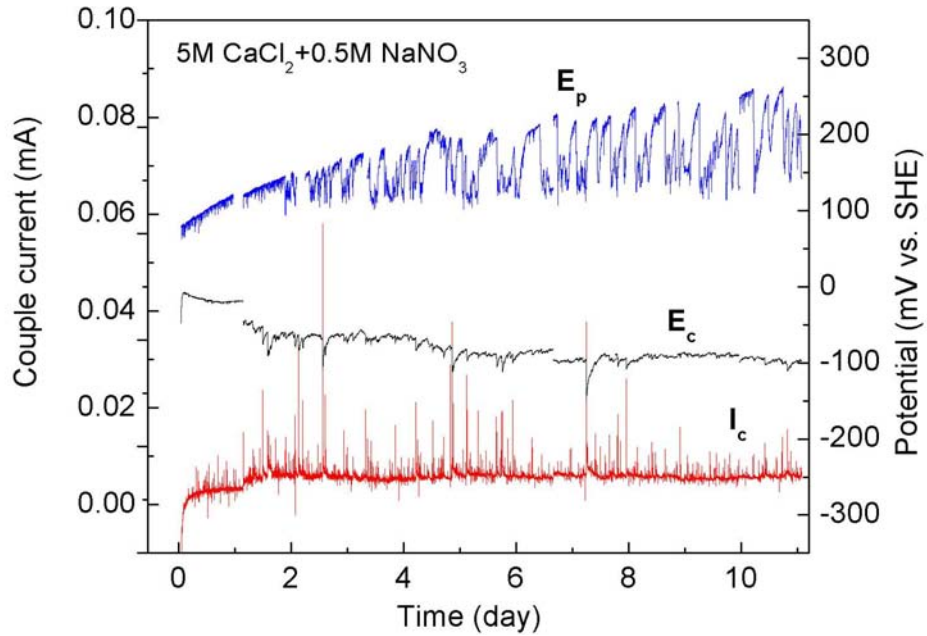
Figure 5-58
Time dependence of the coupled current (I_c) and potential (E_c) and the potential of the planar electrode (E_p) in Solution B (5 mol·dm^{-3} CaCl$_2$ + 0.5 mol·dm^{-3} NaNO$_3$) following initiation at a current density of 10 μA·cm^{-2} initially.

Initiation of localized corrosion was more evident for a [NO$_3^-$]:[Cl$^-$] ratio of 0.05 (Solution B, Figure 5-58). Following the initial galvanostatic polarization, the coupled potential drifted to a potential of –0.1 V$_{SHE}$ and the coupled current was of the order of 5 μA. Post-test examination showed a larger number of attacked sites than in Solution A, indicating an effect of the [NO$_3^-$]:[Cl$^-$] ratio on the extent of initiation. The maximum depth of corrosion was 79 μm after 11 days exposure (average of 7.2 μm/day). Table 5.10.4 summarizes the results of these and the other tests reported below.

Table 5-21
Summary of test results.

Specimen Number	Test solution	$[NO_3]:[Cl]$ ratio	Fully initiated	Inhibited after initiation
Specimen #3	Solution B	0.05	No	No
Specimen #4	Solution A	0.1	No	No
Specimen #5	Solution C	0.05	No	Yes
Specimen #6	Solution C	0.05	No	Yes
Specimen #7	Solution D	0.05	No	Yes
Specimen #15	Solution E	0	Yes	Yes
Specimen #11	Solution F	0.02	Yes	Yes
Specimen #12	Solution F	0.02	Yes	Yes
Specimen #10	Solution G	0.1	No	Yes

5.10.3.2   Dilute $CaCl_2$ + $NaNO_3$ Solution

Initiation of crevice corrosion in the "dilute" solution (0.05 mol·dm^{-3} $CaCl_2$ + 0.005 mol·dm^{-3} $NaNO_3$, Solution C and 0.5 mol·dm^{-3} $CaCl_2$ + 0.05 mol·dm^{-3} $NaNO_3$, Solution D) using the standard galvanostatic polarization current was unsuccessful, despite the relatively low $[NO_3]:[Cl]$ ratio of 0.05 (Figure 5-59). Initiation is characterized by an initial positive shift in potential (to >0.2-0.3 V_{SHE}) followed by a negative shift to <0.1 V_{SHE} as the crevice activates and the material dissolves in the acidic pore solution. The potential transients in concentrated solution (the lower two curves (colored black and light blue) in Figure 5-59) generally displayed these characteristics and some crevice attack was observed, as discussed above. However, in the more dilute solutions, no equivalent fall in potential was observed in any of the tests, even when the initiation current density was increased to 20 µA·cm^{-2} (specimen #6, red curve, Figure 5-59). In this case, although the potential went very positive (close to the transpassive potential), no crevice activation was apparent based on the absence of a negative shift in potential. However, for both specimens #6 and #7 (Table 5-20) there was significant noise in the potential, suggesting repeated attempts at film breakdown.

The lack of initiation implied by the behavior of the initiation potential was confirmed by post-test examination of the creviced coupons. There was no indication of sustained crevice attack for any of the samples. Some minor pitting was observed for tests that exhibited potential transients during the initiation phase.
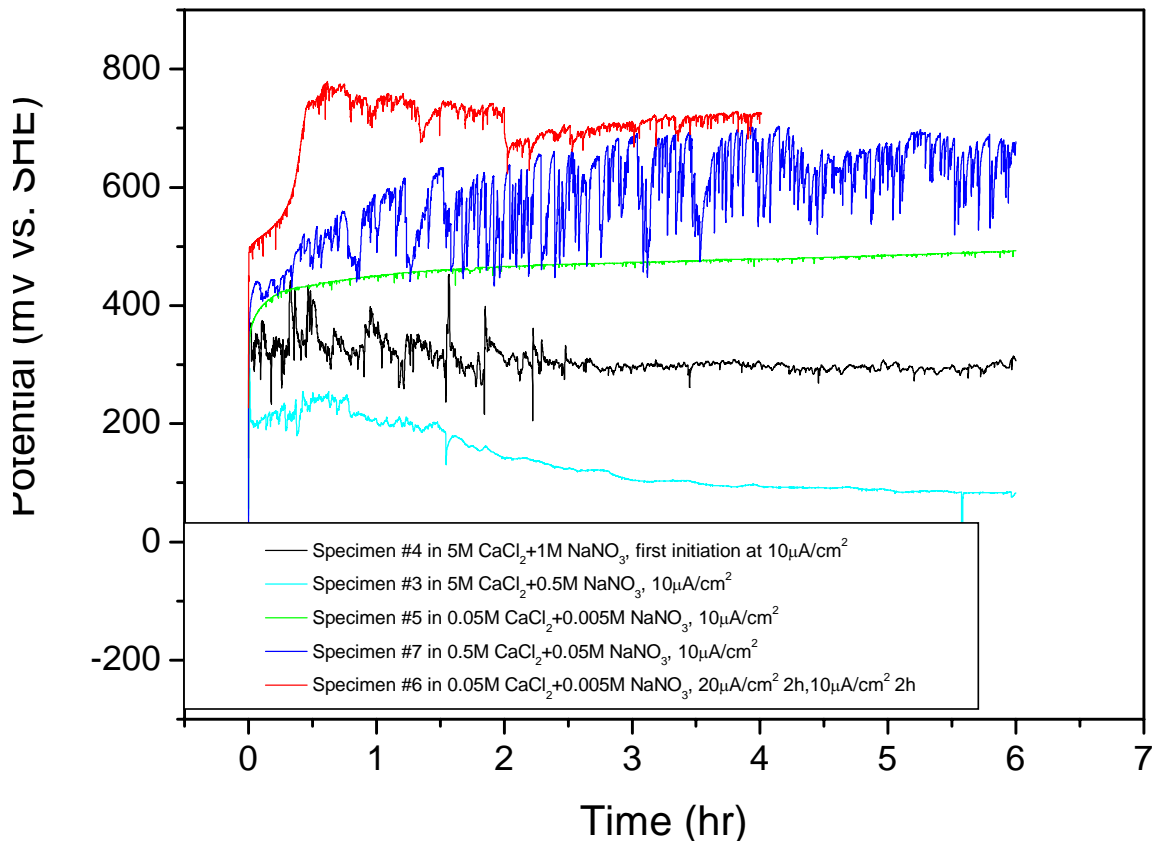
Figure 5-59
Time dependence of the potentials of the creviced electrode during the galvanostatic initiation stage in CaCl$_2$ + NaNO$_3$ solutions.

5.10.3.3   5 mol·dm^{-3} NaCl + NaNO$_3$ Solutions

In contrast to the difficulty found in initiating crevice corrosion in CaNO$_3$ + NaNO$_3$ solutions, initiation was observed readily in 5 mol·dm^{-3} NaCl solutions, both with and without added NO$_3^-$. Figure 5-60 shows the variation of the potential of the creviced samples during an 11-hour initiation period during which a constant current of 10 μA·cm^{-2} was applied. Crevice initiation, as characterized by an initial positive shift in potential followed by a decrease to more-active values, was observed in the absence of NO$_3^-$ (specimen #15, solution E) and for a [NO$_3^-$]:[Cl$^-$] ratio of 0.02 (specimen #11, solution F). The initiation time (as measured by the drop in potential to active values) was shorter in the absence of NO$_3^-$ and the degree of initiation (as indicated by the absolute value of the potential post-initiation) was greater. Visible corrosion was observed following these two tests; interestingly, crevice corrosion initiated at the metal-metal crevice in the absence of NO$_3^-$ (solution E) but at the metal-PTFE crevice in the presence of NO$_3^-$ (solution F). Generally, it is considered that a metal-PTFE crevice is required to initiate localized corrosion of Alloy 22. No explanation for this observed difference in behavior is currently available.

Initiation was more difficult in the 5 mol·dm^{-3} NaCl solution at a [NO$_3$]:[Cl] ratio of 0.1 (specimen #10, solution G, Figure 5-60). An active potential shift characteristic of crevice initiation was observed after 3.8 hours, but the potential appeared to recover and remain relatively constant at ~0.2 V$_{SHE}$. The coupled current after the 11-hour initiation period was small (0.5 µA), suggesting minimal crevice propagation. In order to induce greater crevice corrosion, a second period of galvanostatic initiation was imposed for a further 24 hours with a higher applied current density of 26 µA·cm^{-2} (Figure 5-61). Although the potential once again dropped after several hours of galvanostatic polarization, the more-active potential (of ~0.1 V$_{SHE}$) was not maintained and the potential shifted to more passive values after ~15 hours. No evidence for crevice corrosion was observed visually on the specimen at the end of the test.
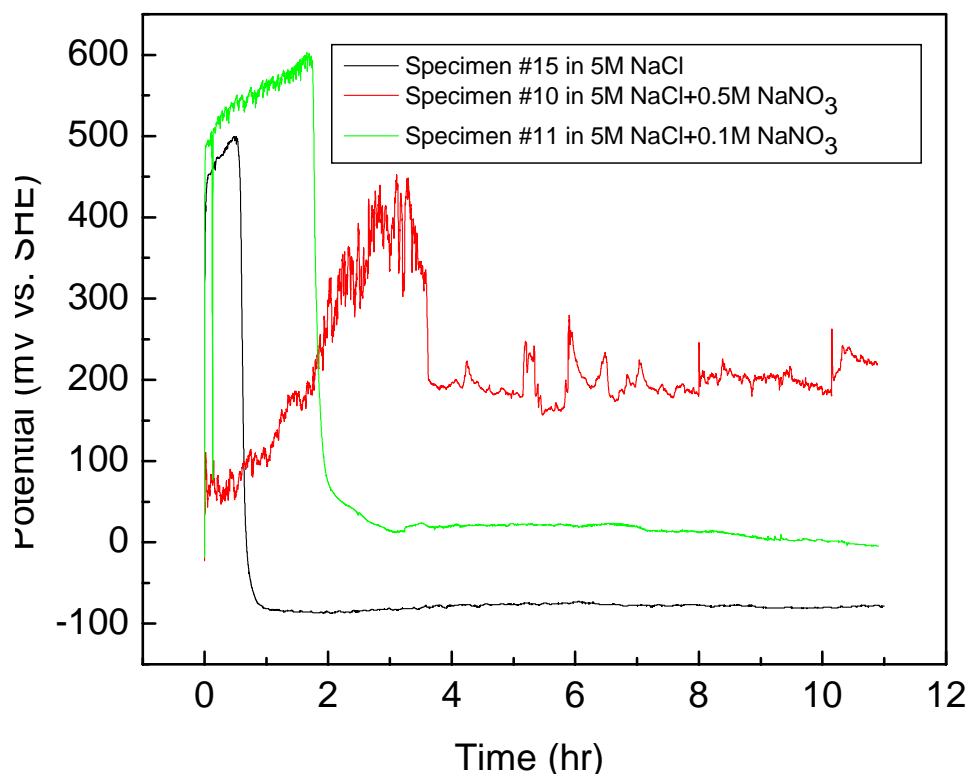
Figure 5-60
Time dependence of the potentials of the creviced electrode during the galvanostatic initiation stage in 5 mol·dm^{-3} NaCl + NaNO$_3$ solutions.

The extent of crevice propagation of those crevices that initiated in solution E (5 mol·dm^{-3} NaCl) and solution F (5 mol·dm^{-3} NaCl + 0.1 mol·dm^{-3} NaNO$_3$) was followed by measuring the time dependence of the coupled current and potential. Figure 5-62 shows the time dependence of the coupled potential and current and of the potential of the planar specimen following initiation of crevice corrosion in 5 mol·dm^{-3} NaCl solution. Over the 11-day period the coupled current remained relatively constant at between 2 µA and 5 µA, with no indication of stifling. However, over the same period, the potential of the creviced sample drifted to more-passive values suggesting that the crevice would passivate eventually. During the course of the measurements, the difference in the creviced and planar electrode potentials decreased from about 200 mV initially to 75 mV after 11 days, consistent with a slow re-passivation process. Grain boundary

pitting was observed on the corroded specimen following the test, although the overall metal loss was minimal.

Following initiation of crevice corrosion in solution F (5 mol·dm^{-3} NaCl + 0.1 mol·dm^{-3} NaNO$_3$), there was an immediate positive shift in the coupled potential followed by a period of relatively constant potential of 0.04-0.05 V$_{SHE}$ (Figure 5.10.9). During the same period, the coupled current was <<1 μA, indicating minimal propagation.
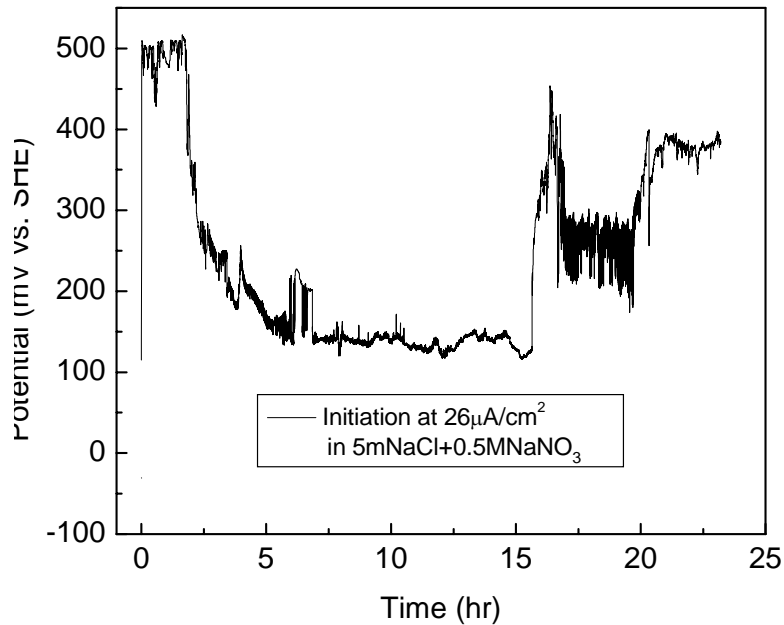
Figure 5-61
Time dependence of the potential of the creviced electrode during the galvanostatic initiation stage in 5 mol·dm^{-3} NaCl + 0.5 mol·dm^{-3} NaNO$_3$ solutions at a current density of 26 μA·cm^{-2}.
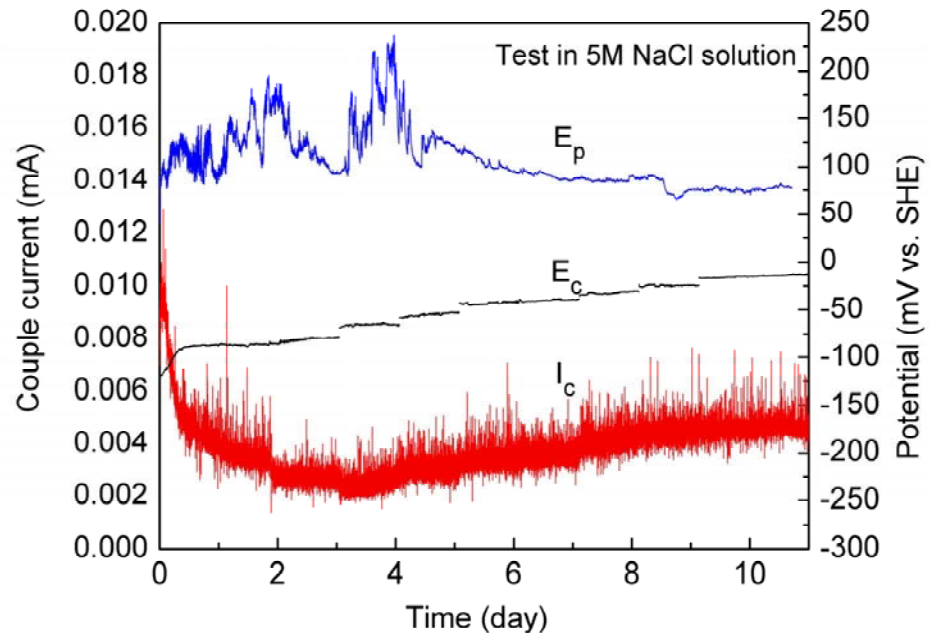
Figure 5-62
Time dependence of the coupled current and potential and of the planar potential following initiation of crevice corrosion of Alloy 22 in solution E (5 mol·dm^{-3} NaCl).
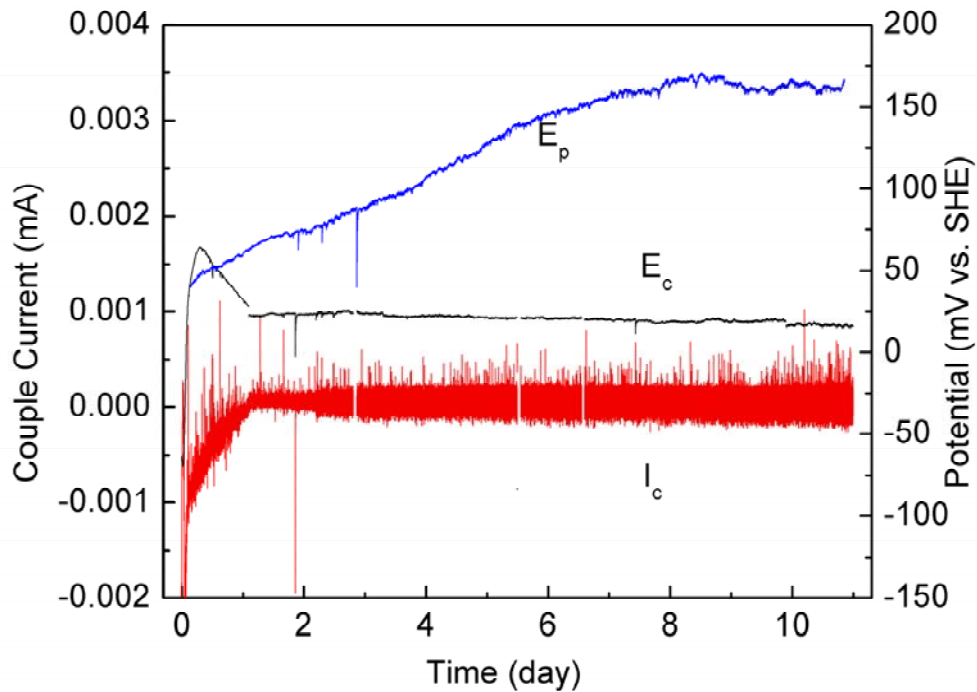
Figure 5-63
Time dependence of the coupled current and potential and of the planar potential following initiation of crevice corrosion of Alloy 22 in solution F (5 mol·dm-3 NaCl + 0.1 mol·dm-3 NaNO3).

5.10.3.4 Surface Analysis

Surface analysis was performed on a number of samples to investigate the degree of selective dissolution within the crevice and to determine whether any information on the crevice solution composition could be obtained.

Auger electron spectroscopy was used to map the elemental distribution on the creviced surface of specimen #11 (5 mol·dm^{-3} NaCl + 0.1 mol·dm^{-3} NaNO$_3$, [NO$_3^-$]:[Cl$^-$] ratio of 0.02). Two areas were investigated, one near the edge and another in the center of the visibly corroded area. There was significant enrichment of Mo with respect to Ni in the nine specific locations investigated within the two areas, although greater enrichment was observed in the center of the visibly corroded area. The mean Mo:Ni atomic ratio for the nine locations was 1.6 (0.66 for four locations around the edge and 2.3 for the five locations in the center), compared with an atomic ratio of 0.12 in the as-received material. Molybdenum was also enriched with respect to Cr, especially in the center of the corroded area. The mean Mo:Cr atomic ratio was 0.36 on the edge and 0.48 in the center of the corroded area, compared with a ratio of 0.34 in the as-received material. The Mo enrichment was more pronounced at grain boundaries in the middle of the corroded area, with a Mo:Cr ratio of 0.63 compared with slight depletion (Mo:Cr = 0.28) in the grain body.

Photoelectron X-ray spectroscopy (XPS) was used to determine the NO_3^-:Cl^- ratio on different areas of the creviced sample. Table 5-22 lists the results of analyses on three of the specimens. There is no evidence that NO_3^- preferentially migrates into the crevice (as has been proposed (King et al., 2006)). However, the methods used here are somewhat limited for the purpose of determining crevice chemistry, and are subject to compositional changes during the cool-down step and sampling procedure.

Table 5-22
Results of Post-test XPS Analysis of the Nitrate:Chloride Ratio in the Creviced Area.

Solution composition	Location of the analysis	Measured [NO₃]:[Cl-] in crevice	[NO₃]:[Cl-] in bulk solution
5 M CaCl$_2$ + 1M NaNO$_3$	Corroded area	0.163	0.1
5 M CaCl$_2$ + 0.5 M NaNO$_3$	Corroded area	0.0835	0.05
5 M NaCl + 0.1M NaNO$_3$	Corroded area	No nitrogen detected	0.02
5 M NaCl + 0.1M NaNO$_3$	Uncorroded area	No nitrogen detected	0.02

5.10.4 Conclusions

The crevice corrosion of Alloy 22 is difficult to initiate, even in concentrated chloride solutions at elevated temperature and with the imposition of a constant current to force initiation. In CaCl$_2$ + NaNO$_3$ solutions, crevice initiation and limited propagation was observed in 5 mol·dm^{-3} CaCl$_2$ solutions with [NO$_3^-$]:[Cl$^-$] ratios of 0.05 and 0.1, although the extent of localized attack decreased with increasing nitrate content. Initiation was not observed (as indicated by a drop in potential in the active direction) in more-dilute CaCl$_2$ solutions, even with a [NO$_3^-$]:[Cl$^-$] ratio of 0.05.

In contrast to the difficulty found in initiating crevice corrosion in CaNO$_3$ + NaNO$_3$ solutions, initiation was observed readily in 5 mol·dm^{-3} NaCl solutions, both with and without added NO$_3^-$. However, in the presence of nitrate, rapid stifling occurred following the period of imposed galvanostatic initiation. Only limited initiation (as evidenced by the value of the potential during the initiation phase and the absence of extensive localized attack) occurred in a solution with a [NO$_3^-$]:[Cl$^-$] ratio of 0.1.

No evidence was found for the enhanced transport of nitrate into the crevice region, which has been proposed as a possible explanation for the inhibitive effect of NO$_3^-$. Significant enrichment of Mo (with respect to both Ni and Cr) was observed in the creviced region, especially at grain boundaries.

The current results indicate that, as well as inhibiting the initiation of crevice corrosion, nitrate ions also inhibit the propagation of localized attack, although the mechanism by which they do so is not understood at present. This work, together with that performed by the DOE and CNWRA, indicates that the rate of crevice propagation of Alloy 22 decreases with time, although the precise mechanism behind this "stifling" process is not currently understood.

5.10.5 References

Apted, M., F. King, D. Langmuir, R. Arthur, and J. Kessler, 2005. The unlikelihood of localized corrosion of nuclear waste packages arising from deliquescent brine formation, *Journal of Materials* 57, 43-48.

BSC, 2005. *Analysis of dust deliquescence for FEP screening*, Bechtel SAIC Company report to DOE, ANL-EBS-MD-000074 Rev 01.

Cragnolino, G., D.S. Dunn and Y.-M. Pan, 2004. Evaluation of Corrosion Processes Affecting the Performance of Alloy 22 as a Proposed Waste Package Material, *Mat. Res. Soc, Symp. Proc.*, 807, pp. 435-440.

DOE, 2008. *Yucca Mountain Repository License Application*, Safety Analysis Report, U.S. Department of Energy, Office of Crystalline Radioactive Waste management, DOE/RW-0573, Rev. 0

EPRI, 2000. *Evaluation of the candidate high-level radioactive waste repository at Yucca Mountain using total system performance assessment: Phase 5*, Electric Power Research Institute, Palo Alto, CA: 2000. 1000802.

EPRI, 2002. *Evaluation of the Proposed High-Level Radioactive Waste Repository at Yucca Mountain Using Total System Performance Assessment: Phase 6*, Electric Power Research Institute, Palo Alto, CA: 2002. 1003031.

EPRI, 2005. *Program on Technology Innovation: Evaluation of a Spent Fuel Repository at Yucca Mountain, Nevada – 2005 Progress Report,* Electric Power Research Institute, Palo Alto, CA: 2005. 1010074.

He, X. and D.S. Dunn, 2006. Crevice corrosion penetration rates of Alloy 22 in chloride-containing waters, *Proc. CORROSION/2006*, NACE International (Houston, TX), paper #06618.

He, X. and D.S. Dunn, 2007. Crevice corrosion penetration rates of Alloy 22 in chloride-containing waters, *Corrosion* 63, 145-158.

King, F. and M. Kolar, 2006. EPRI's Engineered Barrier System Corrosion Model (EBSCOM), *Proc. 11th International High-level Radioactive Waste Management Conference*, American Nuclear Society (La Grange Park, IL), pps. 478-485.

King, F., M. Kolar, J.H. Kessler, and M. Apted, 2008. Yucca Mountain Engineered Barrier System Model (EBSCOM), *J. Nucl. Mater.* 379, 59-67.

King, F., M.G. Bailey, C.F. Clarke, B.M. Ikeda, C.D. Litke and S.R. Ryan, 1989. *A high temperature, high pressure silver-silver chloride reference electrode: a user's guide*, Atomic Energy of Canada Limited Report, AECL-9890.

King, F., R. Arthur, M. Apted, and J. Kessler, 2006. EPRI's analysis of the potential for localized corrosion of Alloy 22 waste packages in multi-salt deliquescent brines, presentation to the Nuclear Waste Technical Review Board, September 25-26. Available from www.nwtrb.gov/meetings/2006/sept/king.pdf.

Rebak, R.B., K. J. Evans and G.O. Ilevbare, 2007. Crevice Repassivation Potentials for Alloy 22 in Simulated Concentrated Ground Waters, *CORROSION/2007*, paper 07584, Nashville, TN, 11-15.

Sandia, 2007. *General and Localized Corrosion of Waste Package Outer Barrier*, ANL-EBS-MD-000003 REV 03C, May 2007.

Shoesmith, D.W. and J.R. Massari, 2001. Predicted performance of the engineered barrier system in the Yucca Mountain repository, *Proc. 9ᵗʰ International High-level Radioactive Waste Management Conference*, American Nuclear Society, LaGrange Park, IL.

Shoesmith, D.W. and M. Kolar, 1998. Waste package performance, *Alternative Approaches to Assessing the Performance and Suitability of Yucca Mountain for Spent Fuel Disposal*, Electric Power Research Institute, Palo Alto, CA: 1998. 108732.

5.11   Comparison of IMARC 9 and DOE TSPA-LA Results

5.11.1 Discussion

This section provides a side-by-side comparison of several key results from the EPRI IMARC 9 and DOE TSPA-LA models. Figure 5-64 compares TSPA results for the "nominal" case, which does not include seismic or igneous events. The nominal scenario for both models shows the effects of long-term EBS degradation, radionuclide release and transport, and uptake by the RMEI assuming no seismic, rockfall, or igneous intrusion or eruption events occur. It should be noted that the IMARC 9 nominal case includes assumption of one early WP failure, whereas DOE's TSPA-LA treats early WP failure as a separate scenario. This difference should have little impact on the direct comparison of the two nominal cases, as the dose contribution from the TSPA-LA early WP failure case is minor relative to the nominal scenario, i.e., 2 – 3 orders of magnitude lower (see Figure 5 – 67). Figure 5-64A presents the IMARC 9 mean RMEI annual dose (mrem/yr) for the nominal case. IMARC 9 estimates dose assuming 100% of the repository is CSNF, i.e., no co-disposal waste packages are modeled in IMARC 9. Figure 5-64B presents the DOE TSPA-LA mean annual RMEI dose for the nominal case. The DOE TSPA-LA model assumes 90% CSNF and 10% co-disposal waste (vitrified HLW and spent fuel from defense related activities) based on the equivalent metric tons of heavy metal.

The peak mean annual dose at 1 million years is approximately 0.02 and 0.5 mrem/yr for the EPRI and DOE models, respectively. There are many factors that contribute to the difference in these dose estimates. Many of the important factors are described in Table 5-23. Dominant

radionuclides (those contributing the most to total mean annual RMEI dose) at later times in DOE's TSPA-LA for the nominal case are I-129, Pu-242, Cs-135, and Np-237; in EPRI's IMARC 9, the dominant radionuclides at later times are I-129; Np-237; and U-233. Although not shown in Figure 5-64A, Pu-242 and Ra-226 are second-tier radionuclides in terms of contribution to RMEI mean annual dose in IMARC 9. Perhaps the most important contributor to the differences in dose estimates and dominant radionuclides are the different solubility values for U, Np, and Pu used in the two TSPA models. Pu solubility in the DOE TSPA-LA is 2 to 3 orders of magnitude higher than in IMARC 9; Np solubility in the DOE TSPA-LA is 3 to 4 orders of magnitude higher than in IMARC 9. Biosphere Dose Conversion Factors (BDCFs) in IMARC 9 for the major actinides are 5 to 10 times larger than those in DOE's TSPA-LA. These two factors alone may explain much of the difference between the two models for total mean annual dose estimates late in the 1 million-year compliance period.

Figure 5-64
Comparison of (A) EPRI IMARC 9 and (B) DOE TSPA-LA annual RMEI dose estimates for the nominal scenario (Figure B adapted from DOE, 2008a; YM-LA Ch. 2, Figure 2.4-22b).

Table 5-23
Comparison of primary features, events, and processes in the DOE and EPRI TSPA models.

Feature, Event or Process	DOE TSPA-LA (DOE, 2008b)	EPRI IMARC 9	Comments
Infiltration	3 pre-10,000 yr climate states: present, monsoon, glacial transition prescribed post-10,000 yr climate	3 pre-10,000 yr climate states: greenhouse, interglacial, glacial maximum prescribed post-10,000 yr climate	EPRI adopting 1 climate state in 0 – 10,000 yr timeframe based on low risk importance of early climate states
Drift seepage	Low seepage rates High seepage fractions (nominal: 30 – 40% of repository)	Higher seepage rates Much lower seepage fractions (nominal: 1.25% of repository)	
Inventory	CSNF and co-disposed HLW	CSNF	
Dominant Alloy 22 failure mechanism	SCC then GC	GC	
Dominant radionuclides	Early: Pu-239, Tc-99 Late: Pu-242, Np-237, Ra-226, I-129	Early: Tc-99, I-129 Late: I-129, Np-237, U-233	EPRI evaluating additional radionuclides; Pu-242 and Ra-226 represent second tier radionuclides for RMEI dose in IMARC analyses
Colloid-facilitated transport	included in TSPA-LA	negligible, not included in IMARC	EPRI (2006)
$\log_{10}$ solubility (mg/L)	Pu: -1.2 to 1.1 Np (NpO2): -1.1 to 2.1	Pu: -4.7 to -0.7 Np (NpO2): -4.0 to -2.0	
UZ Kd's for Pu, Np (mL/g)	Th: 5500 to 15500 U: 0.2 to 0.5 Pu: 70 – 100 Np: 0.5 to 1.0	Th: 2500 U: 2.0 Pu: 50 Np: 1.0	
BDCFs (Sv/y per Bq/m3)	Th-229: 2.62×10^{-6} U:-233: 9.20×10^{-8} Np-237: 2.79×10^{-7} Pu-239: 9.74×10^{-7}	Th-229: 3.09×10^{-5} U:-233: 6.96×10^{-7} Np-237: 1.78×10^{-6} Pu-239: 6.19×10^{-6}	EPRI moving to probabilistic basis for BDCFs

Figure 5-65 compares IMARC 9 and TSPA-LA results from dose calculations incorporating nominal processes and seismic events. Seismic ground motion contributes approximately 0.5 mrem/yr to total dose estimate from the DOE TSPA-LA modeling (Figure 5-65B); this dose contribution is roughly the same as from nominal processes alone. In contrast, EPRI modeling

(Figure 5-65A) shows an incremental increase in dose due to seismic effects of approximately 0.01 mrem/yr, which represents only one-half the contribution from nominal processes. Likely sources of this discrepancy between the two models are:

- The intensity of the peak ground motion for large seismic events. While the DOE model assumes peak ground velocities (PGVs) as high as 4 m/s, the EPRI model assumes a PGV for large seismic events in the range of 0.75 to 1 m/s.

- The predicted amount of damage sustained by waste packages due to seismic activity. Due to the lower PGV estimates in IMARC 9, EPRI finds that damage to the WPs in WP to WP collisions when the drip shields are intact is minimal, such that there is very little potential for subsequent SCC. Furthermore, the less severe damage to WP determined by EPRI modeling also results in part from the important role that drip shield failure and rockfall can play in limiting seismic damage to waste packages through restriction of WP motion. In the EPRI modeling, all drip shields are assumed to fail after the first seismic event (at 50,000 years). Consequently, rockfall caused by subsequent seismic motion serves to pin down waste packages, dampen WP motions, and limit severity of WP to WP collisions; these collisions are primary drivers for potential plastic deformation which, in turn, may initiate SCC. For the DOE TSPA-LA modeling, this beneficial effect of rockfall is less pronounced as drip shield failures do not occur at once but, instead, are distributed over time (DOE, 2008a).

- The EPRI model predicts that approximately 16% of the waste packages will be breached in one million years; only 0.7% of that 16% is due to seismic activity (Figure 5-66).

Table 5-24 summarizes the dominant failure mechanisms for the Alloy 22 outer waste package corrosion barrier in the DOE and EPRI TSPA models for the nominal + seismic scenario. The DOE and EPRI models differ with respect to the dominant Alloy 22 degradation mechanism in the 10^4- to 10^5-year time frame. The DOE model results indicate stress corrosion cracking (SCC) as the primary degradation mechanism during this time frame, whereas EPRI modeling finds general corrosion (GC) as the primary degradation mechanism. Therefore, according to EPRI model estimates, SCC is not expected to play a major role in waste package degradation.

Thus, in addition to the difference in magnitude between dose estimates, the different approaches taken by DOE and EPRI in modeling repository performance lead to differences in the relative ranking of the various processes (nominal, seismic, etc.). Table 5-25 compares RMEI dose rate estimates in the DOE and EPRI TSPA models for the four major scenario classes. The DOE estimate for igneous intrusion contribution contributes the most to peak RMEI dose rate. The significant dose contribution from igneous intrusion in DOE TSPA-LA analyses can be largely attributed to the conservative assumption made by DOE that 100% of waste packages are breached following the intersection of an igneous event with the repository footprint (EPRI, 2005).
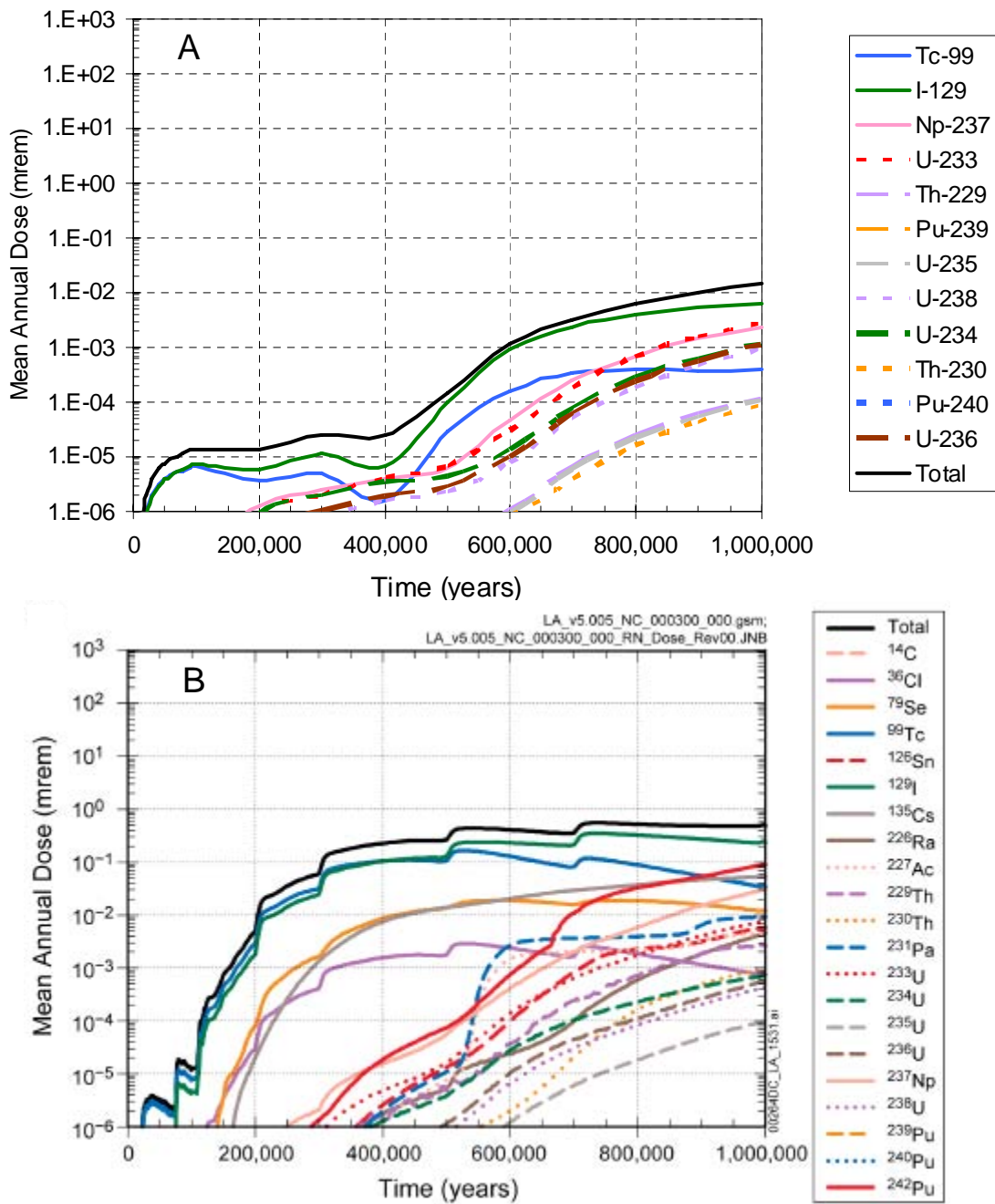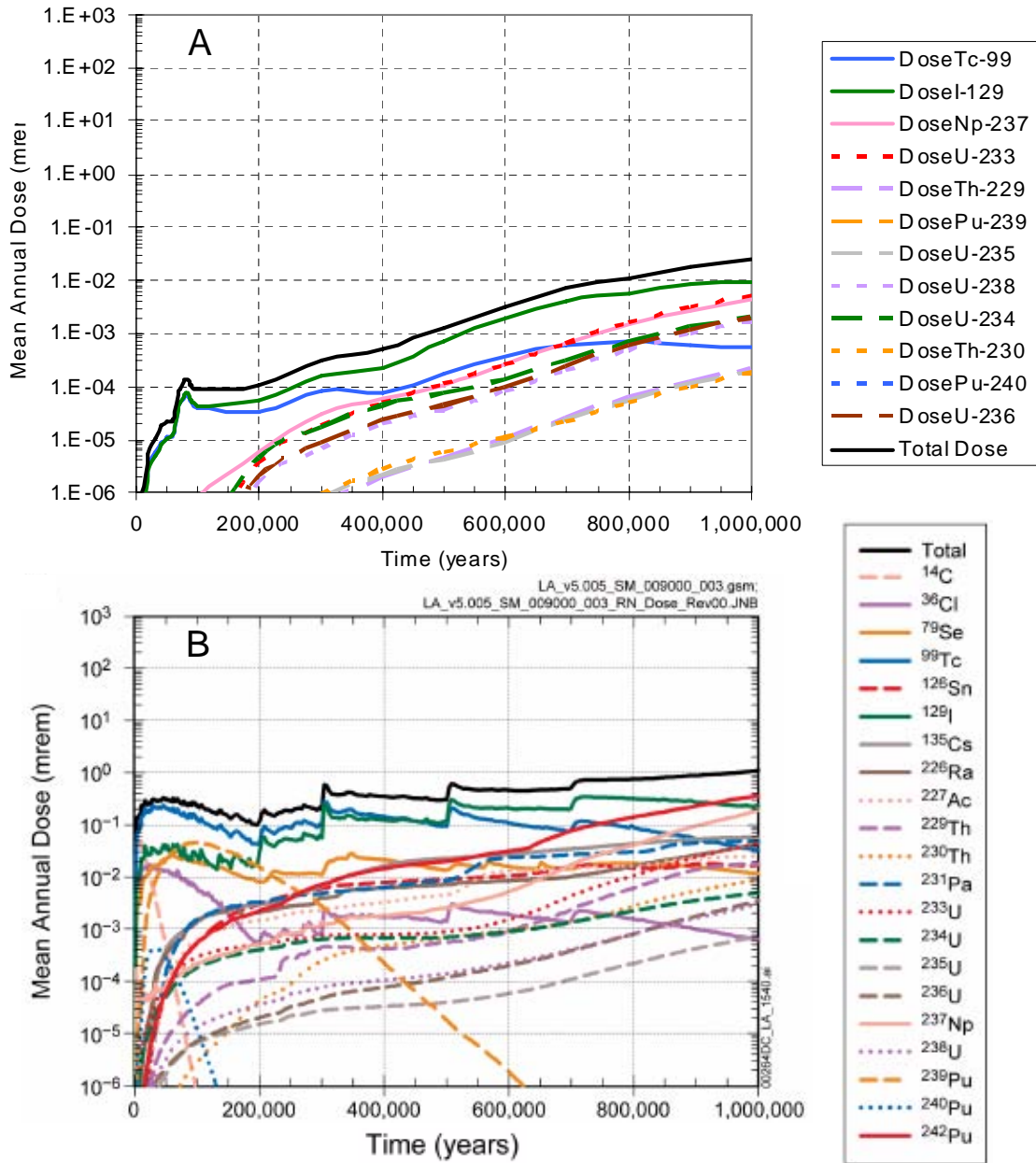
Figure 5-65
Comparison of (A) EPRI IMARC 9 and (B) DOE TSPA-LA annual RMEI dose estimates for the nominal + seismic scenario (Figure B adapted from DOE, 2008a; YM-LA Ch. 2, Figure 2.4-26b).
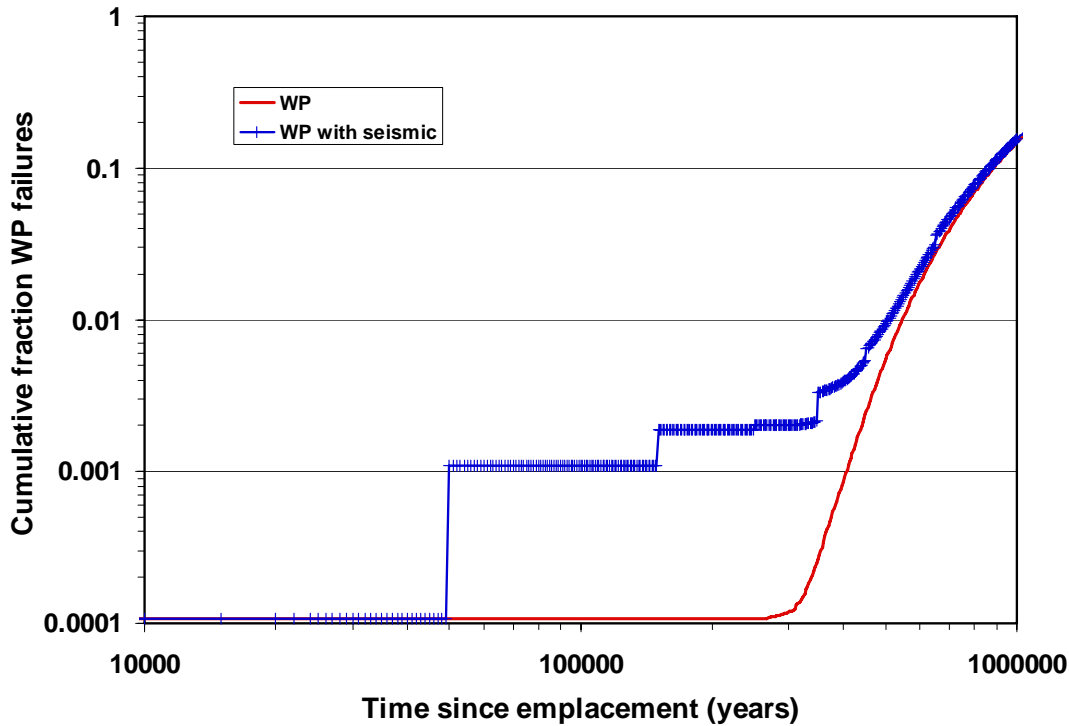
Figure 5-66
Cumulative fraction of waste package failures versus time in the EPRI IMARC 8 model for the nominal ("WP", no seismic activity assumed) and the nominal + seismic ("WP with seismic") scenarios. The EPRI model assumes 100% of the drip shields fail after the first major seismic event at 50,000 years.

A recent independent probabilistic volcanic hazard analysis (PVHA) commissioned by EPRI (EPRI, 2008, summarized in Section 5.5 of this report) finds the annual probability of an igneous event intersecting the repository footprint to be significantly less than the 10^{-8} per year regulatory threshold established in 40 CFR 197. Accordingly, any future EPRI TSPA analysis will not consider the consequences of igneous events intersecting the repository. In light of this determination, the consequences of igneous scenarios are excluded from the total dose estimate due to low probability of occurrence, and both igneous intrusion and volcanic eruption do not appear in the EPRI ranking.[9] Thus, the total dose presented in Figure 5-65A for the nominal + seismic scenario can be viewed as the EPRI dose estimate for *all scenarios*. Figure 5-67 presents the dose estimate contributions from all scenarios considered in the DOE TSPA-LA model. While DOE considers the consequences of volcanic eruptions through the proposed repository, the dose impact is negligible compared to the other scenario classes. Similarly, dose contributions from a number of other process and scenarios considered in the DOE TSPA-LA

---

[9]Previous EPRI analyses, which adopted the 1.6×10^{-8} per year probability estimate from DOE's 1996 PVHA study (CRWMS M&O, 1996), also found igneous intrusion to represent the highest dose contribution (~0.08 mrem/yr) to the RMEI *when included* in the performance assessment; however this estimated dose rate was still an order of magnitude lower than that of DOE. In this case, EPRI's lower dose estimate and ranking for igneous intrusion is likely driven by the assumption, considered by EPRI to be more realistic based on expected magma behavior in the repository, that only a fraction (~14%) of the waste packages would be breached as the result of igneous intrusion (EPRI, 2005).

model, including seismic fault displacement, early waste package failure, and early drip shield failure, are relatively minor compared to doses from the dominant scenarios.

Table 5-24
Dominant Alloy 22 waste package (WP) failure mechanisms in the DOE and EPRI TSPA models for nominal + seismic scenario.

Timeframe	DOE (Sandia, 2008; DOE, 2008b)	EPRI
Early ($T_0 - 10^4$ yr)	Seismic damage to co-disposal WPs	Negligible for CSNF WPs
Intermediate ($10^4 - 10^5$ yr)	SCC failure of CSNF	Limited GC failure of CSNF WPs
Late ($10^5 - 10^6$ yr)	GC failure of co-disposal and CSNF WPs	GC failure of CSNF WPs

SCC: stress corrosion cracking
GC: general corrosion

Table 5-25
Comparison of the DOE and EPRI TSPA estimated annual RMEI dose rates for the major repository evolution scenarios.

Rank	DOE (2008a)	EPRI
1	igneous intrusion 0.9 mrem/yr	nominal 0.02 mrem/yr
2	seismic ground motion 0.5 mrem/yr	seismic 0.01 mrem/yr
3	nominal 0.5 mrem/yr	*Igneous intrusion and volcanic eruption scenarios not considered. Annual probability of igneous event intersecting repository below 10^8 yr^{-1} threshold per EPRI (2008)*
4	volcanic eruption 0.0001 mrem/yr	
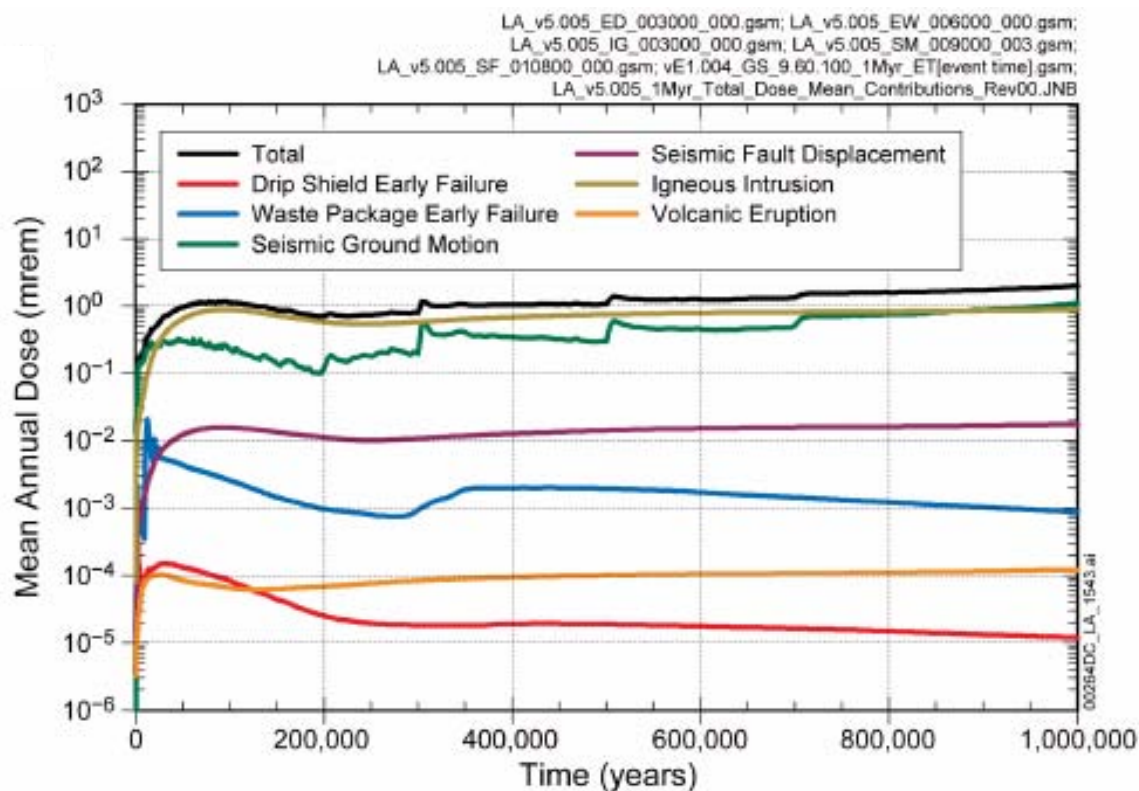
Figure 5-67
Contributions of DOE scenarios to total annual dose estimates versus time (adapted from DOE (2008a), YM-LA Ch. 2, Figure 2.4-18b).

5.11.2 References

CRWMS M&O, 1996. Civilian Radioactive Waste Management System Management and Operating Contractor, 1996. *Probabilistic Volcanic Hazard Analysis for Yucca Mountain, Nevada*. BA0000000-01717-2200-00082 REV 0. Las Vegas, Nevada: CRWMS M&O. ACC: MOL.19971201.0221.

DOE 2008a. *Yucca Mountain Repository License Application*. U.S. Department of Energy, Office of Civilian Radioactive Waste Management, DOE/RW-0573, Rev. 0, June 2008.

DOE, 2008b. *Total System Performance Assessment Model/Analysis for the License Application*. U.S. Department of Energy, Office of Civilian Radioactive Waste Management, MDL-WIS-000005 REV00. January, 2008.

EPRI, 2005. *Potential Igneous Processes Relevant to the Yucca Mountain Repository: Intrusive-Release Scenario.* Electric Power Research Institute, Palo Alto, CA: 2005. 1011165.

EPRI, 2006. *Treatment of Colloid-Facilitated Transport for Yucca Mountain Total System Performance Assessment.* Electric Power Research Institute, Palo Alto, CA: 2006. 1013440

EPRI, 2008. *Independent Probabilistic Volcanic Hazard Analysis for the Yucca Mountain Region*. Electric Power Research Institute, Palo Alto, CA: 2008. 1018059.

Sandia, 2008. *Total System Performance Assessment Results*. Presented to: NRC/DOE Technical Exchange on Total System Performance Assessment for Yucca Mountain. April 3, 2008, Las Vegas, NV.

5.12   Occupational Risk Consequences of the Proposed Repository Design and Operation

5.12.1 Introduction

As part of its on-going activities, EPRI conducted a review of DOE's Yucca Mountain License Application (DOE, 2008), which was submitted to the USNRC in June, 2008, and its technical basis to provide an assessment of potential occupational impacts of the proposed design and operational activities associated with the repository. The results of this review were published in August, 2008, as Technical Update 1018058 entitled, "*Occupational Risk Consequences of the Department of Energy's Approach to Repository Design, Performance Assessment and Operation in the Yucca Mountain License Application*." (EPRI, 2008)

5.12.2 Approach

EPRI's review was based on its prior experience with and knowledge of the DOE Yucca Mountain program, including reviews of the underpinning technical basis, multiple project environmental impact statements, total system performance analysis reports, and extensive DOE interactions with and reports to the public, the NRC, NWTRB, ACNWM, and many other groups in public meetings. EPRI considered both radiological and non-radiological occupational health and safety risks during reactor-site storage, CSNF transfer and loading, CSNF transportation, CSNF management at Yucca Mountain, and construction of appropriate CSNF management facilities at the reactor sites and at Yucca Mountain. The EPRI review also followed the philosophy that YM-related analyses should reflect "cautious but realistic" assumptions, as opposed to "worst case analyses," as recommended by   the National Academy of Sciences in its Technical Bases for Yucca Mountain Standards report (NAS, 1995). This same philosophy has been incorporated into the US EPA's regulation 40 CFR 197 that addresses the environmental requirements for the Yucca Mountain repository. That regulation indicates that an appropriate approach is to perform more realistic analyses that support the concept of "realistic expectation." This is the philosophy that EPRI has followed in all of its YM-related analyses.

EPRI's review addressed the occupational risk consequences associated with such issues and activities as:

- The potential direct disposal of dual purpose canisters (DPC's) within the repository;

- The proposed size of the Transportation, Aging and Disposal (TAD) canisters;

- The amount of commercial spent nuclear fuel that will arrive at Yucca Mountain in a transport container other than TADs;

- The probability that igneous activity will occur within the repository footprint;

- The need for and use of drip shields;

- The design of the surface facilities necessary to withstand seismic ground motion.

- The potential level of seismic energy that should be considered possible during the post-closure period;

- The impact of "Co-disposal waste packages" (i.e., those that contain both spent nuclear fuel and high level radioactive waste) on the peak dose that might result from the repository;

- The sufficiency of the proposed waste handling facility throughput to process the SNF that will be shipped to the repository in transport canisters other than TADs;

- The spacing between repository drifts; and

- Conservatisms in DOE Analyses related to the estimates of post-closure radiological doses.

EPRI recognizes that while some conservatism in the face of uncertainty is warranted, especially given the one million year compliance period for repository performance, repeated application of overly conservative assumptions and estimates in performance assessment will likely result in over designed facilities in order to provide excess performance margins. In addition, the use of such conservatisms may also have important consequences for the utilities that currently manage the spent nuclear fuel onsite in wet and/or dry storage configurations.

As each over-conservatism incorporated in the design and/or operational philosophy of the repository carries with it finite levels of risk to the workers that must carry out the associated activities, the performance of such activities will result in the incurrence of risks that exceeds that which would be incurred if a more realistic design and/or operational approach were taken resulting in a lesser level of associated activity. For the purposes of EPRI's analysis, such additional risk is deemed to be "unnecessary" as it exceeds the level of risk that would exist if only those activities that were absolutely required to provide a facility that complies with the applicable regulatory requirements were performed. EPRI recognizes that there are a certain amount of hazards and risks associated with all such activities and that it is impossible to reduce such hazards and risks to zero. EPRI also recognizes there could be additional, "unnecessary," public and economic consequences of such over-conservatisms although these are not assessed quantitatively in this report.

The independent analyses and data collection conducted by EPRI suggest that there are issues related to the proposed design and/or operational philosophy of the repository that, as a result of using an overly conservative philosophy, have the potential to result in levels of risk to workers in the nuclear industry and other related industries that exceed the minimum necessary to design, construct and operate a facility that would comply with pertinent regulations.

5.12.3 References

EPRI, 2008. *Occupational Risk Consequences of the Department of Energy's Approach to Repository Design, Performance Assessment and Operation in the Yucca Mountain License Application*, Electric Power Research Institute, Palo Alto, CA, 2008. 1018058.

DOE, 2008. License Application for the Construction of a Repository at Yucca Mountain, Nevada for the Disposal of Spent Nuclear Fuel and High-level Radioactive Waste, US Department of Energy, Washington, DC.

NAS. 1995. *Technical Bases for Yucca Mountain Standards*, National Academy Press, Washington DC.

5.13 Criticality and Direct Disposal of Dual-Purpose Canisters

5.13.1 Introduction

The concept of direct disposal of dual-purpose canisters (DPCs) has not been included in the plans for the Yucca Mountain geologic repository because of concerns, among other reasons, about degradation of the aluminum-based reactivity-control material typically used in DPC's over the relatively long period of the repository analyses and the resulting potential for criticality events to occur during the regulatory period of interest. As a complement to work reported in EPRI 1018051 (EPRI, 2008a) on the feasibility of direct disposal of DPCs at Yucca Mountain, which is summarized in Section 5.3 of this report, EPRI performed an evaluation of the criticality concerns associated with direct DPC disposal. A description and the results of this work will be published as EPRI report number 1016629, "Feasibility of Direct Disposal of Dual-Purpose Canisters: Options for Criticality Control" (EPRI, 2008b, *in press*). The results of that evaluation are summarized below.

5.13.2 Approach

To evaluate the potential for a criticality event within a DPC, criticality calculations were performed assuming: a) appropriate burn-up credit; b) a minimal (i.e., 5 years) spent fuel cooling period; c) a fully flooded canister; and d) no aluminum-based neutron absorber material within the DPC. The two latter assumptions are considered to be conservative as it is unlikely that the canister would fail in a manner that would facilitate a fully flooded condition and/or that all of the aluminum-based material would be consumed within the DPC. Two Holtec MPC-32 DPCs located at TVA's Sequoyah Nuclear Plant were arbitrarily selected to serve as the basis for the evaluation. Calculations were performed to determine the potential reactivity using the actual loading positions and isotopic content of each of the 32 spent fuel assemblies within the selected DPC's.

5.13.3 Results

The results of EPRI's evaluation indicate that criticality can be ruled out as a concern for repository performance when best estimate assumptions are made, including application of full burnup credit and incorporation of reasonable biases and uncertainties. The potential for direct disposal of some already loaded dual-purpose casks is further enhanced when the moderator displacement effect of burnable poison rod assemblies (BPRAs) stored in the fuel assemblies is taken into account.

The potential for a criticality event in as yet to be loaded DPCs could be further reduced by using planned reactivity management during loading at the reactor sites through emplacement of the least reactive spent assemblies in the center of the canister. Another option would entail the placement of surrogate control rod assemblies with fresh neutron absorber material into the center of the DPC during reactor site loading. This latter approach would enable the direct disposal of any DPC while satisfying established criticality criteria.

EPRI's evaluation is considered to be extremely conservative as the likelihood of a fully flooded DPC is considered to be minimal as corrosion of the waste package would occur non-preferentially (i.e., equally likely on bottom and sides of waste package), allowing for at least partial drainage of the DPC cavity. Accordingly, partial flooding of a DPC is considered to be a more reasonable scenario. A potential for a criticality event within a DPC is insensitive to the ingress of small volumes of water, and will only approach the reactivity limit when two or three rows of assemblies are submerged. A determination of reactivity versus flooding level provides a basis for risk estimations based upon the probability of intrusion of a given volume of water. The repository temperature during the time period when water ingress into the waste package and contained DPC might occur is of little consequence to criticality events as long as the temperature is below the boiling point at the repository (96°C) and the water is present in liquid form.

5.13.4 Conclusions

When best estimate assumptions are used, the occurrence of a criticality event within a repository at Yucca Mountain can be ruled out for at least some existing (currently loaded) DPCs. In addition, a criticality event associated with any emplaced DPC is considered to be a highly unlikely event given the conditions that will exist within the repository and the manner in which the surrounding waste package is anticipated to fail. Actions can be taken at the reactor sites during the future loading of DPCs to further reduce the potential for such events.

5.13.5 References

EPRI, 2008a. *Feasibility of Direct Disposal of Dual-Purpose Canisters in a High-Level Waste Repository*, Electric Power Research Institute, Palo Alto, CA: 2008. 1018051.

EPRI, 2008b. *Feasibility of Direct Disposal of Dual-Purpose Canisters: Options for Criticality Control*, Electric Power Research Institute, Palo Alto, CA: 2008. 1016629 (*in press*).

5.14 Spent Fuel Transportation

During 2008, EPRI continued its oversight of and involvement with national transportation activities associated with transport of spent nuclear fuel to a repository at Yucca Mountain. The following details the status of such activities and EPRI's involvement in these activities.

5.14.1 U. S. NRC Transportation Activities

In November 2007, the U.S. Nuclear Regulatory Commission (NRC) directed NRC staff to consult with the Advisory Committee on Nuclear Waste and Materials (ACNWM) regarding staff's review of transportation risks. Following its consultation with ACNWM, the Commission directed NRC staff to report to the Commission regarding how the NRC could better inform the public about the risks associated with the transportation of radioactive material compared to other hazardous material transported across the U.S. and the requirements the NRC has put in place to reduce those risks.

In July 2008, NRC staff issued SECY-08-0101 that outlined NRC staff's views regarding how it could better inform the public about the risks of transporting radioactive material. The document focuses on spent fuel transport since the packages used are similar in size to those used to ship other hazardous materials and because there has been a recent focus on spent fuel transport in the public domain.

NRC has developed short and long-term actions associated with communicating with the public regarding the risks of transporting radioactive materials. These actions include:

- In the near term, NRC staff will continue to focus its outreach on interactions with State and local government organizations, focusing on the potential shipments of spent nuclear fuel to a repository or interim storage site. This will include providing States and local governments with information that could be used in own outreach efforts, including comparisons of the overall risks of shipping spent fuel and other hazardous materials.

- NRC staff will expand its outreach efforts to a broader audience in anticipation of increasing spent fuel shipments, and to support NRC's licensing efforts for new power reactors, potential interim storage sites, and a permanent geological repository. As part of this effort, NRC staff is making greater use of web-based materials and is in the process of developing a web-based interactive brochure on the risks associated with the transportation of radioactive materials, including spent nuclear fuel, and how the requirements NRC has put into place for transportation of radioactive materials have reduced those risks.

- NRC staff will continue to participate in the U.S. Department of Energy's Transportation External Coordination (TEC) Working Group's effort to develop more effective ways to communicate transportation safety messages with stakeholders. The TEC working group has recently created a topic group dedicated to transportation safety and risk communication. One of the topics to be explored is how risk comparisons should be used to communicate the safety of spent fuel shipments.

5.14.2 EPRI Analysis of Transportation Accident Risk to Yucca Mountain

During 2006, EPRI re-evaluated transportation accident risk associated with transport of SNF to Yucca Mountain using the RADTRAN 5.5 computer code developed by Sandia National Laboratories (EPRI, 2006). During 2008, EPRI described the objectives and results of this study in a conference paper presented at the 12th International High-level Radioactive Waste Management (IHLRWM) Conference, September 7-11, 2008 in Las Vegas, Nevada (Supko and Kessler, 2008). In brief, EPRI demonstrates that conservative assumptions used in the Yucca Mountain Environmental Impact Statement (DOE, 2002) result in an overestimate of accident dose risk. A companion study that evaluates the incident-free radiological risks for transport of SNF to Yucca Mountain was published in 2005 (EPRI, 2005).

In response to EPRI's IHLRWM Conference presentation, the editor for the American Nuclear Society's publication, Radwaste Solutions, requested a copy of the paper in order to feature it in January/February 2009 issue focused on radioactive materials transportation topics.

5.14.3 U.S. DOE OCRWM Transportation Planning

During 2004, DOE selected the Caliente rail corridor as the preferred rail corridor in Nevada and announced its intent to perform an EIS to examine possible alignments for construction of that rail line. In June 2008, DOE released a Final Supplemental Environmental Impact Statement (FSEIS) for the Yucca Mountain repository and a companion EIS on the Nevada Rail corridor (Rail FEIS) (DOE 2008a, DOE 2008b). EPRI reviewed the FEIS and Rail FEIS to determine what changes, if any, were made to the incident-free and accident risk analysis associated with the transport of SNF to Yucca Mountain. EPRI found that the analysis was generally consistent with that contained in the draft 2007 EIS documents, as discussed below.

The Nevada Rail FEIS evaluates the potential environmental impacts of constructing and operating a railroad for the shipment of SNF and HLW from an existing rail line in Nevada to the Yucca Mountain repository. The purpose of the Nevada Rail FEIS is to assist DOE with a decision regarding whether to construct and operate a railroad in Nevada for transport of SNF and HLW, and if so, to assist with the selection of the rail corridor and its alignment within that corridor. The preferred alternative is to construct and operate a railroad along the Caliente rail alignment and to make the railroad "shared use," that is, it would allow commercial shippers to use the proposed railroad for shipment of commercial freight. DOE issued a Record of Decision (ROD) in October 2008. In the ROD, DOE announced that it has decided to construct and operate a railroad along a rail alignment within the Caliente corridor. DOE also has decided to allow shipments of general freight on the rail line, selecting to implement the shared use option.

In June 2008, DOE issued the FSEIS as an update to the original 2002 Final EIS (FEIS) (DOE, 2002), to address the environmental impacts associated with changes in DOE surface and subsurface facilities and in spent fuel transport operations that result from DOE's decision to utilize transportation, aging and disposal canisters (TADs). DOE does not consider any of the changes to the facility design or operational plans to be significant in terms of the environmental impacts described in the original 2002 FEIS.

The FSEIS addressed a range of issues that affect the transportation SNF to Yucca Mountain, including:

- Updated census information to include the 2000 census population density records and updated rail and truck transportation networks. DOE reevaluated the impacts of severe transportation accidents and sabotage events in urban areas using the updated population density data.

- DOE updated its estimate of the number of SNF shipments to incorporate the use of TAD canisters for transport of approximately 90% of commercial SNF. The new analysis assumes that the remaining SNF would be shipped via rail in dual-purpose canisters or as uncanistered fuel in truck casks, resulting in the shipment of approximately 9,500 rail casks and 2,700 truck casks of SNF and HLW under the Proposed Action (that is a 70,000 MTU repository). The use of lower capacity TAD packages for transport of commercial SNF requires a greater number of packages be loaded at reactor sites and transported to the Yucca Mountain repository. The FSEIS also presents an alternative scenario in which 75% of commercial SNF would be shipped in TAD canister systems, with the remaining SNF shipped in either truck casks or traditional SNF transportation casks having the same capacity as TAD packages.

- DOE updated the radionuclide inventory for commercial SNF to include higher burnup and shorter decay times for commercial PWR and BWR SNF. This resulted in higher radionuclide inventories and increased the risk associated with transportation accidents calculated by DOE in the FSEIS. The impacts of potential sabotage events also increased due to the increase in radionuclide inventories in commercial SNF.

The 2008 FSEIS incident-free radiological transportation risk is higher than calculated in DOE's 2002 FEIS due to the increase in the dose-to-latent cancer fatality conversion factors (using the latest ICRP recommendations); shipment of commercial SNF in lower-capacity TAD packages; the use of additional shipment escorts during transport; and extrapolation of impacts to 2067. The 2002 FEIS calculated transportation risks for a 70,000 MTU repository over a 24-year period ending in 2034. The accident risk is higher due to the increase in dose-to-latent cancer fatality conversion factors; the extrapolation of impacts to 2067; and the increased radionuclide inventory for commercial SNF. While the risks calculated in the 2008 FSEIS are higher than those from the 2002 FEIS, the risks associated with transport of SNF to the repository remain small. For example, the 2008 FSEIS calculated that the radiological risk associated with incident-free transportation was 1.3×10^{-4} LCF for a maximally exposed individual (MEI).

The FSEIS and rail corridor FEIS were submitted to the NRC along with DOE's license application for the Yucca Mountain repository in June 2008. In September 2008, NRC docketed the DOE license application and the NRC staff recommended that the Commission adopt, with further supplementation, DOE's Environmental Impact Statements. The supplemental material requested by NRC was not associated with the transportation analysis

5.14.4 References

DOE, 2002. *Final Environmental Impact Statement for a Geologic Repository for the Disposal of Spent Nuclear Fuel and High-Level Radioactive Waste at Yucca Mountain, Nye County, Nevada*, Volume II, DOE/EIS-0250F, U.S. Department of Energy, Las Vegas NV.

DOE, 2008a, *Final Supplemental Environmental Impact Statement for a Geologic Repository for the Disposal of Spent Nuclear Fuel and High-Level Radioactive Waste at Yucca Mountain, Nye County, Nevada* (DOE/EIS-0250F-S1), U.S. DOE, Office of Civilian Radioactive Waste Management, June 2008.

DOE, 2008b, *Final Supplemental Environmental Impact Statement for a Geologic Repository for the Disposal of Spent Nuclear Fuel and High-Level Radioactive Waste at Yucca Mountain, Nye County, Nevada – Nevada Rail Transportation Corridor and Final Environmental Impact Statement for a Rail Alignment for the Construction and Operation of a Railroad in Nevada to a Geologic Repository at Yucca Mountain, Nye County, Nevada* (DOE/EIS-0250F-S2 and DOE/EIS-0369), U.S. DOE, Office of Civilian Radioactive Waste Management, June 2008.

EPRI, 2005. *Assessment of Incident-Free Transport Risk for Transport of Spent Nuclear Fuel to Yucca Mountain Using RADTRAN 5.5*, Electric Power Research Institute, Palo Alto CA: 2005. 1011821.

EPRI, 2006. *Assessment of Accident Risk for Transport of Spent Nuclear Fuel to Yucca Mountain Using RADTRAN 5.5*, Electric Power Research Institute, Palo Alto, CA: 2006. 1013450.

Supko, E. and Kessler, J, 2008. "Assessment of Spent Nuclear Fuel Transport Accident Risk Using RADTRAN 5.5," International High Level Radioactive Waste Management Conference, September 7-10, 2008, Las Vegas, Nevada.

5.15 EPRI Yucca Mountain-Related 2008 Reports, Papers and Presentations

5.15.1 Introduction

During 2008, EPRI personnel and consultants also continued to monitor on-going YM-related regulatory discussions and activities, and to review YM-related documents issued by all stakeholders and attend and make presentations at numerous technical, scientific and regulatory meetings and forums addressing YM-related subjects of interest.

The following is a list of EPRI reports, technical/scientific papers, and presentations at technical/scientific meetings on Yucca Mountain related topics. The reports represent EPRI deliverables published in 2008 and each are summarized elsewhere in this end-of-year report. The papers represent EPRI research manuscripts published in, submitted to, or under preparation for peer-review journals in 2008. The presentations were presented at prominent scientific/technical meetings and forums by the EPRI HLW and Spent Fuel Management team or its contractors.

5.15.2 Reports

Feasibility of Direct Disposal of Dual-Purpose Canisters – Options for Assuring Criticality Control. EPRI, Palo Alto, CA: 2008. 1016629.

Feasibility of Direct Disposal of Dual-Purpose Canisters in a High-Level Waste Repository. EPRI, Palo Alto, CA: 2008. 1018051.

Occupational Risk Consequences of the Department of Energy's Approach to Repository Design, Performance Assessment and Operation in the Yucca Mountain License Application. EPRI, Palo Alto, CA: 2008. 1018058.

Independent Probabilistic Volcanic Hazard Analysis for the Yucca Mountain Region. EPRI, Palo Alto, CA: 2008. 1018059.

5.15.3 Journal Articles Published, in Press, Submitted or in Preparation

Huber, M. "A climate model-paleoclimate proxy data approach to inferring past and future hydrological conditions in the Southwestern U.S. with a focus on Yucca Mountain," *in preparation for submission to Vadose Zone Journal*.

Kemeny, J. Thermal Spalling in rock and the importance of post-peak material properties, *in preparation for submission to International Journal of Rock Mechanics and Mineral Science.*

King, F. 2008. "MIC of nuclear waste containers," CORROSION, *in press*.

King, F., M. Kolar, J.H. Kessler and M. Apted. 2008. "Yucca Mountain engineered barrier system corrosion model (EBSCOM)," *Journal of Nuclear Material*, *379, 59-67.*

King, F., L. Mao, J. Luo, M. Apted, J. Kessler and A. Sowder. 2008. "Mechanistic studies of the localized corrosion of Alloy 22 in chloride-nitrate solutions," CORROSION 2009, *submitted*.

Morrissey, M. "Natural Analogues For Volcanic Hazards Assessment at the Proposed Site for the High-Level Nuclear Waste Repository At Yucca Mountain, Nevada," *in preparation*.

Smith, G. "Historical development and update of EPRI's post-closure dose assessment for potential releases from the proposed HLW repository at Yucca Mountain," *in preparation for submission to Health Physics*.

Schwartz, F.W., E.A. Sudicky, R. McLaren, Y.J. Park and M. Huber. 2009. "Transient 120,000-year response of a large regional flow system to complex cyclical variability in paleoclimate," *in preparation for submission to Ground Water*.

5.15.4 Presentations to the Nuclear Waste Technical Review Board

Sowder, A., J. Kessler and M. Apted. 2008. "Independent performance assessment Of Yucca Mountain," presented to the U.S. Nuclear Waste Technical Review Board, 29 May 2008, Las Vegas, NV.

5.15.5 Conference Proceedings and Presentations

5.15.5.1   International High-Level Waste Management Conference, 7 – 11 September 2008, Las Vegas NV, USA

Garisto, N.C., D.G. Bennet and J. Andersson. 2008. "A peer review of the Yucca Mountain IMARC total system performance assessment EPRI model," in Proc. 2008 International High-level Radioactive Waste Management Conference, American Nuclear Society (La Grange Park, IL).

King, F. 2008. "The Impact of microbiologically influenced corrosion on the lifetimes of the Yucca Mountain engineered barrier system," in Proc. 2008 International High-level Radioactive Waste Management Conference, American Nuclear Society (La Grange Park, IL).

King, F., M. Kolar and M. Apted. 2008. "A revised EPRI source-term model for the dissolution of commercial spent nuclear fuel," in Proc. 2008 International High-level Radioactive Waste Management Conference, American Nuclear Society (La Grange Park, IL).

King, F., J. Luo, M. Apted and J. Kessler. 2008. "Studies of the effect of chloride and nitrate on the propagation of localized corrosion of Alloy 22," in Proc. 2008 International High-level Radioactive Waste Management Conference, American Nuclear Society (La Grange Park, IL).

Morrissey, M., M. Apted and J. Kessler. 2008. "Expected behavior of basaltic lava at the proposed high level nuclear repository at Yucca Mountain, Nevada" in Proc. 2008 International High-level Radioactive Waste Management Conference, American Nuclear Society (La Grange Park, IL).

Smith, G., J. Merino and M.W. Kozak. 2008. "Uncertainty and variability in biosphere dose conversion factors for the groundwater release scenario for Yucca Mountain," in Proc. 2008 International High-Level Waste Management Conference, American Nuclear Society (La Grange Park, IL).

Stirling, M., N. Field and V. Gupta. 2008. "Simplified probabilistic seismic hazard model for Yucca Mountain," in Proc. 2008 International High-level Radioactive Waste Management Conference, American Nuclear Society (La Grange Park, IL).

Zhou, W., M. Apted and J. Kessler. 2008. "Thermohydrological behavior in rock pillars between emplacement drifts at Yucca Mountain repository," in Proc. 2008 International High-level Radioactive Waste Management Conference, American Nuclear Society (La Grange Park, IL).

5.15.5.2 International Conference on Underground Disposal Unit Design and Emplacement Processes for a Deep Geological Repository, 16-18 June 2008, Prague, Czech Republic

Apted, M., J. Kessler and C. Fairhurst, 2008. "Emplacement and operational feasibility of a multi-tier, expanded capacity repository at Yucca Mountain, Nevada USA," presented at the International Conference on Underground Disposal Unit Design and Emplacement Processes for a Deep Geological Repository, 16-18 June, 2008, Prague.

5.15.5.3 CORROSION 2008, 16 – 20 March 2008, New Orleans LA, USA

King, F. 2008. "MIC of nuclear waste containers." in Proc. CORROSION 2008, Research Topical Symposium, NACE International (Houston, TX).

5.15.5.4 Scientific Basis for Nuclear Waste Management XXXII, 1 – 5 December, Boston MA, USA

King, F., J. Luo, L. Mao, M. Apted, J. Kessler, and A. Sowder. 2008. "Studies of the effect of chloride and nitrate on the propagation of localized corrosion of Alloy 22," in Proc. Scientific Basis for Nuclear Waste Management XXXII, Materials Research Society (Warrendale, PA), *submitted*.

6
FUTURE ROLE OF EPRI

As noted throughout this report, for over 20 years EPRI has performed independent, third party investigations and analyses of technical and scientific issues related to the characterization of the Yucca Mountain site and region, as well as the potential performance of the various engineered systems that have been proposed for use within the repository if a license to construct and operate the facility is granted.

With the docketing (acceptance) of the DOE's Yucca Mountain license application for review by the NRC, the Yucca Mountain Project has entered into a new and fundamentally different phase. In this phase, the investigations and decisions regarding the soundness of the design and the performance of the natural and engineered systems associated with the repository will be made by the NRC staff and the ASLB panels as part of the prescriptive regulatory process that has been set out in the Nuclear Waste Policy Act as well as the Code of Federal Regulations.

In the past, EPRI was one of many entities that had an interest in the Yucca Mountain Project and the capabilities to investigate technical and scientific issues that were believed to be pertinent to the overall soundness of the project. As EPRI will not be a party to the regulatory review and/or the Public Hearing processes (as EPRI's charter precludes it from such participation), EPRI's role regarding the Yucca Mountain Project has changed with this latest Project transition. The performance of further investigations and the putting forth of positions related to the repository are now the responsibility of the various parties admitted to the regulatory process. As such, EPRI is concluding its efforts specific to the Yucca Mountain Project. Accordingly, this will be the last annual End of the Year Report addressing these activities. It is, however, recognized that the results of past EPRI efforts are in the public domain and that any of the parties that continue to be associated with the project may avail themselves of EPRI's work.

A

EXECUTIVE SUMMARY OF A PEER REVIEW OF THE YUCCA MOUNTAIN IMARC TOTAL SYSTEM PERFORMANCE ASSESSMENT EPRI MODEL

In 2007, EPRI commissioned an independent peer review of EPRI's IMARC 9 code (EPRI 2006) for total system performance assessment (TSPA). An International Review Team (IRT) conducted its review during late-2007 and early-2008 following the guidelines and protocols of the International Atomic Energy Agency's (IAEA's) Improvements on Safety Assessment Methodology (ISAM) (IAEA, 2004). This ISAM methodology was adopted as a review framework to ensure a systematic review of the IMARC 9 draft report, as well as to conform to international standards. A paper on the IRT review was presented by one of the IRT members at the 12th International High-level Radioactive Waste Management Conference, September 7-11, 2008 in Las Vegas, Nevada.

The following text is an advanced copy of the IRT report executive summary. It is provided as received from the IRT. An EPRI report detailing the findings of the IRT review will be published in the first quarter of 2009. At the same time, EPRI will publish its IMARC-10 model report, which will include EPRI's response to the IRT review.

A PEER REVIEW
OF THE
YUCCA MOUNTAIN
IMARC TOTAL SYSTEM PERFORMANCE
ASSESSMENT EPRI MODEL

Prepared for:

The Electric Power Research Institute

Prepared by:

International Review Team

April 2008

EXECUTIVE SUMMARY

ES1   BACKGROUND

The "Electric Power Research Institute" (EPRI) has conducted "Total System Performance Assessments" (TSPAs) of the Yucca Mountain repository to gain insight into important repository system features, events and processes with respect to estimates of radiation dose to a hypothetical "reasonably maximally exposed individual" (RMEI) living downstream of the repository, as defined by U.S. EPA (40 CFR197). The EPRI TSPA code, IMARC, was designed to provide an assessment of processes which are likely to occur and their impact on the radiation dose estimate to the RMEI. The focus of the EPRI TSPAs is on the disposal of spent commercial fuel.

This report presents the results of a peer review of EPRI's IMARC methodology for TSPA, keeping in mind the EPRI TSPA objective. This review is the outcome of the work of an international team of three members, over a period of about three months. The main focus of the review has been a draft of the IMARC 9 model documentation (EPRI 2007), with a partial review of key supporting documents. Given the time constraints, the IRT (International Review Team) was primarily concerned with high level features of the model rather than with details.

The International Atomic Energy Agency's (IAEA's) Improvements on Safety Assessment Methodologies (ISAM) methodology (originally developed for near-surface disposal facilities) was adopted as a framework for the peer review to ensure a systematic review of the IMARC 9 draft report by the IRT. The review therefore followed the steps outlined by the ISAM methodology as follows:

ES2   ASSESSMENT CONTEXT

EPRI notes that U.S. NRC 40 CFR 197 and 10 CFR 63 call for the performance of analyses that are consistent with a "reasonable expectation" philosophy as opposed to a "most conservative" philosophy. The IRT considers that EPRI has adopted an appropriate assessment context according to its role and that EPRI's implementation of the IMARC code is consistent with the "reasonable expectation" philosophy and the applicable regulations.

ES3   SYSTEM DESCRIPTION

The IMARC 9 documentation focuses on the IMARC model and does not provide a detailed description of the disposal system and its components, beyond those necessary to understand what the model is seeking to represent. EPRI's reliance on information regarding the disposal system characteristics published by the U.S. DOE and others is appropriate, but the IRT

considers that the current IMARC 9 documentation could be improved by providing more detail on the disposal system and its (geometrical) conceptualization.

ES4   DEVELOPMENT AND JUSTIFICATION OF SCENARIOS

EPRI's development of IMARC has tracked the evolution of Yucca Mountain regulations, disposal system design, and conceptual understanding of the proposed repository over the years and current emphasis is on three primary scenario variants:

- A nominal scenario, which comprises the features, events and processes (FEPs) that are expected to occur (as opposed to unlikely FEPs), including certain seismic effects.

- An igneous intrusive scenario.

- An igneous extrusive scenario.

The igneous intrusive scenario has been addressed using IMARC in EPRI (2005). The FEPs associated with the igneous extrusive scenario are very different than those implemented in IMARC, and as a result, this scenario has been evaluated using a different modeling approach.

The inadvertent human intrusion scenario established in 10 CFR Part 63 has not been addressed in IMARC or in other EPRI analyses for two reasons:

- 10 CFR Part 63 prescribes a stylized examination of inadvertent human intrusion manner and does not permit significant alternative viewpoints.

- Inadvertent human intrusion scenarios are not expected to be significant in licensing of the Yucca Mountain repository (U.S. DOE/OCRWM, 2000).

In general terms, EPRI has followed an approach to the identification and justification of scenarios and models that is largely based on the regulatory context for the assessment of a repository at Yucca Mountain, coupled with expert judgement regarding which FEPs should be included (or excluded) from TSPA models and sub-models. The IRT considers that the EPRI approach to the identification and justification of scenarios is appropriate, given EPRI's assessment context and its focus on developing a model that provides a reasonable representation of expected system behaviour. The focus of the IRT's review has been on the nominal scenario. It is proposed that a future review will address EPRI's application of IMARC to alternative credible scenarios such as igneous events, rockfall and expanded capacity of the repository.

Consistent with its objectives and priorities EPRI has not conducted a formal FEPs audit to confirm that all relevant FEPs are appropriately accounted for (or eliminated from) its chosen scenarios and models. A systematic formal audit of FEPs would be expected of the U.S. DOE as

potential implementer of the repository at Yucca Mountain. However, it is recommended that EPRI reviews the U.S. DOE FEPs documentation for comparison with its assessment models.

ES5   MODEL FORMULATION AND IMPLEMENTATION

EPRI's approach to model formulation and implementation has been to contract a team of experts, collectively possessing expertise in a wide variety of relevant disciplines. Individuals from this team have been given responsibility for developing detailed conceptual models and software to represent various parts of the disposal system, according to their areas of expertise. A lead contracting organisation (Monitor Scientific) maintains and runs the IMARC code, which provides a TSPA capability based on the various detailed models or their outputs.

The IRT considers that the model formulation process is reasonable; it relies on 'cross-review' of work by other members of the assessment team and by peer reviewers, as well as controls over the quality of the work and software development. The IRT suggests that EPRI should consider reviewing and adopting centralised methods for recording and controlling changes to model assumptions, data and parameter values, and for making these readily available across the expert team (e.g. the Vignette knowledge management system used by the Belgian Agency for Radioactive Waste). Overall, the model formulation process followed by EPRI results in a very efficient, high quality, well integrated and "fit for purpose" TSPA model.

The following paragraphs comment on the IMARC 9 component models.

ES5.1 Climate Change

Climate and climate change are likely to be important controls on the amount of water that flows through Yucca Mountain and may, thus, affect repository system performance. Over extremely long periods, major changes in the global climate could occur, for example, leading to a transition to a glacial climate.

EPRI's approach to representing climate and climate change in IMARC 9 is generally clear, although the terms 'present-day interglacial', 'greenhouse', and 'full glacial maximum' should be clearly defined and their use made more consistent in the next revision of the IMARC documentation. Perhaps more importantly the draft IMARC 9 report does not present the rationale for the assumed durations of the first two climate states.

Nevertheless, the IRT considers that the overall EPRI approach to representing climate change in IMARC 9 is generally consistent with the proposed regulations. An approximation is however introduced because IMARC 9 represents the U.S. NRC proposed log-uniform distribution for infiltration rate using a three-point discrete distribution) (see also ES5.2 and ES6.2).

The IRT recommends that EPRI incorporates a discussion of the potential effects of global warming into the document.

ES5.2 Infiltration

Net infiltration is a hydrologic parameter that controls the rate of deep percolation, radionuclide transport, groundwater recharge and groundwater seepage into the repository.

Net infiltration is largely dependent on the climatic conditions. It is therefore appropriate that the net infiltration modelling in IMARC is climate dependent. Furthermore, the assignment of low, moderate and high values to the net infiltration event-tree branches is a reasonable approach for capturing uncertainty and variability in this parameter value, and is commensurate with the available meteorological data.

In addition, this simple approach is justified because in the very long-term, i.e. beyond 10^4 years (when infiltration could affect the dose risk from the repository, by affecting radionuclide transport from Engineered Barriers (EBS) which are expected to gradually fail in the long-term) the infiltration rate in the TSPA has been proposed by U.S. NRC.

Specific suggestions for improved documentation of the infiltration model include:

- addition of a water balance diagram;
- explanation of the coupling between infiltration, percolation and seepage in IMARC 9;
- clarification of the effect (or lack thereof) of infiltration on EBS degradation rates;
- addition of the model equations which use the infiltration rates (or reference to other sections where these may appear);
- reference to the literature source(s) where the model and model parameters are derived.

As IMARC is periodically updated to reflect scientific progress, the IRT suggests that it would be beneficial to use the IMARC 9 tool to evaluate the dose/risk implications of uncertainties related to selecting the (EPRI, 1998) range of net infiltration rates versus other recent work (e.g., Faybishenko, 2007) or other recent assessments. Since infiltration rates affect percolation through the Unsaturated Zone (UZ) and groundwater recharge, it would also be useful to carry out a sensitivity analysis to evaluate how sensitive the UZ and Saturated Zone (SZ) radionuclide transport are to uncertainty in the net infiltration rate over the first ten thousand years after disposal.

ES5.3 Seepage

Seepage, i.e. free water flow, into the disposal drift, is a function of the infiltration and is affected by the capillary barrier of the open drift, which at small infiltration rates will allow the water to flow around the drift without any seepage into it. Furthermore, the heterogeneous nature of the fractured tuff implies that the average net infiltration is focused into some areas and away from other areas.

The IMARC 9 seepage model is based on a critical assessment of U.S. DOE work in this area and appears to be state-of-the-art. The EPRI model seems justified and not unnecessarily conservative. However, a few remarks are warranted regarding clarity of the documentation.

Initially it was not clear how the different seepage assessments made by U.S. DOE had been used in justifying EPRI's model. Only after discussions with the IMARC team, did it become evident that the model justification is based on the critical review of U.S. DOE reports presented in (EPRI 2000).

There is a need to expand the justification for omitting episodic flows. The fracture asperity argument presented in EPRI (2002a) is plausible, but does not provide sufficient evidence. The argument would be much enhanced if combined with observations from the existing drift at Yucca Mountain.

The handling of seepage during high sub-boiling temperatures would benefit from additional discussion. The IRT agrees that it is reasonable to omit this aspect from the model, because the containment model is not coupled to the seepage model, and because containment is generally long-term (i.e. it is functioning well into the temperate region when the IMARC seepage model becomes valid). However, should either of these conditions become invalid (e.g. by future updates of IMARC 9 or by new data on containment times), then it would be necessary to revisit the seepage model. The IRT, thus, recommends that this, as well as other critical assumptions, be clearly documented at an overview level.

ES5.4 Containment

Containment failure (i.e. a breach of the engineered barriers) would lead to the release of radionuclides from the wasteform. Containment failure encompasses several aspects including: corrosion processes, undetected initial defects and geotechnical issues.

ES5.4.1   Corrosion Aspects

IMARC's EBSCOM code assesses the rate of failure of the components of the engineered barriers system. It includes models for the rate of failure of:

- The cladding;
- The titanium Drip Shield (DS);
- The Alloy 22 Waste Package Shell (WP) and Waste Package Closure welds.

The cladding failure model in IMARC 9 addresses the following modes of failure:

- Initial cladding failure;
- Localized corrosion (LC) – this process (e.g. pitting in oxidizing saline conditions), is acknowledged in the text but not taken explicitly into account because the consequences of pitting failures are not expected to be significant, since the apertures are expected to be small and at least partially blocked by corrosion products;
- General corrosion (GC for wet and dry conditions);
- Hydride reorientation – this process is neglected because cladding temperatures for higher burn-up spent fuels during drying operations (prior to transfer from pool to dry storage) are limited to 400ºC. This operational limit ensures that little or no hydride reorientation should occur.

The IRT concurs that relevant failure mechanisms are addressed in the IMARC 9 description of the cladding failure model and supports the consideration of the cladding as part of the EBS in IMARC 9. Furthermore, the IRT concurs with the argument that pitting corrosion is unlikely to lead to a major exposure of fuel for dissolution. However, the IRT recommends that EPRI adds a discussion providing rationale for this argument and showing that neglecting this process will not have a significant impact on the estimated dose.

The drip shield (DS) failure model in IMARC 9 addresses the following modes of failure:

- GC – This is represented by a temperature dependent Arrhenius expression. The modelling keeps track of the fraction of GC of the drip shield supported by the cathodic reduction of O_2, which does not result in hydrogen absorption. This is important because it affects the probability of drip-shield failure by Hydrogen-Induced-Cracking (HIC).

- Hydrogen Induced Cracking (HIC) – The corrosion of Ti by H_2O produces hydrogen atoms that can be absorbed by the DS and lead to hydrogen-induced cracking. Failure of the DS by HIC can occur once the absorbed hydrogen concentration reaches a critical value.

The IRT agrees that relevant modes of failure are addressed in the IMARC 9 description of DS failure. Furthermore, the IRT concurs with the modelling of these corrosion processes. In particular the IRT supports the recent modification in the HIC model which now takes into account the release of absorbed H as the Ti matrix corrodes and converts to TiO_2.

The waste package (WP) failure model in IMARC 9 addresses the following modes of failure:

- GC – this is represented by a temperature dependent Arhenius relationship. No enhancement factor is included to account for thermal aging. A factor is used to represent reduction in the tensile stress that would reduce the rate of GC for the laser-peened closure weld on the outer lid.

- LC – this is represented through initiation (under specific conditions) and a rate of propagation. If LC initiates, it is assumed to continue to propagate at a time dependent and temperature-dependent rate. The rate of propagation is assumed to decrease with time, essentially stifling LC growth after a certain period of time.

- Microbial Influenced Corrosion (MIC) – The WP is susceptible to MIC when the temperature is below a threshold temperature. Therefore, MIC of the WP is potentially important in the long-term once environmental conditions in the drift have ameliorated sufficiently to allow microbial activity. One of the major stressors for microbial activity in the repository is the general lack of water, characterized by the low % Relative Humidity (RH) in the drift. The time dependence of the %RH in the drifts is not explicitly included in EBSCOM but, as RH and temperature are closely linked, the conditions for the onset of microbial activity in the repository following the thermal pulse are defined by a threshold temperature. Once active, MIC is represented in IMARC 9 through two factors that enhance the rates of GC and LC.

- Stress Corrosion Cracking (SCC) - In the nominal scenario, SCC only affects the WP closure lid welds. The WP shell (including the non-closure lid) is heat treated to relieve manufacturing stresses prior to loading of the spent nuclear fuel. Once filled with the wasteform and sealed, the WP cannot be stress relieved through heat treatment, although the surface of the outer closure lid weld is stress relieved by laser peening or low-plasticity burnishing.

The IRT concludes that relevant failure mechanisms are addressed in the IMARC description of the WP failure model and that the models are appropriate. Furthermore, the IRT concurs with neglecting the effect of thermal ageing on the rate of GC in Alloy 22. Such enhancement was only observed in aggressive boiling 50% H_2SO_4 + 42 g/L $Fe_2(SO_4)_3$. However, tests in more relevant environmental conditions indicated no enhancement (BSC, 2003; 2004a). Therefore, neglecting this factor makes sense.

The IRT suggests that EPRI carry out a Sensitivity Analysis to assess the risk importance of the stifling model. If this is important, the IRT recommends that EPRI provides further evidence to support the stifling model for the expected repository conditions.

ES5.4.2   Failures Caused by Initial Defects

There is a very low probability that some Engineered Barriers (EBS) components placed in the repository would have significant initial defects. These defects would be either detectable faults missed by the inspection procedure, or undetectable, small faults located so as to lead to premature container failure. Failure would occur when the full wall thickness of the EBS component (e.g., DS, WP, WP lid welds) was penetrated. Subsequently, irrespective of the size of the penetration, the EBS component is assumed to offer no further protection. A variety of defects, depending on their type (crack, void, inclusion, etc.), position (weld, sidewall), and size, can be expected.

Some of these defects would lead to rapid failure, whereas others would require some time to grow before perforation occurred.

The IRT concurs that the consideration of initial defects in the containment model makes sense. Furthermore, the assumption of complete failure regardless of defect size is clearly conservative. Regarding documentation of the model in the IMARC 9 report, the IRT had difficulty understanding what specific probability was used for initial defects and what it was based on.

ES5.4.3   Rock Mechanics

IMARC 9 considers rock fall resulting from drift degradation and thermal stresses as part of the nominal scenario. The possibilities for such rock fall were assessed by EPRI, using both EPRI and U.S. DOE analyses. EPRI concluded that U.S. DOE's Drift Degradation model is appropriate for analyzing drift degradation due to thermal loading and seismic events. Furthermore, supplementary EPRI numerical analyses were conducted using UDEC, a two-dimensional code produced by Itasca.

Overall, the IMARC approach follows the U.S. DOE development. The IRT concurs that the U.S. DOE approach and the subsequent EPRI analyses seem to be state-of-the-art.

ES5.5 Radionuclide Release from the Engineered Barriers System

The source-term model in IMARC 9 calculates the release rates of selected radionuclides from spent fuel upon containment failure and contact with water. The list of radionuclides is developed by screening. Other components of the source-term model include:

- instant and congruent release models;
- wasteform degradation model;
- element-dependent solubility limits.

The release of radionuclides from the EBS and into the Unsaturated Zone (UZ) is also affected by mass transport through the EBS and the EBS-UZ interface. These various aspects are commented on below.

ES5.5.1   Screening

IMARC 9 tracks selected radionuclides based on a screening assessment. The radionuclides assessed in IMARC 9 include: Tc-99, I-129, Th-229, U-233, U-234, U-235, U-236, Np-237, U-238, Pu-239 and Pu-240. Potentially important radionuclides in other assessments of spent nuclear fuel disposal include Cl-36, Se-79, and Ra-226 and its progeny. The IRT recommends that EPRI documents the radionuclide screening assessment within the IMARC 9 documentation.

ES5.5.2   Instant Release

The instant release model in IMARC 9 represents both gap inventory and grain-boundary release through the use of an instant release fraction (IRF). This is a conservative and adequate model for the assessment purposes. However, there is no discussion of the derivation of the IRF in the IMARC 9 document. The IRT recommends that EPRI includes a section on the selection of IRF parameter values, their justification and the mathematical implementation of instant release in the model.

ES5.5.3   Wasteform Degradation

Spent fuel is assumed to undergo rapid alteration in the Yucca Mountain repository following waste package and cladding failure because of assumed oxidizing conditions. Radionuclides bound within the spent-fuel matrix are assumed to dissolve into water congruently with spent fuel alteration. A constant spent-fuel alternation rate is assumed. The IRT believes that this alteration time is very conservative for the following reasons:

- The dissolution rates were determined from once-through flow tests. As uranium concentrations in the surrounding solution increase, there will be a smaller diffusive gradient driving dissolution.
- No credit was taken for the precipitation of alteration products, especially in the presence of Ca and Si. Although the absolute protective nature of such a precipitates is uncertain, they would be expected to at least partially block the underlying UO_2 surface and thus reduce the rate of dissolution.

The IRT recommends that EPRI continues current efforts to evaluate the applicability of more mechanistic spent fuel alteration models.

ES5.5.4   *Element-Dependent Solubilities*

IMARC 9 assumes that the concentrations of dissolved radionuclides cannot exceed their element-dependent solubilities. The IRT focussed the review of element-dependent solubilities on Np-237, because of its potential contribution to the RMEI dose (due to its long half-life, potential mobility in oxidizing conditions and its radiotoxicity).

The IMARC 9 model assumes that Np co-precipitates with secondary uranyl minerals in which Np (V) substitutes for U (VI), with charge balance maintained by substitution of divalent alkaline earth cations by H^+ or monovalent alkali metal cations.

The IRT concurs that this assumption is consistent with empirical data, although such a precipitate has not been directly identified in dripping experiments under Yucca Mountain repository conditions. The EPRI assumption of an Np co-precipitate with secondary uranyl minerals is also consistent with Burns and Klingensmith (2006). Furthermore, the IRT believes that the consideration of schoepite as an end-member of the assumed solid solution, rather than more stable U minerals such as uranophane, is conservative.

The IRT notes that there is some uncertainty surrounding the precise nature of the solid precipitate and because of this the IRT recommends that EPRI carries out a sensitivity analysis to explore the effect of uncertainty in the value of Np solubility on the overall dose results.

ES5.5.5   *Mass Transport through the Engineered Barriers and UZ Interface*

In IMARC 9, mass transport through the EBS is modelled using the COMPASS code. The IMARC 9 document only describes the COMPASS and COMPASS-UZ interface in general terms. A detailed description of this interface is provided by Wei (2007).

The radionuclide release rate from COMPASS is given by the sum of the advective and diffusive fluxes calculated assuming a zero outer concentration boundary condition. In order to provide input to the unsaturated zone code, which has been implemented with a concentration boundary condition at the upper edge of the unsaturated zone solution domain, the output from COMPASS is translated into a concentration boundary condition using the average advective flow into the unsaturated zone. As pointed out by the IMARC team, this approach of prescribing the input mass flux to UZ may underestimate concentrations at the interface between the near field and the

unsaturated zone, but since it ensures consistency in the total mass flux between COMPASS and UZ, it is appropriate.

It appears to the IRT that dripping conditions in the near-field should be correlated to fracture flowing conditions in UZ, but this correlation could not be fully implemented using a single UZ column (see below). It might have been more realistic to use two different columns of the UZ model, where dripping sections discharge to a UZ column with high rate seepage and the non-dripping parts discharge to a diffusion dominated UZ column. However, since currently used UZ boundary conditions imply that migration though the UZ is dominated by seepage, using a single vertical column is justified.

The IRT encourages the detailed documentation of COMPASS, recently undertaken by EPRI and recommends that it is included in the IMARC 9 document. It is also recommended that EPRI should provide an Assessment Model Flowchart (AMF) that gives an overview of IMARC 9 and its various sub-models.

ES5.6 Unsaturated Zone Flow and Transport- UZ – SZ Interface

The IMARC 9 model of the unsaturated zone (UZ) could be used to represent several one-dimensional vertical columns allowing approximation of the spatial variations of repository releases from the repository horizon. However, in its current implementation only one column is used. It is reasonably assumed that the flow and the transport of the radionuclides are directed downwards only. The one-dimensional columns are represented either as a single-porosity, single-permeability or double porosity/double permeability medium thus describing the coupled matrix/fractures interactions.

The IMARC model of the unsaturated flow allows exploration of the sensitivity of the system to the different hydraulic and migration processes that may be active in the unsaturated zone. The simplification to one-dimensional transport appears justified – and its justification has also been explored by sensitivity analyses.

The IRT is concerned about the use of a single vertical column, since this, in principle, would not represent the spatial variability of the rock properties. However, the IRT accepts the argument provided by the IMARC team that in IMARC 9, migration though the UZ is dominated by seepage so that the spatial variability is relatively unimportant. Therefore, using a single vertical column is justified. However, the IRT recommends that the IMARC document explicitly discusses this, and also generally remarks that the selection of a single vertical column is justified for current properties and boundary conditions.

ES5.7 Saturated Zone Flow and Transport

The IMARC conceptual model for flow and transport in the saturated zone is one of fracture flow, but allowing for matrix diffusion (and sorption) into the rock between the flowing fractures. EPRI has assessed the U.S. DOE approach of channelized flow or flowing intervals, but assumed, in contrast to U.S. DOE, that within the flowing interval, the fracture spacings and resulting block sizes will be much smaller than flowing-interval spacing. The SZ (Saturated Zone) code is a general double porosity groundwater flow and transport code composed of two sub-blocks: one block for the water velocity field computation and one block for the radionuclides transport computation. Originally, the model was implemented as three-dimensional, but based on sensitivity studies the present model uses a 2-dimensional representation, set up as two segments: A fractured tuff segment extending from beneath the repository to 15 km down gradient, and an alluvial segment extending from 15 km down gradient to the location of the Reasonably Maximally Exposed Individual (RMEI) 18 km down gradient, the "compliance point." as established by the U.S. EPA. The flow boundary conditions are the spatially variable water inflow rate at the upstream boundary of the SZ computational domain, a temporally variable water infiltration rate at the bottom of the UZ column(s) under the repository, and as a constant infiltration rate over the rest of the water table. The values used are derived from U.S. DOE analyses. The output from the saturated zone is calculated as the total discharge in the plume divided by the representative volume to produce concentrations.

The overall conceptual model appears consistent with the U.S. DOE assessment of the saturated zone, but the resulting retention offered by the saturated zone depends critically on the boundary conditions (infiltration at the top surface and inflow rate at the upstream boundary), the used block size, and flow "focusing" caused by the flowing intervals and the matrix diffusivity and sorption. The IRT agrees that it is correct to only consider the flow over the flowing intervals, and increase the flux in the SZ by dividing the average flux by the percentage of the vertical profile representing flowing intervals. The IRT also agrees that block sizes determined by the distances between flowing intervals, rather than the distance between the flowing fractures within the flowing intervals is unnecessarily conservative. However, the IRT notes that basing the block size on the fracture spacing is strictly only valid in case the flow is equal in all fractures and flowing intervals. In case of uneven flow between fractures, the effective block size is a function of the distance between the fractures carrying most of the flow. Furthermore, while the applied boundary conditions for flow and transport are generally justified, it should be noted that flow, and thus retention, in the saturated zone will depend critically on the inflow rate at the upstream boundary of the SZ computational domain and the constant infiltration rate over the rest of the water table. These aspects should be better acknowledged in the IMARC documentation and the input values used, when deviating from U.S. DOE values, need better justification.

The SZ code appears fit-for-purpose, and the sensitivity tests carried out fully support the reduction to two-dimensions – and possibly even to a one-dimensional solution – , given the fact the current biosphere endpoint makes transverse dispersion a non-issue. The approach for calculating concentration at the compliance point appears justified.

ES5.8 Biosphere

EPRI's biosphere model is a compartmental model which includes the following exposure pathways:

- Drinking of domestic water;
- Bathing in domestic water;
- Inhalation of soil and other dust suspended in air;
- Inhalation of irrigation water;
- Ingestion of soil;
- External exposure to soil;
- Ingestion of food products, including crops (root and green vegetable, grain and fruit) and animal products (beef, chicken and eggs).

This compartment model is used separately from IMARC to calculate a set of Biosphere Dose Conversion Factors (BCDFs), which are used as inputs to the IMARC TSPA calculations. EPRI's overall approach to developing and justifying its compartment model of the biosphere is appropriate and consistent with international practice. The approach is also similar to that of the U.S. DOE.

The IRT has suggestions for improvement of the biosphere model regarding the following aspects:

ES5.8.1   Biosphere Climate Change

The IRT notes that some features of the biosphere are likely to be climate dependent (e.g., irrigation rates). However, the model assumptions are consistent with the regulatory context for the assessment.

ES5.8.2   Exposure Pathways

The IRT notes that the U.S. DOE (2007) biosphere model includes a pathway that is not considered in the EPRI model, namely consumption of fish, farmed in radionuclide-contaminated water. The basis for the inclusion of this pathway in the US DOE biosphere model

is that fish-farming is currently practiced in the Amargosa Valley. The IRT recommends that EPRI considers the potential significance of such a pathway.

ES5.8.3   Biosphere Transfer Model

IMARC 9 uses a K_d for modelling radionuclide retardation in soil. This is commonly the approach used in safety assessments. It should be noted that for some radionuclides, such as Tc-99, this is a conservative approach because processes, such as chemical reduction and co-precipitation (e.g., Abdelouas *et al.* 2005; Zachara *et al.* 2007) may tend to further retard migration. The IRT notes that it would be useful to add a discussion on these processes in the report.

ES5.8.4   Data and Parameter Values

The IRT has found that the traceability of the data used in EPRI's biosphere modelling is very good. Nevertheless, it would be useful to improve the IMARC 9 documentation and explain the reasons for changes to the BDCFs that have occurred in IMARC 9 BDCFs as compared to IMARC 6 and 7. With regard to data selection and the use of up to date data, it is noted that EPRI (2007) cites Ashton and Sumerling (1988) as the source of dose coefficients for external irradiation from soil, whereas more recent data may be available (e.g., U.S. EPA, 2002). The IRT recommends therefore, that at an appropriate stage in its safety assessment process, EPRI reviews and updates its documentation and biosphere data.

ES5.8.5   Parameter Uncertainty

EPRI's biosphere modeling involves a large number of parameters, many of which are uncertain. For example, animal product transfer factors and retardation coefficients may well vary over several orders of magnitude. IMARC 9, however, uses single BDCFs for each radionuclide. The IRT suggests that EPRI considers undertaking further analysis of the significance of uncertainties in the values of biosphere input parameters, and clarifies which BDCFs it is taking forward into TSPA (i.e., best estimates, distributions, means, medians or other type of central value), and explains why the values used in TSPA are consistent with its assessment context.

ES6   INTEGRATED MODEL AND INTERPRETATION OF THE RESULTS

IMARC 9 provides an integrated presentation of the total repository system and captures the main processes and their interactions. In addition to comments on specific sub-models (above), the IRT reviewed overarching issues related to the integrated model and interpretation of the modelling results. Comments on these issues are provided in the following paragraphs.

ES6.1 Conservatism and Realism

The IRT concurs that IMARC 9 is "fit for purpose" in the sense that it provides a risk-based methodology for integrating information from various disciplines affecting long-term repository performance and focuses on a reasonable expectation of the dose consequence to the RMEI as defined by U.S. NRC. IMARC 9 is a very well integrated model which focuses on those processes which could affect the long-term performance of the repository.

The U.S. NRC 40 CFR 197 and 10 CFR 63 call for the performance of analyses that are consistent with a "reasonable expectation" philosophy as opposed, for example, to a "most conservative" philosophy. The IMARC 9 code is generally consistent with the "reasonable expectation" philosophy and the applicable regulations, although some conservatisms in the IMARC models remain (e.g., the spent fuel dissolution rate, neglecting defect size in the modelling of instant containment failure).

The IRT strongly supports work carried out by the EPRI team on the deliquescent brines scenario. This is an important study showing that such brines are unlikely to form, would not be stable if formed, and would not lead to LC, even if they formed and were stable (EPRI 2004b; Apted et al. 2006). The IRT agrees therefore that eliminating deliquescent brine formation and consequent early failure of WPs by LC is justified.

The IRT recommends that EPRI continues to study ways to move away from conservative assumptions (which are essential in the absence of sufficient data and full mechanistic understanding) towards more scientifically credible and realistic assumptions. This is important, particularly for risk-sensitive processes. For example, if a sensitivity analysis shows that the spent fuel dissolution rate in IMARC 9 is risk sensitive over the time-frame of interest, it would be useful to study the availability of data and the feasibility of developing a less conservative, and a more mechanistic fuel alteration model. The IRT supports an initiative being undertaken in this regard, by EPRI.

ES6.2 Treatment of Uncertainty

Uncertainty in input parameters is propagated using two different methods. The primary method of uncertainty propagation in IMARC 9 is based on a logic tree approach. In this approach, parameters are specified as high, moderate, and low values with probabilities associated with each. The second method of uncertainty propagation is based on Monte Carlo (MC) methods. MC analysis has been used in the areas of EBS degradation and BDCF calculation to generate distributions, means or median values for use in the TSPA.

The event tree approach is an approximation to a full MC with continuous pdf's. EPRI should consider carrying out sensitivity analyses to assess whether the approximation introduced by using discrete pdfs significantly affects calculated dose to the RMEI. Furthermore, it is recommended that EPRI justifies the selection of the various pdfs in IMARC. The focus of this documentation effort should be risk-informed.

ES6.3 Sensitivity Analysis

The IMARC 9 draft document focuses on description of assessment methodology and its justification, and less on results and their interpretation. Some sensitivity analyses are presented as part of the rationale for the development of some of the component models, but the dose consequences of the nominal evolution scenario are only shown in the IMARC 9 document for a best-estimate case.

The IRT recommends that the results of the IMARC 9 probabilistic assessment be subject to a systematic sensitivity analysis to identify which parameter uncertainties contribute most to the uncertainty in the calculated total dose rates.

In addition, IMARC 9 includes model uncertainties. Some of these uncertainties are not captured in the IMARC 9 probabilistic calculations (they are represented by parameter values which are means or medians derived outside of IMARC). The IRT recommends that model uncertainties be addressed in a systematic sensitivity analysis. This sensitivity analysis could be based on risk insight from existing assessments and detailed modelling work which could guide priorities towards risk-sensitive areas.

ES6.4 Code Inter-Comparison

According to the IMARC 9 report, ongoing verification activities ensure that the code and its constituent parts are correctly implemented. The code is maintained under a configuration management system. Thorough testing is conducted of all changes to the code that are implemented, and this includes benchmarking against analytical solutions and alternative computer codes, as appropriate.

The IRT concurs with EPRI's statement on the importance of code-intercomparison activities for the various "sub models" that make up IMARC 9. Such comparisons are useful for understanding assumptions and modelling approaches, as well as the effects of certain parameter values and data. Benchmarking is also important for understanding differences between different modelling approaches, and whether these differences are methodological or related to particular sets of parameter values. Once the differences are understood and resolved, the similarity between results using different models can be used to enhance the scientific credibility

of the models. The IRT recommends that significant benchmarking activities should be documented.

ES6.5 System Understanding

Many of the U.S. DOE models are incorporated in IMARC 9 via either lookup tables or failure distribution curves. When IMARC 9 deviates from the U.S. DOE conceptual model – this is generally justified based on an independent assessment of the issue and with focus on processes which are important for system performance. The IMARC team has also developed system understanding by its previous sensitivity analyses. Overall IMARC 9 appears to provide very good insight into risk-important processes of the explored repository system.

The IRT understands that the system understanding and model selection are based on critical reviews of the U.S. DOE work by the EPRI team. Such reviews are documented in several of the IMARC reports. However, the IRT recommends that EPRI improves the overall documentation on the final judgements made based on these critical reviews. This would enhance traceability and credibility of the model.

ES6.6 Information Quality and Management

The IMARC 9 document does not include a description of EPRI's approaches to assessing input data quality or data management. In the IMARC 9 report the adequacy of data is generally justified by reference to U.S. DOE work and documents, but there is no pre-defined procedure for justifying and accepting EPRI's input data. The IRT has found no specific examples of non-justified data being used, but the IRT recommends that EPRI should consider making the use of suitable information quality procedures an integral part of conducting assessments with the IMARC code.

EPRI is currently developing and implementing a configuration management system to demonstrate even better control of its code development activities - the IRT encourages EPRI to describe this work in the IMARC report.

The IRT notes that the justification for omitting particular processes or features from certain IMARC sub-models is sometimes based on the expected or actual output of other sub-models. While such an approach is acceptable, the justifications for the sub-models may be interdependent and there might be a risk that these interdependencies could be forgotten by individual team members when further developing a sub-model or if there is an important change in input data. To mitigate this potential problem the IRT recommends that EPRI should maintain a central record of the modelling assumptions made.

The Electric Power Research Institute (EPRI), with major locations in Palo Alto, California; Charlotte, North Carolina; and Knoxville, Tennessee, was established in 1973 as an independent, nonprofit center for public interest energy and environmental research. EPRI brings together members, participants, the Institute's scientists and engineers, and other leading experts to work collaboratively on solutions to the challenges of electric power. These solutions span nearly every area of electricity generation, delivery, and use, including health, safety, and environment. EPRI's members represent over 90% of the electricity generated in the United States. International participation represents nearly 15% of EPRI's total research, development, and demonstration program.

Together...Shaping the Future of Electricity

Program:

Nuclear Power

1016631